



## City Research Online

### City, University of London Institutional Repository

---

**Citation:** Ragupathy, P. (1994). Nonlinear behaviour of precast concrete frames.  
(Unpublished Doctoral thesis, City University London)

This is the accepted version of the paper.

This version of the publication may differ from the final published version.

---

**Permanent repository link:** <https://openaccess.city.ac.uk/id/eprint/8380/>

**Link to published version:**

**Copyright:** City Research Online aims to make research outputs of City, University of London available to a wider audience. Copyright and Moral Rights remain with the author(s) and/or copyright holders. URLs from City Research Online may be freely distributed and linked to.

**Reuse:** Copies of full items can be used for personal research or study, educational, or not-for-profit purposes without prior permission or charge. Provided that the authors, title and full bibliographic details are credited, a hyperlink and/or URL is given for the original metadata page and the content is not changed in any way.

**NONLINEAR BEHAVIOUR OF  
PRECAST CONCRETE FRAMES**

by

**PASUPATHY RAGUPATHY**

Submitted in fulfilment of the  
requirement for the award of  
Degree of Doctor of Philosophy  
in Civil Engineering

Structures Research Centre  
Department of Civil Engineering  
City University  
London  
February 1994

## ABSTRACT

This thesis describes a new technique for studying the non-linear behaviour of reinforced concrete frames with flexible joints. The method is based on the concept of establishing an equilibrium deflected shape of a structure. The computations involve two basic levels of iteration. First, starting with an assumed nodal deformation, equilibrium deflected shapes and end forces of individual members in a structure are calculated using moment-thrust-curvature relations. The out of balance forces are computed by considering equilibrium of member forces at nodal points. In the second level of iteration based on a numerically computed nonlinear stiffness matrix, the nodal deformation are updated until the out of balance forces are negligible. The interaction of torsion with flexure has been assumed to be independent and further, the members are assumed to behave linearly in torsion. The influence of floors and cladding is ignored and only the skeleton frame is considered in the analysis. The associated computer program SWANSA based on the above method can be used as a design tool for sway and nonsway concrete frames with or without flexible joints. An interactive data entry facility allows the user to enter data by answering simple questions or by returning default values.

Full scale experiments were carried out on eight column beam subframes to validate the computer program. Each subframe consisted of a two storey column with a short length of a typical mid-storey beam. Four types of connection commonly used in precast construction were selected to connect the beam to the column at mid height. Two sets of subframes were made for each connection, one each of a pair of subframes was tested for upward and

downward rotations. The numerical technique is further validated with results published in literature, including experiments and the finite element method. All the comparisons show that the analysis developed in this thesis can be used to predict the behaviour of precast and other reinforced concrete frames for deflections, strains and for the ultimate loads.

Finally, it is shown how a computer program based on the new numerical method can be used as an alternative method of designing rigid jointed or semi-rigid jointed precast concrete 3-dimensional frames, taking into account material and geometrical nonlinearities.

## ACKNOWLEDGEMENTS

I wish to express my thanks to Prof. K S Viridi, under whose supervision this investigation was carried out, for his continuous guidance and constructive criticism throughout this project.

I am grateful to the technical staff in the Heavy Structures Laboratory for their help in constructing the test rig and in carrying out the experiments.

I would also like to thank several members of the precast concrete frame industry: Atcost Building Limited, Composite Structures, and members of the Precast Concrete Frame Association for their technical advice and for providing the test specimens.

I am grateful to Dr Stuart Robson, lecturer in Department of Civil engineering, for patiently going through my thesis and suggesting corrections.

Finally, I sincerely thank my wife for providing me with continuous support throughout the duration of this work.

## TABLE OF CONTENTS

	Page
Abstract	ii
Acknowledgements	iv
List of Figures	viii
List of Tables	xiii
Notation	xiv
<b>1. INTRODUCTION</b>	
1.1 General	1
1.2 Objectives	4
1.3 Summary of work	4
<b>2. SURVEY OF PREVIOUS WORK</b>	
2.1 Introduction	9
2.2 General structural analysis	9
2.3 Previous work on beam-column analysis	10
2.4 Previous work on frame analysis	15
2.5 Previous work on joint flexibility	21
2.6 Conclusion	24
<b>3. NUMERICAL ANALYSIS OF PRECAST CONCRETE FRAMES</b>	
3.1 Introduction	27
3.2 Assumptions made in numerical model	27
3.3 Modelling of frames	28
3.4 Condition of equilibrium and compatibility	28

3.5	Outline of the method of analysis	29
3.6	Development of the numerical model	30
3.7	Ultimate load	50
3.8	Description of computer program 'SWANSA'	50
<b>4.</b>	<b>EXPERIMENTS</b>	
4.1	Introduction	63
4.2	Specimens	64
4.3	Testing rig	65
4.4	Loading	66
4.5	Manufacture of specimens	67
4.6	Instrumentation	68
4.7	Preparation for the tests	68
4.8	Test procedure	70
4.9	Material properties	71
4.10	Failure of the subframes	72
<b>5.</b>	<b>COMPARISON OF EXPERIMENTAL RESULTS WITH COMPUTED RESULTS</b>	
5.1	Introduction	94
5.2	Material model used in the analysis	94
5.3	Modelling subframes for computer analysis	95
5.4	Comparison and discussion of results	96
5.5	Comparison of ultimate loads	102
5.6	Moment rotation relation for the joints	104
<b>6.</b>	<b>VALIDATION OF 'SWANSA' WITH EXPERIMENTS FROM OTHER SOURCES</b>	
6.1	Introduction	155

6.2	Reinforced concrete portal frames	155
6.3	Comparison with finite element method	159
6.4	Conclusion	161
<b>7.</b>	<b>EXAMPLE ON DESIGN APPLICATION</b>	
7.1	Introduction	171
7.2	Modelling the structure	171
7.3	Material models	172
7.4	Loadings	172
7.5	Joint types	173
7.6	Results	174
<b>8.</b>	<b>CONCLUSION</b>	
8.1	Introduction	187
8.2	Analytical method	187
8.3	Computer program	188
8.4	Experimental study	189
8.5	Comparison of computed results with experiments	189
8.6	Comparison with other results	190
8.7	Design example	190
8.8	Future work	191
	<b>REFERENCES</b>	192
<b>APPENDIX</b>	<b>DETAIL OF THE CONCRETE MIX</b>	198

## LIST OF FIGURES

FIG. 1.1	NOSWAY PORTAL FRAME	7
FIG. 1.2	SWAY PORTAL FRAME	8
FIG. 2.1	EULER BUCKLING LOAD	25
FIG. 2.2	MODULUS OF ELASTICITY	25
FIG. 2.3	BUCKLING OF COLUMNS AND BOUNDARY CONDITION	26
FIG. 3.1	TYPICAL MEMBER IN A SPACE FRAME	57
FIG. 3.2	BEAM-COLUMN AS CONSIDERED IN THE ANALYSIS	58
FIG. 3.3	TYPICAL MEMBER	59
FIG. 3.4	STRAIN DISTRIBUTION ACROSS A SECTION	60
FIG. 3.5	RELATIVE ROTATION IN FLEXIBLE CONNECTION	61
FIG. 3.6	FLOW CHART FOR FRAME ANALYSIS PROGRAM 'SWANSA'	62
FIG. 4.1	COLUMN AND BEAM GEOMETRICAL DATA (TEST CT1&CT2)	74
FIG. 4.2	COLUMN AND BEAM GEOMETRICAL DATA (TEST CT3&CT4)	75
FIG. 4.3	COLUMN AND BEAM GEOMETRICAL DATA (TEST CT5&CT6)	76
FIG. 4.4	COLUMN AND BEAM GEOMETRICAL DATA (TEST CT7&CT8)	77
FIG. 4.5	CONNECTION DETAIL FOR EXPERIMENT CT1&CT2	78
FIG. 4.6	CONNECTION DETAIL FOR EXPERIMENT CT3&CT4	79
FIG. 4.7	CONNECTION DETAIL FOR EXPERIMENT CT5&CT6	80
FIG. 4.8	CONNECTION DETAIL FOR EXPERIMENT CT7&CT8	81
FIG. 4.9	TEST RIG GENERAL LAYOUT	82
FIG. 4.10	GENERAL LAYOUT OF THE TEST RIG	83

FIG. 4.11	TWO LOADING CASES FOR WHICH SUBFRAMES ARE TESTED	84
FIG. 4.12	LAYOUT OF JACKS	85
FIG. 4.13	COLUMN BEAM ASSEMBLY ON THE TEST RIG	86
FIG. 4.14	INTERNAL STRAIN GAUGES	87
FIG. 4.15	DIGITAL READ-OUT DIAL GAUGES AND INCLINOMETER	88
FIG. 4.16	COLUMN BEAM SUBFRAME IN POSITION	89
FIG. 4.17	COLUMN FAILURE	90
FIG. 4.18	CRACK PATTERN IN THE UPPER COLUMN	91
FIG. 4.19	CRACK PATTERN IN THE LOWER COLUMN	92
FIG. 4.20	FAILURE OF BEAM COLUMN JOINT (CT7)	93
FIG. 5.0	TYPICAL STRESS STRAIN CURVE FOR STEEL AND CONCRETE	105
FIG. 5.1	COMPARISON OF CALCULATED DEFLECTION WITH EXPERIMENTAL VALUES (TEST CT1)	106
FIG. 5.2	LOAD DISPLACEMENT CURVE FOR UPPER COLUMN (TEST CT1)	107
FIG. 5.3	LOAD DISPLACEMENT CURVE FOR LOWER COLUMN (TEST CT1)	108
FIG. 5.4	COMPARISON OF CALCULATED DEFLECTION WITH EXPERIMENTAL VALUES (TEST CT2)	109
FIG. 5.5	LOAD DISPLACEMENT CURVE FOR UPPER COLUMN (TEST CT2)	110
FIG. 5.6	LOAD DISPLACEMENT CURVE FOR LOWER COLUMN (TEST CT2)	111
FIG. 5.7	COMPARISON OF CALCULATED DEFLECTION WITH EXPERIMENTAL VALUES (TEST CT3)	112
FIG. 5.8	LOAD DISPLACEMENT CURVE FOR UPPER COLUMN (TEST CT3)	113
FIG. 5.9	LOAD DISPLACEMENT CURVE FOR LOWER COLUMN (TEST CT3)	114
FIG. 5.10	COMPARISON OF CALCULATED DEFLECTION WITH EXPERIMENTAL VALUES (TEST CT4)	115
FIG. 5.11	LOAD DISPLACEMENT CURVE FOR UPPER COLUMN (TEST CT4)	116
FIG. 5.12	LOAD DISPLACEMENT CURVE FOR LOWER COLUMN (TEST CT4)	117

FIG. 5.13	COMPARISON OF CALCULATED DEFLECTION WITH EXPERIMENTAL VALUES (TEST CT5)	118
FIG. 5.14	LOAD DISPLACEMENT CURVE FOR UPPER COLUMN (TEST CT5)	119
FIG. 5.15	LOAD DISPLACEMENT CURVE FOR LOWER COLUMN (TEST CT5)	120
FIG. 5.16	COMPARISON OF CALCULATED DEFLECTION WITH EXPERIMENTAL VALUES (TEST CT6)	121
FIG. 5.17	LOAD DISPLACEMENT CURVE FOR UPPER COLUMN (TEST CT46)	122
FIG. 5.18	LOAD DISPLACEMENT CURVE FOR LOWER COLUMN (TEST CT6)	123
FIG. 5.19	COMPARISON OF CALCULATED DEFLECTION WITH EXPERIMENTAL VALUES (TEST CT7)	124
FIG. 5.20	LOAD DISPLACEMENT CURVE FOR UPPER COLUMN (TEST CT7)	125
FIG. 5.21	LOAD DISPLACEMENT CURVE FOR LOWER COLUMN (TEST CT7)	126
FIG. 5.22	COMPARISON OF CALCULATED DEFLECTION WITH EXPERIMENTAL VALUES (TEST CT8)	127
FIG. 5.23	LOAD DISPLACEMENT CURVE FOR UPPER COLUMN (TEST CT8)	128
FIG. 5.24	LOAD DISPLACEMENT CURVE FOR LOWER COLUMN (TEST CT8)	129
FIG. 5.25	LOAD-STRAIN RESPONSE FOR THE UPPER COLUMN (TEST CT1)	130
FIG. 5.26	LOAD-STRAIN RESPONSE FOR THE LOWER COLUMN (TEST CT1)	131
FIG. 5.27	STRAIN PROFILE IN THE COLUMN (TEST CT1)	132
FIG. 5.28	LOAD-STRAIN RESPONSE FOR THE UPPER COLUMN (TEST CT2)	133
FIG. 5.29	LOAD-STRAIN RESPONSE FOR THE LOWER COLUMN (TEST CT2)	134
FIG. 5.30	STRAIN PROFILE IN THE COLUMN (TEST CT2)	135
FIG. 5.31	LOAD-STRAIN RESPONSE FOR THE UPPER COLUMN (TEST CT3)	136
FIG. 5.32	LOAD-STRAIN RESPONSE FOR THE LOWER COLUMN (TEST CT3)	137

FIG. 5.33	STRAIN PROFILE IN THE COLUMN (TEST CT3)	138
FIG. 5.34	LOAD-STRAIN RESPONSE FOR THE UPPER COLUMN (TEST CT4)	139
FIG. 5.35	LOAD-STRAIN RESPONSE FOR THE LOWER COLUMN (TEST CT4)	140
FIG. 5.36	STRAIN PROFILE IN THE COLUMN (TEST CT4)	141
FIG. 5.37	LOAD-STRAIN RESPONSE FOR THE UPPER COLUMN (TEST CT5)	142
FIG. 5.38	LOAD-STRAIN RESPONSE FOR THE LOWER COLUMN (TEST CT5)	143
FIG. 5.39	STRAIN PROFILE IN THE COLUMN (TEST CT5)	144
FIG. 5.40	LOAD-STRAIN RESPONSE FOR THE UPPER COLUMN (TEST CT6)	145
FIG. 5.41	LOAD-STRAIN RESPONSE FOR THE LOWER COLUMN (TEST CT6)	146
FIG. 5.42	STRAIN PROFILE IN THE COLUMN (TEST CT6)	147
FIG. 5.43	LOAD-STRAIN RESPONSE FOR THE UPPER COLUMN (TEST CT7)	148
FIG. 5.44	LOAD-STRAIN RESPONSE FOR THE LOWER COLUMN (TEST CT7)	149
FIG. 5.45	STRAIN PROFILE IN THE COLUMN (TEST CT7)	150
FIG. 5.46	LOAD-STRAIN RESPONSE FOR THE UPPER COLUMN (TEST CT8)	151
FIG. 5.47	LOAD-STRAIN RESPONSE FOR THE LOWER COLUMN (TEST CT8)	152
FIG. 5.48	STRAIN PROFILE IN THE COLUMN (TEST CT8)	153
FIG. 5.49	MOMENT ROTATION RELATION FOR THE JOINTS	154
FIG. 6.1	COMPUTED AND EXPERIMENTAL MIDSPAN DEFLECTION FOR FRAME A40	162
FIG. 6.2	COMPUTED AND EXPERIMENTAL MIDSPAN DEFLECTION FOR FRAME A60	163
FIG. 6.3	COMPUTED AND EXPERIMENTAL MIDSPAN DEFLECTION FOR FRAME B40	164
FIG. 6.4	COMPUTED AND EXPERIMENTAL MIDSPAN DEFLECTION FOR FRAME B60	165
FIG. 6.5	COMPUTED AND EXPERIMENTAL MIDSPAN DEFLECTION FOR FRAME C40	166

FIG. 6.6	COMPUTED AND EXPERIMENTAL MIDSPAN DEFLECTION FOR FRAME C60	167
FIG. 6.7	GEOMETRICAL DATA FOR FRANKLIN'S FRAMES	168
FIG. 6.8	DEFLECTION AT THE FIRST FLOOR LEVEL FOR FRAME 1	169
FIG. 6.9	DEFLECTION AT THE SECOND FLOOR LEVEL FOR FRAME 2	170
FIG. 7.1	GEOMETRICAL DATA OF THE FRAME	177
FIG. 7.2	BENDING MOMENT DIAGRAM FRAME1, LOAD CASE 1	178
FIG. 7.3	BENDING MOMENT DIAGRAM FRAME1, LOAD CASE 2	179
FIG. 7.4	BENDING MOMENT DIAGRAM FRAME1, LOAD CASE 3	180
FIG. 7.5	BENDING MOMENT DIAGRAM FRAME2, LOAD CASE 1	181
FIG. 7.6	BENDING MOMENT DIAGRAM FRAME2, LOAD CASE 2	182
FIG. 7.7	BENDING MOMENT DIAGRAM FRAME2, LOAD CASE 3	183
FIG. 7.8	BENDING MOMENT DIAGRAM FRAME3, LOAD CASE 1	184
FIG. 7.9	BENDING MOMENT DIAGRAM FRAME3, LOAD CASE 2	185
FIG. 7.10	BENDING MOMENT DIAGRAM FRAME3, LOAD CASE 3	186

## LIST OF TABLES

TABLE 4.1	PROPERTIES OF CONCRETE AND REINFORCEMENT	72
TABLE 5.1	EXPERIMENTAL AND THEORETICAL FAILURE LOADS	103
TABLE 5.2	EXPERIMENTAL AND THEORETICAL FAILURE MOMENTS	103
TABLE 6.1	GENERAL DATA FOR THE FRAMES CONSIDERED	156
TABLE 6.2	DETAILS OF BEAMS AND COLUMNS	156
TABLE 6.3	COMPARISON OF ULTIMATE LOADS	157
TABLE 6.4	COMPARISON OF ULTIMATE LOADS	160
TABLE 7.1	COMPARISON OF LOAD FACTOR FOR PROPOSED METHOD AND THE OLD METHOD	175

## NOTATIONS

F	force
M	moment
A	end A of beam-column (subscript)
B	end B of beam-column (subscript)
n	number of division in beam-column
p	axial load in column = $F_{ZA}$
e	load eccentricity
u	column deflection in x-axis
v	column deflection in y-axis
f	curvature
X	global ordinate axis-X (subscript)
Y	global ordinate axis-Y (subscript)
Z	global ordinate axis-Z (subscript)
l,m,n	direction cosines
d	displacements in local axis
q	rotations in local axis

# CHAPTER 1

## INTRODUCTION

### 1.1 GENERAL

Precast concrete construction has been a competitive solution for single and multi-storey buildings for a number of years. It is possible to construct almost an entire structure, for industrial, commercial or residential purposes, using precast components [1-6]. The components like column, beam, wall, staircase and slabs are cast separately in a factory and assembled at site. Casting these components in a factory gives the advantage of achieving quality products. Precast components can be produced with good quality finish so that no extra effort is needed on site. By using suitable connections to assemble the components, the work involved at the construction site is minimised and thereby the construction time is shortened considerably.

Practices in precast construction differ significantly from contractor to contractor in terms of percentage of precast components used in forming the structure and in the type of connections used in assembling the precast components. In the UK most of the precast companies are involved in both design and construction of precast structures. Design and construction by the same company gives freedom to the contractor to develop and use their own connections, developed and perfected over a long period. Four types of beam column connections used by four different contractors in the UK are shown in Fig4548. This does not cover the entire range of connections used in the UK but represents a typical range. The four types shown may be described as Cleat connector, Welded connector, Billet connector and Web connector.

General guidance for the design of precast structures is covered by the code of practice on structural use of concrete, BS8110[28]. There is also a helpful document available, "The Manual of Structural joints in precast concrete"[7], which gives detailed guidance in designing and constructing precast concrete structures.

In precast construction, the components are connected on site. In design, these connections have traditionally been considered as pin-joints for the purpose of structural analysis of the frame. The moment of resistance of the mechanical connections is not taken into consideration in determining the strength of the structure. Thus, beams are designed as simply supported members. The stability of a frame against lateral loading is normally provided by rigid structures like, lift walls, shear walls, the cantilever action of the columns, or by a combination of these.

A typical bending moment diagram of a portal frame with pin connections is shown in Fig 1.1a and the moment diagram for a portal frame with monolithic connections is shown in Fig 1.1b. The maximum sagging beam moment in the beam is reduced considerably when the connection is monolithic.

When the frame is subjected to lateral load as shown in Fig 1.2, it is seen that the moment at the base of the column is reduced considerably for the frame with rigid connections. The reduction in column moment can have a great effect on the design as the frame height increases. Multi-storey buildings with pin connections have to resist lateral loads by cantilever action of the columns or by introducing structural bracing. The connections used in precast construction specially with cast in slab have considerable connection stiffness, which could be used to advantage if taken into account.

The real behaviour of precast connections would be semi-rigid, that is, somewhere between that of a pin and a rigid connection.

The behaviour of precast connections is not well understood at the moment and hence the designers ignore moment capacity of connections. This simplifies the design, but makes the structure somewhat over-conservative. If the knowledge of precast concrete connections could be developed to a point, where a frame could be designed incorporating the strength and stiffness of the connection, it would become possible to produce more economical precast concrete structures.

The principal objective of this project, thus, was to develop a numerical method incorporating the realistic behaviour of connections in determining the ultimate strength of precast concrete frames and to verify the mathematical model by means of full scale experiments.

A detailed literature survey revealed that there were two methods of analysis that could be adopted for the purpose: the finite element method and the finite difference method. The finite element method was not adopted on the basis that modelling and computation can be time consuming and would not be suitable for day-to-day application. The finite difference method based on establishing equilibrium deflected shape [8] offered the prospect of a rapid analysis, suitable for use with engineering workstations.

The method to be developed was kept simple by assuming the following:

1. Influence of slab and cladding through diaphragm action on beams and columns and torsional moment on end beams is ignored and all the loads

such as dead load, live load and wind load are transferred to beams and columns.

2. Only the skeletal frame is considered in the analysis.
3. Plane section of a member remains plane after deformation.
4. Members behave linearly in torsion. Thus interaction of torsion with flexure is ignored.

## **1.2. OBJECTIVES**

- 1 Developing a numerical model to study the behaviour of precast concrete frames with flexible (semi-rigid) joints.
- 2 Obtaining experimental values for the ultimate load, member forces and member deflections for precast column beam subframes under different loading conditions and verifying the numerical model with the values obtained from experiments.
- 3 Verifying the numerical model with other available experimental and analytical results.
- 4 Producing a design approach.

## **1.3 SUMMARY OF WORK**

Chapter 1: An introduction to the current practice in precast industry is given. The need for a numerical method to analyse precast concrete frames with flexible joints is discussed.

Chapter 2: In this chapter a literature review is presented under three headings. a.) The analysis of individual members under elasto-plastic behaviour, b.) analysis of nonlinear frames, and c.) influence of joint flexibility in overall stability of frames.

Chapter 3: A new numerical technique for analysing reinforced concrete frames with flexible joints using moment-thrust-curvature relations [8] is developed in this chapter. An associated computer program SWANSA is described in a later part of the chapter.

Chapter 4: This chapter deals with the experiments carried out to verify the new numerical method. A detailed description of the testing rig is given with illustrative diagram and photographs. The manufacturing, storing, erecting and testing of the column beam subframes used in the experiments are detailed.

Chapter 5: The experimental results of the subframes tested are presented along with the computed values for individual experiments. The attention is given to the reliability of the computer program in calculating deflected shape and the ultimate load. The comparison includes the deflections of the two storey columns, strain values at critical positions and ultimate loads.

Chapter 6: Experimental and analytical study carried out by other researchers on precast concrete frames are used to validate further the computer program SWANSA. In this, six no-sway frames and two sway frames are included.

Chapter 7: The design method proposed in this thesis is illustrated through an example, where a two bay, three storey frame is designed using the computer program SWANSA. Three types of connections are considered in the analysis: one a monolithically cast frame, second a frame with flexible connections and third with pin connections. The benefit obtained from

considering the strength and stiffness of the precast connection is demonstrated.

Chapter 8: The results of the theoretical and experimental work carried out in this project are discussed and conclusions from the work are drawn.

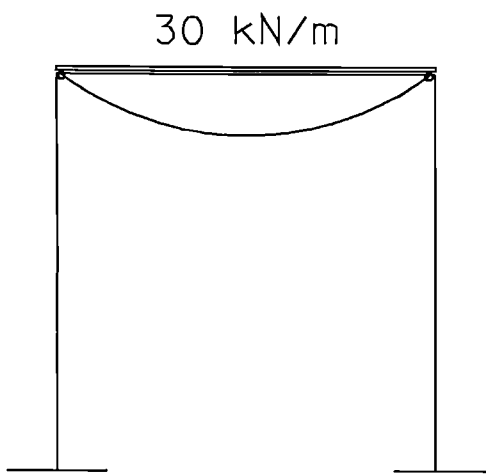


Fig 1.1a  
PIN CONNECTION

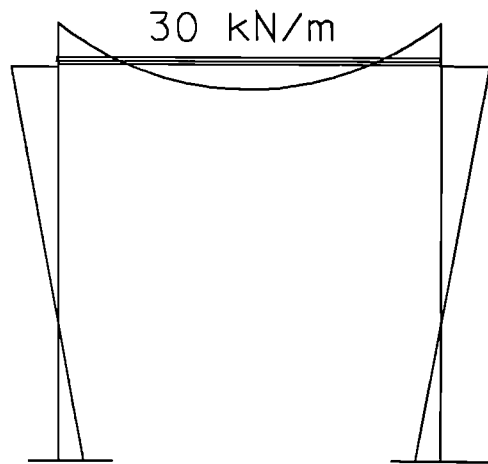


Fig 1.1b  
RIGID CONNECTION

**FIG 1.1 NOSWAY PORTAL FRAME**

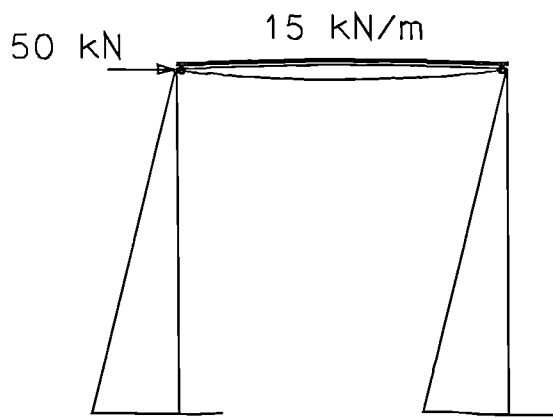


Fig 1.2a  
PIN CONNECTION

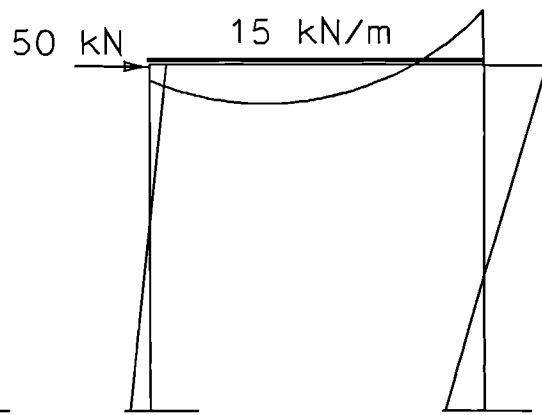


Fig 1.2b  
RIGID CONNECTION

**FIG 1.2 SWAY PORTAL FRAME**

## **CHAPTER 2.**

### **SURVEY OF PREVIOUS WORK**

#### **2.1 INTRODUCTION**

This literature review covers the theoretical development of the following aspects:

The behaviour of beam-columns

The behaviour of joints used in precast concrete construction

The behaviour of structural frames with flexible joints.

The principal object of the review is to gather available knowledge that would be useful in developing a numerical model for the analysis of precast concrete frame. Both nonlinear numerical techniques and methods of linear elastic analysis are reported.

#### **2.2 GENERAL STRUCTURAL ANALYSIS**

The behaviour of a structure depends on the geometry of the cross-section of the members, boundary conditions, any initial imperfections and the material properties of its members. The basic problem for the designer is to specify the section details of the members to resist given external forces. The designer has to assure that the structure has a stable equilibrium deflected shape and the deflections in the members are acceptable under given loading.

Advanced theoretical analysis methods may be used to accurately predict the capacity of a structure. In the absence of analytical methods, the strength of the members may be obtained from experiments. Experiments are also

essential for validating theoretical models, but once a theory is validated it should be applicable to other similar circumstances.

## **2.3 PREVIOUS WORK ON BEAM-COLUMN ANALYSIS**

### **BUCKLING ANALYSIS**

The theoretical analysis of column behaviour is first attributed to Euler [10]. He considered a pin ended geometrically perfect column subjected to compressive load acting along the column axis as shown in Fig 2.1. He stated that the buckling load of a column is the load that a column can support without bending and he further stated that the buckling load is inversely proportional to the square of the height of the column. He defines the buckling load as  $\pi^2 E_{kk} / a^2$ . Where  $a$  is the length of the column and  $E_{kk}$  is the stiffness moment which has to be evaluated experimentally. As defined by Euler,  $E_{kk}$  is a function of sectional dimension of the column and the stiffness of the material, equivalent in current definition to the product of the modulus of elasticity and the second moment of area. Euler concluded that the  $E_{kk}$  value is a constant for columns of same cross-section and material. A corollary of the equation given by Euler is that very high values for buckling load are obtained as the length of the column is reduced.

If a geometrically perfect column subjected to axial compressive load is considered, the strain across the section will be uniform. When the axial load is increased, at a critical load the column has two paths available. For slender columns the buckling load is reached before stress in the cross-section of the column reaches the yield value, resulting in the column failing by buckling. If the column is short then the stress in the cross-section reaches the ultimate

stress before the load reaches the Euler buckling load, and the column fails in crushing.

Lamarle [11] observed that the Euler formula for predicting the buckling load is applicable only if the column is not stressed beyond the elastic limit prior buckling. Later, Considere and Engesser [11,12] modified Euler's formula for the inelastic zone by replacing the Young's modulus by the tangent modulus of elasticity, which is defined as shown in Fig 2.2. This modification enabled a failure load to be predicted for short columns stressed into the inelastic range before buckling. Shanley [13] observed that the actual buckling load was close to the critical load calculated using the tangent-modulus method.

A pin ended column bends in a single smooth curve when buckling load is reached. For a fixed ended column, the ends are prevented from rotating and the column bends as shown in Fig 2.3. This gives rise to the concept of effective length. By using the distance between the points of contraflexure as the effective length to be used in the Euler formula, the failure loads of columns with different end-conditions, can be obtained. The effective length method of designing a column is the outcome of the buckling analysis and is widely used for steel and concrete structures.

By considering a column in its deflected shape under an axial load, a differential equation governing the equilibrium of the column can be obtained. The above equation can then be solved for the applicable boundary conditions [14].

## **SIMPLIFIED METHODS OF ELASTIC BUCKLING ANALYSIS**

The following simplified methods to calculate the buckling load are available if the cross-section of a column varies along its length.

**Principle of stationary potential energy:** This is also known as the Rayleigh-Ritz [15] method. In this method a suitable deflected shape in the form of algebraic or trigonometric series is assumed and the solution is obtained by considering that the sum of the strain energy in the column and the potential energy of loading will not change at equilibrium. The critical load, obtained by this method, depends on the accuracy of the approximation for the deflections.

The Finite Difference Method was developed by Collatz [16]. Finite differences are used to represent the differential coefficients at nodes along the beam-column by a linear combination of deflections. This allows the differential equation governing the behaviour of the beam-column to be replaced by a series of linear equations. The advantage in using this method is that sufficiently accurate answers can be found for problems involving a change of cross-section along the length.

**Finite Integral Method:** This method was developed by Brown and Trahair [17]. This is a reversal of the finite difference method. It is claimed that the numerical integration gives greater accuracy than that provided by numerical differentiation[11].

## NON-LINEAR ANALYSIS

Commonly used columns are not perfect and often subjected to loads other than the axial load. Columns in this category do not have a buckling load but maintain an equilibrium deflected shape from the beginning of loading. Lack of strength to support the load is indicated by excessive deflections.

There are three modes of deflections anticipated in a beam-column, namely: single axis bending, bi-axial bending and lateral torsional buckling. Lateral torsional buckling is not covered in this study since reinforced concrete columns have a relatively large torsional rigidity, reducing the influence of torsional effects.

A theoretical analysis of eccentrically loaded column was first considered by von Karman [11,18]. A strain pattern was assumed for the column section and an expression was derived for the axial load and bending moment at the section. The above expression was equated to the axial load and the external moment at that point. The resulting equation was solved for deflections using the stress-strain curve for the material with the assumption that the concave side of the column reaches a maximum strain. A graphical integration method was used to evaluate the integral.

The above method was later simplified by Westergaard and Osgood [19] by assuming a suitable shape for the column deflection.

A procedure based on moment-thrust-curvature relations for computing deflected shape, using a stress strain table, was proposed by Wilson [20]. His procedure, however, was limited for beam-column with prismatic sections. This method was later adapted for irregular sections by Gesund

[21]. The deflected shape of the column was assumed and the curvature of the column was calculated at selected stations along the column. By varying the neutral axis position, axial thrust in the column was calculated using stress-strain data. The difference between the von Karman method and this method is that no assumption for strain and boundaries are made. The bending moment was then calculated at the neutral axis position for which the axial thrust equals the column load. This procedure was repeated at all the stations and the station moments were equated to the moments due to external forces. Iterative technique was then used to modify the deflection.

Another computer method, applicable for single axis bending, was developed based on the moment-thrust-curvature relations by Cranston [22]. He used a computer program based on the above method to do an extensive study on ultimate load of concrete columns subjected to varying end conditions. The findings of the above study were later included in CP110 [72] both for the column effective length calculations, and for the added moments to be included for second order deflections. The area integration for axial load and bending moment in a section was carried out by subdividing the section into smaller elements. Warner [23] described a method applicable to short reinforced concrete columns subjected to biaxial bending based on moment-thrust-curvature relation. It is similar in concept to the method proposed by Gesund. Milner [24] also developed a concept to calculate the ultimate load for restrained H-columns under biaxial bending using moment thrust curvature interaction. Virdi [8] further extended this method by using numerical integration techniques and a better iterative method which leads to faster convergence. Virdi's modification provides an advantage when analysing members with section consisting of different materials and arbitrary boundaries. The method is based on the determination of the actual deflected shape of the beam-column and hence gives an almost exact solution

to the problem. The above method has been verified extensively for steel, reinforced, and composite columns [25,26,27]

The finite element method could also be used to perform linear and non-linear analyses of reinforced concrete beam-column. This is discussed in some detail under the literature review on frame analysis.

## **2.4 PREVIOUS WORK ON FRAME ANALYSIS**

### **GENERAL**

Cast-in-situ reinforced concrete frames are an example of rigid frame construction where the beam-column connections have sufficient rigidity to maintain the original angle between members at the junction. Precast concrete frames are usually considered as simple frames in current design practice assuming that the beam-column connections have little moment resistance and are free to rotate. The semi-rigid frames are those where the beam-to-column connections have finite moment capacity ranging between the capacity of monolithic connection at one extreme and a pin connection at the other.

The design specification for reinforced concrete frames as specified in BS8110 [28] suggests that non-sway frames can be divided into sub-frames in order to calculate the member forces due to vertical load. A moment distribution method is then applied to the subframe to calculate the member forces. The lateral loads on non-sway frame are assumed to be taken by stiffer components like lift walls within the structure.

In sway frames the member forces are calculated by combining the forces obtained from non-sway analysis and the forces obtained from lateral loads. The cantilever method or portal method [29] is used to calculate the member forces due to lateral loads.

## **LINEAR ANALYSIS**

Moment distribution was first introduced by Hardy Cross [32,33]. The method is a mechanical process to calculate the member forces in an indeterminate structure. The stiffness and carry over factor of the member are calculated assuming an elastic behaviour of the material. Starting from the fixed end moments of the beam, the moments are progressively distributed at the joints in proportion to the stiffness of the members connected at each joint and carried over to the far end of the members. The distribution of moments is continued until the out of balance moment in each joint is zero. The subframes suggested in BS8110, could be analysed using the moment distribution method. This method is still considered by designers as a valuable tool for solving structural problems.

When considering sway frames, the Hardy Cross method requires additional analyses to be performed considering shear in each storey separately. Naylor [34] developed a faster converging method based on the Hardy Cross method, to analyse single-bay multistorey frames with sway.

The slope deflection method to analyse multistorey frames was given by Chwalla and Jokisch [35]. The Moment distribution method is a procedure for solving the equations in the slope deflection method. The slope deflection method is used widely for linear analysis of frames. In the basic method the axial shortening effect is not considered in the analysis. The effect of axial

load on the flexural behaviour of the member is considered by using stability functions[36]. Ekhande et al[37] detail stability functions that could be included in three-dimensional analysis.

Frazer, Duncan, and Collier [38] proposed the concept of analysing a frame by combining the structural solution with matrix theory. Their method is basically a slope deflection method adding axial shortening and axial load effects to flexural behaviour. It's full development occurred after computer became widely available.

The P-delta effect, that is taking into account the eccentricity of axial load, was considered in elastic analysis of concrete frames by MacGregor et al [39].

As the structures become tall and slender non-linear and secondary effects become more important. Over the past 20-30 years, considerable research effort has been directed towards the nonlinear behaviour of frames.

## **BUCKLING ANALYSIS**

Bleich [11,30] first presented a systematic analysis of the stability of frames. He used the fundamental differential equation of the tangent modulus theory and defined the stability factors. Then equilibrium and stability were considered in the analysis of the frame. Bleich also developed buckling analysis of frames using energy methods[11,30]. By applying the principle of virtual work to the frame, a condition of equilibrium could be obtained for internal and external forces.

The influence of axial load effect on torsional stiffness was included in an elastic stability analysis of frames by Vaart [31].

## NON-LINEAR ANALYSIS

The plastic theory of analysing frames started after the Steel Structures Research Committee pointed out, in 1930[51,52], the uncertainties in designing the structure using the elastic method. The elastic method does not provide the designer with a knowledge of the exact behaviour of structures which approach their failure load. The theory assumes that whenever the fully plastic moment is attained at any section, a plastic hinge is formed which can undergo rotation of any magnitude as the moment at the hinge remains unchanged at plastic moment value. The plastic method of design was first used in 1949 [40,41]. Plastic theory was used to estimate the collapse load of the structure.

The plastic theory has the following limitations;

1. Loads are carried mainly by bending, and the effects of axial load and shear force on a member are assumed to be small.
2. The checks on deflections have to be made separately.

Majid [42] developed a theory to analyse the geometrically nonlinear, elasto-plastic behaviour of frames up to collapse. He traced the load deflection history of the frame by varying the applied load in small increment. When the bending moment was equal to plastic moment a hinge was introduced at that point and the procedure carried on until the frame had lost all its stiffness.

Design methods were formulated to include the additional moment created due to the eccentric action of vertical load due to side sway. A numerical

method presented by Gharpuray [43] calculates the elastic plastic response including the P-Delta effects and the reduction in plastic moment capacity due to the presence of axial load. The method gives reasonable agreement with the experimental results.

Turner et al [44] developed a numerical technique called the finite element method and Zienkiewicz [45] has contributed a considerable amount of work in further development of finite element analysis. The technique is widely used for elastic analysis. Structures of any shape can be analysed using this method. However, it can be an expensive method in terms of computer time, for day to day use in a design office.

A finite element method for elasto-plastic analysis was presented by Hsiao et al [46]. This method uses beam elements and solves the nonlinear equilibrium equations. This method is applicable for analysing frames with large displacement.

The finite element model for non-linear behaviour of concrete members was developed some 25 years ago by Ngo and Scordelis [47]. The basic difficulty in modeling concrete in the finite element method is that the method has to locate zones of cracking and then estimate the effect of cracking on the overall behaviour of the structure. Several current computer programs (e.g. LUSAS) can perform analysis of reinforced concrete frames with flexible joints. Non-linear material models for concrete in finite element packages usually have limitations. The stress strain relation for concrete in compression is assumed to be linear. The computer time required to perform the analysis also makes the program unusable in daily practice.

Gesund [21] proposed a method to analyse space frames based on the finite difference method. Using the stress-strain relation of the member material

and sectional dimension, moment thrust relations are obtained over a possible range of curvatures. The axial load and the trial moment at the ends of the members are calculated using elastic analysis. The members of the frame are divided in to a number of segments and the bending moment at each node is calculated from the end forces. By using these moments together with the help of a moment thrust curvature table, corresponding curvature at all the nodes can be found. The curvatures are then converted to displacements, subject to boundary conditions. This method assumes that the axial load remains constant during the calculation. The procedure is repeated until the deflections converge. The method of analysis is limited to regular frames.

A concrete portal frame was analysed by Chang [48] using moment-thrust-curvature relation. Good correlation was obtained when compared with experimental results.

Virdi [49] proposed a method to analyse space frames using the moment-thrust-curvature relation. The method was an adaptation of his theory for biaxially loaded columns. It takes into account the change in direction of member forces along the member stations. Equilibrium is considered at all the stations and at nodal points. For an assumed deflected shape internal forces at the stations are calculated and by using equilibrium equation corrections for the deflection can be calculated.

The moment-thrust-curvature method provides the flexibility necessary to introduce semi-rigid joints at the end of the members. An incremental stiffness matrix can be formed which incorporates the behaviour of the joints. This will be discussed in more detail in Chapter 3.

The effect of torsional moments on the flexural behaviour of steel members was considered in the analysis of columns [50]. In general, the effect of torsion on reinforced concrete members is considered separately from flexural effects.

## **2.5 PREVIOUS WORK ON EFFECT OF JOINT FLEXIBILITY**

### **GENERAL**

Steel frames are treated as rigid frames and the existence of connection is ignored in the overall analysis. Any connections are designed to have minimum rotation when subjected to bending moment.

The importance of considering the flexible connection into the behaviour of frames was first pointed out by the Steel Structures Research Committee in 1930 [51,52]. Considerable research has been carried out since then in incorporating the effect of flexible joints in the design of steel frames.

Reinforced concrete frames are also treated as rigid frames and the frames are cast monolithically to ensure rigid frame action. In the case of precast concrete frames the analysis is normally carried out on the assumption that the connection has no rigidity and only serves as a shear connector from member to member. The actual connections do have considerable strength in flexure [53] and if this is considered in the overall analysis of the frame it is anticipated that the precast frame would have the advantage of having better resistance against lateral load and also lesser mid span moments in the beam.

The requirements of steel frames and precast frames seem to have a common ground so that the knowledge in both the fields could be shared to advantage.

## **LINEAR ANALYSIS**

Early researchers on the linear analysis of frames with flexible connections are Wilson and Moore [56], Baker [57], and Rathburn [58]. The slope deflection method was modified by Baker to include the flexibility of the joint given that the behaviour of the joint was linear.

The moment distribution method of analysing frames was modified by Rathburn, by considering that the behaviour of a connection was linear.

The matrix method of analysis was modified by Monforton and Wu [59] to incorporate flexible joints. A linear behaviour of connections is assumed and a modified stiffness matrix incorporating connection stiffness is used in the analysis.

## **BUCKLING ANALYSIS**

Very little work has been carried out on the stability aspect of flexibly connected frames. The matrix stability analysis method was modified by Romstad and Subramanian [54] by adding a correction factor for coefficients of end rotations. The analysis was based on an elastic stiffness matrix. The above method can be used to calculate the buckling load of flexibly connected frames. A similar stiffness matrix method was proposed by Yu and Shanmugan [55] to include the  $P-\Delta$  effects and also the effect of axial load on flexural stiffness in analysing flexibly connected frames.

## NON-LINEAR ANALYSIS

Two types of non-linearities are discussed under this heading. One is the non-linear behaviour of connections and the other is the non-linear stress-strain behaviour of the material.

The non-linear behaviour of connections was first considered by Batho [60]. He developed a method called the Beam Line method to calculate the moment distribution in a member connected by flexible connections. The member is considered as behaving elastically and the connections as behaving non-linearly.

A matrix stiffness method incorporating the axial force bending moment interaction was proposed by Chen and Lui [61]. The tangent stiffness matrix of the beam column was formed for an assumed deflected shape and modified for the connection behaviour by assuming an exponential function for the moment rotation behaviour of the connection. The procedure was continued by calculating the correction factor for the assumed deflection and was repeated until convergence for deflection is achieved. The stress strain behaviour of the beam-column itself was considered linear.

One method which considers the non-linear behaviour of the frame with flexible connections is the plastic hinge method suggested by Melchers and Kaur [62]. It is similar to the collapse mechanism discussed in the analysis of frames. Hinges forming at the connections are based on the moment rotation characteristic of the connections and are included in the analysis.

A finite element method of analysis was developed by Hsieh and Deierlein [ 63] to analyse steel space frames with flexible connections. The biaxial behaviour of connections is considered in the analysis.

## **2.6 CONCLUSION**

Since faster computers with more memory are becoming available for an affordable price in design offices, it is considered that a numerical method that could perform non-linear analysis of precast concrete space frame with flexible joint would be an asset to the designer.

A finite element method of analysis, however, is anticipated to be time consuming in terms of preparing the data and computing. As an alternative, the moment-thrust-curvature method of analysing beam-columns was seen as a potentially rapid approach for predicting a solution closer to the exact behaviour of frames. This is developed fully in the next chapter.

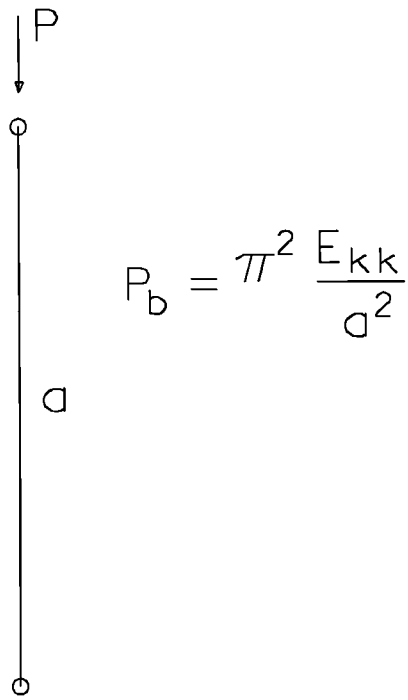


**FIG 2.1 EULER BUCKLING LOAD**

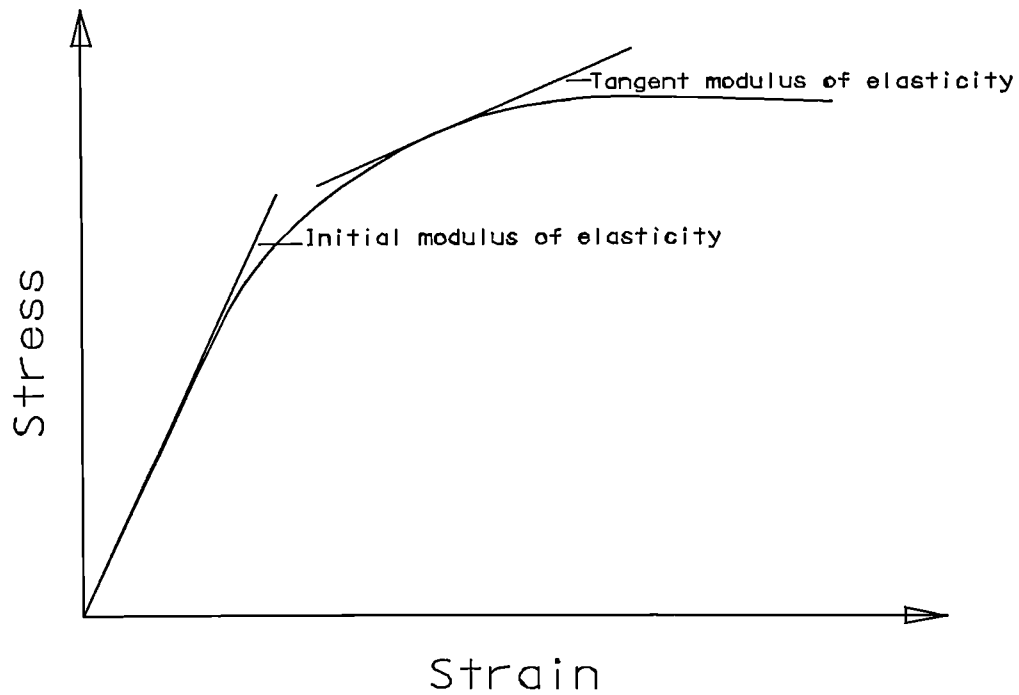


**FIG 2.2 MODULUS OF ELASTICITY**

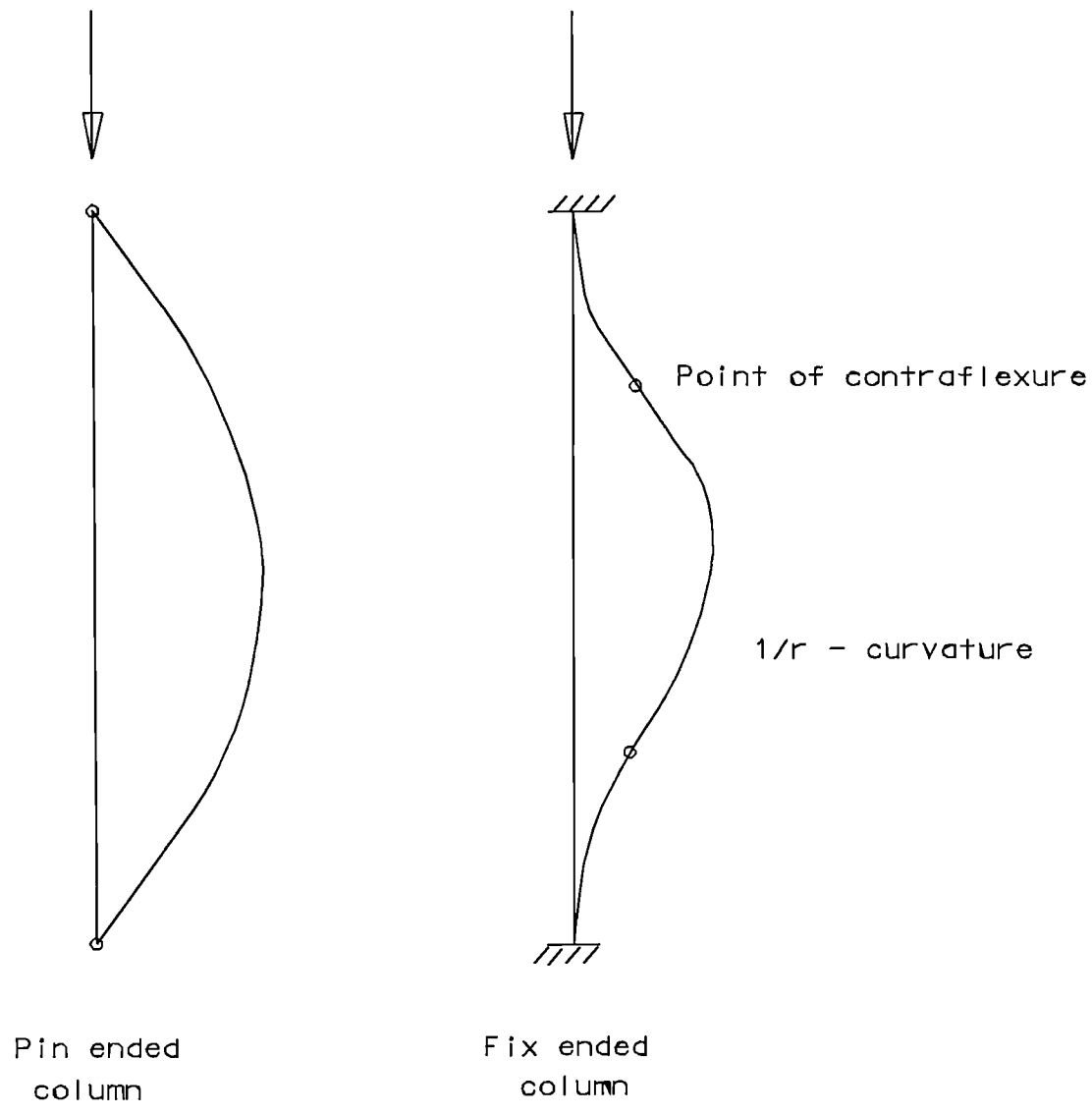


**FIG 2.3 BUCKLING OF COLUMN & BOUNDARY CONDITIONS**

## CHAPTER 3.

### NUMERICAL ANALYSIS OF PRECAST CONCRETE FRAMES

#### 3.1 INTRODUCTION

It is customary to study the nonlinear behaviour of structural frames by following their load-deflection response. Frames generally exhibit reduction in stiffness with increase in external loading. The ultimate load is determined when the structure stiffness reduces to zero.

The overall nonlinear behaviour of a structure can be attributed to the following two parameters.

1. Actual nonlinear stress-strain behaviour of the material.
2. Geometrical nonlinearity, associated with the need to satisfy equilibrium in the deflected state of the structure or its members.

This chapter describes a new numerical method of analysis of precast concrete frames with semi-rigid joints. The procedure is based on the calculation of the equilibrium deflected shape of the frame and its members for increasing levels of applied external loading. The procedure incorporates both material and geometrical nonlinearities. Nonlinear behaviour of semi-rigid joints is taken into account.

### **3.2 ASSUMPTIONS MADE IN THE NUMERICAL MODEL**

The following assumptions are made for formulating the numerical model to analyse the precast concrete frames with flexible joints.

1. Influence of slab and cladding diaphragm action on beams and columns, and torsional moment on end beams, are ignored and all the loads such as dead load, live load and wind load are transferred to beams and columns.
2. Only the skeletal frame is considered in the analysis.
3. Plane section of a member remains plane after deformation.
4. Members behave linearly in torsion
5. Torsional or shear forces do not affect the calculation of axial load and moment using moment-thrust-curvature relations of a section.

### **3.3 MODELLING OF FRAMES**

Precast concrete frames may be viewed as an assembly of members forming a structure skeleton. A general member in the structure can be represented by a beam-column of finite length, connected on either side through flexible joints. A flexible joint is an element with zero length but has defined rotation for a given moment. Monolithic joints may be assumed to be flexible joints with zero rotation for any given moment. In the case of a pin connection, the joint has zero moment of resistance for any joint rotation.

### **3.4 CONDITION OF EQUILIBRIUM AND COMPATIBILITY**

For a frame at its equilibrium deflected shape the nodes in the frame have specific rotations. A typical beam-column also has an equilibrium deflected shape. There exists a set of end forces and end deformations relating to this

beam-column deflected shape. A flexible joint transmits the forces from one end to the other end without any change in magnitude. The member end deformation is thus equal to the nodal deformation. The difference in member end rotation and beam-column end rotation is due to the rotation in the joint. For the equilibrium deflected shape of a frame at a given load level, the following basic conditions need to be satisfied.

1. Beam-column is in equilibrium with end forces.
2. Joint moments and rotations are in accordance with joint characteristic.
3. Member end forces at a node are in equilibrium with external nodal forces.
4. Compatibility of member end deformation at nodal points must be satisfied.

### **3.5 OUTLINE OF THE METHOD OF ANALYSIS**

It may be helpful to state the overall scheme of computations.

1. Consider a frame with assumed or previously calculated nodal deformations.
2. Nodal deformations in global coordinates are converted to member end deformations by using a transformation matrix.
3. Member end forces required to hold the member in equilibrium deflected shape, retaining the end deformation obtained in the above step, are calculated.
4. Member end forces are then transferred to global axes and assembled at the nodes. These forces are then checked for equilibrium with external forces.
5. If member end forces are not in equilibrium with the external forces, an iterative technique is used to calculate the corrections to the nodal deformations.
6. Steps 1-5 are repeated until convergence in global deformations is obtained.

These steps are also shown in the flow chart of Fig. 3.6.

### 3.6 DEVELOPMENT OF THE NUMERICAL MODEL

#### 3.6.1 NODAL AND MEMBER DEFORMATIONS

A typical member A-B in a space frame is shown in Fig. 3.1. A global coordinate system is used to define the nodal points on the frame. Each member has its own local coordinate system to represent member forces. The member A-B has global node  $i$  at end A and global node  $j$  at end B. The deflections of the global node  $i$  and  $j$  at the two ends of the member are expressed in terms of its components.

$$\Delta_i = \begin{bmatrix} \delta_{1i} \\ \delta_{2i} \\ \delta_{3i} \end{bmatrix} \quad \Delta_j = \begin{bmatrix} \delta_{1j} \\ \delta_{2j} \\ \delta_{3j} \end{bmatrix} \quad 3.1$$

Similarly, the rotation of the global nodes  $i$  and  $j$  are

$$\theta_i = \begin{bmatrix} \theta_{1i} \\ \theta_{2i} \\ \theta_{3i} \end{bmatrix} \quad \theta_j = \begin{bmatrix} \theta_{1j} \\ \theta_{2j} \\ \theta_{3j} \end{bmatrix} \quad 3.2$$

These deflections and rotations are transferred to member axes by the following transformation

$$\{\delta\} = [T]\{\Delta\} \quad 3.3$$

where  $\{\delta\}$  is the vector of member deformations at end A and end B with respect to member axes.

In expanded form, the above equation may be written as:

$$\begin{bmatrix} \delta_{zA} \\ \delta_{xA} \\ \delta_{yA} \\ \theta_{zA} \\ \theta_{xA} \\ \theta_{yA} \\ \delta_{zB} \\ \delta_{xB} \\ \delta_{yB} \\ \theta_{zB} \\ \theta_{xB} \\ \theta_{yB} \end{bmatrix} = \begin{bmatrix} l_1 & m_1 & n_1 & 0 & 0 & 0 & 0 & 0 & 0 & 0 & 0 & 0 \\ l_2 & m_2 & n_2 & 0 & 0 & 0 & 0 & 0 & 0 & 0 & 0 & 0 \\ l_3 & m_3 & n_3 & 0 & 0 & 0 & 0 & 0 & 0 & 0 & 0 & 0 \\ 0 & 0 & 0 & l_1 & m_1 & n_1 & 0 & 0 & 0 & 0 & 0 & 0 \\ 0 & 0 & 0 & l_2 & m_2 & n_2 & 0 & 0 & 0 & 0 & 0 & 0 \\ 0 & 0 & 0 & l_3 & m_3 & n_3 & 0 & 0 & 0 & 0 & 0 & 0 \\ 0 & 0 & 0 & 0 & 0 & 0 & l_1 & m_1 & n_1 & 0 & 0 & 0 \\ 0 & 0 & 0 & 0 & 0 & 0 & l_2 & m_2 & n_2 & 0 & 0 & 0 \\ 0 & 0 & 0 & 0 & 0 & 0 & l_3 & m_3 & n_3 & 0 & 0 & 0 \\ 0 & 0 & 0 & 0 & 0 & 0 & 0 & 0 & 0 & l_1 & m_1 & n_1 \\ 0 & 0 & 0 & 0 & 0 & 0 & 0 & 0 & 0 & l_2 & m_2 & n_2 \\ 0 & 0 & 0 & 0 & 0 & 0 & 0 & 0 & 0 & l_3 & m_3 & n_3 \end{bmatrix} \begin{bmatrix} \delta_{1i} \\ \delta_{2i} \\ \delta_{3i} \\ \theta_{1i} \\ \theta_{2i} \\ \theta_{3i} \\ \delta_{1j} \\ \delta_{2j} \\ \delta_{3j} \\ \theta_{1j} \\ \theta_{2j} \\ \theta_{3j} \end{bmatrix} \tag{3.4}$$

Where the  $l_k, m_k, n_k$  ( $k=1,3$ ) are the direction cosines of the member axes.

### 3.6.2 EQUILIBRIUM DEFLECTED SHAPE OF MEMBERS

#### TYPICAL MEMBER

Typical member from a frame is shown in the left hand side of Fig 3.2. All the members in a frame can be represented by a unified representation without losing its functionality by shifting member z-axis to pass through end B as shown in the right hand side of Fig 3.2. By developing a method to calculate an equilibrium deflected shape of this typical member all the members in a frame can be analysed for equilibrium deflected shape.

The stability behaviour of isolated restrained columns has previously been studied by Virdi [8]. The method, and the associated computer program *VARCOLS*, enables computation of the ultimate load of no-sway isolated columns. Columns of a variety of cross-sections, including material and geometrical nonlinearities, a variety of load paths, as well as variability of cross-section along the length of the column can be analysed. The method has been extensively verified by tests on composite and reinforced concrete columns[25-27] For member equilibrium, Virdi's method has been adopted with no major modifications.

Fig 3.3 shows a beam-column of length  $L$  with flexible joints at the ends. The axial load is  $P$ , the biaxial end moments at A are  $M_{xA}$  and  $M_{yA}$ , and the end moments at B are  $M_{xB}$  and  $M_{yB}$ . The end B is restrained in all six directions. The end A is restrained in all the directions except for the displacement along  $z$ -axis.

The stable equilibrium shape of a deflected beam-column is obtained by subdividing the column into a number of segments and establishing conditions of equilibrium at the stations where segments are connected. For given end forces, the moments produced at a station by the external forces need to be in equilibrium with the internal moments derived from the curvature.

The beam-column is subdivided into  $n$  segments. The stations at the end of the segments are numbered, starting from end A to end B, as 1 to  $(n+1)$ . The length of each segment  $h$  is equal to  $L/n$ . Let the lateral displacements of the centroid of the cross section at station  $i$  be  $u_i$  and  $v_i$  and the moments due to external forces be  $M_{exi}$  and  $M_{eyi}$ .

## MOMENT-THRUST-CURVATURE RELATION

For small deflections, the total curvature in the x and y planes,  $\phi_x$  and  $\phi_y$ , can be expressed in the form of second derivatives of deflections, which can be simplified using finite differences as follows.

$$\phi_{xi} = -\frac{\partial^2 v}{\partial z^2} = (v_{i-1} - 2v_i + v_{i+1}) \frac{1}{h^2} \quad 3.5$$

$$\phi_{yi} = -\frac{\partial^2 u}{\partial z^2} = (u_{i-1} - 2u_i + u_{i+1}) \frac{1}{h^2} \quad 3.6$$

Thus, the curvatures can be calculated from the assumed deflections. These curvatures are combined to obtain the principal curvature  $\phi$ , with the neutral axis lying at an angle  $\theta$  measured from x-axis anti-clockwise Fig 3.3.

$$\phi = \sqrt{(\phi_x^2 + \phi_y^2)} \quad 3.7$$

$$\theta = \frac{\pi}{2} + \tan^{-1}(\phi_y / \phi_x) \quad 3.8$$

The strain distribution across a section is a function of the corresponding curvature  $\phi$ , the direction of neutral axis  $\theta$ , and the location of neutral axis  $d_n$ .

$$\varepsilon = \varepsilon(x, y, \phi, \theta, d_n) \quad 3.9$$

From the assumption that plane sections remain plane upon flexure, it follows that

$$\varepsilon = \phi d \quad 3.10$$

Where  $d$  is the perpendicular distance of the point from the neutral axis.

The material stress-strain curves are represented by

$$\{\sigma\} = \{\sigma(\epsilon)\} \quad 3.11$$

Stress is interpolated for a given strain from the provided material stress strain data. The internal forces of the section may then be expressed as

$$P = \int_A \sigma \, dA \quad 3.12$$

$$M_x = \int_A \sigma \, x \, dA \quad 3.13$$

$$M_y = \int_A \sigma \, y \, dA \quad 3.14$$

This area integration over an arbitrary cross section with nonlinear stress distribution is very complex. The above calculation is simplified by discretising the section into a number of quadrilaterals. Using transformation of natural coordinates and Gauss quadrature, the area integral can be replaced by weighted double summation [1]. By systematic correction, it is possible to calculate the position of the neutral axis for which the internal axial load equals the external load. Internal moments are then calculated for this position of the neutral axis.

## **MOMENT ALONG THE MEMBER DUE TO EXTERNAL FORCES**

General equations for moments at a distance  $d$  from the end A can be written as follows. These expressions are based on uniformly distributed lateral load  $W$ . For other loads, similar expressions can be obtained.

$$M_{ex} = + P v_A - P v_d + M_{xA} - F_{yA} d - W_y \frac{d^2}{2} \quad 3.15$$

$$M_{ey} = - P u_A + P u_d + M_{yA} + F_{xA} d + W_x \frac{d^2}{2} \quad 3.16$$

$$\text{where } F_{xA} L = - M_{yA} - M_{yB} + P u_A - W_x \frac{L^2}{2} \quad 3.17$$

$$F_{yA} L = M_{xA} + M_{xB} + P v_A - W_y \frac{L^2}{2} \quad 3.18$$

and P represents  $F_{zA}$ .

by substituting for  $F_{xA}$  and  $F_{yA}$  in equation 3.15 and 3.16

$$M_{ex} = P v_A - P v_d + M_{xA} - \left( M_{xA} + M_{xB} + P v_A - W_y \frac{L^2}{2} \right) \frac{d}{L} - W_y \frac{d^2}{2} \quad 3.19$$

$$M_{ey} = - P u_A + P u_d + M_{yA} + \left( -M_{yA} - M_{yB} + P u_A - W_x \frac{L^2}{2} \right) \frac{d}{L} + W_x \frac{d^2}{2} \quad 3.20$$

The moments due to external moments at station i can be written by substituting  $d = L \cdot (i-1)/n$ . The simplified equations after substitution are as follows.

$$M_{exi} = P v_A - P v_i + \left( \frac{n-i+1}{n} \right) M_{xA} - \left( \frac{i-1}{n} \right) (M_{xB} + P v_A) + W_y \frac{(i-1)(n-i+1)}{2n^2} L^2 \quad 3.21$$

$$M_{eyi} = - P u_A + P u_i + \left( \frac{n-i+1}{n} \right) M_{yA} - \left( \frac{i-1}{n} \right) (M_{yB} - P u_A) - W_x \frac{(i-1)(n-i+1)}{2n^2} L^2 \quad 3.22$$

Where  $u_A$  and  $v_A$  are lateral deformations at end A in the x and y directions respectively, relative to end B as shown in Fig 3.3.

### END ROTATIONS AND END MOMENTS

The following finite difference form is used to calculate the end rotations of the beam-column.

$$\theta_{xA} = -(v_3 - 4v_2 + 3v_1) / 2h \quad \theta_{yA} = -(u_3 - 4u_2 + 3u_1) / 2h \quad 3.23$$

$$\theta_{yB} = -(v_{n-1} - 4v_n) / 2h \quad \theta_{xB} = -(u_{n-1} - 4u_n) / 2h \quad 3.24$$

The end rotations of the members are directly obtained from nodal deformations of the frame. The joint rotations are given by relative rotation between the beam-column and the corresponding member end. In the presence of flexible joints at the ends, the joint moments are related to joint rotation through the characteristic of the joint, Fig 3.5. As already mentioned, rigid joints can be analysed using very high values for joint stiffness. Similarly, pinned connections are assumed to have zero stiffness.

The following expressions may be written for the joint rotations and member end moments.

$$M_{xA} = M_{xA}(\theta_{xAr}) \quad M_{xB} = M_{xB}(\theta_{xBr}) \quad 3.25$$

$$M_{yA} = M_{yA}(\theta_{yAr}) \quad M_{yB} = M_{yB}(\theta_{yBr}) \quad 3.26$$

Where  $\theta_r$ 's are joint rotations as shown in Fig. 3.4

After the calculation of internal and external moments, an iterative technique is required to obtain a solution for the beam-column deflections.

### ITERATION SCHEME

A simple iterative scheme to arrive at equilibrium deflected shape is explained below. Equations 3.21 and 3.22 can be rewritten as follows.

$$\begin{aligned}
 Pv_i = & Pv_A - M_{exi} + \left(\frac{n-i+1}{n}\right)M_{xA} - \left(\frac{i-1}{n}\right)(M_{xB} + Pv_A) \\
 & + W_y \frac{(i-1)(n-i+1)}{2n^2} L^2
 \end{aligned} \tag{3.27}$$

$$\begin{aligned}
 Pu_i = & Pu_A + M_{exi} - \left(\frac{n-i+1}{n}\right)M_{yA} + \left(\frac{i-1}{n}\right)(M_{yB} - Pu_A) \\
 & + W_x \frac{(i-1)(n-i+1)}{2n^2} L^2
 \end{aligned} \tag{3.28}$$

For equilibrium deflected shape, the external moment must be equal to the internal moment calculated from curvature. Let the deflection be  $\{u, v\}^k$  and the next correct deflection be  $\{u, v\}^{k+1}$ . It can be shown that:

$$\begin{aligned}
 Pv_i^{k+1} = & -M_{xi}^k + Pv_A + \left(\frac{n-i+1}{n}\right)M_{xA}^k - \left(\frac{i-1}{n}\right)(M_{xB}^k + Pv_A) \\
 & + W_y \frac{(i-1)(n-i+1)}{2n^2} L^2
 \end{aligned} \tag{3.29}$$

$$\begin{aligned}
 Pu_i^{k+1} = & M_{xi}^k + Pu_A - \left(\frac{n-i+1}{n}\right)M_{yA}^k + \left(\frac{i-1}{n}\right)(M_{yB}^k - Pu_A) \\
 & + W_x \frac{(i-1)(n-i+1)}{2n^2} L^2
 \end{aligned} \tag{3.30}$$

Where  $M_{xi}^k$  and  $M_{yi}^k$  are the internal moments at deflection  $\{u,v\}^k$

The equilibrium-deflected-shape can be calculated from the above four equations by modifying the deflections iteratively and also modifying the end moments if they are functions of end rotations.

By going through the above cycle, starting from an assumed deflected shape, convergence will be reached if an equilibrium shape exists for the given load condition.

## SECOND ORDER ITERATION

By using a Newton-Raphson iterative technique, the convergence can be accelerated considerably. The Newton-Raphson method suggests that if  $M(w)=0$  is a function of  $w$ , a better approximation  $w_{k+1}$  for an assumed value  $w_k$  can be given by.

$$w_{k+1} = w_k - [M'(w_k)]^{-1}M(w_k) \quad 3.31$$

Where  $M'(w_k)$  is the matrix of derivatives of  $M(w_k)$  with respect to  $w$  at  $w_k$ . by replacing the function  $M$  by  $\{M_{in}(w)-M_e(w)\}$  and rearranging

$$[M'_{in}-M'_e]\{w_{k+1}-w_k\} = -\{M_{in}+M_e\} \quad 3.32$$

$\{M_{in}-M_e\}$  is the vector of difference of internal moment to external moment and has  $(2n+2)$  elements, where  $n$  is the number of subdivisions in the

member.  $\{w_{k+1}-w_k\}$  is the vector of correction to the deflections and also has  $(2n+2)$  elements.

It follows that the  $[M'_{in}-M'_e]$  term is a matrix of  $(2n+2) \times (2n+2)$  elements. This matrix can be considered as a difference of matrices,  $[M'_{in}]$  based on internal moments and  $[M'_e]$  based on external moments, each of  $(2n+2) \times (2n+2)$  elements. The method of forming these matrices is examined next.

### Formation of matrix $[M'_{in}]$

Internal moments  $M_{xi}$  and  $M_{yi}$  are functions of curvatures in the x and y axes at station i. Therefore they may be regarded as functions of  $u_{i+1}$ ,  $u_i$ ,  $u_{i-1}$ ,  $v_{i+1}$ ,  $v_i$  and  $v_{i-1}$ . The non zero derivatives of internal moment at station i with respect to deflections can be written as follows.

$$\begin{array}{cccccc} \frac{\partial M_{xi}}{\partial u_{i-1}}, & \frac{\partial M_{xi}}{\partial u_i}, & \frac{\partial M_{xi}}{\partial u_{i+1}}, & \frac{\partial M_{xi}}{\partial v_{i-1}}, & \frac{\partial M_{xi}}{\partial v_i}, & \frac{\partial M_{xi}}{\partial v_{i+1}} \\ \frac{\partial M_{yi}}{\partial u_{i-1}}, & \frac{\partial M_{yi}}{\partial u_i}, & \frac{\partial M_{yi}}{\partial u_{i+1}}, & \frac{\partial M_{yi}}{\partial v_{i-1}}, & \frac{\partial M_{yi}}{\partial v_i}, & \frac{\partial M_{yi}}{\partial v_{i+1}} \end{array}$$

where  $i=2,n$

For a small increase  $\Delta$  in displacement  $u_i$  at station i new curvature is calculated. As described before new internal moment  $M_{xi}$  and  $M_{yi}$  are calculated using moment-thrust-curvature relations. Difference in moment divided by the increase in displacement gives the derivative of moment with

respect to  $u$  at station  $i$ . Similarly by repeating the analysis for displacement  $v$  derivatives of moments with respect to  $v$  at station  $i$  can be obtained.

Using Equations 3.5 and 3.6 the following relationships are obtained.

$$\frac{\partial M_{xi}}{\partial u_{i-1}} = \frac{\partial M_{xi}}{\partial u_{i+1}} = -2 \frac{\partial M_{xi}}{\partial u_i} \qquad \frac{\partial M_{yi}}{\partial u_{i-1}} = \frac{\partial M_{yi}}{\partial u_{i+1}} = -2 \frac{\partial M_{yi}}{\partial u_i} \qquad 3.33$$

$$\frac{\partial M_{xi}}{\partial v_{i-1}} = \frac{\partial M_{xi}}{\partial v_{i+1}} = -2 \frac{\partial M_{xi}}{\partial v_i} \qquad \frac{\partial M_{yi}}{\partial v_{i-1}} = \frac{\partial M_{yi}}{\partial v_{i+1}} = -2 \frac{\partial M_{yi}}{\partial v_i} \qquad 3.34$$

The above relationships are used to calculate the rest of the nonzero derivatives in matrix  $[M'_{in}]$ .

### Formation of Matrix $[M'_{e}]$

The moment due to external loading consists of two components, one due to axial load and the other due to external moments.

In the equilibrium state, the external moments along the length of the member depend upon the end rotations, which in turn are functions of the deflections of points used to calculate the end rotations. Therefore, the end moments may be regarded as functions of  $u_A, u_2, u_3, v_A, v_2, v_3, u_{n-1}, u_n, v_{n-1}, v_n$ . If the external moment at end A in the y-axis is  $M^0_{yA}$ , due to an increase of  $\Delta$  in  $u_3$  the contribution of external moment at station  $i$  is given by

$$\frac{\partial M_{exi}}{\partial u_3} = -\left(\frac{n-i+1}{n}\right) \left(\frac{M^0_{yA} - M_{yA}}{\Delta}\right) \qquad 3.35$$

similarly for a  $\Delta$  increase in  $u_{n-1}$

$$\frac{\partial M_{exi}}{\partial u_{n-1}} = \left(\frac{i-1}{n}\right) \left(\frac{M_{yB}^0 - M_{yB}}{\Delta}\right) \quad 3.36$$

for a  $\Delta$  increase in  $v_3$

$$\frac{\partial M_{eyi}}{\partial v_3} = \left(\frac{n-i+1}{n}\right) \left(\frac{M_{xA}^0 - M_{xA}}{\Delta}\right) \quad 3.37$$

for  $\Delta$  increase in  $v_{n-1}$

$$\frac{\partial M_{eyi}}{\partial v_{n-1}} = \left(\frac{i-1}{n}\right) \left(\frac{M_{xB}^0 - M_{xB}}{\Delta}\right) \quad 3.38$$

By using equations 3.23 and 3.24 the following expressions are obtained.

$$\frac{\partial M_{exi}}{\partial u_2} = -\left(\frac{1}{4}\right) \frac{\partial M_{exi}}{\partial u_3} \quad \frac{\partial M_{eyi}}{\partial v_2} = -\left(\frac{1}{4}\right) \frac{\partial M_{eyi}}{\partial v_3} \quad 3.39$$

$$\frac{\partial M_{exi}}{\partial u_n} = -\left(\frac{1}{4}\right) \frac{\partial M_{exi}}{\partial u_{n-1}} \quad \frac{\partial M_{eyi}}{\partial v_n} = -\left(\frac{1}{4}\right) \frac{\partial M_{eyi}}{\partial v_{n-1}} \quad 3.40$$

The moment along the member due to axial force is a linear function of deflection. Hence the derivative of this moments with respect to deflections may be expressed as a diagonal matrix with axial load as the uniform diagonal member.

The above derivatives together with the uniform diagonal matrix with axial load are combined to form the matrix  $[M'_e]$ .

### **Solution technique for member equilibrium deflected shape**

A systematic procedure for solving the nonlinear equations 3.31 is outlined below.

1. Assume a deflected shape.
2. Calculate curvatures.
3. Calculate internal moments. Using a small increment calculate the matrix  $[M']$ .
4. Calculate end rotation of the beam-column.
5. Calculate joint rotation and then obtain joint moment.
6. Calculate moments along the stations due to external forces.
7. Solve the simultaneous equation 3.32
8. If the correction for deflections are not small enough, steps 1 to 8 are repeated until convergence in deflections is obtained.

This step by step procedure gives member equilibrium deflected shape for a given end rotations and member loadings. It is important to notice that the axial load in the member is not altered in the above procedure. As mentioned earlier end A is free to move in z-direction. The axial deformation at the equilibrium deflected shape can be obtained by summing up the axial shortening of the individual segments between two stations. Axial shortening of a segment can be calculated by multiplying the average strain along its geometrical centre line by the original length of the segment.

For the purpose of the frame analysis the deflected length of the member must be equal to the distance between the corresponding nodal points in the frame. This necessitates another iteration that systematically alters the axial load until the above condition is satisfied.

### 3.6.3 EQUILIBRIUM DEFLECTED SHAPE OF FRAMES

#### NODAL EQUILIBRIUM

The end forces obtained from member equilibrium deflected shape calculation is now checked for equilibrium at nodal points. If the two are not in equilibrium then corrections to nodal deformations must be calculated.

Consider a beam-column as shown in Fig.3.2. The member end forces  $\{p\}$  are functions of member deformation  $\{\delta\}$ .

$$\{p\} = \{p(\delta)\} \quad 3.41$$

These end forces are transferred to the global axis system by multiplying by a transformation matrix. The member forces in global coordinates become:

$$\{P\} = \{p(\Delta)\} \quad 3.42$$

where  $\{\Delta\} = [T]^{-1} \{d\}$  are the global deformations. In the context of iterative procedures, if the external nodal forces were represented by  $\{F\}$ , and unbalanced nodal forces by  $\{R\}$  the global unbalanced nodal forces may be written as:

$$\{P\} - \{F\} = \{R(\Delta_r)\} \quad 3.43$$

where  $\{\Delta_r\}$  are the global deformations at the  $r$ th iteration. The aim of the iteration is to reduce all the unbalanced forces to an acceptably small value.

The generalised Newton-Raphson method for iterative solution suggests that an improved set of deformations  $\{\Delta_{r+1}\}$  is given by

$$\{\Delta_{r+1}-\Delta_r\} = -[R'(\Delta_r)]^{-1}\{R(\Delta_r)\} \quad 3.44$$

By substituting  $\{R\}$  in terms of  $\{P\}$  and  $\{F\}$

$$\{\Delta_{r+1}-\Delta_r\} = -[P_r' - F']^{-1}\{\{P_r\} - \{F\}\} \quad 3.45$$

Since applied  $\{F\}$  are constant for a load case,  $\{F'\} = 0$ . Thus,

$$\{\Delta_{r+1}-\Delta_r\} = -[P_r']^{-1}\{\{P_r\} - \{F\}\} \quad 3.46$$

By multiplying both side by  $[P_r']$

$$[P_r']\{\Delta_{r+1}-\Delta_r\} = -\{P_r\} + \{F\} \quad 3.47$$

where  $[P_r']$  is an assembly of member incremental matrices  $[K]$ .

The member incremental stiffness matrix can be represented by

$$K_{ij} = \frac{dP(\delta_i)}{d\delta_j} \quad 3.48$$

where  $i, j = 1, 12$

## INCREMENTAL STIFFNESS MATRIX

In the general case, the incremental stiffness matrix would be a 12x12 full matrix. By the assumption mentioned earlier that the torsion is independent of all the other deformations, the columns and rows representing the torsional force and torsional rotation in the above matrix are made zero except for the derivative of torsional force with twisting rotation, which represents the torsional rigidity.

$$[K] = \begin{bmatrix} \frac{\partial F_{zA}}{\partial \delta_{zA}} & \frac{\partial F_{zA}}{\partial \delta_{xA}} & \frac{\partial F_{zA}}{\partial \delta_{yA}} & 0 & \frac{\partial F_{zA}}{\partial \theta_{xA}} & \frac{\partial F_{zA}}{\partial \theta_{yA}} & \frac{\partial F_{zA}}{\partial \delta_{zB}} & \frac{\partial F_{zA}}{\partial \delta_{xB}} & \frac{\partial F_{zA}}{\partial \delta_{yB}} & 0 & \frac{\partial F_{zA}}{\partial \theta_{xB}} & \frac{\partial F_{zA}}{\partial \theta_{yB}} \\ \frac{\partial F_{xA}}{\partial \delta_{zA}} & \frac{\partial F_{xA}}{\partial \delta_{xA}} & \frac{\partial F_{xA}}{\partial \delta_{yA}} & 0 & \frac{\partial F_{xA}}{\partial \theta_{xA}} & \frac{\partial F_{xA}}{\partial \theta_{yA}} & \frac{\partial F_{xA}}{\partial \delta_{zB}} & \frac{\partial F_{xA}}{\partial \delta_{xB}} & \frac{\partial F_{xA}}{\partial \delta_{yB}} & 0 & \frac{\partial F_{xA}}{\partial \theta_{xB}} & \frac{\partial F_{xA}}{\partial \theta_{yB}} \\ \frac{\partial F_{yA}}{\partial \delta_{zA}} & \frac{\partial F_{yA}}{\partial \delta_{xA}} & \frac{\partial F_{yA}}{\partial \delta_{yA}} & 0 & \frac{\partial F_{yA}}{\partial \theta_{xA}} & \frac{\partial F_{yA}}{\partial \theta_{yA}} & \frac{\partial F_{yA}}{\partial \delta_{zB}} & \frac{\partial F_{yA}}{\partial \delta_{xB}} & \frac{\partial F_{yA}}{\partial \delta_{yB}} & 0 & \frac{\partial F_{yA}}{\partial \theta_{xB}} & \frac{\partial F_{yA}}{\partial \theta_{yB}} \\ 0 & 0 & 0 & \frac{\partial M_{zA}}{\partial \theta_{zA}} & 0 & 0 & 0 & 0 & 0 & \frac{\partial M_{zA}}{\partial \theta_{zB}} & 0 & 0 \\ \frac{\partial M_{xA}}{\partial \delta_{zA}} & \frac{\partial M_{xA}}{\partial \delta_{xA}} & \frac{\partial M_{xA}}{\partial \delta_{yA}} & 0 & \frac{\partial M_{xA}}{\partial \theta_{xA}} & \frac{\partial M_{xA}}{\partial \theta_{yA}} & \frac{\partial M_{xA}}{\partial \delta_{zB}} & \frac{\partial M_{xA}}{\partial \delta_{xB}} & \frac{\partial M_{xA}}{\partial \delta_{yB}} & 0 & \frac{\partial M_{xA}}{\partial \theta_{xB}} & \frac{\partial M_{xA}}{\partial \theta_{yB}} \\ \frac{\partial M_{yA}}{\partial \delta_{zA}} & \frac{\partial M_{yA}}{\partial \delta_{xA}} & \frac{\partial M_{yA}}{\partial \delta_{yA}} & 0 & \frac{\partial M_{yA}}{\partial \theta_{xA}} & \frac{\partial M_{yA}}{\partial \theta_{yA}} & \frac{\partial M_{yA}}{\partial \delta_{zB}} & \frac{\partial M_{yA}}{\partial \delta_{xB}} & \frac{\partial M_{yA}}{\partial \delta_{yB}} & 0 & \frac{\partial M_{yA}}{\partial \theta_{xB}} & \frac{\partial M_{yA}}{\partial \theta_{yB}} \\ \frac{\partial F_{zB}}{\partial \delta_{zA}} & \frac{\partial F_{zB}}{\partial \delta_{xA}} & \frac{\partial F_{zB}}{\partial \delta_{yA}} & 0 & \frac{\partial F_{zB}}{\partial \theta_{xA}} & \frac{\partial F_{zB}}{\partial \theta_{yA}} & \frac{\partial F_{zB}}{\partial \delta_{zB}} & \frac{\partial F_{zB}}{\partial \delta_{xB}} & \frac{\partial F_{zB}}{\partial \delta_{yB}} & 0 & \frac{\partial F_{zB}}{\partial \theta_{xB}} & \frac{\partial F_{zB}}{\partial \theta_{yB}} \\ \frac{\partial F_{xB}}{\partial \delta_{zA}} & \frac{\partial F_{xB}}{\partial \delta_{xA}} & \frac{\partial F_{xB}}{\partial \delta_{yA}} & 0 & \frac{\partial F_{xB}}{\partial \theta_{xA}} & \frac{\partial F_{xB}}{\partial \theta_{yA}} & \frac{\partial F_{xB}}{\partial \delta_{zB}} & \frac{\partial F_{xB}}{\partial \delta_{xB}} & \frac{\partial F_{xB}}{\partial \delta_{yB}} & 0 & \frac{\partial F_{xB}}{\partial \theta_{xB}} & \frac{\partial F_{xB}}{\partial \theta_{yB}} \\ \frac{\partial F_{yB}}{\partial \delta_{zA}} & \frac{\partial F_{yB}}{\partial \delta_{xA}} & \frac{\partial F_{yB}}{\partial \delta_{yA}} & 0 & \frac{\partial F_{yB}}{\partial \theta_{xA}} & \frac{\partial F_{yB}}{\partial \theta_{yA}} & \frac{\partial F_{yB}}{\partial \delta_{zB}} & \frac{\partial F_{yB}}{\partial \delta_{xB}} & \frac{\partial F_{yB}}{\partial \delta_{yB}} & 0 & \frac{\partial F_{yB}}{\partial \theta_{xB}} & \frac{\partial F_{yB}}{\partial \theta_{yB}} \\ 0 & 0 & 0 & \frac{\partial M_{zB}}{\partial \theta_{zA}} & 0 & 0 & 0 & 0 & 0 & \frac{\partial M_{zB}}{\partial \theta_{zB}} & 0 & 0 \\ \frac{\partial M_{xB}}{\partial \delta_{zA}} & \frac{\partial M_{xB}}{\partial \delta_{xA}} & \frac{\partial M_{xB}}{\partial \delta_{yA}} & 0 & \frac{\partial M_{xB}}{\partial \theta_{xA}} & \frac{\partial M_{xB}}{\partial \theta_{yA}} & \frac{\partial M_{xB}}{\partial \delta_{zB}} & \frac{\partial M_{xB}}{\partial \delta_{xB}} & \frac{\partial M_{xB}}{\partial \delta_{yB}} & 0 & \frac{\partial M_{xB}}{\partial \theta_{xB}} & \frac{\partial M_{xB}}{\partial \theta_{yB}} \\ \frac{\partial M_{yB}}{\partial \delta_{zA}} & \frac{\partial M_{yB}}{\partial \delta_{xA}} & \frac{\partial M_{yB}}{\partial \delta_{yA}} & 0 & \frac{\partial M_{yB}}{\partial \theta_{xA}} & \frac{\partial M_{yB}}{\partial \theta_{yA}} & \frac{\partial M_{yB}}{\partial \delta_{zB}} & \frac{\partial M_{yB}}{\partial \delta_{xB}} & \frac{\partial M_{yB}}{\partial \delta_{yB}} & 0 & \frac{\partial M_{yB}}{\partial \theta_{xB}} & \frac{\partial M_{yB}}{\partial \theta_{yB}} \end{bmatrix}$$

The procedure for calculating the terms in the incremental stiffness matrix is now explained using a step by step approach.

### **STEP 1**

The member equilibrium position is calculated by keeping the end displacements  $\theta_{xA}$ ,  $\theta_{yA}$ ,  $\theta_{xB}$ ,  $\theta_{yB}$  and  $(\delta_{zA} - \delta_{zB})$  constant as described in section 3.6.2. End moments  $M_{xA}$ ,  $M_{yA}$ ,  $M_{xB}$  and  $M_{yB}$  and end forces  $F_{zA}$ ,  $F_{xA}$ ,  $F_{yA}$ ,  $F_{xB}$ , and  $F_{yB}$  are obtained from the above calculation.

### **STEP 2**

The member equilibrium position is calculated for an increment  $dF_{zA}$  to the existing axial load  $F_{zA}$ , while all the end rotations are kept constant. Axial deformation  $\delta_{zA}^{ii}$ , end moments  $M_{xA}^{ii}$ ,  $M_{yA}^{ii}$ ,  $M_{xB}^{ii}$  and  $M_{yB}^{ii}$  and end transverse forces  $F_{xA}^{ii}$ ,  $F_{yA}^{ii}$ ,  $F_{xB}^{ii}$  and  $F_{yB}^{ii}$  are obtained from the above calculation. The following components of the matrix are then formed using the above information.

$$d\delta_{zA} = (\delta_{zA}^{ii} - \delta_{zA} + \delta_{zB})$$

$$k(1,1)=-k(1,7)=-k(7,1)=k(7,7)=dF_{zA}/d\delta_{zA}$$

$$k(2,1)=-k(2,7)=(F_{xA}^{ii}-F_{xA})/d\delta_{zA}$$

$$k(3,1)=-k(3,7)=(F_{yA}^{ii}-F_{yA})/d\delta_{zA}$$

$$k(8,1)=-k(8,7)=(F_{xB}^{ii}-F_{xB})/d\delta_{zA}$$

$$k(9,1)=-k(9,7)=(F_{yB}^{ii}-F_{yB})/d\delta_{zA}$$

$$k(5,1)=-k(5,7)=(M_{xA}^{ii}-M_{xA})/d\delta_{zA}$$

$$k(6,1)=-k(6,7)=(M_{yA}^{ii}-M_{yA})/d\delta_{zA}$$

$$k(11,1)=-k(11,7)=(M_{xB}^{ii}-M_{xB})/d\delta_{zA}$$

$$k(12,1)=-k(12,7)=(M_{yB}^{ii}-M_{yB})/d\delta_{zA}$$

### STEP 3

The member equilibrium position is calculated for a displacement of  $d\delta_{xA}$  at the end A along x axis while all the end rotations are kept constant.

Axial deformation  $\delta^{iii}_{zA}$ , end moments  $M^{iii}_{xA}$ ,  $M^{iii}_{yA}$ ,  $M^{iii}_{xB}$  and  $M^{iii}_{yB}$  and end transverse forces  $F^{iii}_{xA}$ ,  $F^{iii}_{yA}$ ,  $F^{iii}_{xB}$  and  $F^{iii}_{yB}$  are obtained from the above calculation. The following components of the matrix can then be formed using the above information.

$$d\delta_{zA} = (\delta^{iii}_{zA} - \delta_{zA} + \delta_{zB})$$

$$k(1,2) = -k(7,2) = -k(1,8) = k(7,8) = -k(1,1) * d\delta_{zA} / d\delta_{xA}$$

$$k(2,2) = -k(2,8) = \{(F^{iii}_{xA} - F_{xA}) - k(2,1) * d\delta_{zA}\} / d\delta_{xA}$$

$$k(3,2) = -k(3,8) = \{(F^{iii}_{yA} - F_{yA}) - k(3,1) * d\delta_{zA}\} / d\delta_{xA}$$

$$k(8,2) = -k(8,8) = \{(F^{iii}_{xB} - F_{xB}) - k(8,1) * d\delta_{zA}\} / d\delta_{xA}$$

$$k(9,2) = -k(9,8) = \{(F^{iii}_{yB} - F_{yB}) - k(9,1) * d\delta_{zA}\} / d\delta_{xA}$$

$$k(5,2) = -k(5,8) = \{(M^{iii}_{xA} - M_{xA}) - k(5,1) * d\delta_{zA}\} / d\delta_{xA}$$

$$k(6,2) = -k(6,8) = \{(M^{iii}_{yA} - M_{yA}) - k(6,1) * d\delta_{zA}\} / d\delta_{xA}$$

$$k(11,2) = -k(11,8) = \{(M^{iii}_{xB} - M_{xB}) - k(11,1) * d\delta_{zA}\} / d\delta_{xA}$$

$$k(12,2) = -k(12,8) = \{(M^{iii}_{yB} - M_{yB}) - k(12,1) * d\delta_{zA}\} / d\delta_{xA}$$

### STEP 4

Similar to the procedure shown in step 3 the member equilibrium position is calculated for a displacement of  $d\delta_{yA}$  at the end A along y-axis while all the end rotations are kept constant.

Axial deformation, end moments, and end transverse forces are obtained from the above calculation. Using the above information column 3 and 9 of the element matrix can be formed following the same procedure as given in step 3.

### **STEP 5**

The member equilibrium position is calculated for an increment of  $d\theta_{xA}$  in rotation  $\theta_{xA}$  while all the other end rotations are kept constant.

Axial deformation  $\delta^V_{zA}$ , end moments  $M^V_{xA}$ ,  $M^V_{yA}$ ,  $M^V_{xB}$  and  $M^V_{yB}$  and end transverse forces  $F^V_{xA}$ ,  $F^V_{yA}$ ,  $F^V_{xB}$  and  $F^V_{yB}$  are obtained from the above calculation. The following components of the matrix may then be formed using the above information.

$$d\delta_{zA} = (\delta^V_{zA} - \delta_{zA} + \delta_{zB})$$

$$k(1,5) = -k(7,5) = -k(1,1) * d\delta_{zA} / d\theta_{xA}$$

$$k(2,5) = \{(F^V_{xA} - F_{xA}) - k(2,1) * d\delta_{zA}\} / d\theta_{xA}$$

$$k(3,5) = \{(F^V_{yA} - F_{yA}) - k(3,1) * d\delta_{zA}\} / d\theta_{xA}$$

$$k(8,5) = \{(F^V_{xB} - F_{xB}) - k(8,1) * d\delta_{zA}\} / d\theta_{xA}$$

$$k(9,5) = \{(F^V_{yB} - F_{yB}) - k(9,1) * d\delta_{zA}\} / d\theta_{xA}$$

$$k(5,5) = \{(M^V_{xA} - M_{xA}) - k(5,1) * d\delta_{zA}\} / d\theta_{xA}$$

$$k(6,5) = \{(M^V_{yA} - M_{yA}) - k(6,1) * d\delta_{zA}\} / d\theta_{xA}$$

$$k(11,5) = \{(M^V_{xB} - M_{xB}) - k(11,1) * d\delta_{zA}\} / d\theta_{xA}$$

$$k(12,5) = \{(M^V_{yB} - M_{yB}) - k(12,1) * d\delta_{zA}\} / d\theta_{xA}$$

### **STEPS 6, 7, 8**

The member equilibrium position is calculated for an increment of  $d\theta$  in rotation  $\theta_{yA}$ ,  $\theta_{xB}$ ,  $\theta_{yB}$  respectively while all the other end rotations are kept constant.

Axial deformation, end moments and end transverse forces are obtained from the above calculation. The columns 6, 11 and 12 of the matrix may then be formed following the same procedure as detailed in step 5.

The above step by step procedure enables the member stiffness matrix to be evaluated by a numerical procedure. Major advantages are that this procedure has no limitation on the constitutive relations of the materials or on the geometric shape and constitution of the cross-section.

### **SOLUTION TECHNIQUE**

The element incremental matrices and the end force matrices are transformed to the global axis system using standard transformation matrices. By considering the equilibrium at nodes, the following simultaneous equations are obtained:

$$-\{P_r\} + \{F\} = [K]\{d\Delta\}$$

The above simultaneous equations are solved for incremental nodal deformations, such that the frame deformations are modified. The above values are in turn used as the new nodal deformation in the procedure

described in section 3.5. The process is repeated until the displacements and rotations converge.

### **3.7 ULTIMATE LOAD**

The equilibrium deflected shapes of a frame are calculated as described in previous chapters for increasing values of applied loads. As the load is increased the stiffness of the structure reduces and eventually vanishes. The load at which equilibrium deflected shape for a member or a converged solution for nodal deformations can not be found is defined as the ultimate load of the structure.

### **3.8 DESCRIPTION OF COMPUTER PROGRAM "SWANSA"**

#### **INTRODUCTION**

A computer program *SWANSA* (*SWay And No-Sway Analysis*) has been developed based on the above procedure. A user friendly interactive data entry facility has been written in C programming language. It allows the user to modify an existing data file or to accept the default values. The main program has been written in FORTRAN 77 and the full version can be installed on any machine with UNIX or OS2 operating system. A limited version, mainly due to memory limitations, can be installed on any personal computer that works under DOS.

A user manual for the above program has been written[70].

## MODELLING OF THE STRUCTURE

The structure is simplified as an assembly of nominally straight members. The nodal points where members are assembled are defined by a global coordinate system. The nodes are numbered in sequence starting from one. In addition to global coordinate system each member is given a coordinate system unique to that member so that member end forces and deformations can be defined. The z-axis of the member coordinate system passes through the member centre line from one end to the other. This defines the direction of members. Assembly of members are defined by their node numbers at the two ends, referred to as End A and End B. The member coordinate system though fixed along the z-axis requires x-axis to be fixed in direction. This is defined by giving the global coordinates of a point along the positive direction of x-axis. This global and member coordinate system defines the frame in a unique manner.

Member subdivision to be considered in the analysis is specified for each member. The subdivisions are numbered starting from one at End A to End B. Different sections occurring in all the stations in all the members are classified and numbered. The shape of the cross section of a member is defined in terms of constituent quadrilateral components. A given cross section can consist of a combination of elements of different material properties. An axis parallel to member x and y axis and containing the cross-section in its positive quadrant is selected to define the coordinates of quadrilateral components in a section. The member axis, normally the geometrical centre, is fixed along the member z-axis. The coordinates of this member axis relative to section x, y axis are also given while defining the section data. Stress strain relations for each material are given as data.

The members are connected through flexible joints. The moment rotation characteristics of flexible joints are given as data. By default the program assumes monolithic connection. The boundary conditions are given as fixed or free for all six degrees of freedom (3 deflections and 3 rotations) wherever it is required. By default the nodes are assumed to be free in all six directions.

## **LOADING**

The external nodal loads are given at respective nodes in global axes. The member loads such as distributed and point loads are given in terms of member axis. It must be noted that the initial load factor to calculate equilibrium deflected shape of a frame must be much lower than its expected failure load factor. The facility is there in the computer program to maintain a set of loading constant while the other set of loading is increased proportionally with the load factor upto the failure of the structure.

## **ANALYSIS TYPES**

The program *SWANSA* has the following options:

1. Non-linear analysis of 3-dimensional precast concrete frames. This analysis can be carried out by providing non-linear stress strain data. Geometrical nonlinearity is also considered in this analysis. Joints can be rigid, pinned, or flexible. The data for joint characteristic is provided as multi-linear curve.
2. Linear analysis of 3-dimensional precast concrete frames. This analysis can be carried out by providing linear stress strain data. Geometrical nonlinearity is considered in this analysis. Joints can be rigid, pinned, or flexible. The data for joint characteristic is provided as multi-linear curve.

3. Any one or a combination of external forces can be increased to reach the ultimate load. If the load increment is specified as zero, an equilibrium deflected shape for the given loading can be obtained.
4. The output includes deflections, moments, shear forces, axial forces and torsion at all the member stations and at global nodes.

## **STRUCTURE OF THE COMPUTER PROGRAM**

Figure 3.6 shows a flowchart of the computer program *SWANSA*. The geometrical, material and loading data are first read. The data file is identified with ".dat" as its extension and any file submitted as data file without this extension will result in termination of the program with a message suggesting to submit a data file with ".dat" extension. The data are first checked for validity and the interrelation. The data can be printed out for verification purposes. If there is any data found to be invalid, the program would be terminated printing out appropriate message with suggestions (if any). Successful reading of data will initiate a routine to create a result file with the same first name as data file but with ".res" extension. Similarly a file is created for writing results on strain with ".stn" extension and a file for writing information on plotting with ".plo" extension.

### *INITIAL CALCULATION*

Values that will remain constant throughout the analysis are calculated at the beginning of the program. The transformation matrix and the lengths of all the members are calculated at the beginning. Gauss point coordinates and weights of all the cross-sections are also calculated. Facility is provided for using up to 10 Gauss points for each quadrilateral in the analysis. If the initial

deflected shape is to be obtained from an elastic analysis, coefficients of linear stiffness matrix are calculated as explained above. The initial imperfections in members are calculated from the central deflection data provided, if sinusoidal imperfection is to be included in the analysis.

### *ELASTIC ANALYSIS*

Nodal and member loads are obtained by multiplying the given loads by initial load factor. Elastic stiffness matrix and fixed end moments for each member are calculated. The member stiffness matrix and fixed end moments are then transformed to global axes. The out of balance force vector is formed by considering equilibrium at the nodal points. The overall stiffness matrix is modified according to boundary conditions. The solution of the above simultaneous equation is obtained by Gaussian elimination, and used as trial deformation for the frame nonlinear analysis.

### *NONLINEAR ANALYSIS*

Nodal deformations are transformed to member deformation using transformation matrix. Using material nonlinear data and joint moment rotation characteristics member end forces are calculated for all the members corresponding to their member end deformation. Equilibrium deflected shape of a member is confirmed when member deflections at its stations converge to a value. The tolerance for convergence is a predetermined percentage of the summation of absolute values of deflections at all stations. If no convergence in deflection is reached with prescribed number of iterations the load factor is reduced. Recalculation starts from the last converged load factor. The process is repeated until the load factor increments are reduced to the prescribed accuracy.

Incremental stiffness matrices for all the members are calculated step by step as detailed in the previous sections. When the type of iteration used is the modified Newton-Raphson technique, the Incremental stiffness matrix is not recalculated and the last calculated stiffness matrix is used instead. The vector of member end force and the Incremental stiffness matrix of each member are transformed back to global axes using appropriate transformation matrices. The overall incremental matrix is then modified according to the boundary condition. If the boundary condition at any node is rigid then the column and row in the overall matrix corresponding to that deformation are made zero and the diagonal element of that row and column is assigned a value of 1. The corresponding row in the out of balance force vector is also made zero so that the modification to that particular deformation will work out to be zero in the solution of the matrix equation.

This matrix equation is then solved using Gaussian elimination for increment in nodal deformation. Deflections and rotations at each node are checked for convergence separately. Current deflections at all the nodes are compared with the previous deflection. If the difference in deflection is less than a percentage of absolute total of all nodal deflections then the deflections are considered converged. Similar check is made for rotations at nodal points and convergence is determined. If the deformation converges, the structure is considered to be in equilibrium deflected shape, otherwise nonlinear procedure is repeated with the latest nodal deformation until convergence is reached. The member deformation, member end forces and nodal deformation are printed to the result file and to the plotfile after convergence. The curvatures in x and y axis at all stations along the members with neutral axis position are printed in to strain file for future extraction of strain profile across member sections.

The final value of the load factor for which a converged solution is obtained, is taken as the ultimate load factor.

## **OUTPUT**

A post processor for the above program has been developed for use with the drafting system *MICROSTATION* from *INTERGRAPH*. The post processor reads data from the plotfile and writes user command files as used in Microstation drafting system. Microstation software has been customised by modifying the side bar menu to include the commands necessary for viewing the frame, deflected shape, bending moment diagram and shear force diagram. The postprocessor will automatically activate Microstation with a default drawing. The menu also allows the option to produce hard copy of deflected shapes, bending moment diagrams and shear force diagrams. This form of graphical presentation has been found to be very convenient for use by practising engineers from the participating concrete firms.

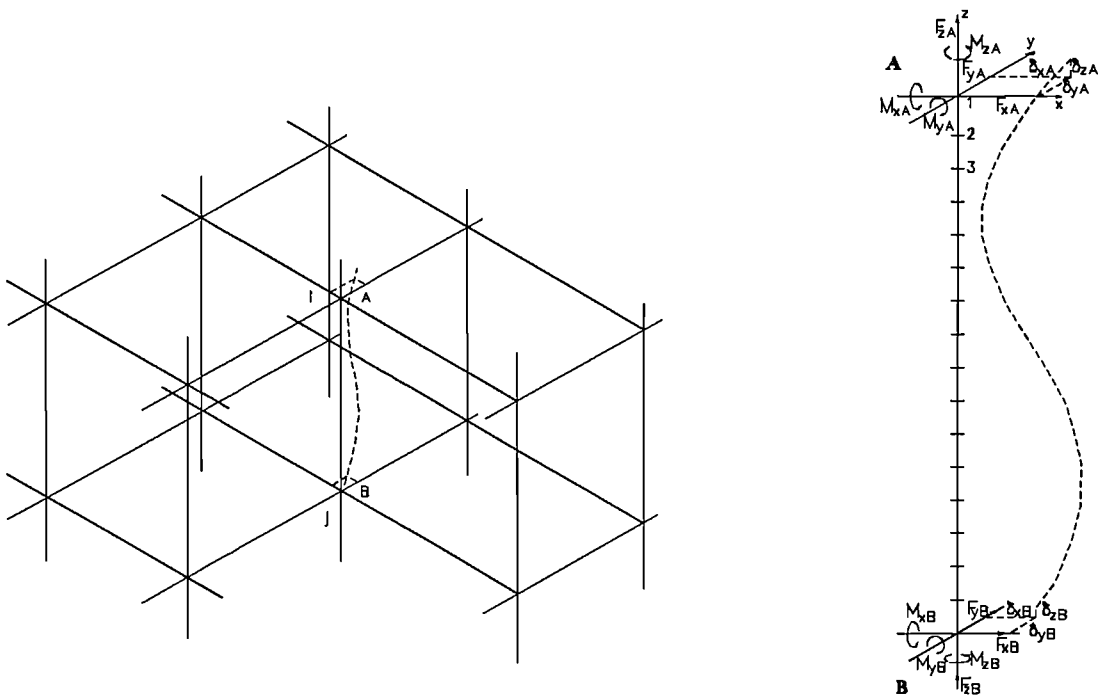


**FIG.3.1 TYPICAL MEMBER IN A SPACE FRAME**

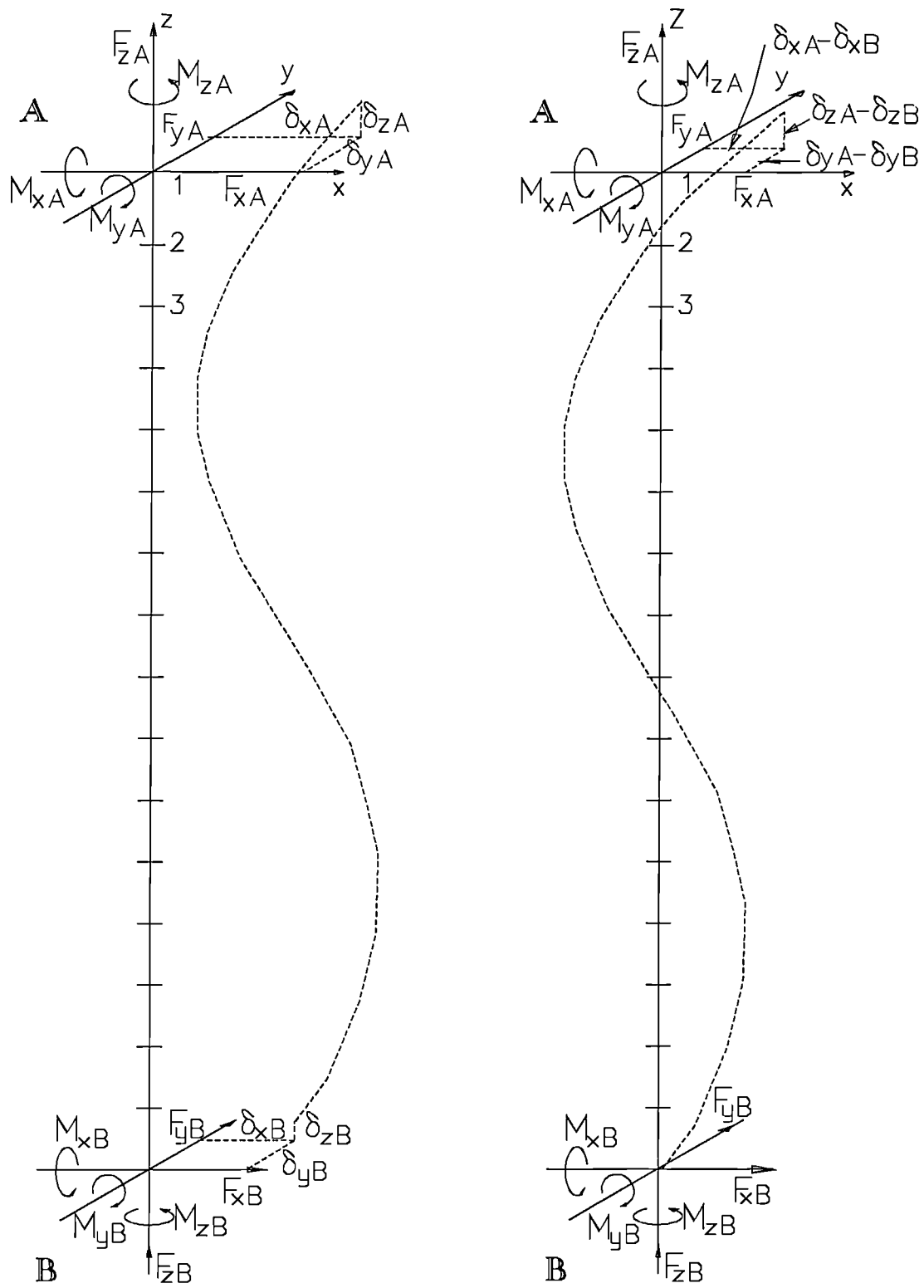


**FIG.3.2 BEAM-COLUMN AS CONSIDERED IN THE ANALYSIS**

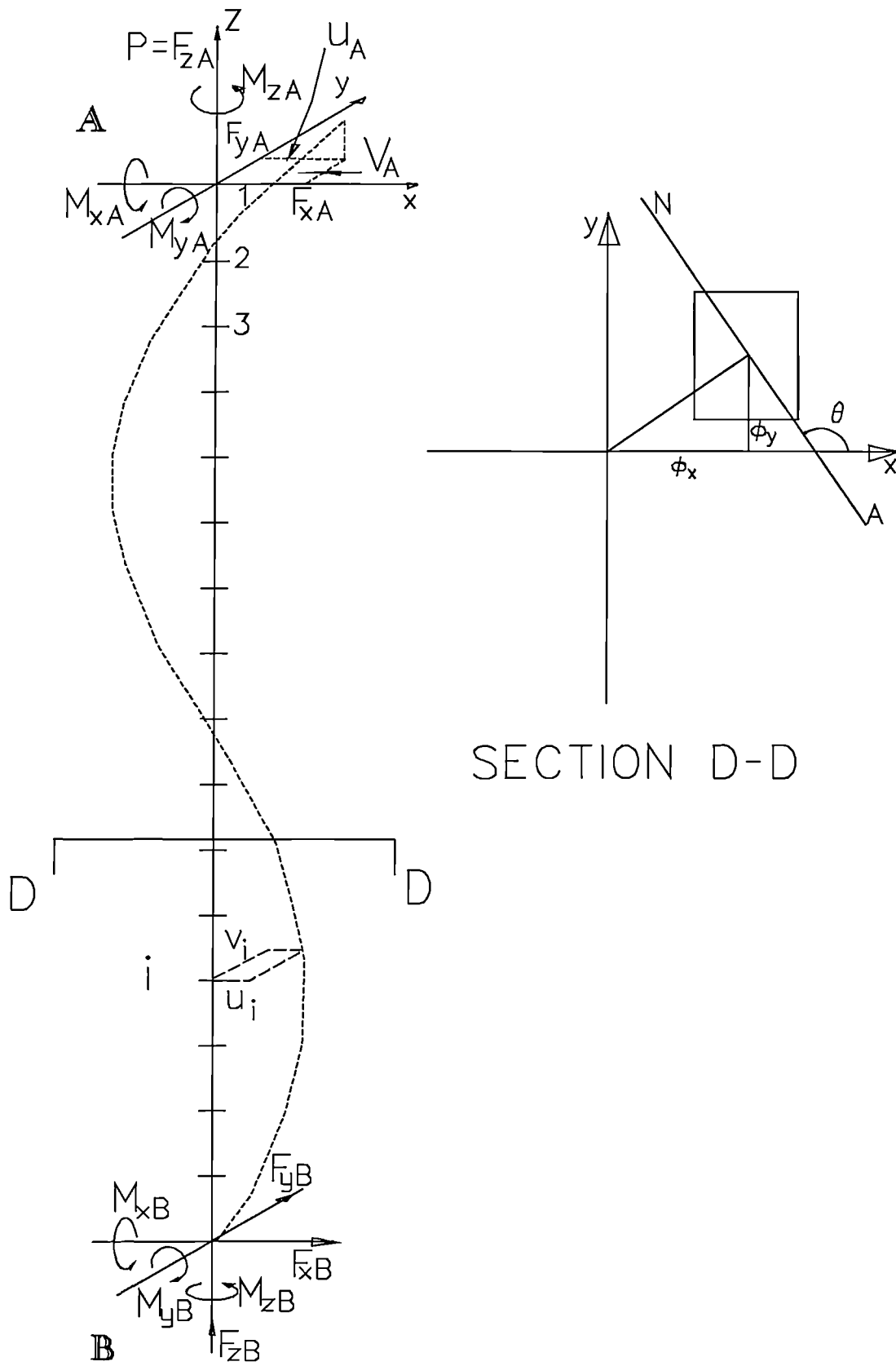


**FIG.3.3 TYPICAL MEMBER**

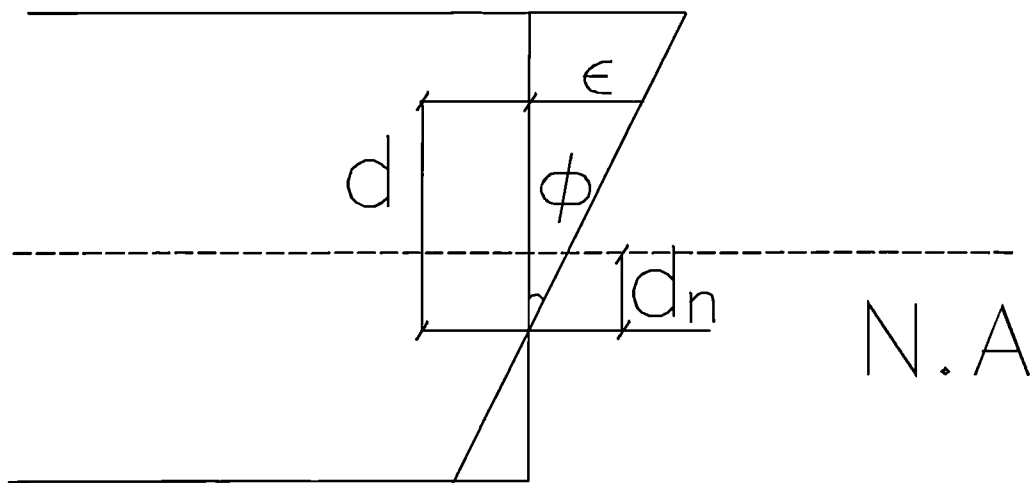
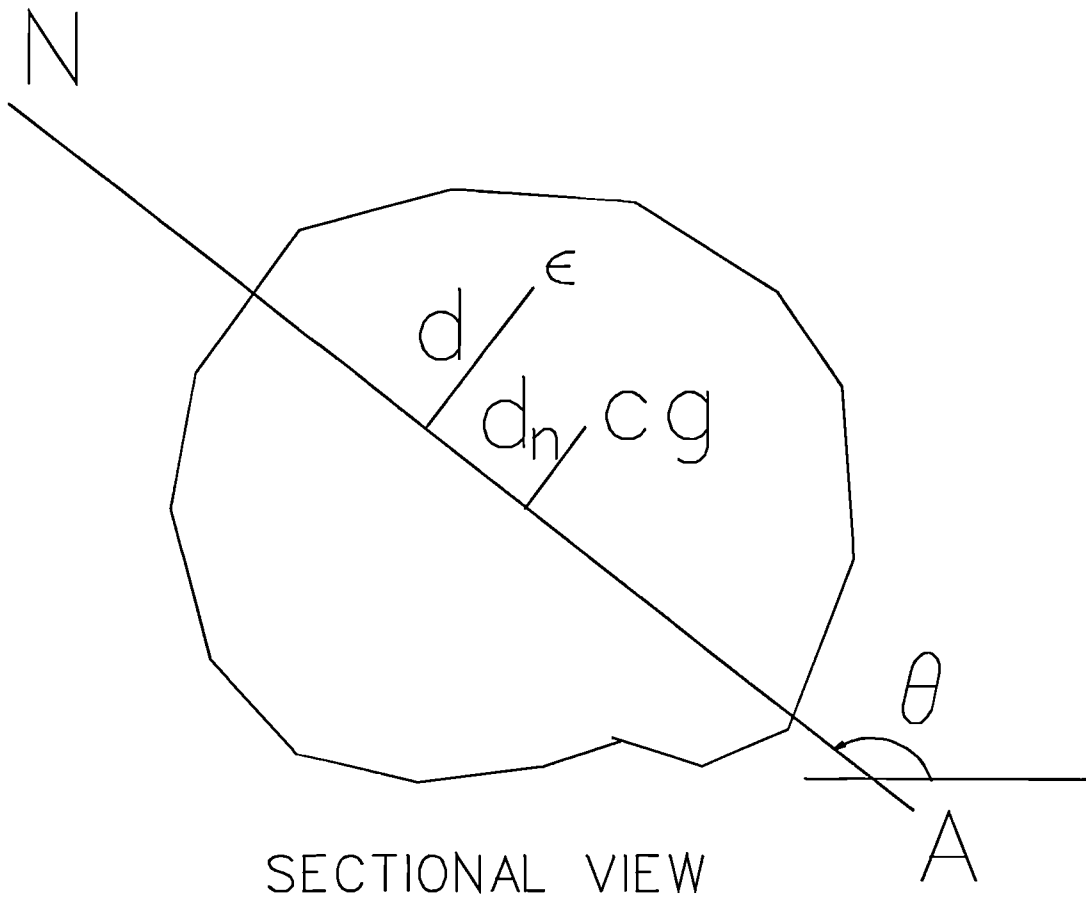


**FIG.3.4 STRAIN DISTRIBUTION ACROSS SECTION**

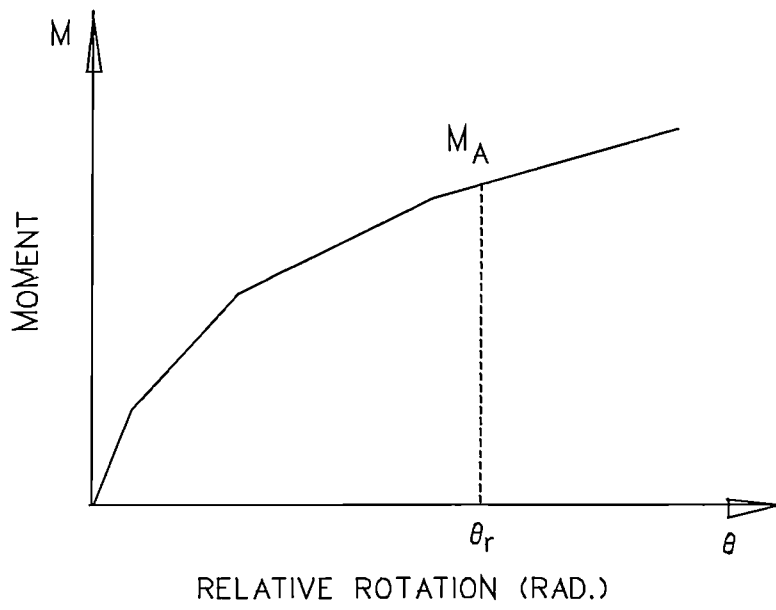
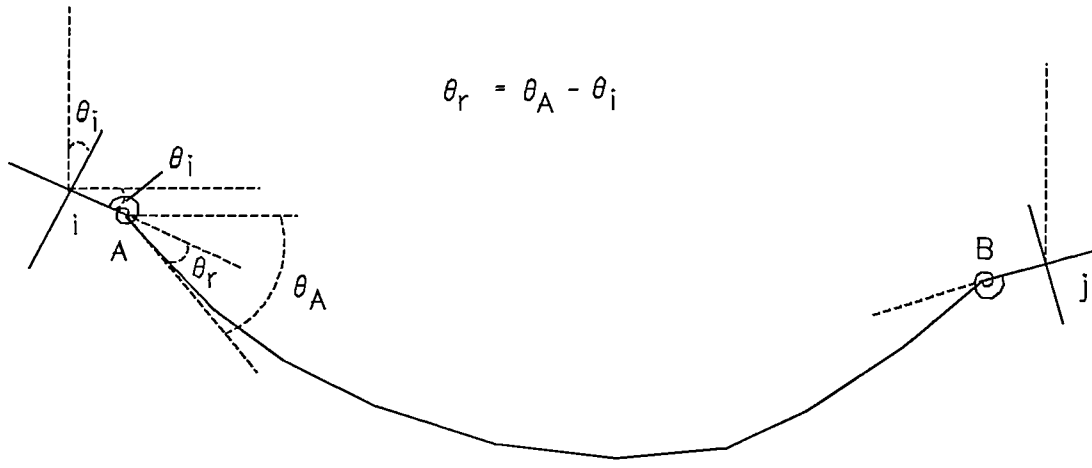


**FIG.3.5 RELATIVE ROTATION IN FLEXIBLE CONNECTION**

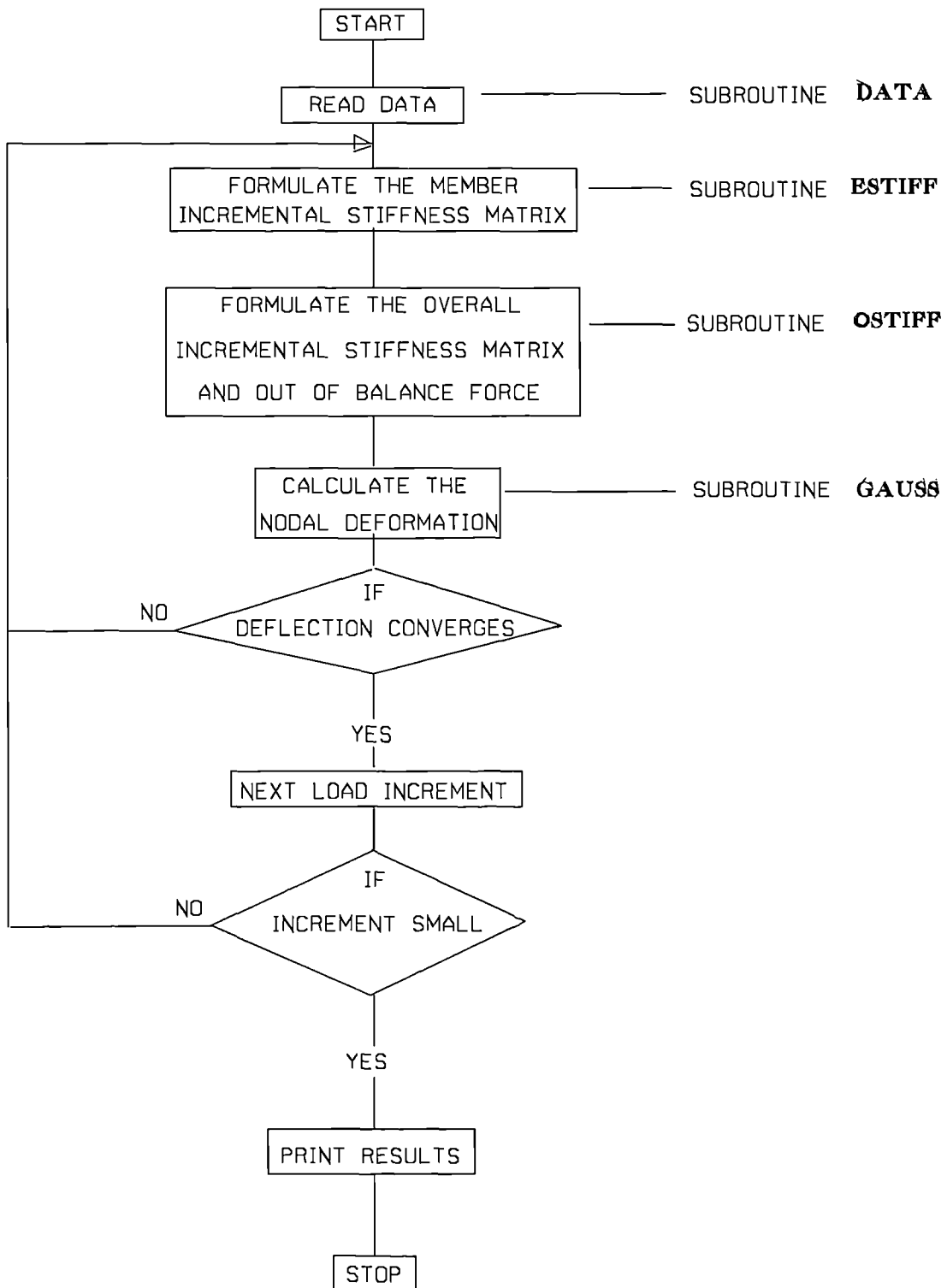


**FIG.3.6 FLOW CHART FOR SPACE FRAME ANALYSIS**

# CHAPTER 4.

## EXPERIMENTS

### 4.1 INTRODUCTION

As noted in the literature review, experimental results on flexibly connected precast concrete frames or subframes are not readily available. In order to fill this void, eight full scale experiments on column beam subframes CT1 to CT8 have been conducted to test the capability of the new theory discussed in Chapter 3, and to validate the associated computer program for eventual use in design or for developing design aids.

Each subframe consisted of a two storey column together with a short length of a typical mid storey beam. In each case the beam was connected to the column at mid height through a mechanical joint. Four types of connection commonly used in precast construction were selected to construct the subframes. These were selected so that a range of strengths and stiffnesses of the connection could be covered. The four connections chosen are used by four different firms, participating in the project. Two sets of subframes were made for each connection type so that the behaviour of subframes could be tested for upward and downward rotations of each connection. The continuous two storey column in the subframes was considered pin-ended at top and bottom. The end moments were introduced by eccentric column loads. The lateral movements of the column at both ends and at mid height were restrained to simulate nosway plane frame behaviour. The free end of the beam in the subframe was allowed to move freely in the vertical direction. This free movement was adopted in order to have control over moment

transferred from beam to column through the connection. This subframes were tested to collapse.

## 4.2 SPECIMENS

Originally, it was planned to use columns of size 200mmx200mm. However, in discussions with the participating firms, it became clear that the minimum size used in precast construction practice was 300mmx300mm. In order to remove any problems with reduced scale specimens, it was agreed that a column size of 300mmx300mm should be adopted for these tests. Columns of these dimensions are used in the construction of structures up to four stories high. The detail of the connection and the additional reinforcements were available only for the above column size and a reduction in column size was thought not to represent realistic connection behaviour. The size of the stub beam was decided in accordance with the standard dimensions used in practice with contractors' connection details. The two storey continuous columns were of 6m height, resulting in storey heights of 3m. The length of the stub beam was 1.5m in each case.

The reinforcement in the beam and the two storey column was determined so as to be representative of typical members used in practice. Four 20mm bars were used as the main reinforcement in all the columns. In order to ensure efficient transfer of end moments to the column, an end steel plate of 18mm thick was welded to the main reinforcements at both ends of the columns. The links used in the columns were of 6mm mild steel at 200mm spacing. The detail of the connection and the additional reinforcement around the connection were those used commonly by the participating firms. Though the length of the stub beam used in the subframe was 1.5m for all

the test frames, the sectional dimension varied according to the connection detail. The reinforcement and sectional details of the column and beam used in the experiments are given in Fig.4.1 to 4.4. The connections used in the respective tests are shown in Fig. 4.4 to Fig. 4.8.

### **4.3 TESTING RIG**

During the planning stage two methods of testing were considered. One method is to test the subframe horizontally to eliminate difficult handling of heavy members of subframes. The other method was to test the subframe vertically so that the effect of self weight, specially when the portion of the slab was included in the subframes, will not have an adverse effect on the behaviour of the subframe. It was decided to adopt the latter option.

A special testing rig was designed to accommodate the subframe. A perspective view of the rig with the subframe in place is shown in Fig. 4.9 and Fig. 4.10. The rig consists of two parallel rectangular plane frames consisting of two columns of section 254x254x73 UC connected by "C" channels at top and bottom of the frame. The top and bottom horizontal beams of the front frame were an assembly of three steel beams. One steel beam of 254x254x132 UC was in the centre connected to the steel column with end plates using 6 bolts of 24mm dia. Two 305x305x198 UB sections were arranged on either side of the first beam and were fixed to the column using stiffened angular bracket welded to the column. The layout of the beams and the connections is shown in Fig.4.9. The front frame of the rig was capable of carrying 2500 kN at the centre of the horizontal support beam. This would be the limiting axial force on the column under test. The total

height available for the specimens was little over 6m. This parallel arrangement of beams enabled a realistic two storey subframe to be tested. The intermediate beam of section 254x254x73 UC in the rear frame was capable of carrying a maximum load of 250 kN, acting upwards or downwards. Axial load in the column was applied by three 900 kN hydraulic jacks with a manifold to permit simultaneous loading. The jacks were clamped together to the base as shown in Fig. 4.11 and Fig. 4.12. Three jacks of low capacity were preferred to a single 2500 kN jack, because the latter would have occupied a greater length of valuable clear height available in the Heavy Structures Laboratory.

The whole rig was assembled vertically from the basement through a purpose made opening in the structural floor of the Heavy Structures Laboratory.

#### **4.4 LOADING**

The load was transferred to the column through a ball bearing on the column cap. By locating the centre of the ball bearing eccentrically with respect to the column centre, as shown in Fig. 4.11 and Fig. 4.12 end moments on the column could be introduced. The column and the beam are loaded so as to bend in one plane only. The eccentricities at the two ends of the continuous column are kept opposite to each other in order to allow each column of the two storey subframe to bend in single curvature. It was felt that this would result in maximum instability effects through combined bending and axial compression. This arrangement corresponds to patterned load combinations used in the design of columns in frames. Provision was made at the top and bottom of the frame to reverse the direction of eccentricity to enhance the

effect of the moment applied to the cantilever beam of the subframe. This is illustrated in Fig.4.11, Cases 1 and 2.

Three horizontal channel sections fixed to the upright columns of the rig are provided at the top, middle and bottom of the column to prevent the horizontal movement of the column at nodal points. The connection between the channels and the column is such as to prevent translation, but to permit rotations in the plane of bending. This is shown schematically in Fig. 4.13.

#### **4.5 MANUFACTURE OF SPECIMENS**

The manufacture of the specimens was carried out at casting yards normally used by the manufacturers. This procedure was adopted to make sure that the specimens tested were representative of those available on site. Internal electrical resistance strain gauges, with marked output leads, were pasted on to prepared surfaces of the reinforcement in the column prior to casting (Fig.4.14). The pasting of the gauges was carried out at the casting yards by the City University staff, under supervision from one of the investigators. Specimens were stripped out of formwork 24 hours after casting. All gauges were tested for integrity of the electrical circuits, before casting took place. Curing procedures were the same as those adopted for prototype frames. Specimens were transported to the Heavy Structures Laboratories at City University, some two weeks after casting.

## **4.6 INSTRUMENTATION**

To measure the axial load in the column a load cell of 2500 kN capacity was located between the assembly of the three jacks and the ball bearing. A load cell of 500 kN capacity was located in series with the jack used for applying the lateral load on the cantilever beam as shown in Fig. 4.12 and 4.13.

In order to measure displacements an isolated scaffolding frame was erected around the test subframe as shown in Fig. 4.11. Digital readout dial gauges, supported by the scaffolding frame, were positioned at 500 mm spacing along the height of the continuous column and along the cantilever beam (Fig. 4.15).

Two inclinometers were also used, one at middle of the column and the other, on the beam near the beam column junction, to assist with the measurement of rotations (Fig.4.15). Vertical beam displacements at three points close to the column face were also used to measure the beam rotations.

Eight external strain gauges were fixed on the clear concrete surface at selected points as shown in Fig.4.1 to 4.8 for recording concrete strains.

## **4.7 PREPARATION FOR THE TESTS**

The test column was erected in position and located on the bearing of the three-jack assembly. The column was tied through pins to the restraining channels located at the top, middle and bottom of the rig (Fig. 4.9).

The cantilever beam was then connected to the column by the mechanical joint provided, and temporarily held in place by slings. When the alignment of the connection was correct, the connection was grouted. The method of grouting was determined in consultation with the participating firms. The grout was allowed to gain strength for a minimum of 7 days before testing.

The connections used in subframes CT1 and CT2 were cleat connection and were grouted with cement sand grout with CONVEX100 admixture. The subframes CT3 and CT4 were assembled using welded plate connection and the connection area was covered with a concrete mix poured into a mould set around the joint. The connections used in subframes CT5 and CT6 were of similar type to those used in CT1 and CT2 but from a different contractor and were grouted using cement sand mix with CONVEX100 admixture. The subframes CT7 and CT8 were of special type with newly designed web connection with steel plate packing to fill the tolerance in construction. The beam was cast with the top part of the reinforcement exposed to have monolithic connection with slab. Formwork was made on either side of the beam to include 200mm thick 500mm width slab. The cast-in socket in the precast column just above the joint was connected to threaded reinforcement to have dowel action in to the slab. The reinforced slab was cast with structural concrete. The detail of the concrete mix and the strengths are given in Appendix 2.

The test column and beam were painted with a thin coat of emulsion paint for clearer visibility of tension cracks. The first specimen was not so painted, and it was found that in this case crack detection was difficult.

All gauges were tested to check that the wiring was still intact before connected to data logger. The three column jacks were connected to a hand

pump in parallel to ensure uniform pressure on all three jacks. The beam jack was connected to another hand pump. The load cells were connected to an electronic display meter separately. A separate display meter was connected to inclinometers.

Trial runs with small loads were carried out to check the functioning of the instruments before starting actual experiments.

At this stage the specimen subframe was ready for testing.

#### **4.8 TEST PROCEDURE**

In general, the column was first loaded until any initial slack in the top support was taken up. After embedding the specimen, and before applying further load, initial readings of all displacements, applied loads, rotations and strains were recorded. Subsequently the column load was increased through a series of predetermined steps to a level approximately 10% of the failure load expected. The beam load was increased next. Once the beam load had reached the desired level, which varied from about 50% of the estimated capacity to about 95%, the beam load was kept constant, and the column load was increased in steps, until either the column visibly failed through spalling, or the column failed to take any further loads. At all steps of loading, lateral displacements, axial loads, cantilever beam loads, rotations and strains were recorded. Visual checks such as appearance of cracks were also made, and subsequently photographed if considered important. The sequence was changed when subframe CT7 was tested where the column load was kept constant at 10% of the expected failure load and the beam load was increased

until subframe failed to take further beam moment. It was intended to follow the same procedure for CT8 but after observing the shear failure near the joint in CT7 due to high moment it decided not to load the subframe with high joint moment. The loading sequence followed for CT8 was similar to that of CT1 to CT6.

The detailed loading sequences are given separately for each test in Refs. [68,69]. The subframe CT1, CT4, CT6 and CT7 were tested for upward connection rotation and the subframes CT2, CT3, CT5 and CT8 were tested for downward connection rotation.

#### **4.9 MATERIAL PROPERTIES**

In order to assess the strength of the concrete in the specimens, 150 mm concrete cubes were cast together with the column and beam specimens. The cubes were tested on the same date as the corresponding subframe. Three 500 mm steel reinforcement bars were also cut at random from the lengths used in the test specimens. The steel bars were tested for strength and elastic modulus in an INSTRON testing machine available for the purpose in the Laboratory. The machine can record load elongation data at predefined interval. A delicate elongation gauge was used for measuring elongation up to yielding.

**TABLE 4.1 PROPERTIES OF CONCRETE AND REINFORCEMENT**

	CT1	CT2	CT3	CT4	CT5	CT6	CT7	CT8
Cube strength N/mm <sup>2</sup>	59.0	59.0	59.9	65.2	69.5	60.2	64.9	68.2
Strength of grout N/mm <sup>2</sup>	53.3	50.2	49.8	55.3	30.1	44.6	55.2	48.7
Steel Yield stress N/mm <sup>2</sup>	533.4	533.4	522.5	522.5	538.6	538.6	522.7	522.7
Ultimate stress N/mm <sup>2</sup>	642.7	642.7	602.5	602.5	627.3	627.3	618.2	618.2
Yield strain	0.00267	0.00267	0.00261	0.00261	0.00269	0.00269	0.00261	0.00261
Ultimate strain	0.240	0.240	0.240	0.24	0.236	0.236	0.240	0.240

#### **4.10 FAILURE OF THE SUBFRAMES**

During erection the column specimen for subframe CT1 was slightly damaged at the base. It was decided, nevertheless to proceed with the test, as it was considered useful to complete the full test procedure and to check the rig performance. As anticipated the column failed abruptly and prematurely. The results are, however, perfectly acceptable for the primary purpose of verification of the numerical model, up to the load that the column was able to sustain.

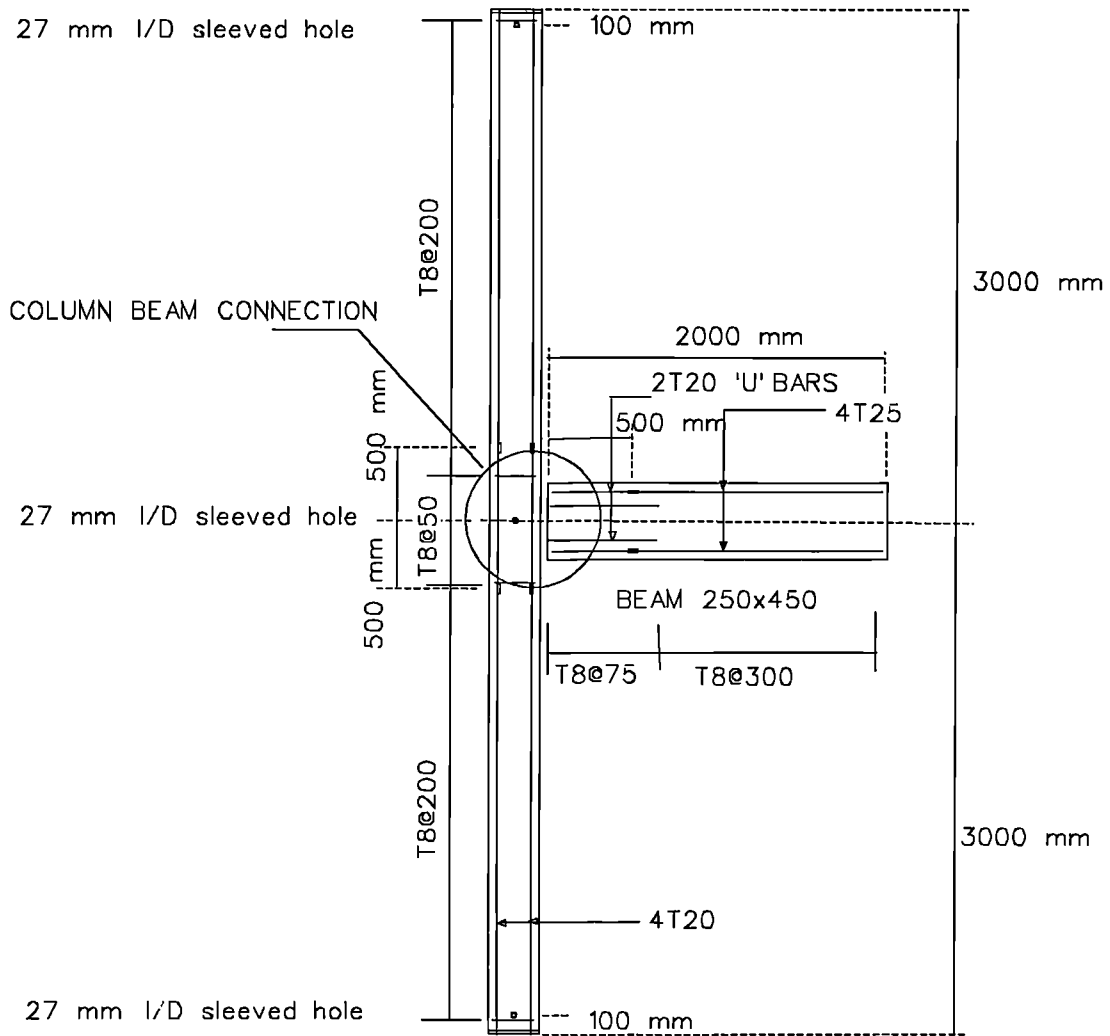
The subframes CT2,CT3,CT5,CT6 and CT8 were loaded up to failure. In all these cases, the column failed suddenly at an end of the column, with concrete bursting away. The subframes CT2,CT3 and CT8 failed at the

bottom end of the column and subframe CT5 and CT6 failed at the top end of the column. The subframe CT5 was expected to fail at the bottom according to the loading arrangement, however it failed at the top. This failure could be due to some imperfection in the material since the beam load applied was relatively small.

The test on subframe CT4 was terminated just below the failure load. The failure appeared imminent at the top of the column and it was considered unsafe at that time to continue with the test. The subframe CT7 was tested with a very high beam moment and the column failed in transverse shear near the junction. The failure was not well defined as the connection failed before it could be verified that the column could take no further moment. It should be mentioned that no special shear reinforcement had been provided to cater for this form of loading.

A sample subframe assembly before testing is shown in Fig 4.16. The same frame is shown after failure at the base of the column, in Fig 4.17. Figure 4.18 and Fig 4.19 show the crack patterns which appeared in the upper and lower column during the test. The crack pattern was consistent but the width of the crack was very fine even near the failure load. This behaviour is expected for a column of  $l/h$  ratio of 15. The failure of the column above the beam column joint in CT7 is shown in Fig 4.20.

The experimental results obtained are presented in detail together with the theoretical results in Chapter 5.

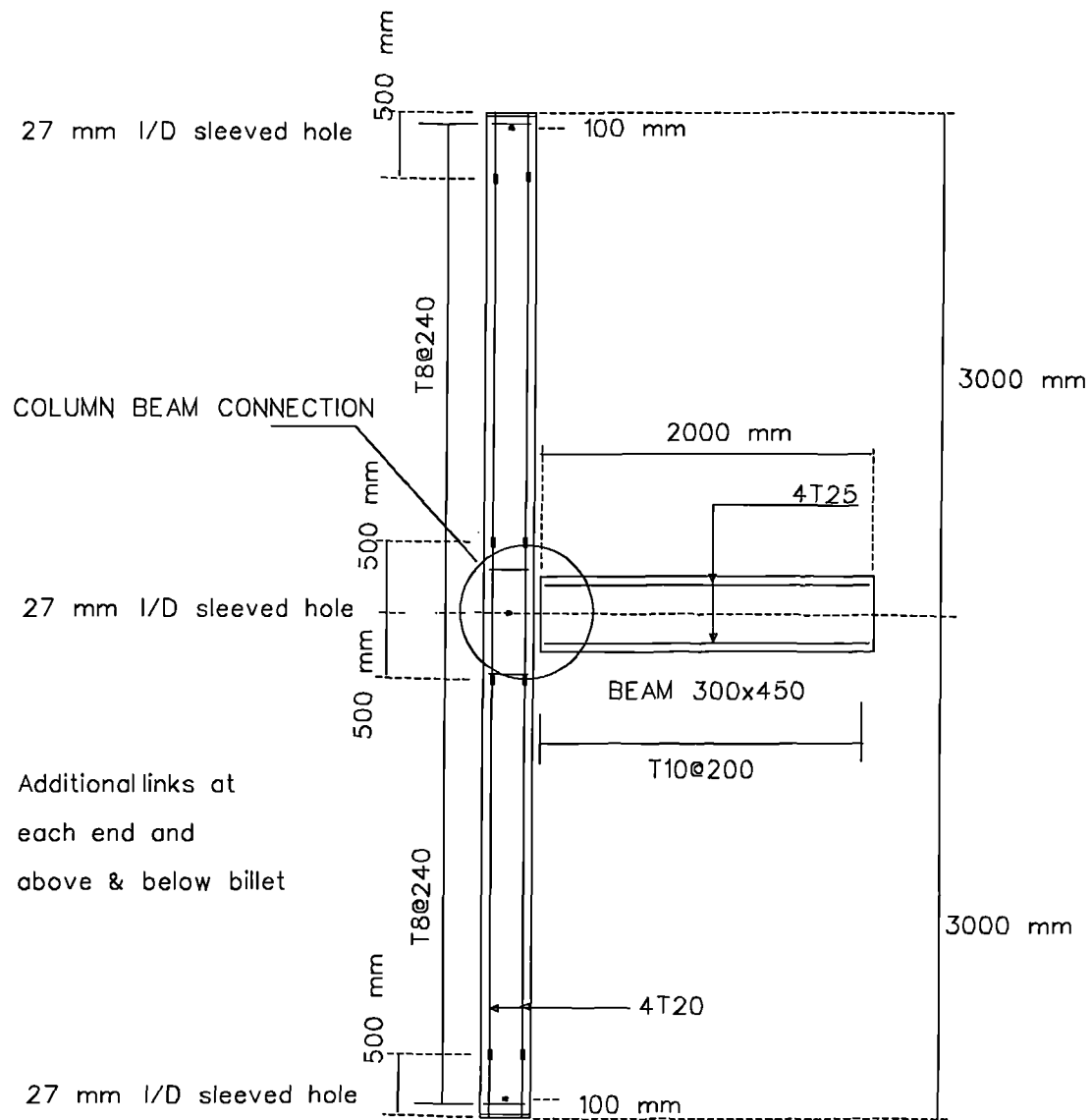


COLUMN 300x300

50 mm COVER TO CENTRE OF THE MAIN BAR

- · · · · EXTERNAL STRAIN GAGUES
- - - - - INTERNAL STRAIN GAUGES

**Fig.4.1 COLUMN AND BEAM GEOMETRICAL DATA (TEST CT1 & CT2)**



COLUMN 300x300

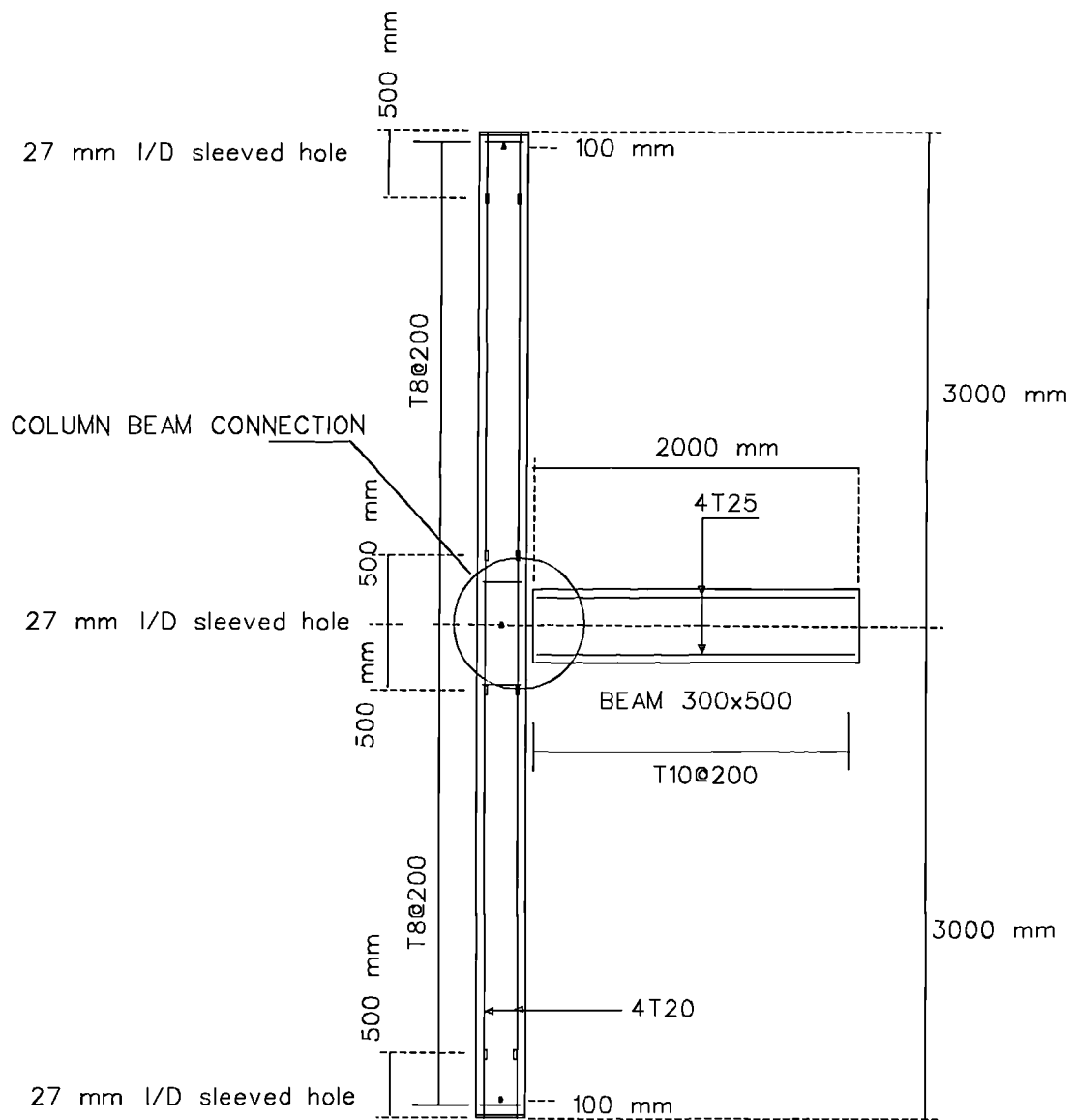
62 mm COVER TO CENTRE OF THE MAIN BAR

300x300x20 mm plate welded to main bar at both ends

EXTERNAL STRAIN GAGUES

- — INTERNAL STRAIN GAUGES

**FIG.4.2 COLUMN AND BEAM GEOMETRICAL DATA (TEST CT3 & CT4)**



COLUMN 300x300

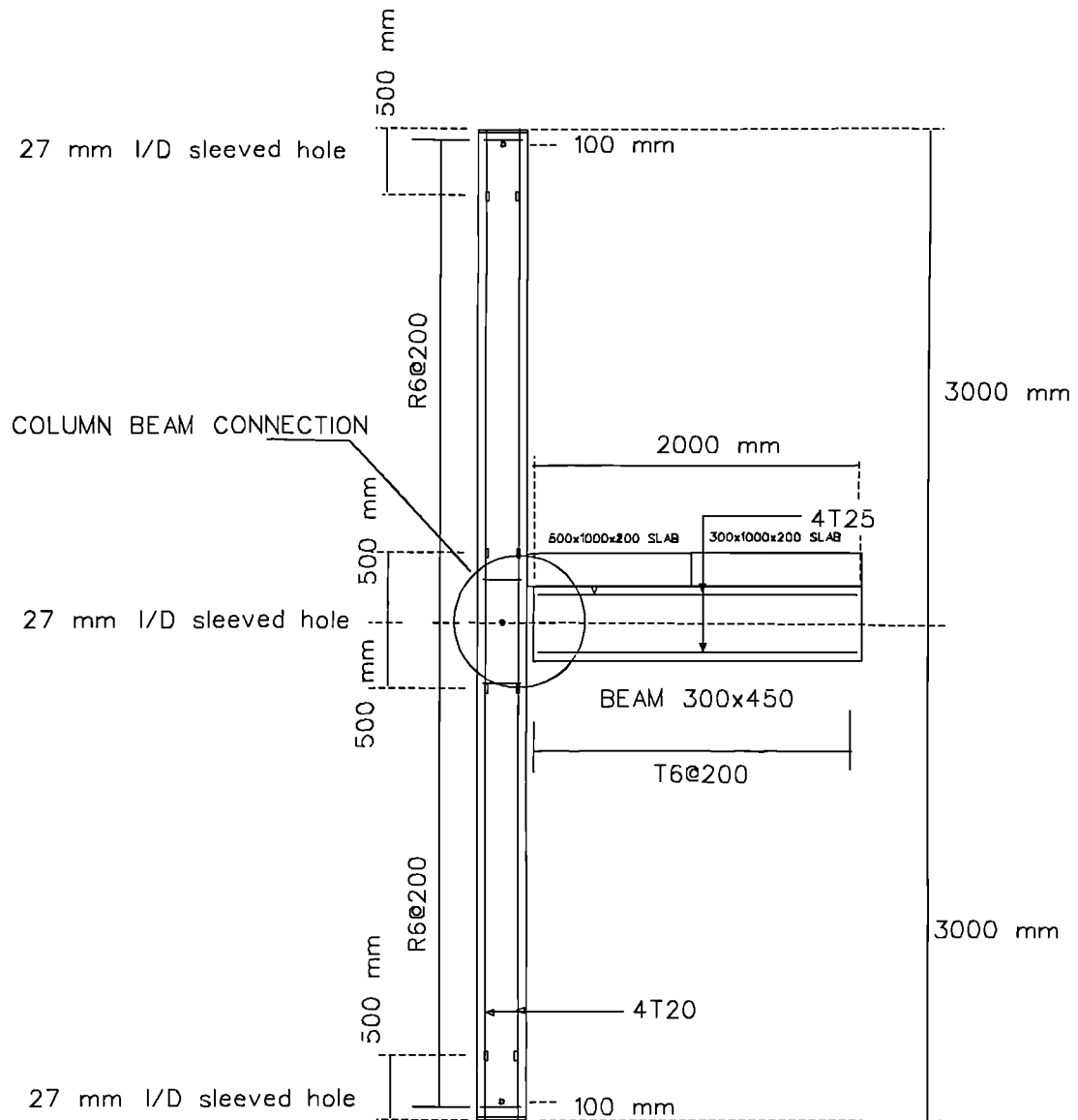
37 mm COVER TO CENTRE OF THE MAIN BAR

300x300x20 mm plate welded to main bar at both ends

EXTERNAL STRAIN GAGUES

- — INTERNAL STRAIN GAUGES

**FIG.4.3 COLUMN AND BEAM GEOMETRICAL DATA (TEST CT5 & CT6)**



COLUMN 300x300

37 mm COVER TO CENTRE OF THE MAIN BAR

300x300x20 mm plate welded to main bar at both ends

EXTERNAL STRAIN GAGUES

- — INTERNAL STRAIN GAUGES

**FIG.4.4 COLUMN AND BEAM GEOMETRICAL DATA (TEST CT7 & CT8)**

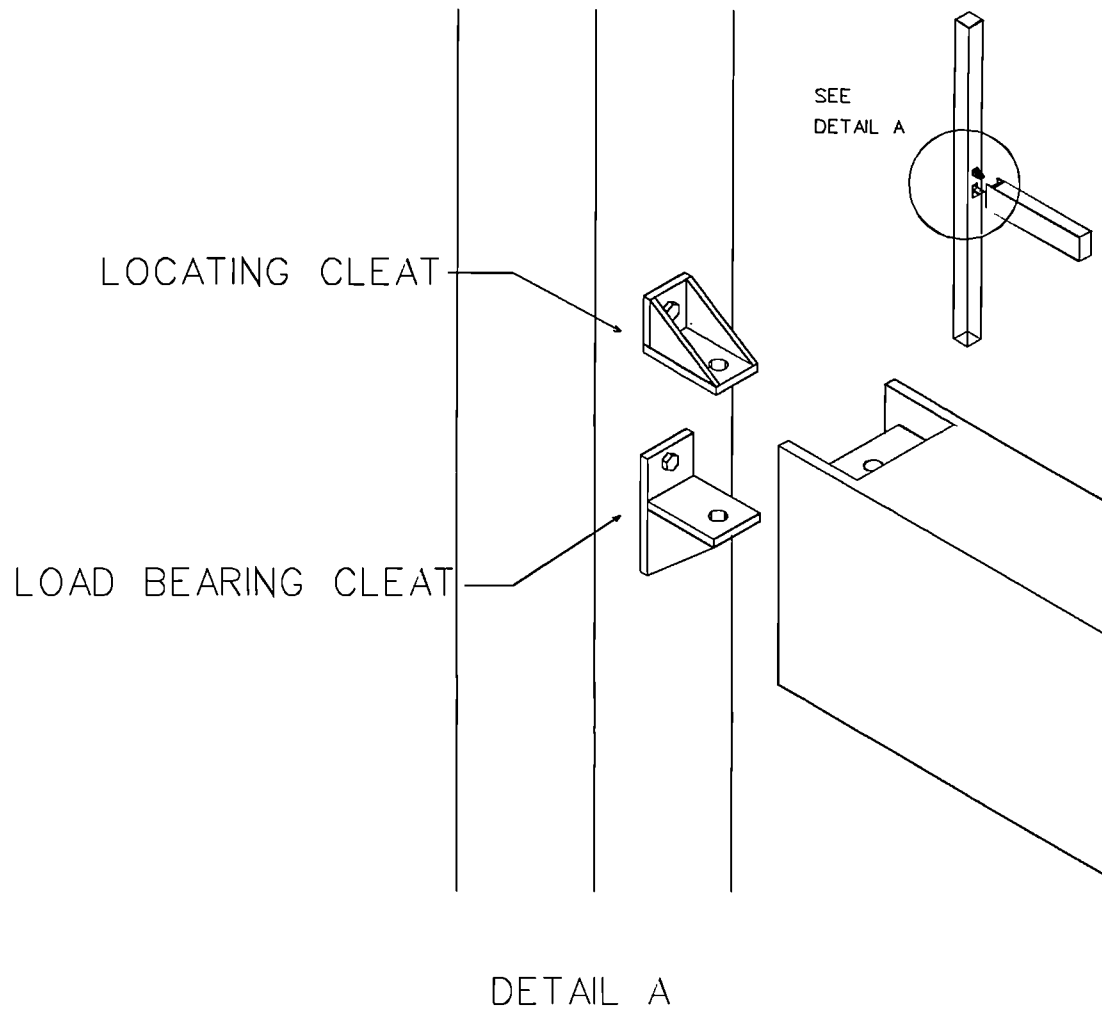


**FIG.4.5 CONNECTION DETAIL FOR TEST CT1 & CT2**

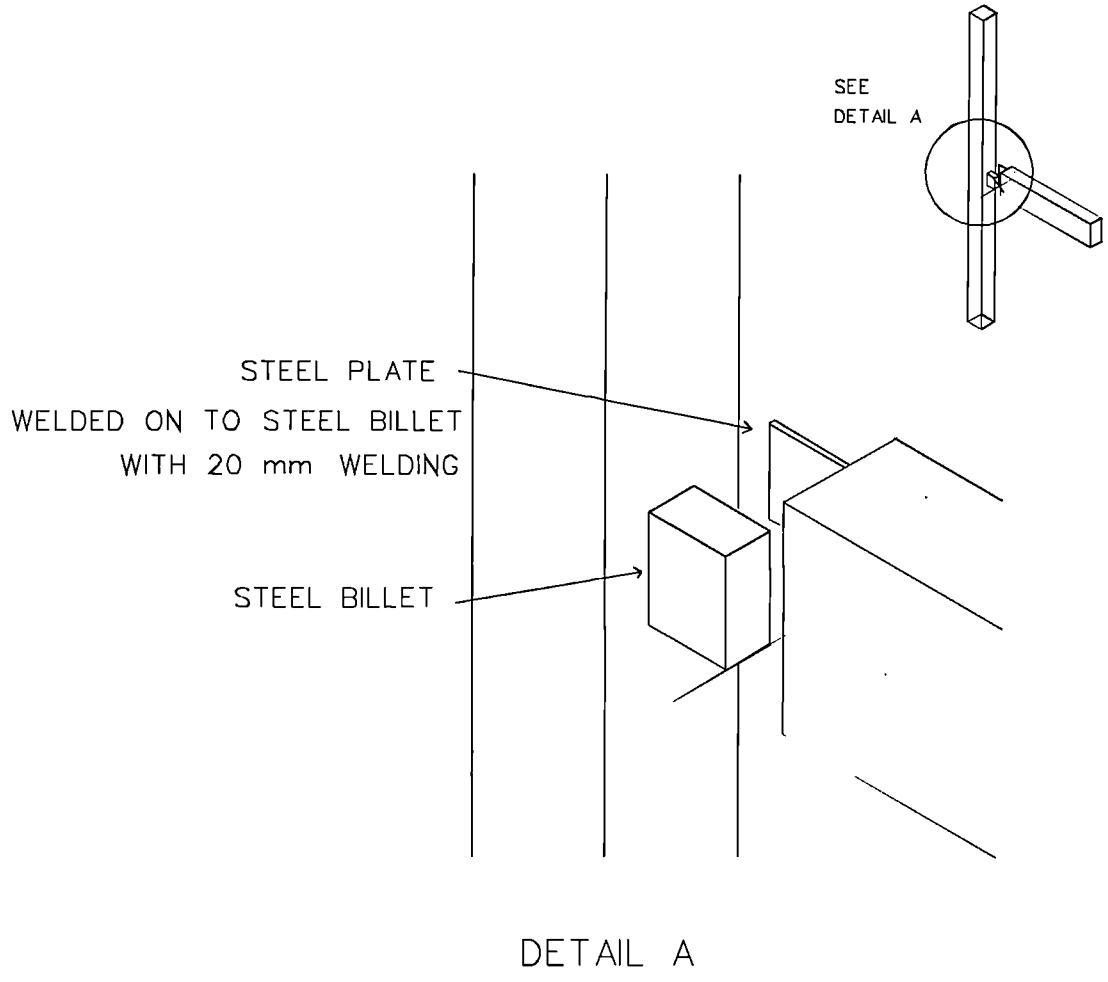


**FIG.4.6 CONNECTION DETAIL FOR TEST CT3 & CT4**

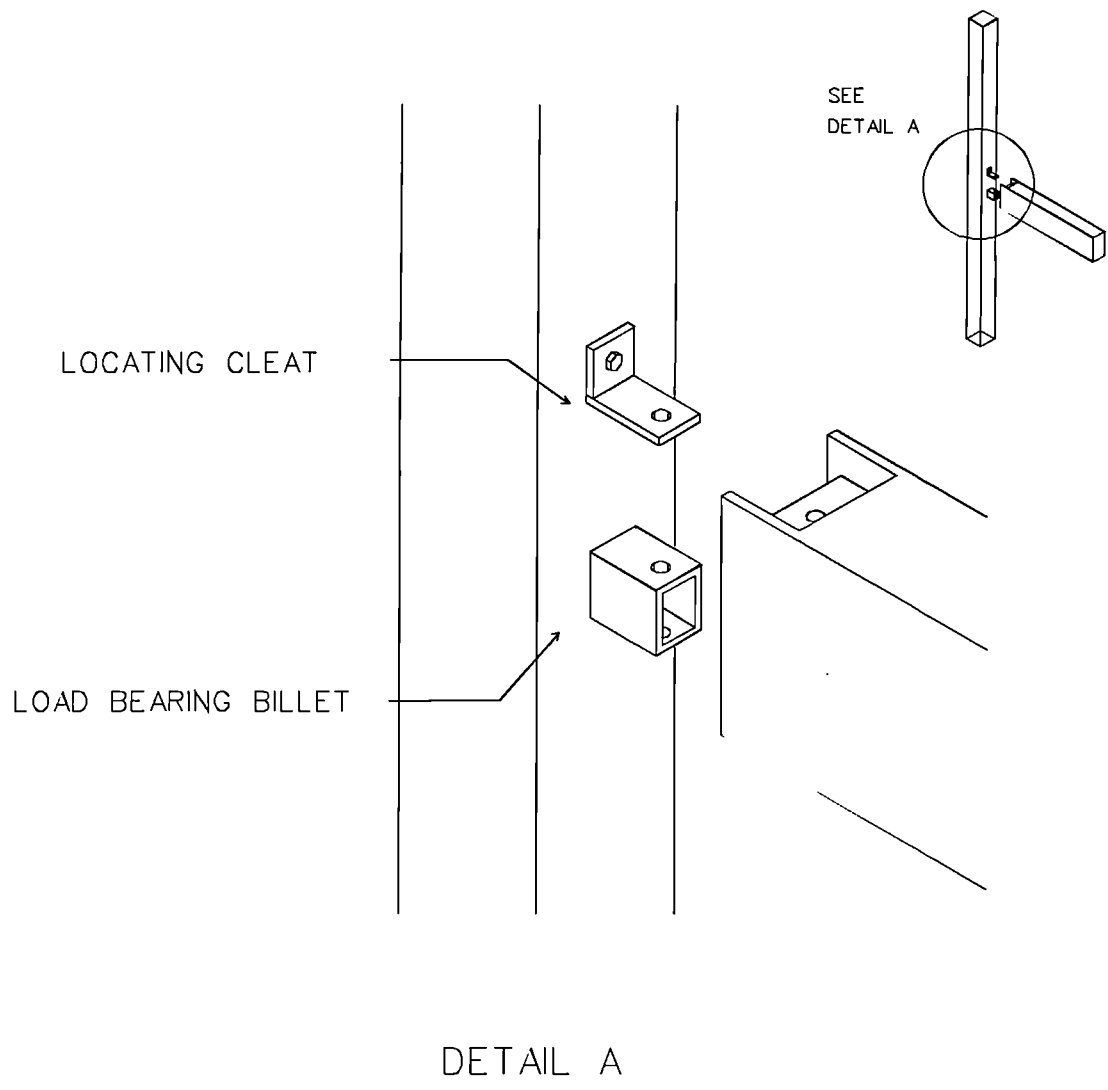
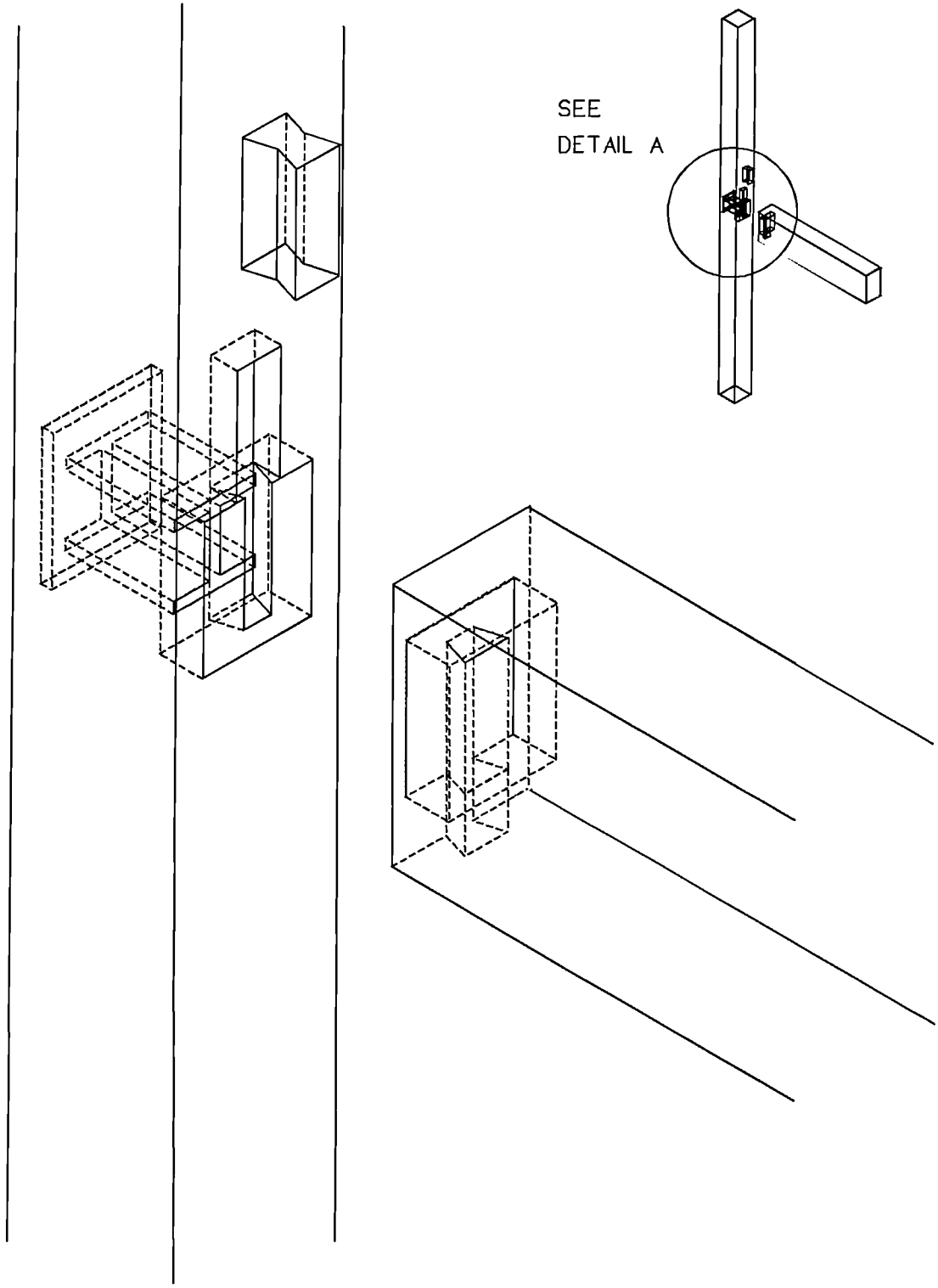


**FIG.4.7 CONNECTION DETAIL FOR TEST CT5 & CT6**



DETAIL A

**FIG.4.8 CONNECTION DETAIL FOR TEST CT7 & CT8**

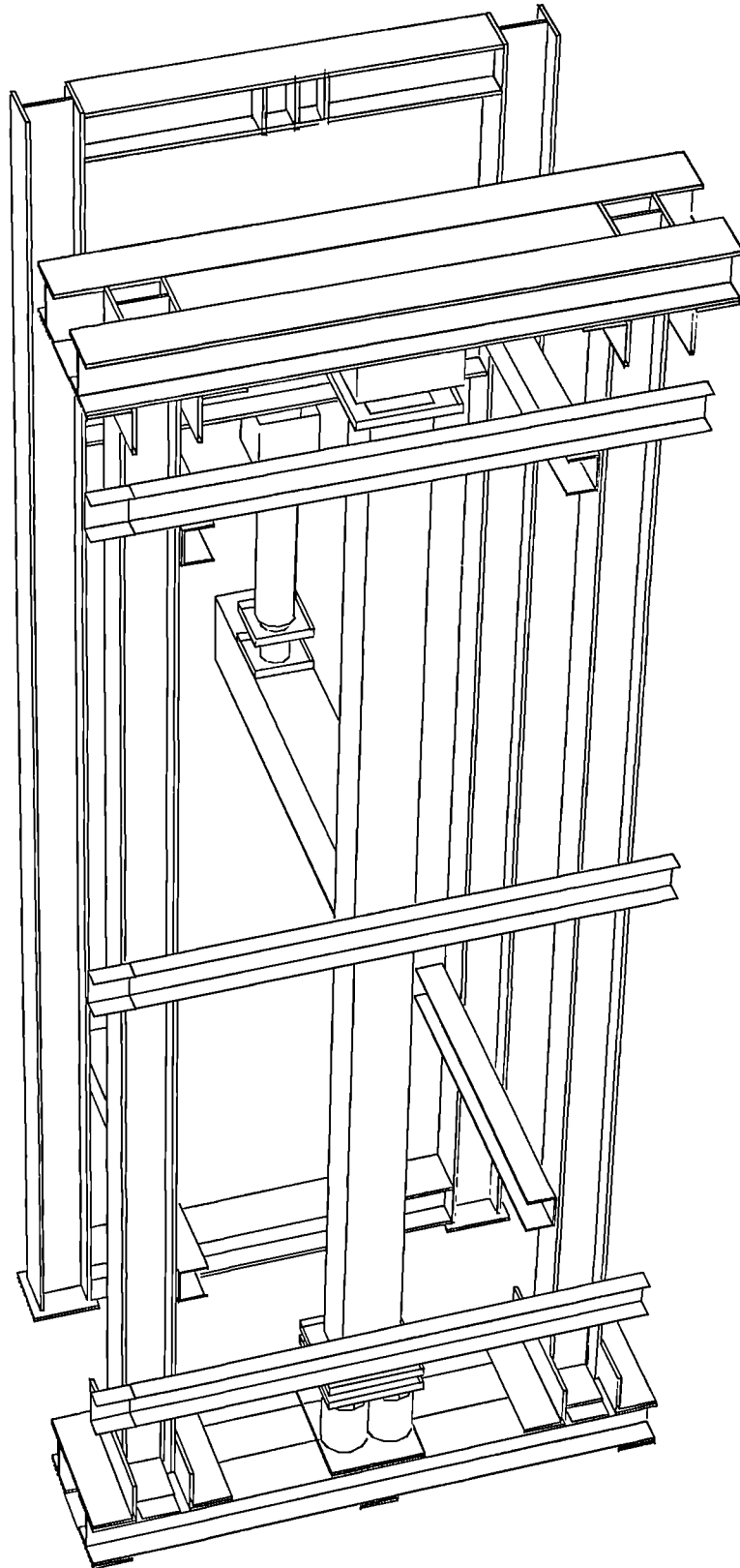


**FIG.4.9 TEST RIG GENERAL LAYOUT**

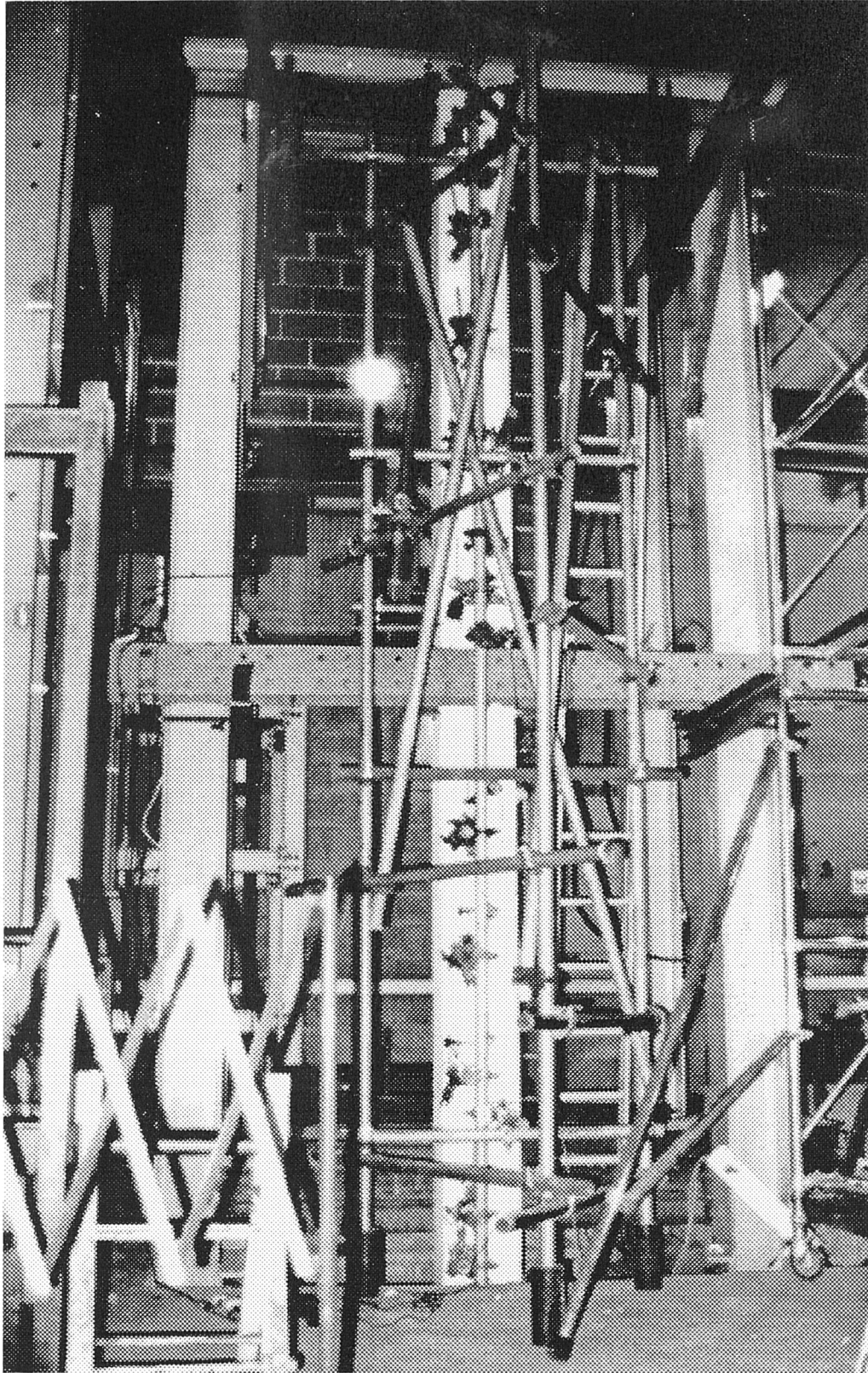


**FIG.4.10 GENERAL LAYOUT OF THE TEST RIG**

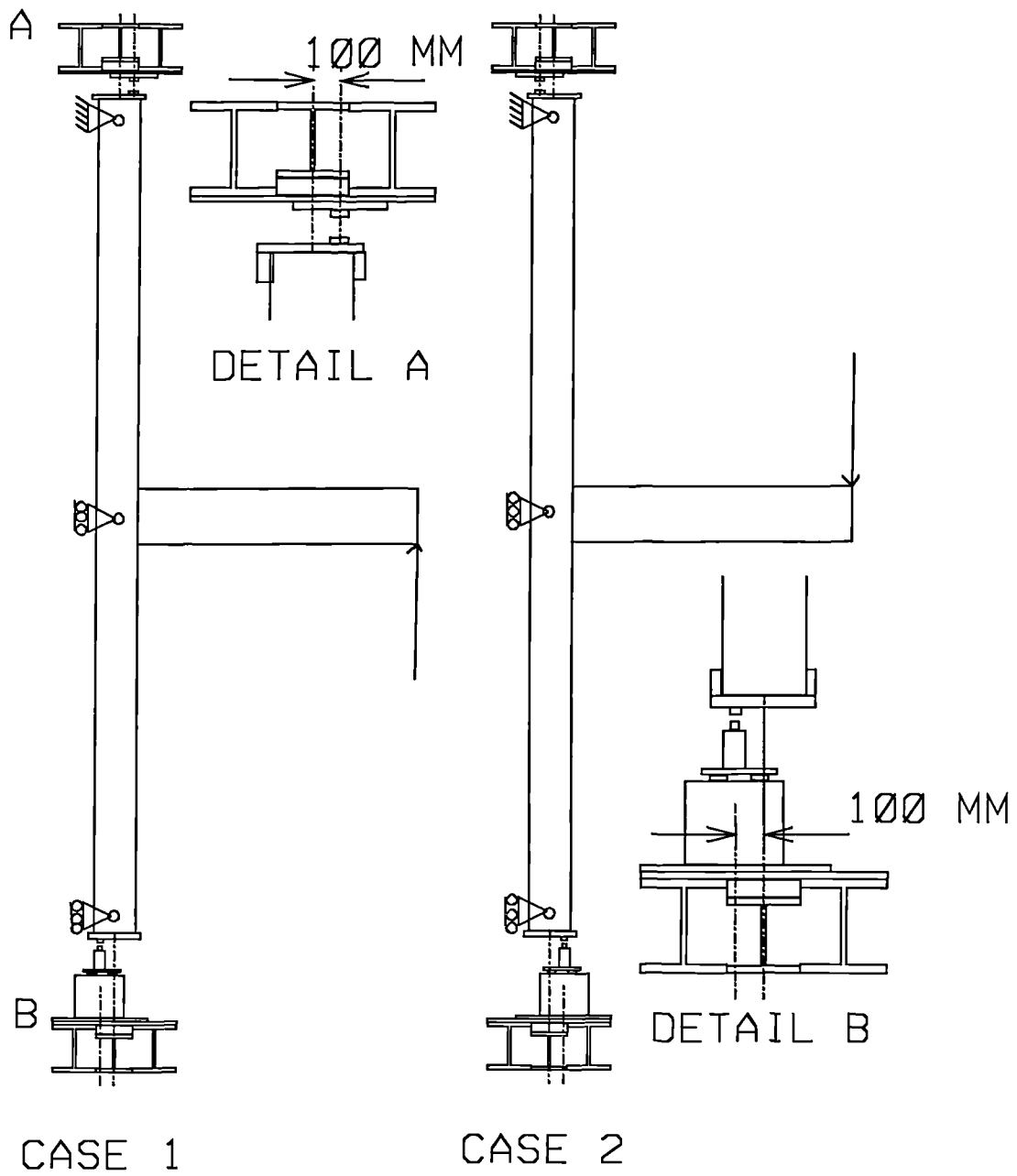


**FIG.4.11 TWO LOADING CASES FOR WHICH SUBFRAMES ARE**

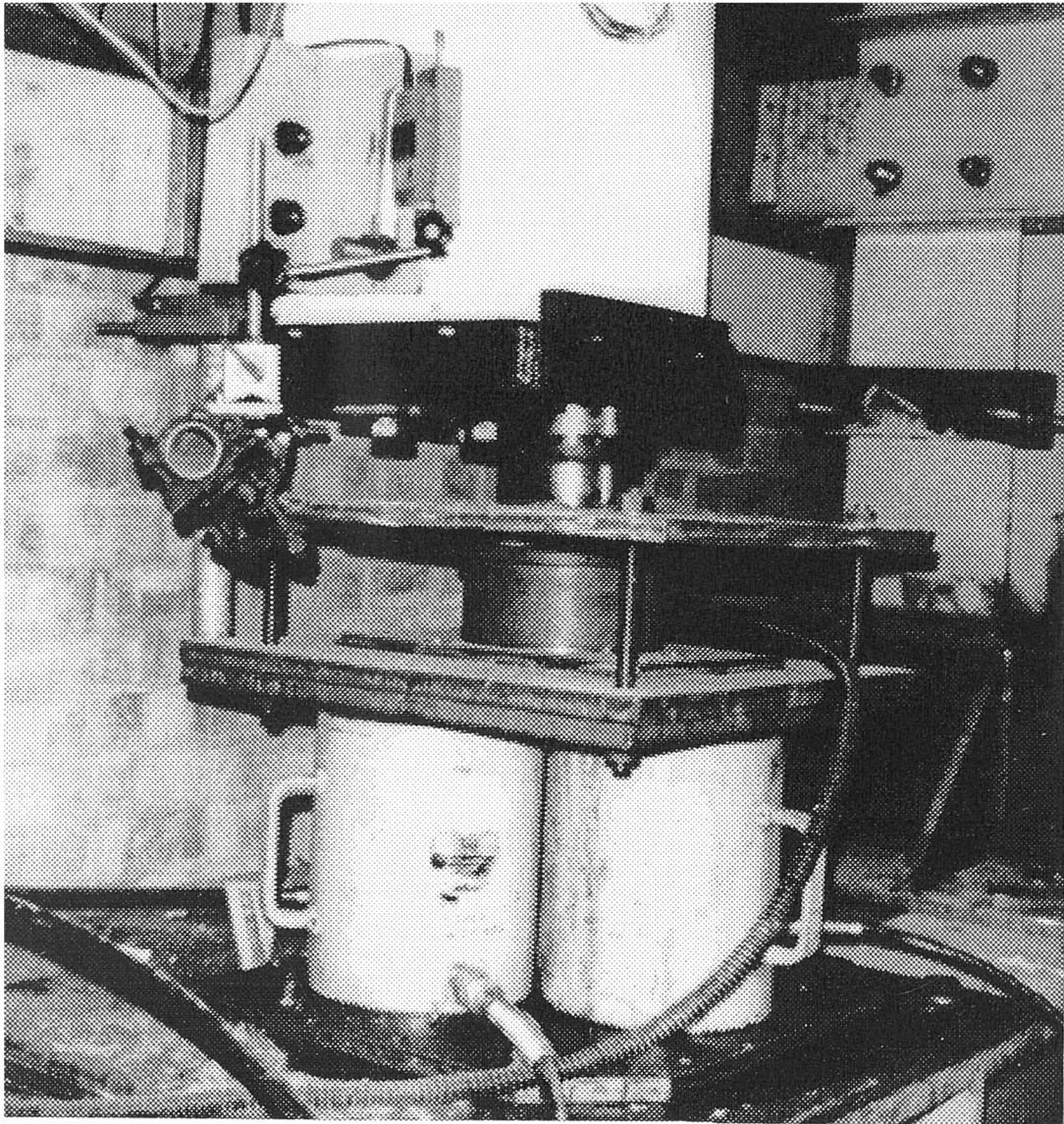


**FIG.4.12 LAYOUT OF JACKS**

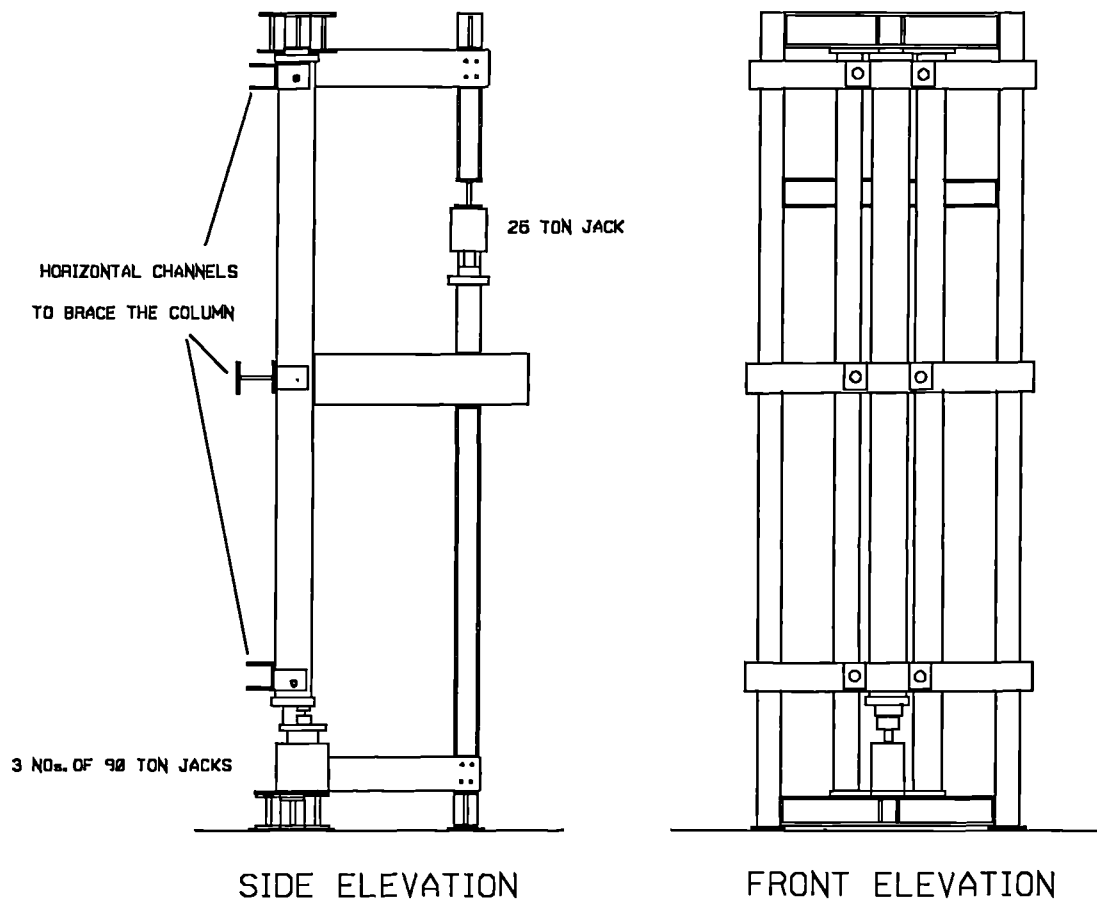


**FIG.4.13 COLUMN BEAM ASSEMBLY ON THE TEST RIG**

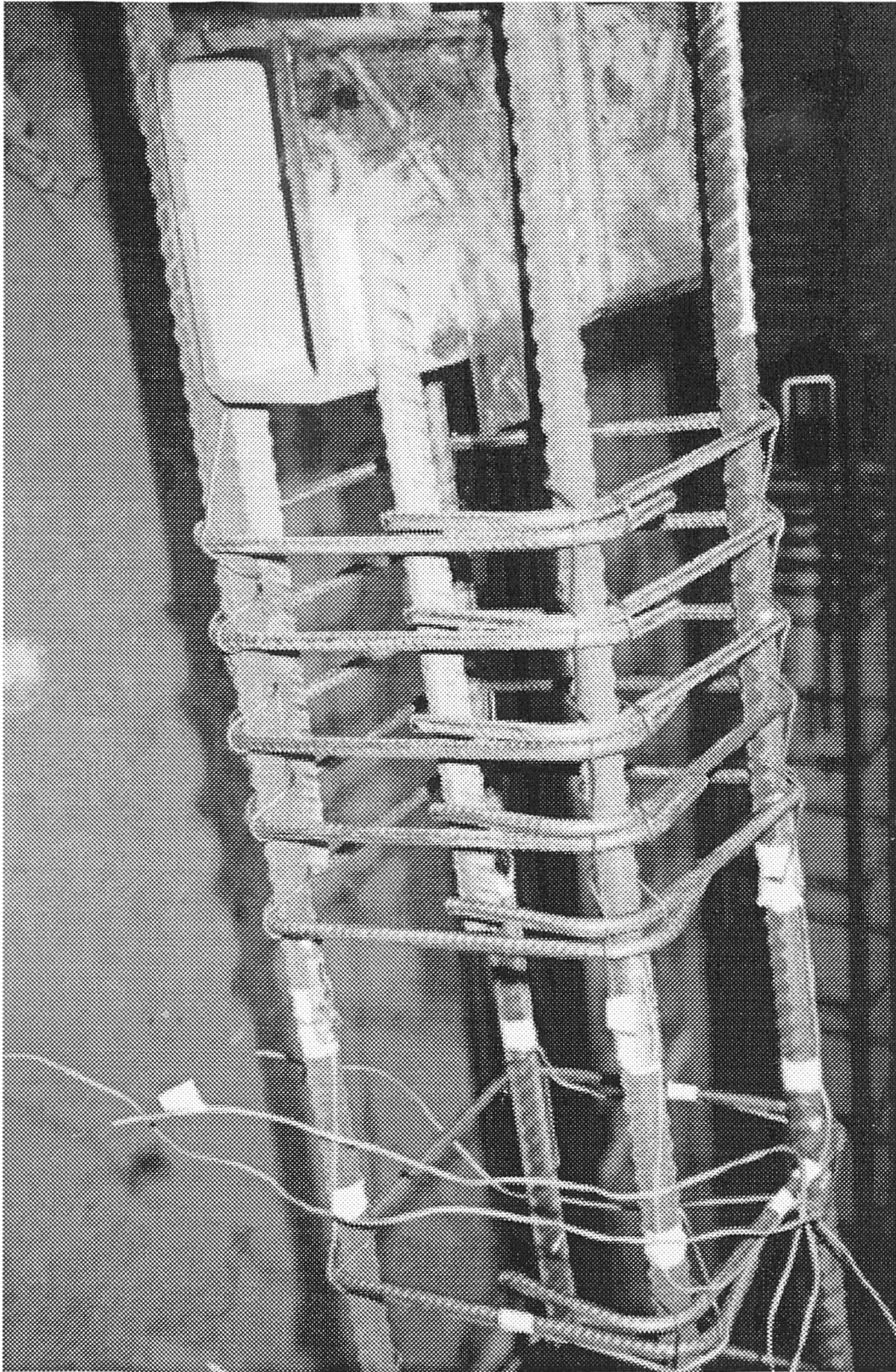


**FIG.4.14 INTERNAL STRAIN GAUGES**

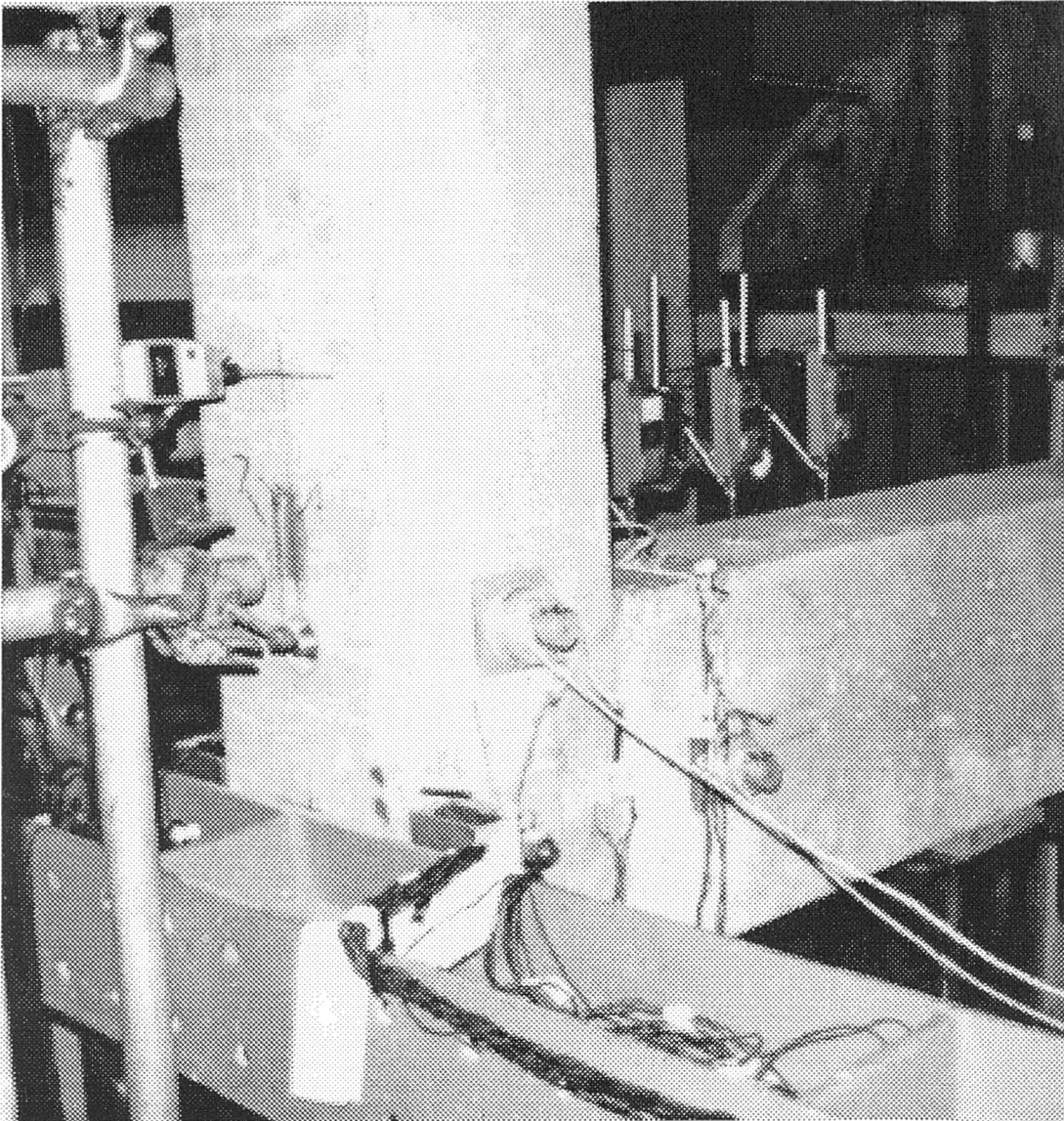


**FIG.4.15 DIGITAL READOUT DIAL GAUGES AND INCLINOMETERS**

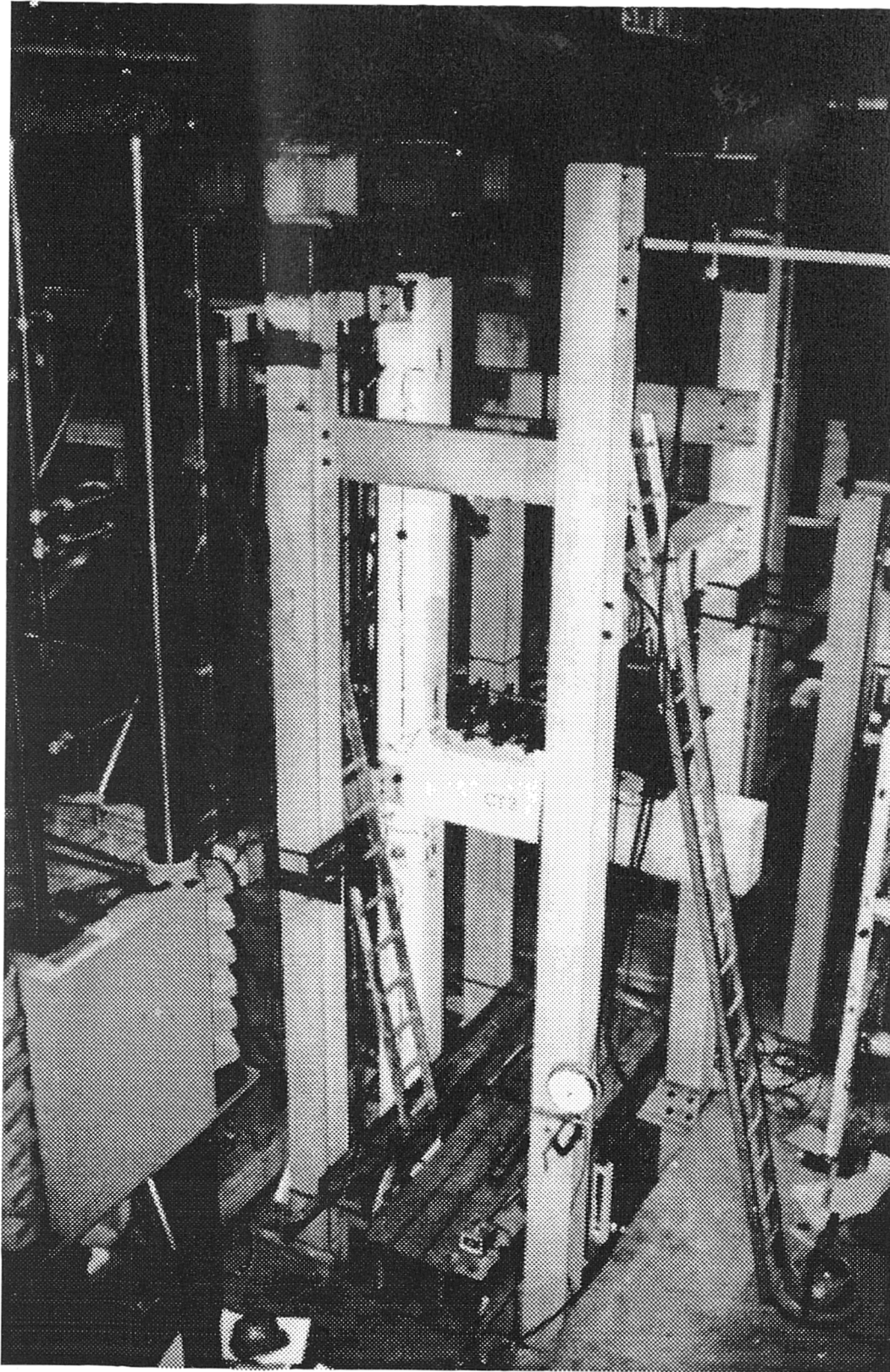


**FIG.4.16 COLUMN BEAM SUBFRAME IN POSITION**

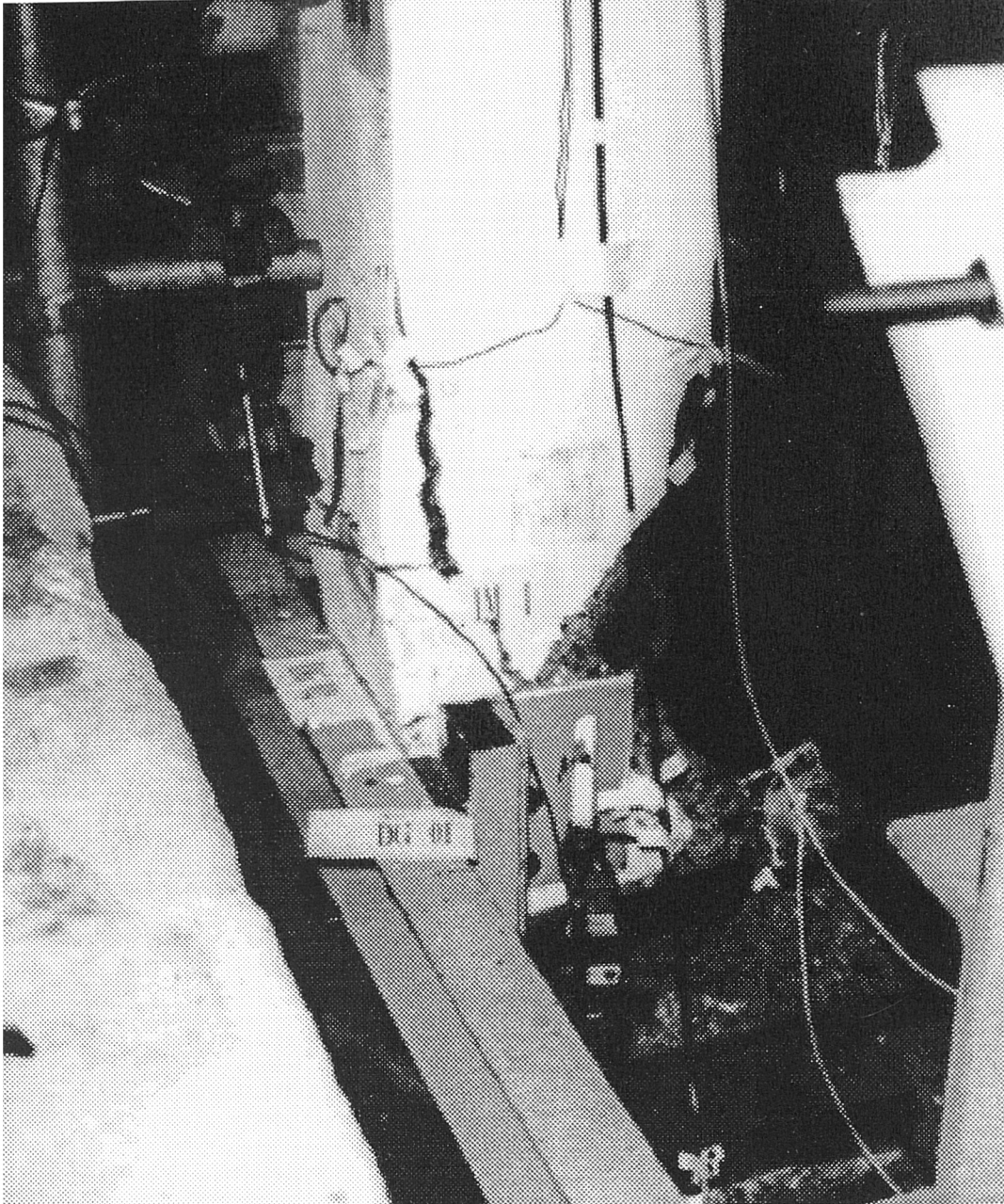


**FIG.4.17 COLUMN FAILURE (CT3)**



**FIG.4.18 CRACK PATTERN IN THE UPPER COLUMN**

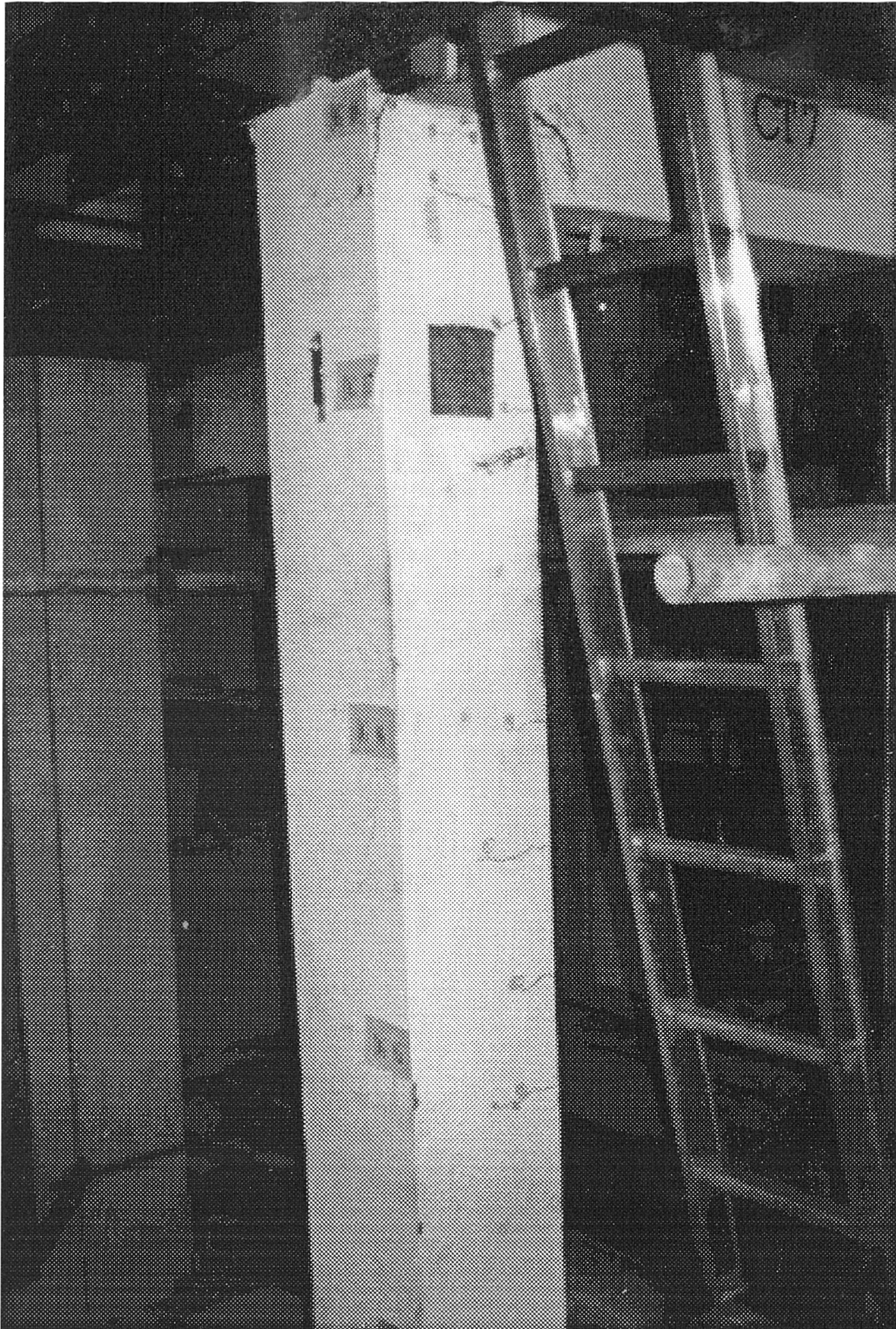


**FIG.4.19 CRACK PATTERN IN THE LOWER COLUMN**



**FIG.4.20 FAILURE OF BEAM COLUMN JOINT (CT7)**

## **CHAPTER 5.**

### **COMPARISON OF EXPERIMENTAL RESULTS WITH COMPUTED RESULTS**

#### **5.1 INTRODUCTION**

In Chapter 3, a new method of analysis of precast concrete frames with semi-rigid joints was described. Tests on eight subframes consisting of 2-storey precast column connected to precast beams with semi-rigid joints were described in Chapter 4. The behaviour of eight test subframes CT1 to CT8 is now compared with computed results from the new method of analysis. The non-linear analysis is based on observed stress-strain data of concrete and steel used in manufacturing the subframes. The equilibrium deflected shapes of the subframes were calculated at all the recorded load combinations used in the experiment. The analytical and test results are compared below.

#### **5.2 MATERIAL MODEL USED IN THE ANALYSIS**

The average cube strength obtained for each subframe was used to define the stress-strain characteristic of concrete. The ultimate stress of concrete in the column was obtained by multiplying the cube strength by 0.67 in accordance with BS8110. Material partial safety factor for concrete was assumed as 1.0, a factor commonly used to compare experimental results. A parabolic variation upto maximum compressive stress and a constant stress variation upto crushing of concrete were assumed as given in BS8110,Part1:1985. The tensile strength of concrete was assumed to be zero.

The average yield strength of cut steel bar of each subframe was used to define the stress-strain characteristic of reinforcement steel. An elastic perfectly plastic bi-linear relation was assumed as suggested in BS8110:Part 1:1985. Material partial safety factors used was 1.0. A sample stress-strain curve for concrete and steel is shown in Fig 5.0.

### **5.3 MODELLING SUBFRAMES FOR COMPUTER ANALYSIS**

As mentioned in Chapter 3 the section of the members was represented by single rectangular element with eight Gauss points. The reinforcements were treated as additional Gauss points with the steel area as weight of that Gauss point. The two storey continuous column was treated as pin-ended at all the two ends. The top end of the column was considered restrained in all three directions of displacements but allowing only inplane rotation. The mid-point and the bottom supports of the continuous column were restrained against inplane and out of plane movement but were allowed to slide vertically and to rotate inplane. The column load was applied vertically at the bottom end of the column with an eccentricity of 100mm. The reaction at the top end of the column was set at 100mm eccentricity in an opposite direction to that at the bottom end.

The beam load and the moment transferred from the beam were directed at the mid-point of the two storey column. Both the upper and lower columns were subdivided in to 12 segments for the analysis.

The equilibrium deflected shape analysis of the subframe was carried out for each of the load cases as observed in the experiment. The deflection at stations and strain pattern across the sections were obtained for the

continuous column. These calculated deflections and strains are compared in the following section with the values obtained from the experimental values.

For the final beam load an ultimate load analysis was carried out by increasing the column load until further equilibrium deflected shape could not be found. This ultimate load analysis was carried out to compare the failure column loads (for specimens CT1-CT6 and CT8) or failure beam moment (in case of specimen CT7) with the experimental values.

#### **5.4 COMPARISON AND DISCUSSION OF RESULTS**

The comparison between experimental and analytical behaviour of the two storey columns is discussed under the headings of deflection and strain to highlight the accuracy of the analytical prediction and to explain the discrepancies if any.

1. Deflected shape of the two storey column for increasing axial load.
2. Deflection at the centre of the upper column with axial load.
3. Deflection at the centre of the lower column with axial load.
4. Strains at selected points in the upper column against axial load.
5. Strains at selected points in the lower column against axial load.
6. Strains across the section for increasing axial load.

A point to note while assessing the graphs is that there are two variables, namely column axial load and beam moment. The graphs demonstrate deflection or strain for only one variable. Thus, for example, when the column axial load is kept constant while beam load is varied, a flat line is observed. The numerical values in all the graph presented here are tabulated

in the Refs.[68,69]. The loading sequences followed for each test are also detailed in Refs.[68,69].

## **COLUMN DEFLECTIONS**

The variation of deflections with the axial load applied to the two storey column for all the tests is shown in Figs 5.1 to 5.24. Change in beam moment varied with axial load is noted in parenthesis. A set of three graphs are presented for each test. The first graph in the set shows the computed and experimental deflections for the two storey column. The following two graphs show the deflection at the centre of the upper and lower column, respectively.

As explained in Chapter 4, test CT1 unfortunately did not reach the expected failure load. The column failed prematurely at the base due to an earlier slight damage at that end during the erection procedure. Nevertheless the performance of the column up to the observed premature failure is compared (Fig 5.1- 5.3) with the computed values and it shows good agreement. The difference in analytical and experimental deflection of the lower column becomes almost zero at the last observed column load. The observed upper column deflection is consistent with the computed deflection but the magnitude of the initial discrepancy remains constant with the increment in axial load.

It should be noted that the computed and experimental deflected shapes are in excellent agreement for the tests CT2 and CT5 over the full range of applied loading (Fig 5.4 - 5.6, 5.13 - 5.15). The uneven experimental deformation of the upper and lower columns in test CT2 are difficult to explain, this behaviour was not observed in the other seven experiments. The

uniform variation of the observed strain on the column shown in Fig 5.28 and 5.29 supports this argument. The observed deflection profile shown for CT5 is uniform and in excellent agreement with the calculated deflections.

For test CT3 (Fig 5.7 - 5.9) the computed and experimental deflections for the lower column are in good agreement. However in the upper column the computed and experimental deflections show some divergence particularly near failure. Reversing of calculated deflection between column loads of 126kN to 402 kN was observed as shown in Fig.5.8 and 5.9. The mid span deflection of the column for low axial load and high end moment was reduced as the column load increased while the beam moment remained constant. This is similar to pre-stressing effect. The actual behaviour of the column did not exhibit this except for the steeper load deflection curve in that region. Even though the observed load deflection profile of the upper column was similar in nature, the deviation with increase in column axial load is attributable only to the movement of the test rig as the beam load was increased to develop high connection moment while the column axial load was low.

For experiment CT4 (Figs 5.10 - 5.12) the computed deflections show consistently good agreement with the experimental deflections, the agreement improving with increasing axial load. The beam load was increased in two stages to avoid rig movement at high beam load as observed in experiment CT3. The two stages of beam load increment could be observed by two horizontal load mid-span deflections shown in Fig5.11, 5.12. However, subframe CT4 was not loaded right up to failure and the test was terminated just slightly prematurely. Bursting failure appeared imminent at the top of the column and it was considered unsafe to continue with the test.

Experiment CT6 (Figs 5.16 - 5.18) shows consistently good agreement between the computed and experimental deflections. The agreement improves with increasing axial load. The mid-span deflection is almost the same near failure for both upper and lower columns. The upper column displayed larger displacement at mid point than the calculated value and the difference reduce considerably near failure.

Experiment CT7 was conducted in a slightly different manner, compared with all the other experiments. The aim was to fail the column by applying excessive beam moment while the axial load in the column remained constant. Accordingly, the deflections are shown against beam moment (Figs 5.19 - 5.21). The computed and experimental deflected profile of the lower column show very good agreement. However the upper column, which suffered local shear damage near the joint, shows divergence between calculated and experimental deflections. Due to the high moment in the column beam joint the column section just above the joint cracked diagonally. The crack width was found to increase with increasing beam moment.

The deflected shape for test CT8 (Fig 5.22 - 5.24) is consistent over the full range of loading. The difference between the computed and experimental deflections decreases with increasing axial load. This subframe was also expected to have a very high connection moment. From the experience gained from experiment on CT7 it was decided not to fail the column by excessive beam moment. The column was loaded upto axial load of 500kN before increasing the beam load. The beam load was increased up to a point to produce 75% of the expected connection moment capacity. The wavy pattern that may be observed in the flat portion of the load displacement curve in

Fig 5.23 and 5.24 is due to observed increment in column axial load as the beam load was increased.

## **STRAIN ACROSS THE SECTION**

The calculated and experimental strains at preselected positions are shown in Figures 5.25 to 5.48 for all the tests. A set of three graphs are presented for each test. The first two graphs show the computed and experimental strains at the positions marked on the subframe diagram shown within each graph. The third diagram is an alternative way of presenting the data from the above two graphs, by showing the strain variation across the sections.

Strain measurement near the beam column joint is presented for experiment CT1 in Figs 5.25 to 5.27. The strain gauges near the ends of the column failed to function therefore the strain at the critical area, near the ends could not be recorded. The failure was expected to occur near the columns ends. The computed and experimental strain values are shown in Figs 5.25 and 5.26. The magnitudes of the strains compared are generally very small. Little correlation could be found in this experiment for strain. The strain profiles across the sections are shown in Fig 5.27.

The computed and experimental values of strain for test CT2 are given in Figs.5.28 and 5.29. The compressive strains (strain gauges SG2, SG7) show fair agreement, but the strain gauge SG8 shows some erratic response towards the failure load. The strain gauge SG1 did not show any response and it could be due to some defect in the strain gauge. The above information is additionally shown as strain profile across the section in Fig. 5.30.

The results of strains for experiment CT3 are shown in Figs 5.31 and 5.32. Although the experimental and computed results do not show good agreement, over the loading range, strains in gauges SG1 and SG8 demonstrate good agreement near failure. The strain gauges SG2 and SG7 show good agreement in the early part of the curve. The strain profiles shown in Fig 5.33 show good agreement at lower load levels but the discrepancy increases at higher loads.

The strain profile for experiment CT4 is shown in Figs 5.34 and 5.35 and strain gauges SG1, SG2 and SG7 show excellent agreement but strain gauge SG8 shows diverging results. The strain profiles shown in Fig.5.36 show very good correlation except for compressive strain in section 1. The predicted strain pattern and the deflection pattern as shown in Figs 5.10 - 5.12 are in good agreement with the experimental observations.

In experiment CT5 the strain gauges SG2 and SG7 (Figs 5.37 and 5.38) show excellent agreement. Also, strain gauge SG8 shows consistent and good correlation with the experimental values. The strain Gauge SG1 seems to have an initial set back which is maintained through out the load range. This is reflected well in the section profile for strain shown in Fig.5.39.

All the strain gauges SG1, SG2, SG7 and SG8 in experiments CT6 and CT8 show excellent agreement (Figs 5.40, 5.41, 5.46 and 5.47). It may be noted that the displacement also showed good agreement for tests CT6 and CT8 between computed and experiment results. The strain profiles across the sections for tests CT6 and CT8 are shown in Figs 5.42 and 5.48 and it may be noted that the correlation between computed and experimental strains is excellent for both the tests.

As explained before for subframe CT7 the moment near the beam column joint was very high and therefore the strain near the joint was selected for comparison. The strains are shown with respect to beam moment in Figs 5.43 and 5.44. The calculated and experimental strains show good agreement in the lower column. Strain gauge SG6 shows close agreement in the initial loading and deviates towards the end. A vertical crack appeared in the upper part of the column, passing through strain gauge SG5, and it may be noted that the experiment terminated abruptly. The strain profile shown at section2 in Fig.5.45 shows very good agreement.

Correlation of deflection and strain in the behaviour of most of the subframes is an moderate indicator of the reliability of results predicted by the computer program "SWANSA" for varying moment and axial load conditions.

## **5.5 COMPARISON OF ULTIMATE LOADS**

As discussed in the previous section the prediction of deflections of the members and the strain patterns across the sections are very much in agreement with the observed values. The reliability of the numerical model in predicting the failure load in addition to the equilibrium deflected shape at intermediate loads is also an important factor to consider. Predicted failure loads for all the eight experiments are compared with the actual failure column load below in Tables 5.5.1 and 5.5.2.

**TABLE 5.1 EXPERIMENTAL AND THEORETICAL FAILURE LOADS****LOADS IN kN**

TEST NO.	EXPERIMENT	SWANSA	%ERROR	REMARKS
1	1140.4	1801.0	-----	Note 1
2	1939.1	1818.1	-6.2	
3	1862.2	1737.8	-6.7	
4	1704.9	1796.5	-----	Note 2
5	2042.8	2132.4	4.4	
6	2023.6	1899.2	-6.1	
8	2038.0	2086.1	2.4	

**TABLE 5.2 EXPERIMENTAL AND THEORETICAL FAILURE MOMENTS****MOMENTS IN kNmm**

TEST NO.	EXPERIMENT	SWANSA	%ERROR	REMARKS
7	180,136.0	238,489.0	32.4	Note 3

**NOTES**

1. Experiment CT1 did not reach the expected failure load due to accidental damage at the base during the erection procedure. This resulted in premature failure at the damaged end. The test was continued nevertheless to the end in order to gain experience for subsequent tests.
2. Experiment CT4 was terminated just below the failure load. The failure appeared imminent at the top of the column with the likelihood of bursting failure of concrete, and it was considered unsafe to continue with the test.

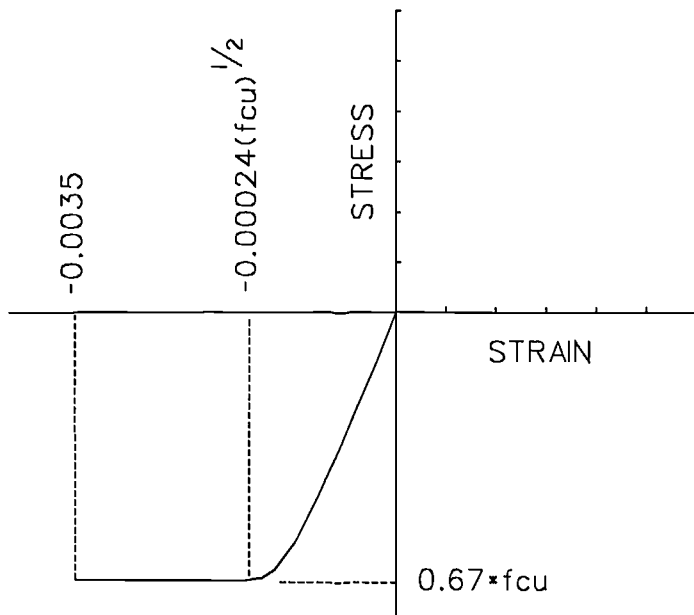
3. Experiment CT7 was tested with a very high beam moment and the column failed in transverse shear near the junction. The failure load is compared in terms of beam moment.

As noted above the failure of a two storey column due to its rather stocky nature was by sudden crushing of concrete. The analytical method also predicted this mode of failure. Except for the subframes CT1, CT4 and CT7 the analytical prediction of failure load is within 7%. This may be regarded as an excellent accuracy as far as concrete structures are concerned.

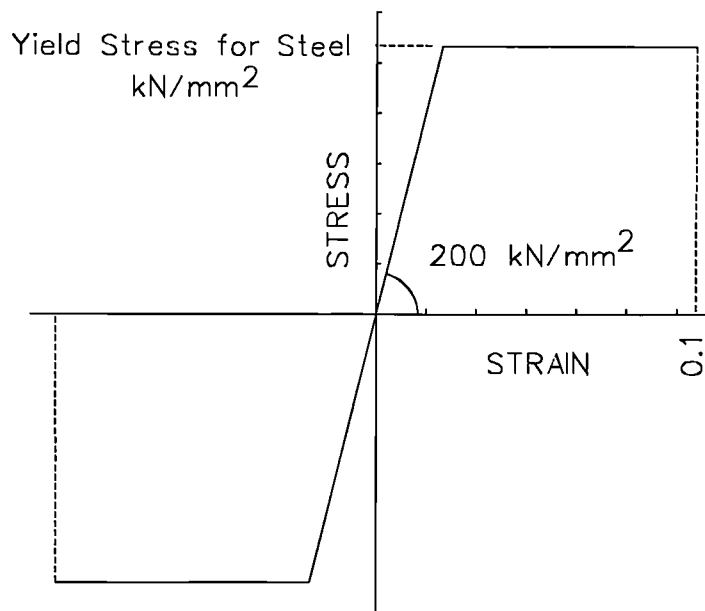
The behaviour of frames with slender members should also be considered before the acceptance of the results from the analytical method. In Chapter 6, the analytical results from portal frames with slender members are compared with experimental results obtained from published literature.

## **5.6 MOMENT ROTATION RELATION FOR THE JOINT**

From the measured rotations of the beams and the columns the relative rotation of the joints and the moments exerted by the beams in the centre of the columns were computed. The joint moments are shown with the relative rotation for all the joint tested in Fig 5.49. The response due to hogging and sagging moments for a joint is shown in one diagram for easy comparison. This data together with the moment rotation data collected by Nottingham University[71] could be used for future analytical study.



CONCRETE STRESS STRAIN CURVE



STRESS STRAIN CURVE FOR STEEL

**FIG.5.0 TYPICAL STRESS-STRAIN CURVE FOR CONCRETE & STEEL**

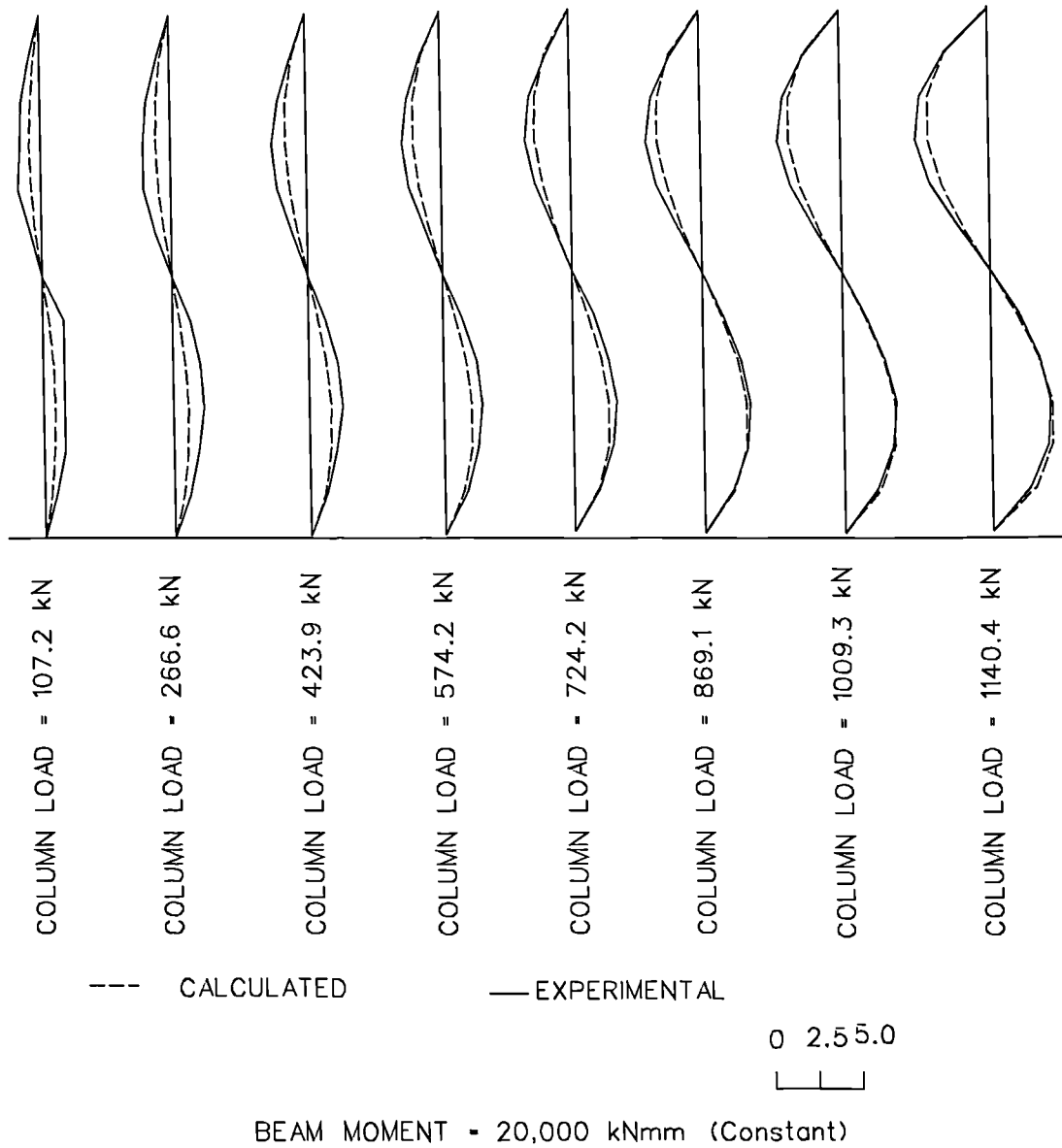


**FIG.5.1 COMPARISON OF CALCULATED DEFLECTION WITH EXPERIMENTAL VALUES (TEST CT1)**

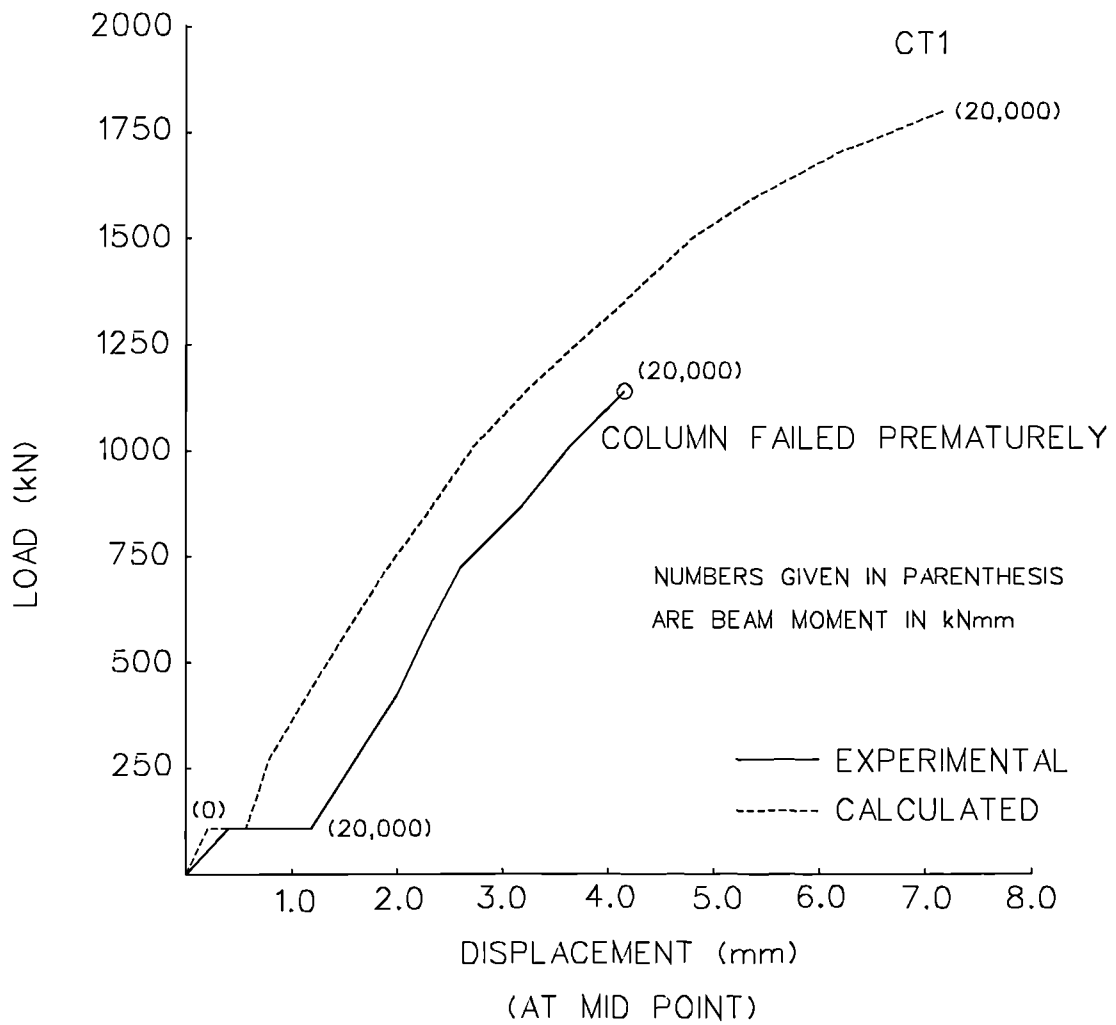


**FIG.5.2 LOAD DEFLECTION CURVE FOR UPPER COLUMN**

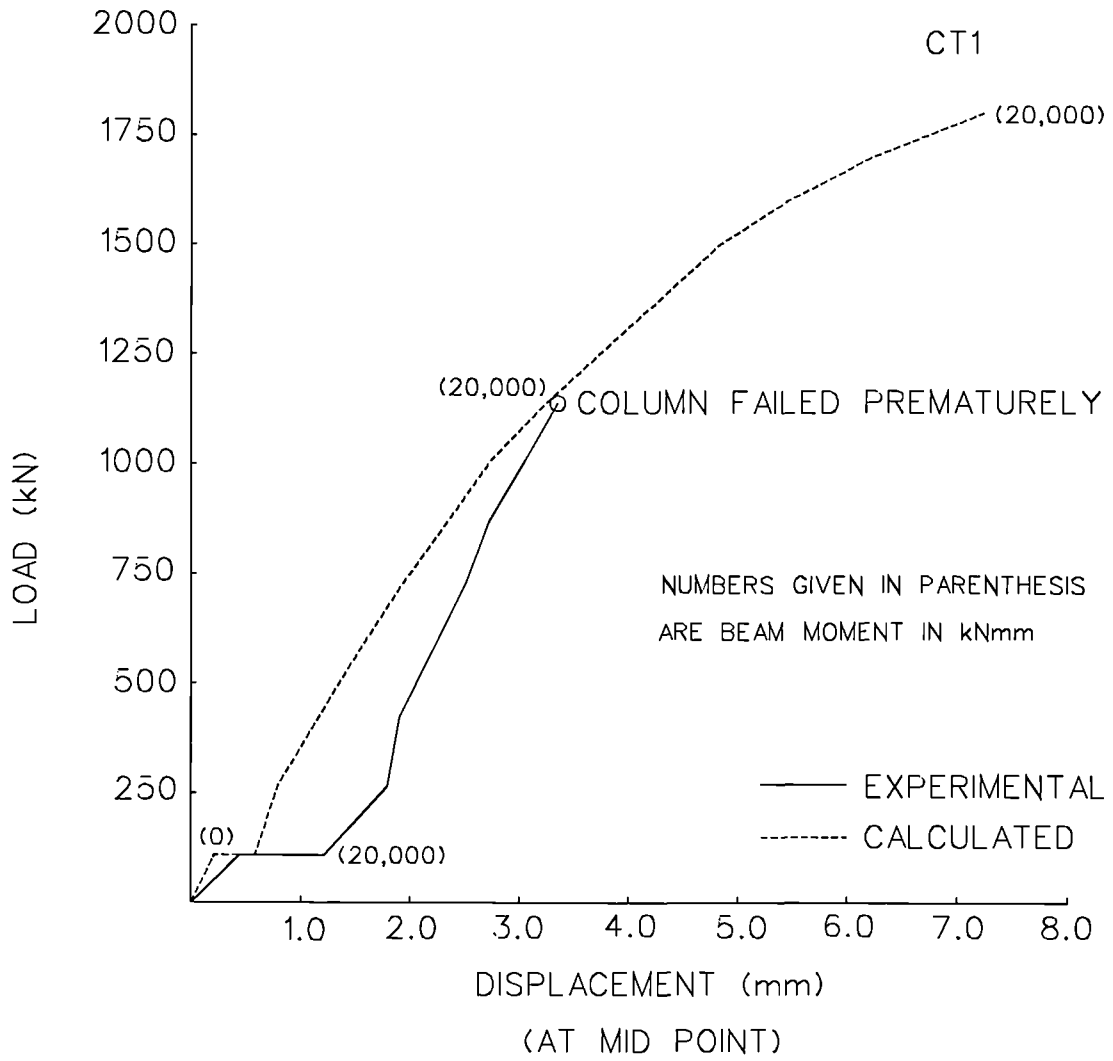


**FIG.5.3 LOAD DEFLECTION CURVE FOR LOWER COLUMN**

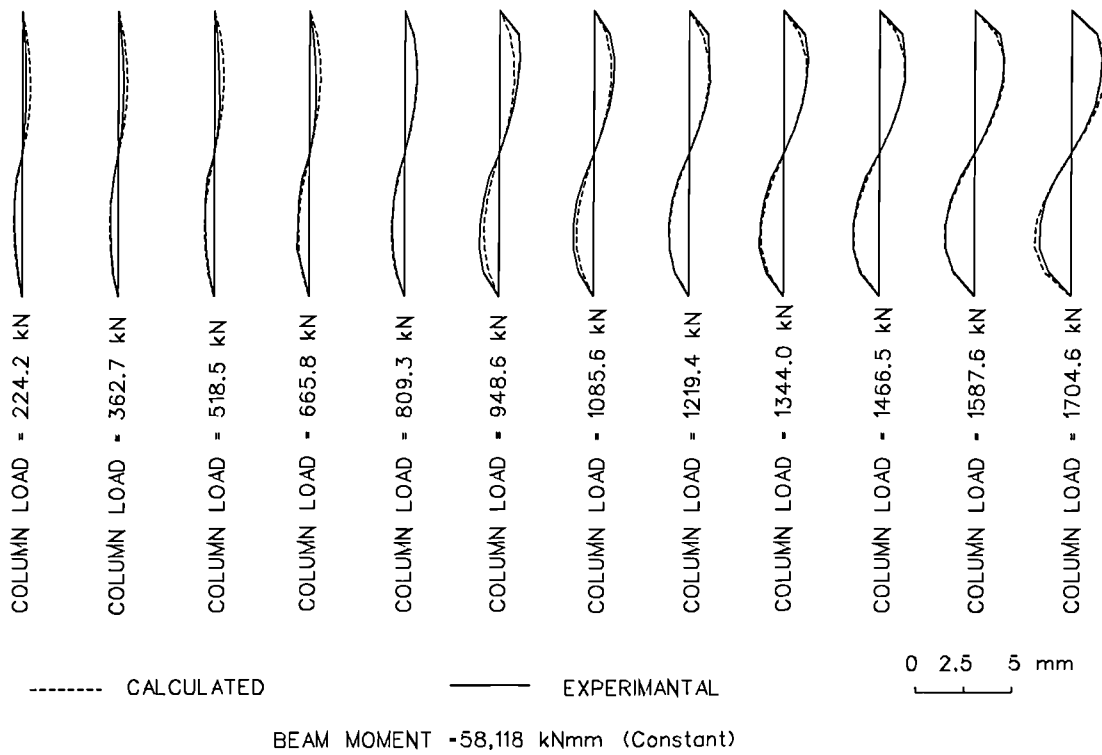


**FIG.5.4 COMPARISON OF CALCULATED DEFLECTION WITH EXPERIMENTAL VALUES (TEST CT2)**

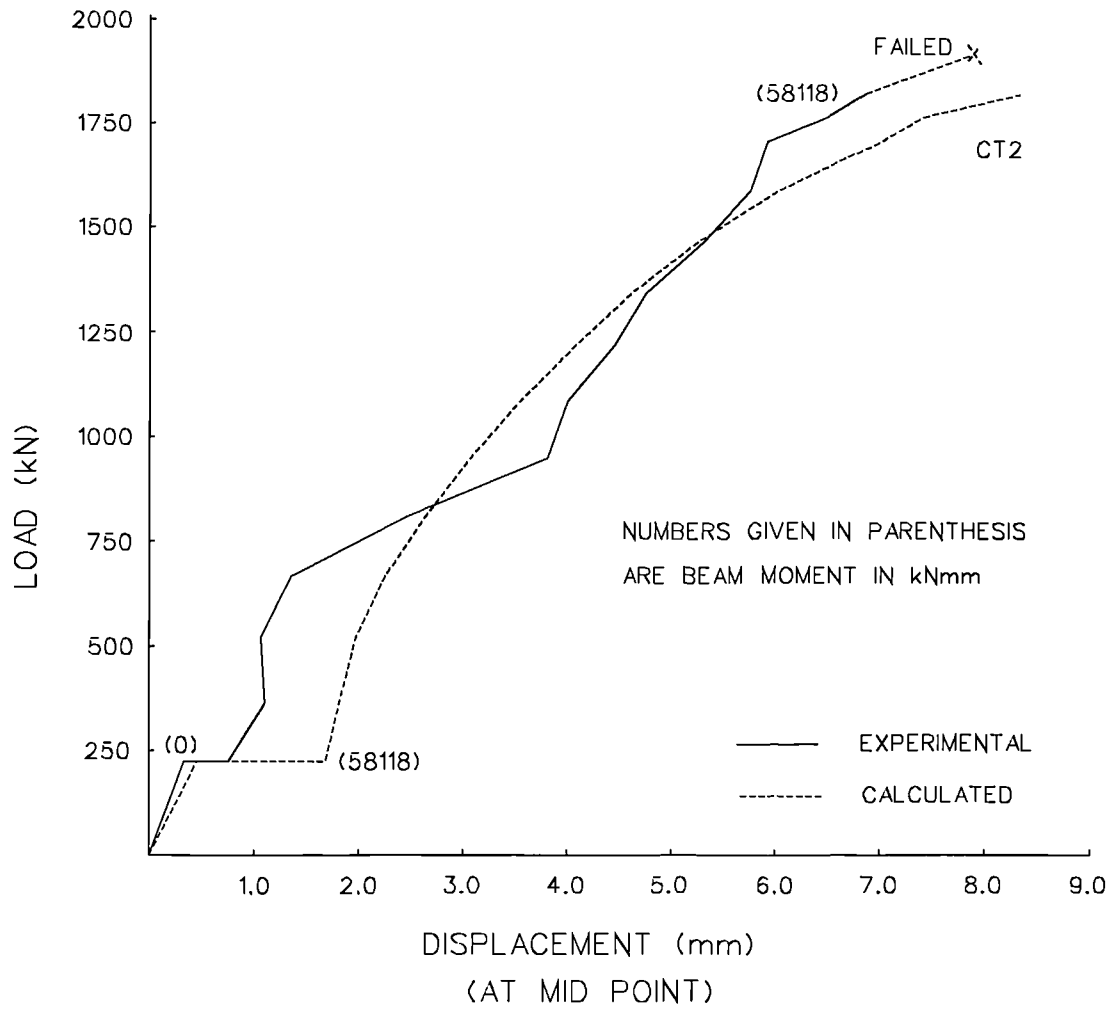


**FIG.5.5 LOAD DEFLECTION CURVE FOR UPPER COLUMN**

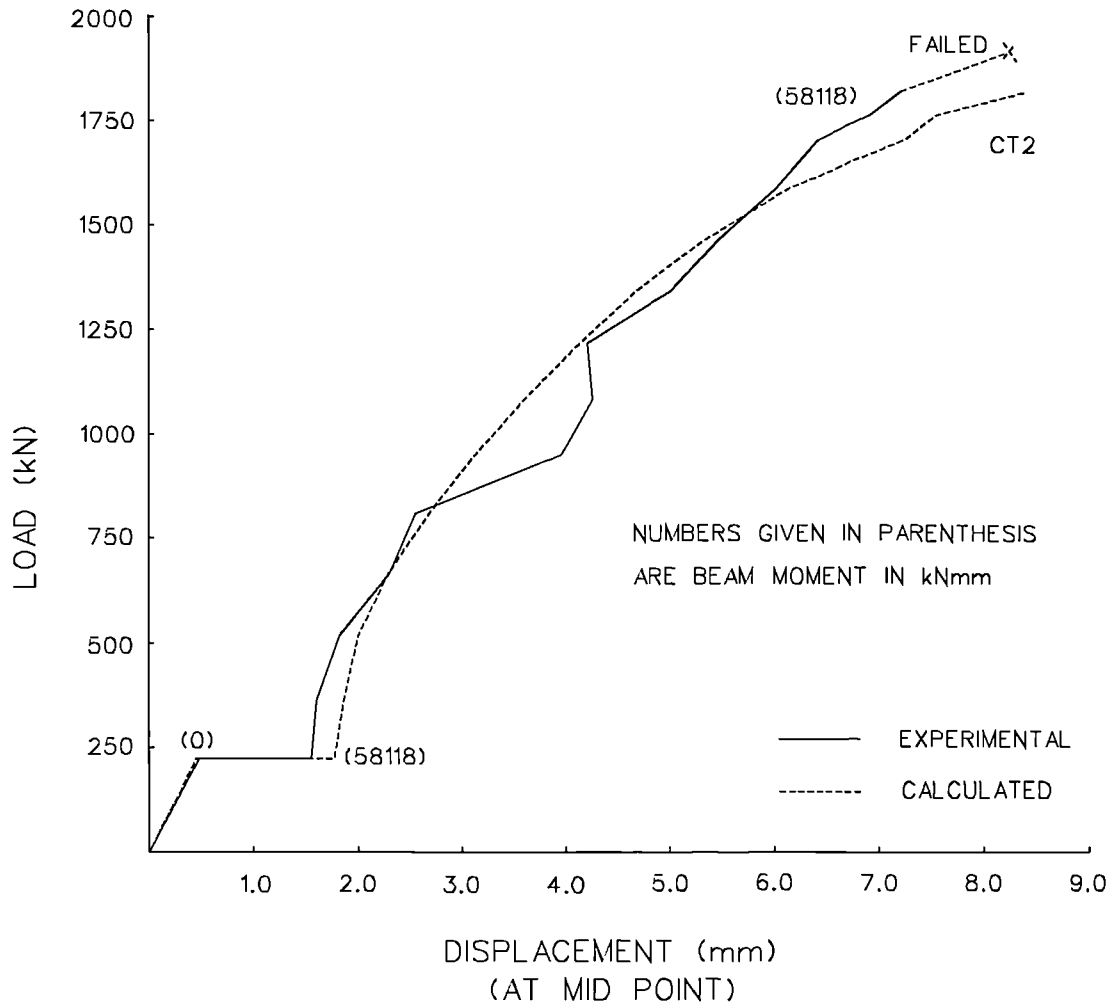


**FIG.5.6 LOAD DEFLECTION CURVE FOR LOWER COLUMN**

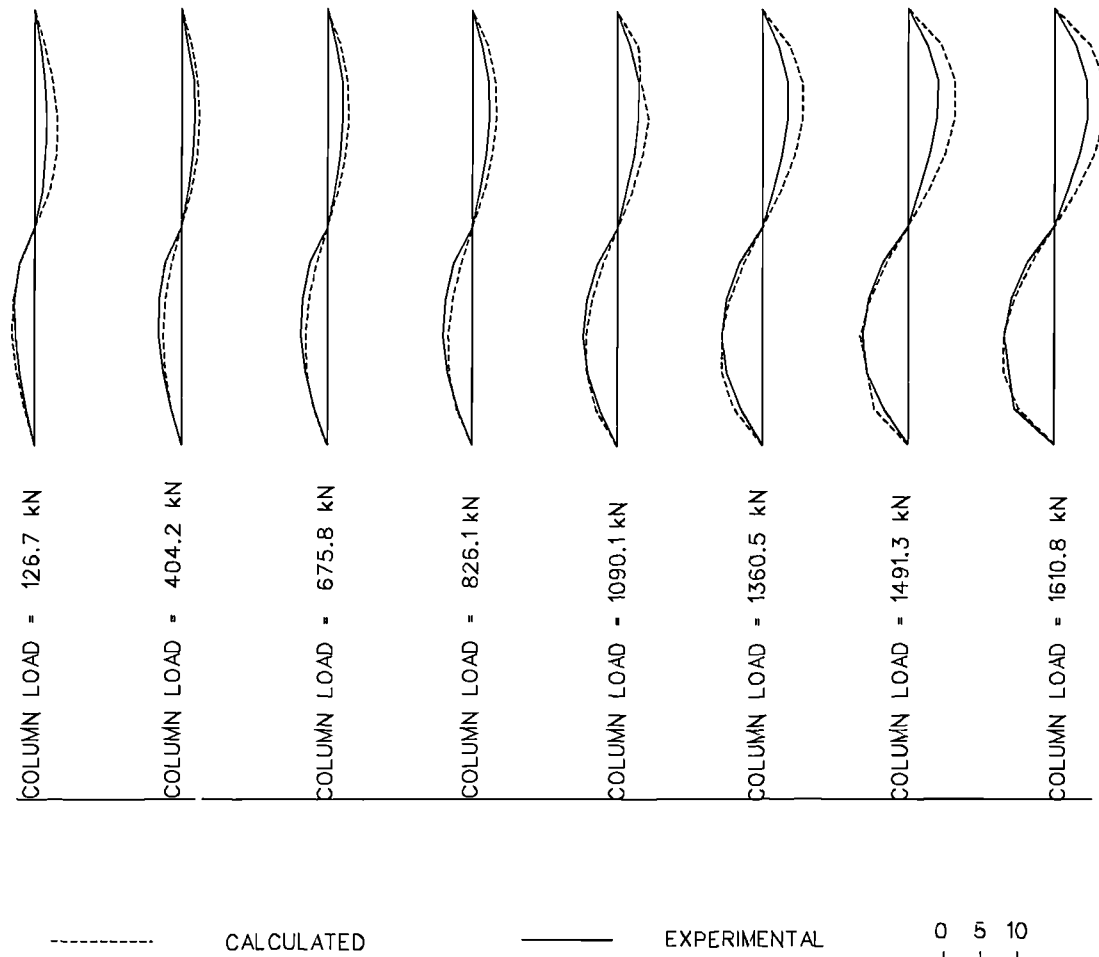


**FIG.5.7 COMPARISON OF CALCULATED DEFLECTION WITH EXPERIMENTAL VALUES (TEST CT3)**

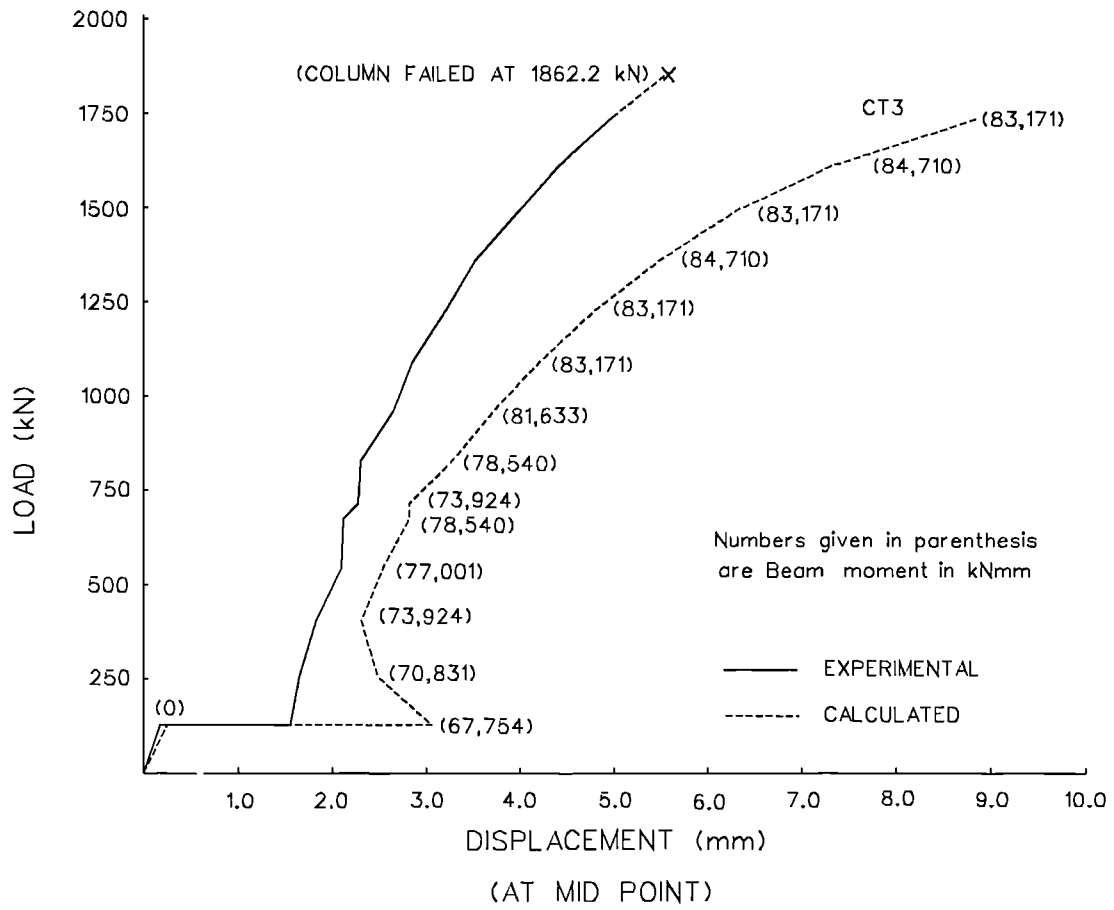


**FIG.5.8 LOAD DEFLECTION CURVE FOR UPPER COLUMN**

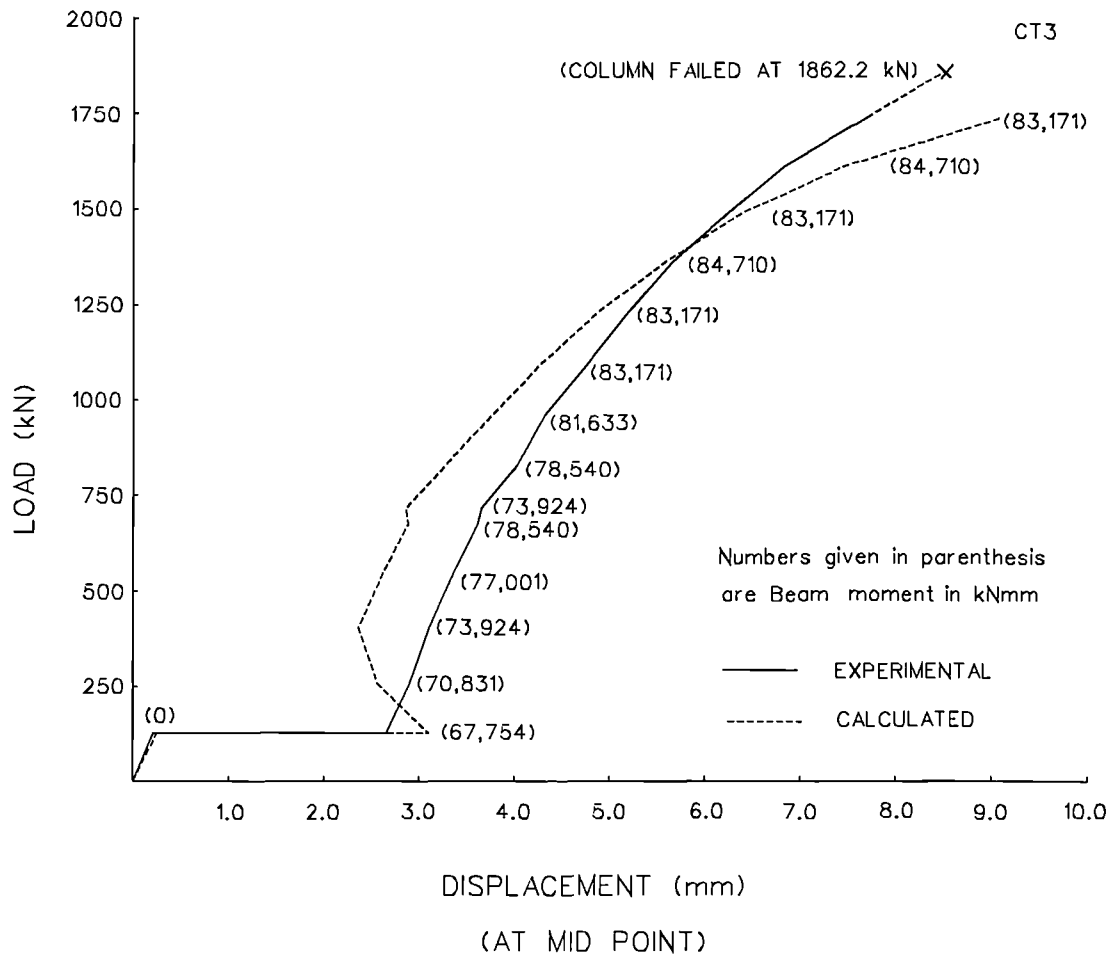


**FIG.5.9 LOAD DEFLECTION CURVE FOR LOWER COLUMN**

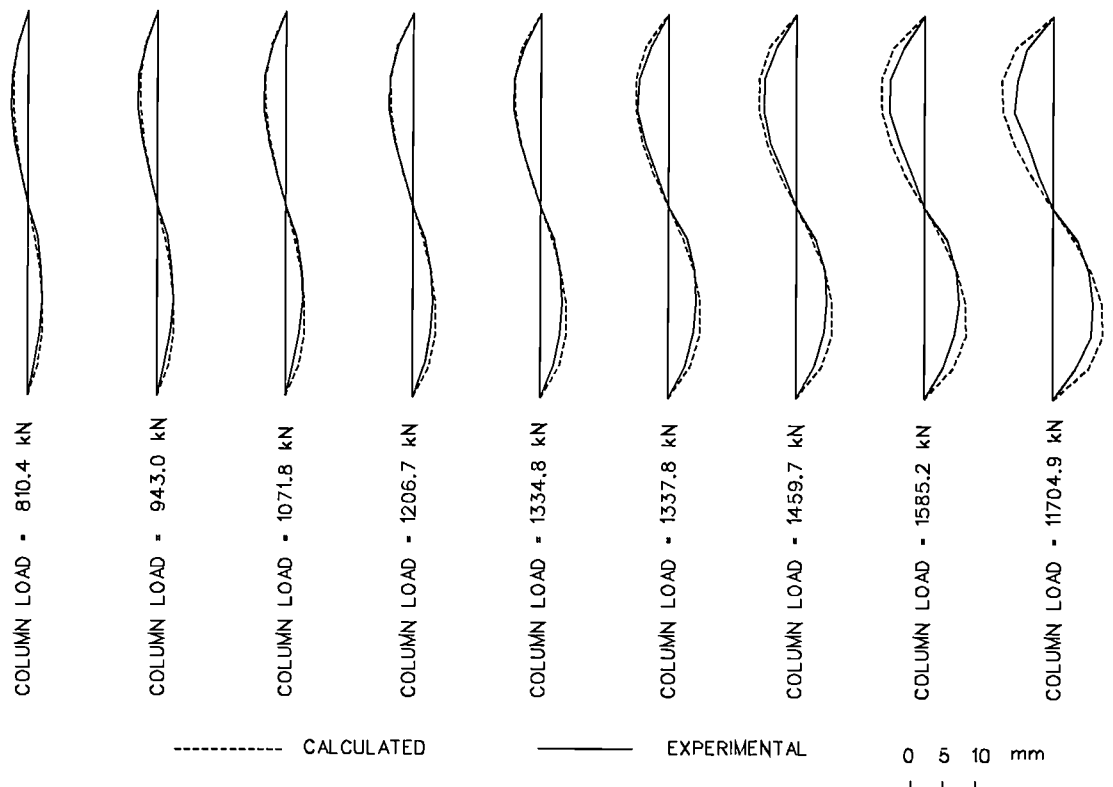


**FIG.5.10 COMPARISON OF CALCULATED DEFLECTION WITH EXPERIMENTAL VALUES (TEST CT4)**

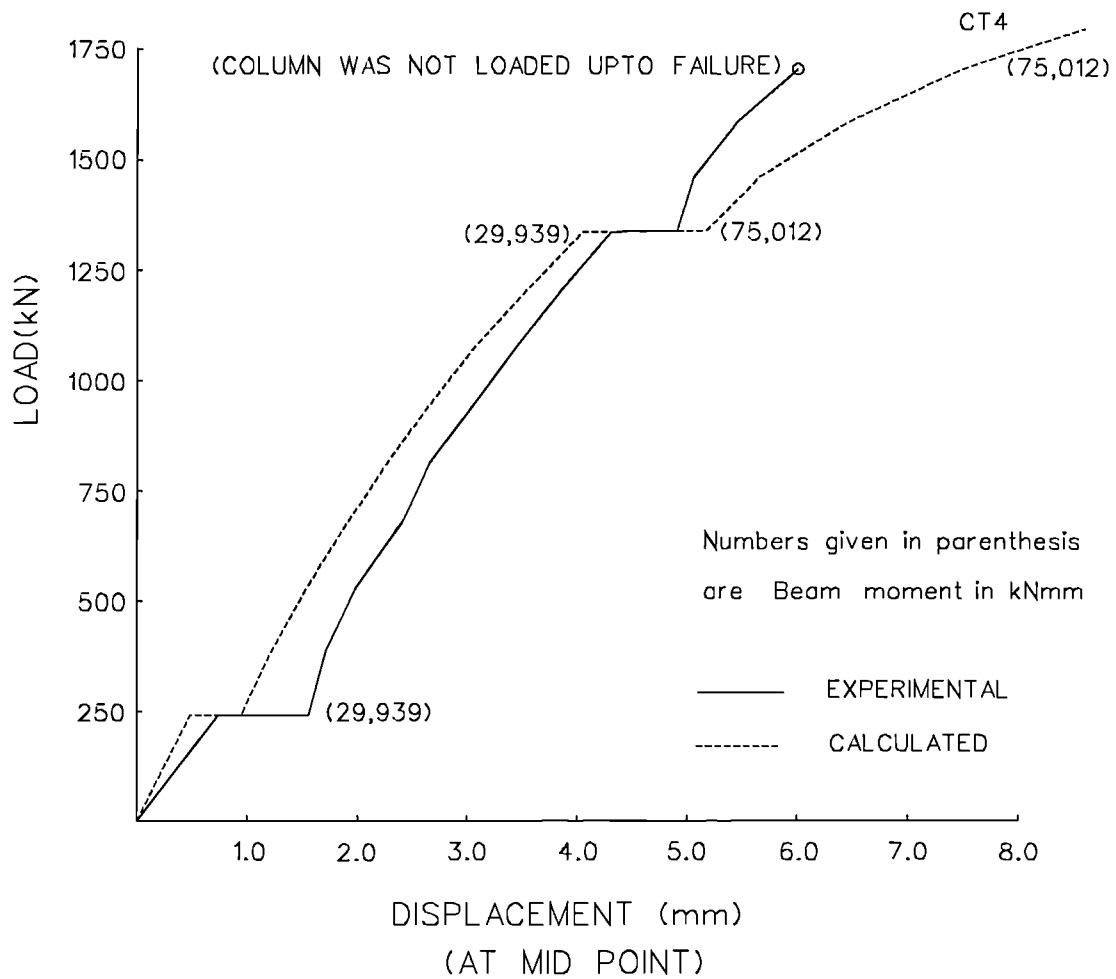


**FIG.5.11 LOAD DEFLECTION CURVE FOR UPPER COLUMN**

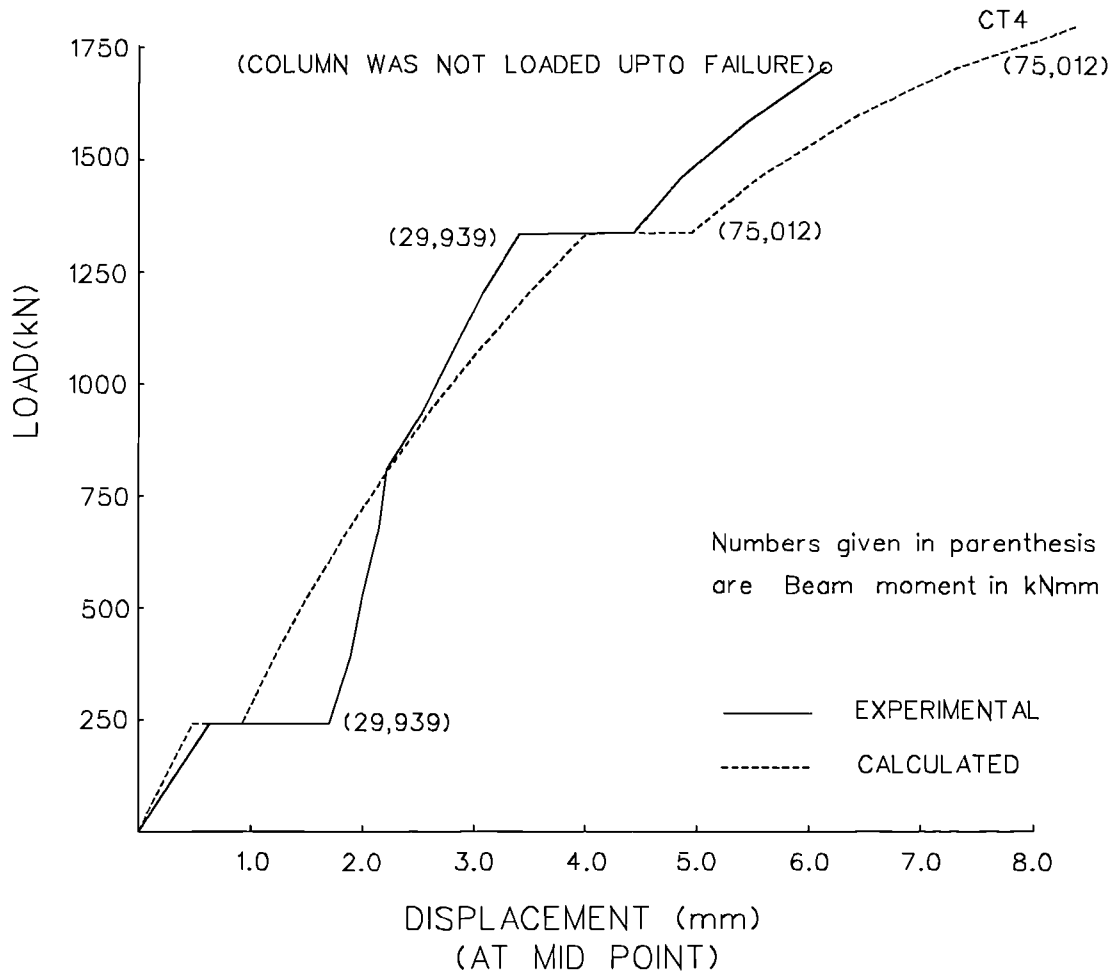


**FIG.5.12 LOAD DEFLECTION CURVE FOR LOWER COLUMN**

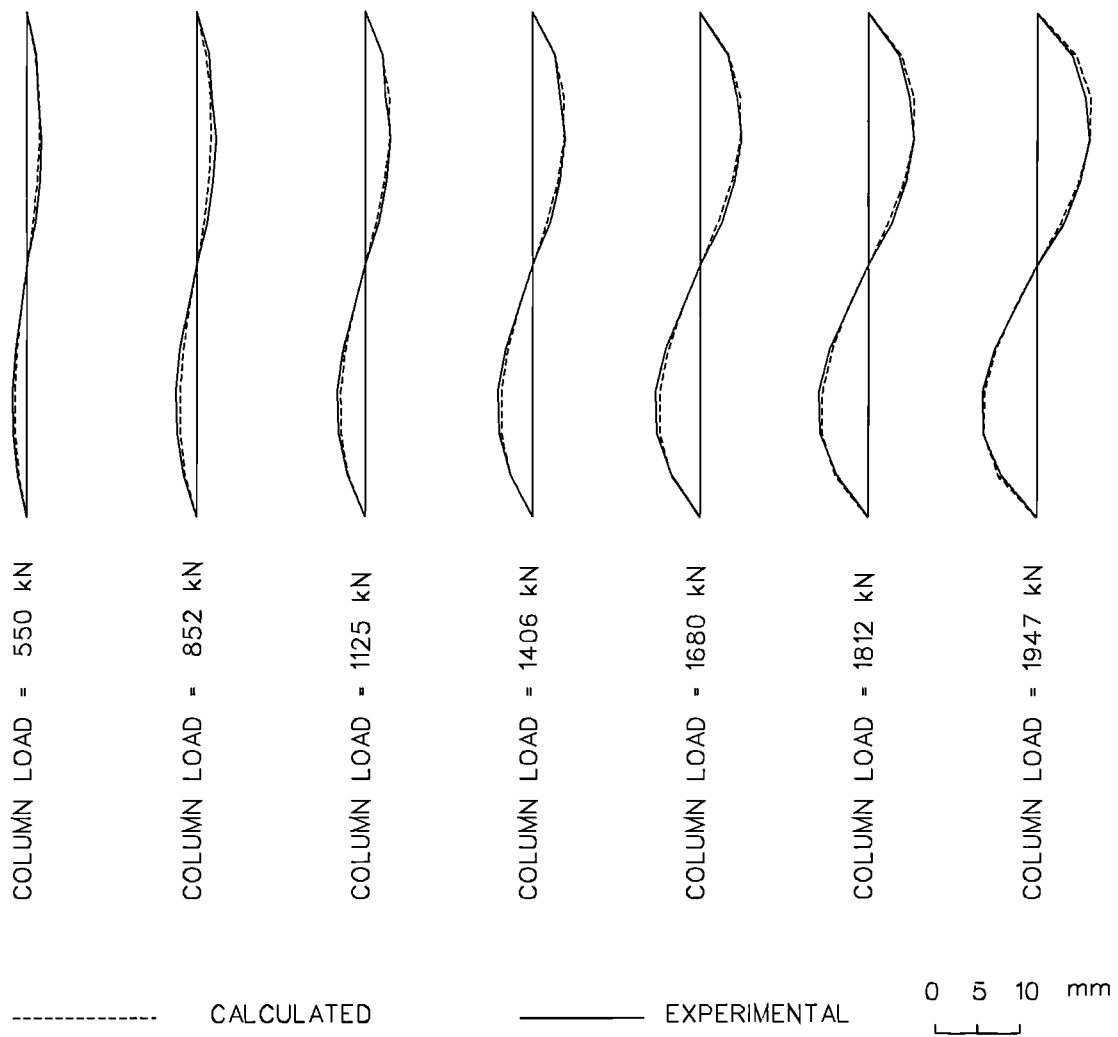


**FIG.5.13 COMPARISON OF CALCULATED DEFLECTION WITH EXPERIMENTAL VALUES (TEST CT5)**

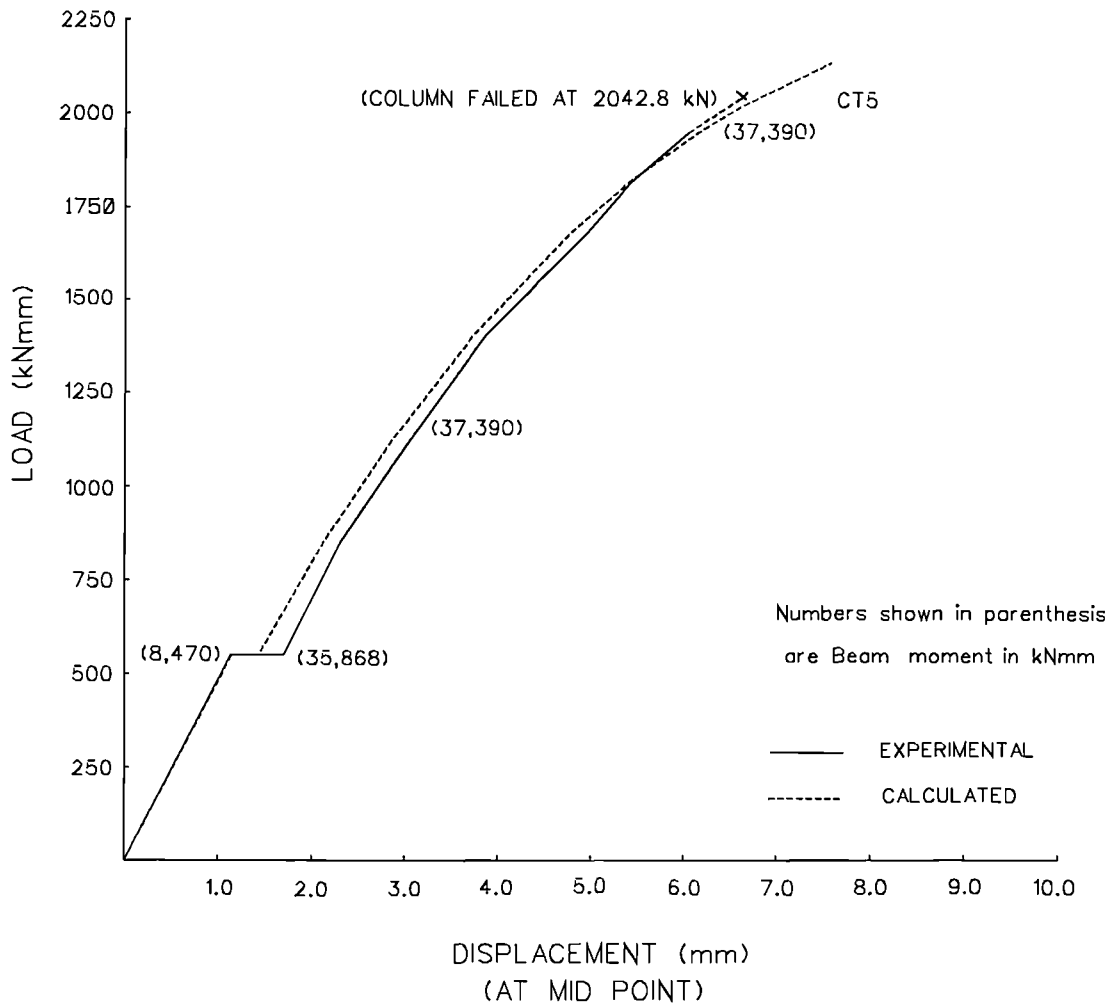


**FIG.5.14 LOAD DEFLECTION CURVE FOR UPPER COLUMN**

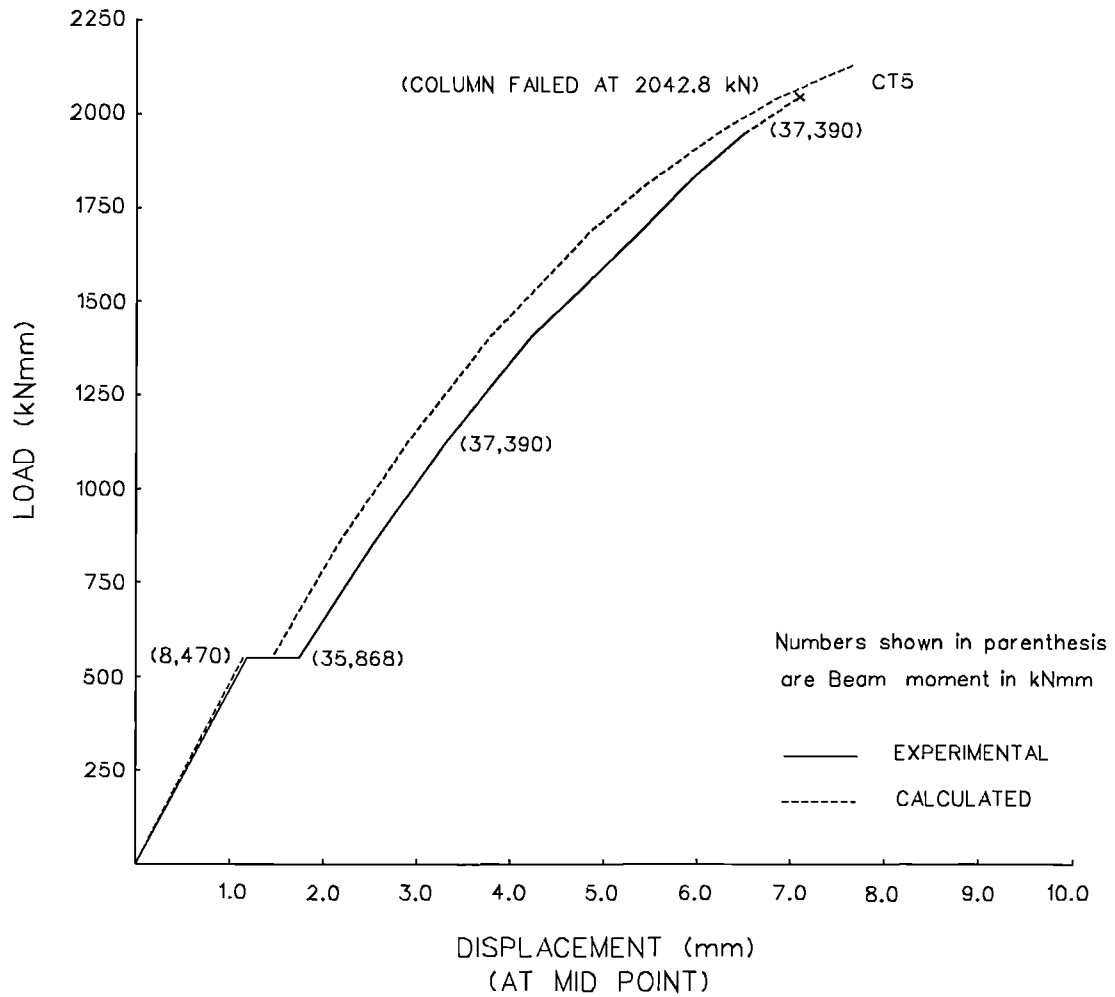


**FIG.5.15 LOAD DEFLECTION CURVE FOR LOWER COLUMN**

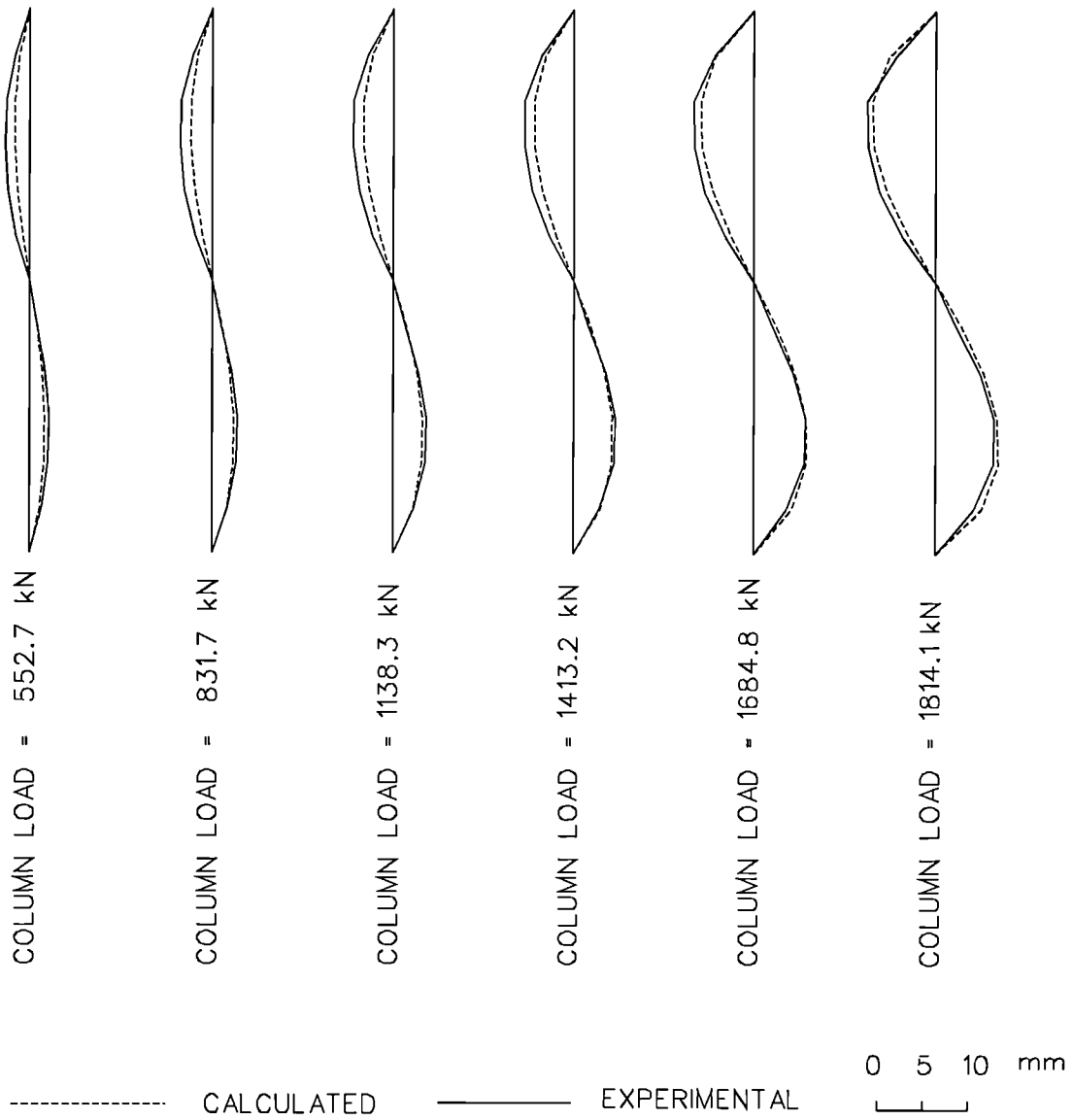


**FIG.5.16 COMPARISON OF CALCULATED DEFLECTION WITH EXPERIMENTAL VALUES (TEST CT6)**

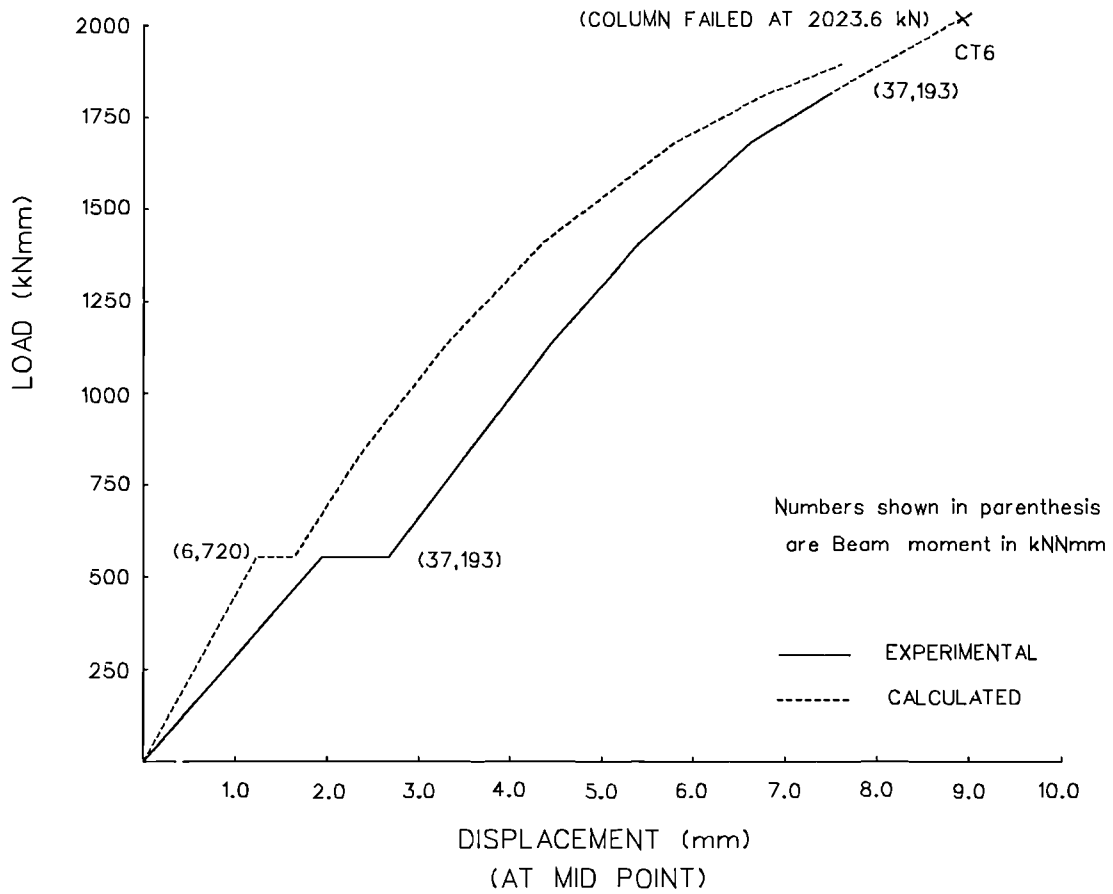


**FIG.5.17 LOAD DEFLECTION CURVE FOR UPPER COLUMN**

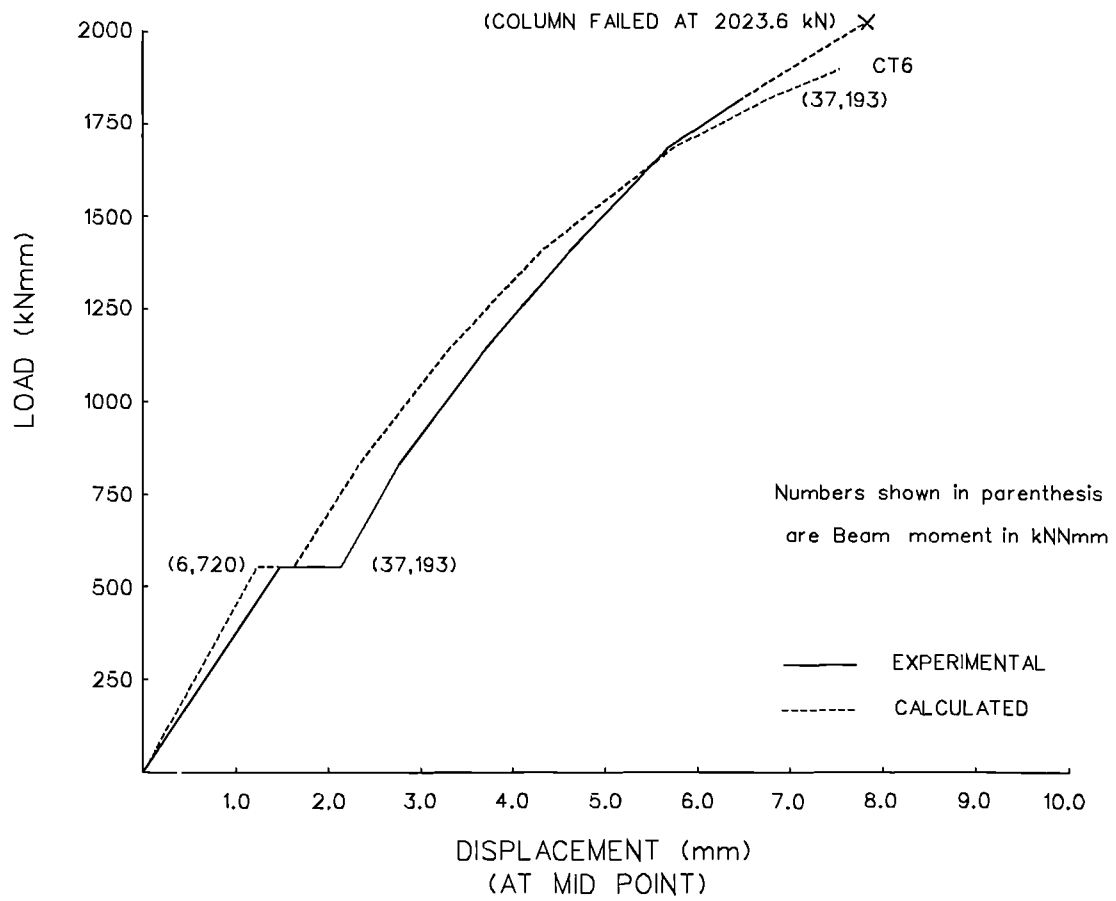


**FIG.5.18 LOAD DEFLECTION CURVE FOR LOWER COLUMN**

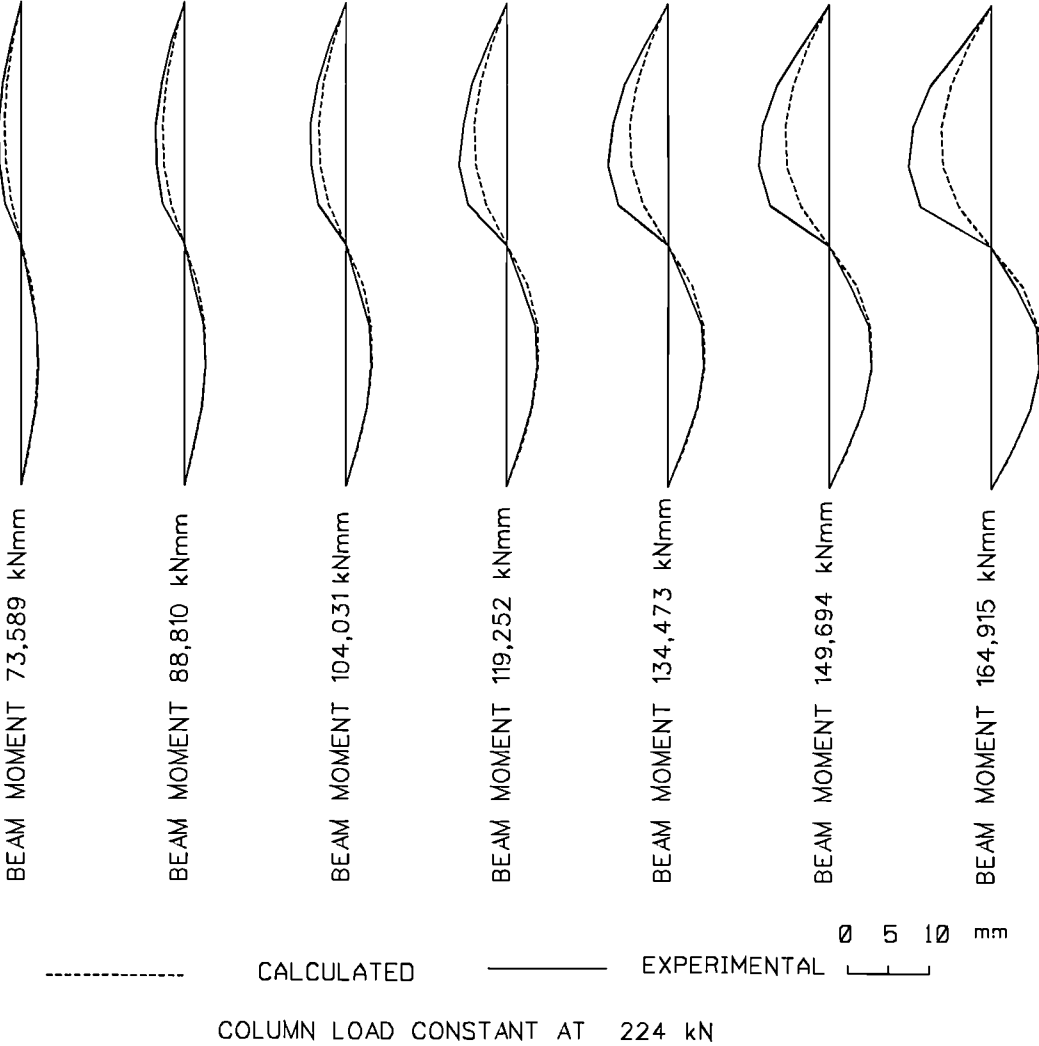


**FIG.5.19 COMPARISON OF CALCULATED DEFLECTION WITH EXPERIMENTAL VALUES (TEST CT7)**

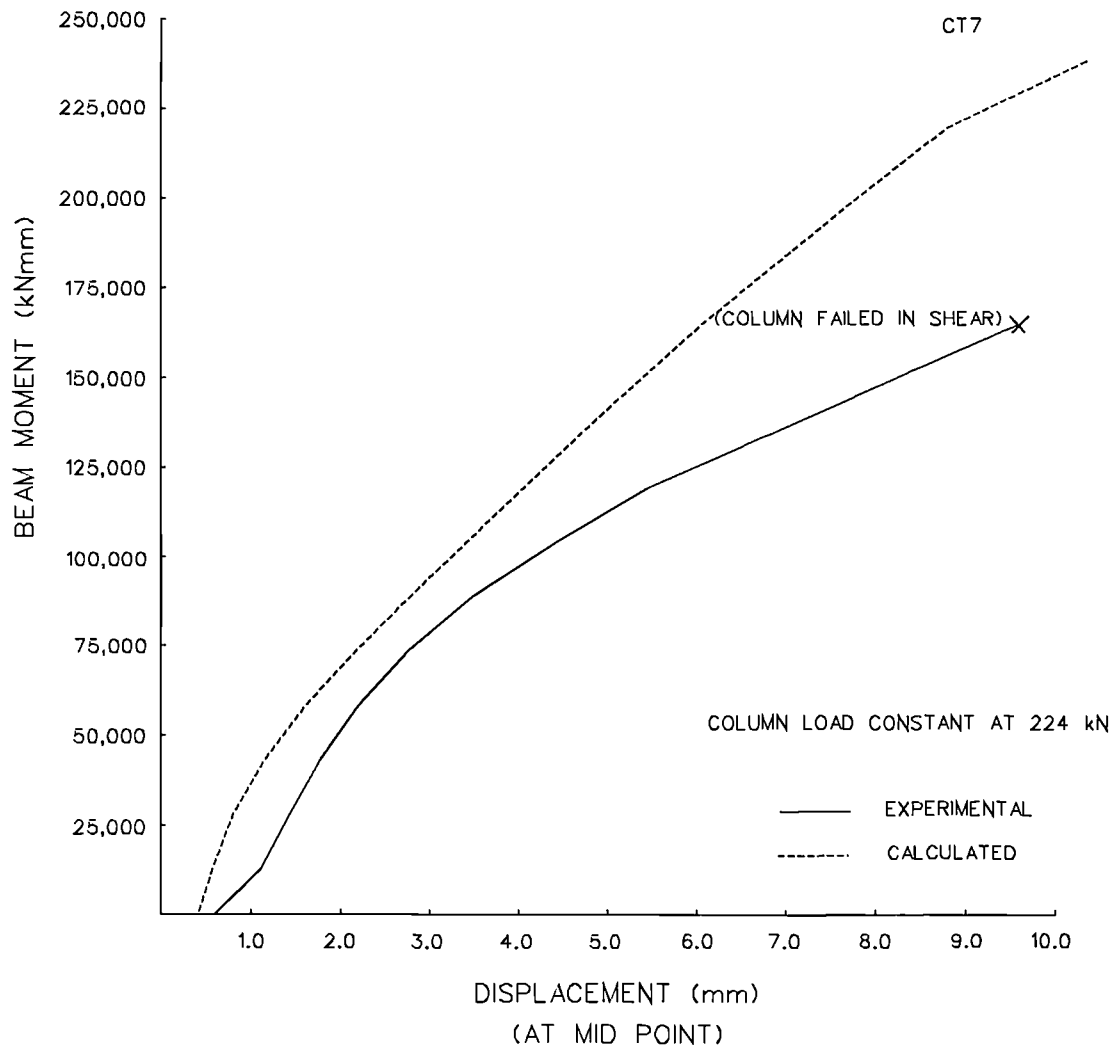


**FIG.5.20 LOAD DEFLECTION CURVE FOR UPPER COLUMN**

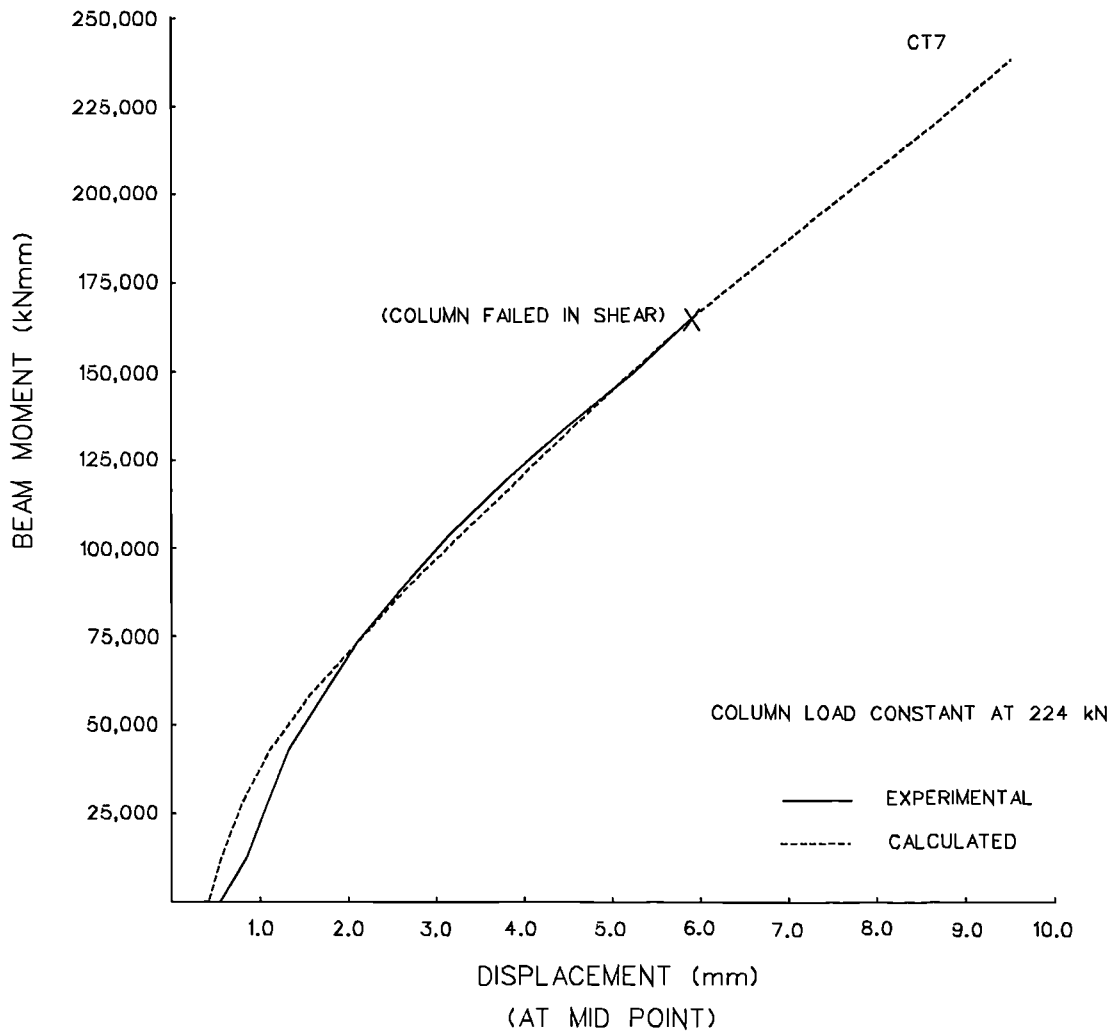


**FIG.5.21 LOAD DEFLECTION CURVE FOR LOWER COLUMN**

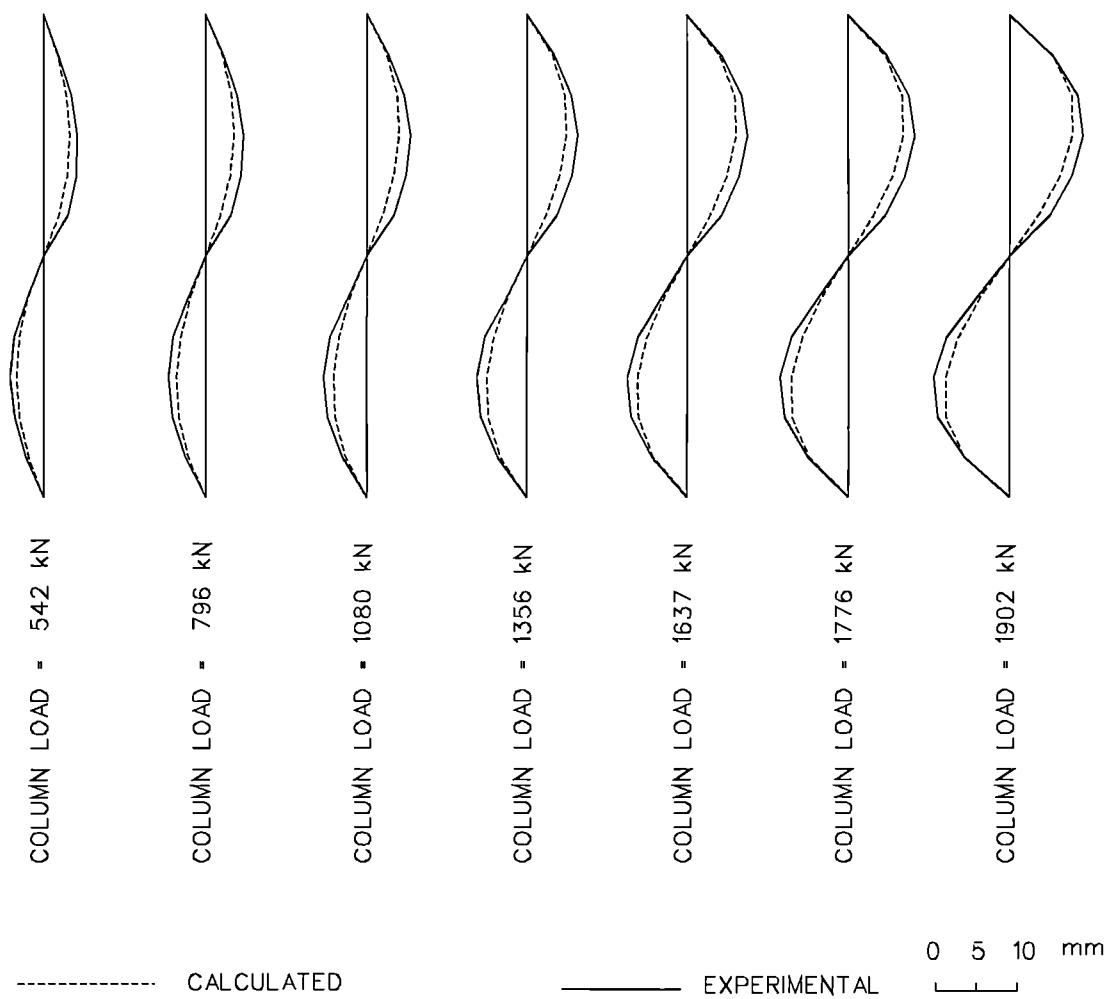


**FIG.5.22 COMPARISON OF CALCULATED DEFLECTION WITH EXPERIMENTAL VALUES (TEST CT8)**

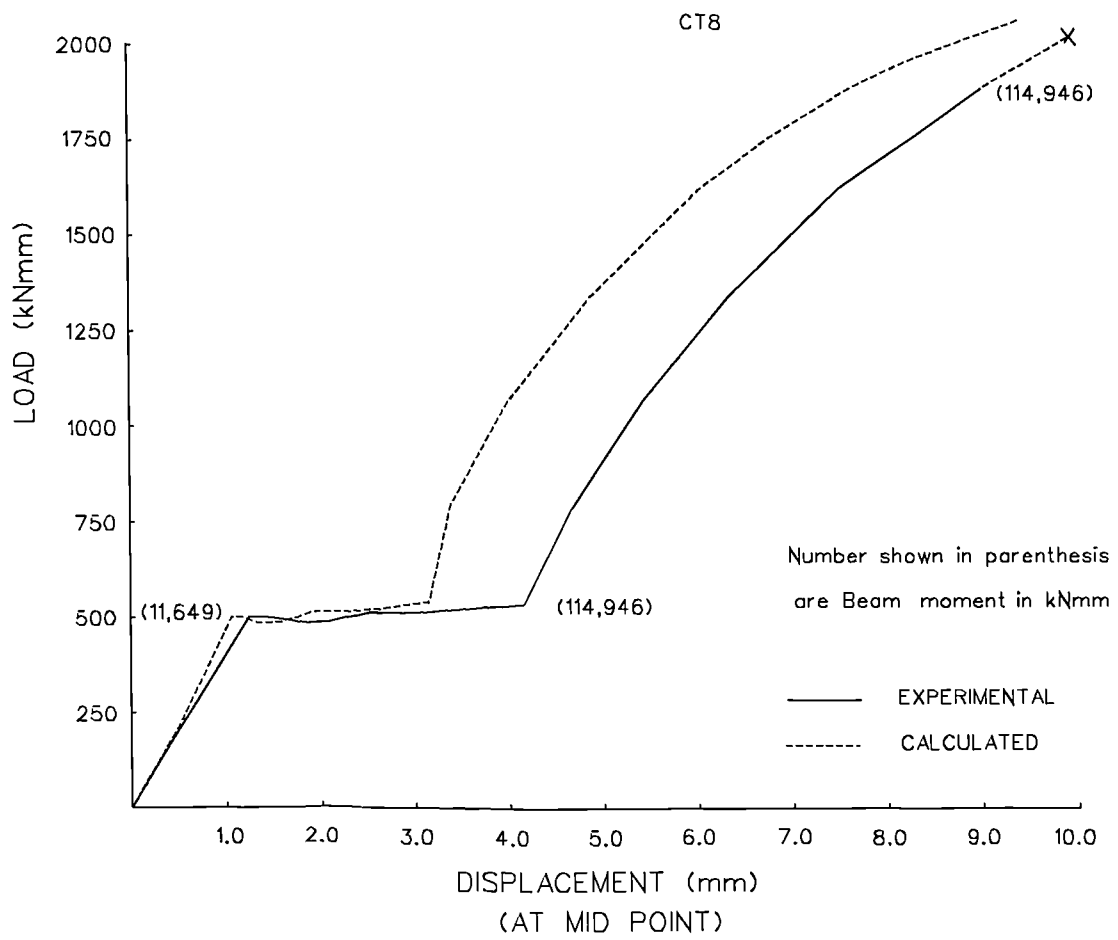


**FIG.5.23 LOAD DEFLECTION CURVE FOR UPPER COLUMN**

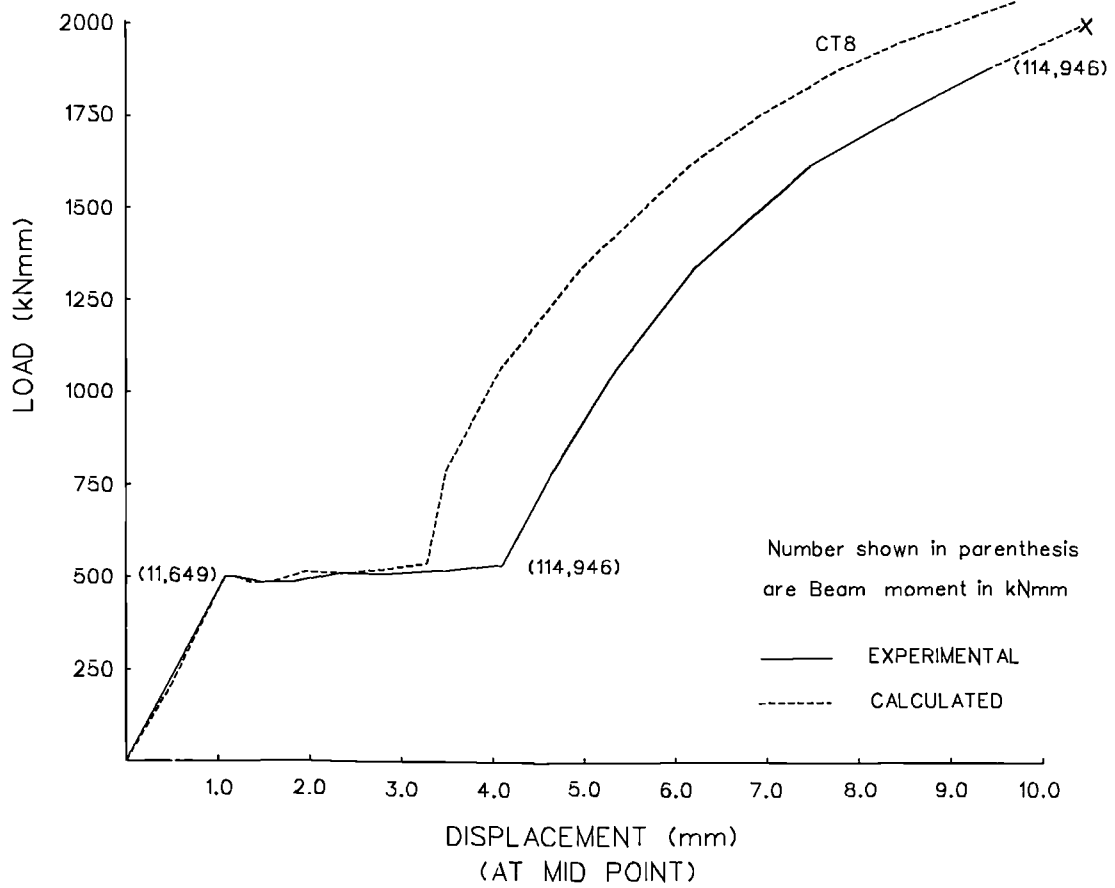


**FIG.5.24 LOAD DEFLECTION CURVE FOR LOWER COLUMN**

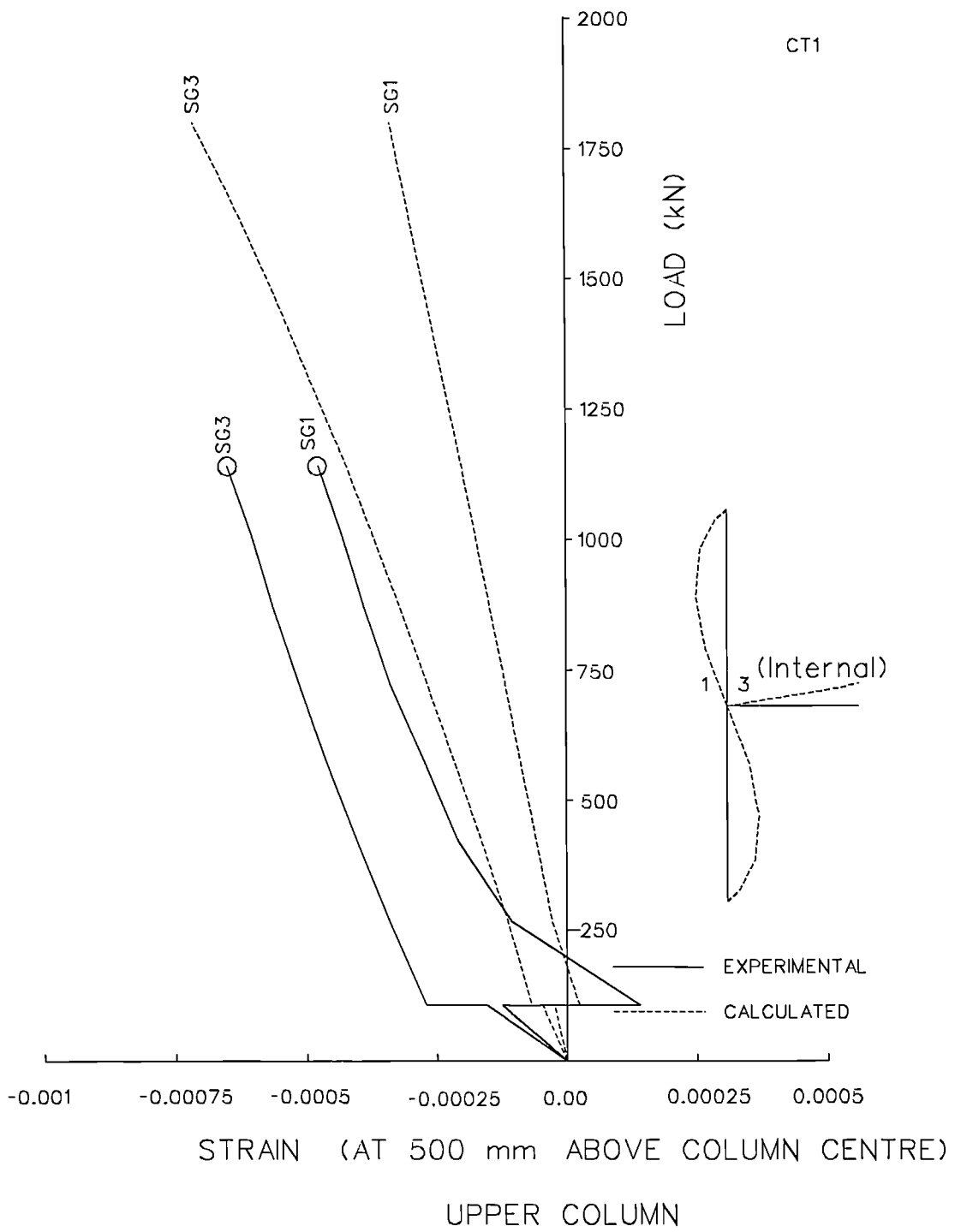


**FIG.5.25 LOAD-STRAIN RESPONSE FOR THE UPPER COLUMN  
(TEST CT1)**

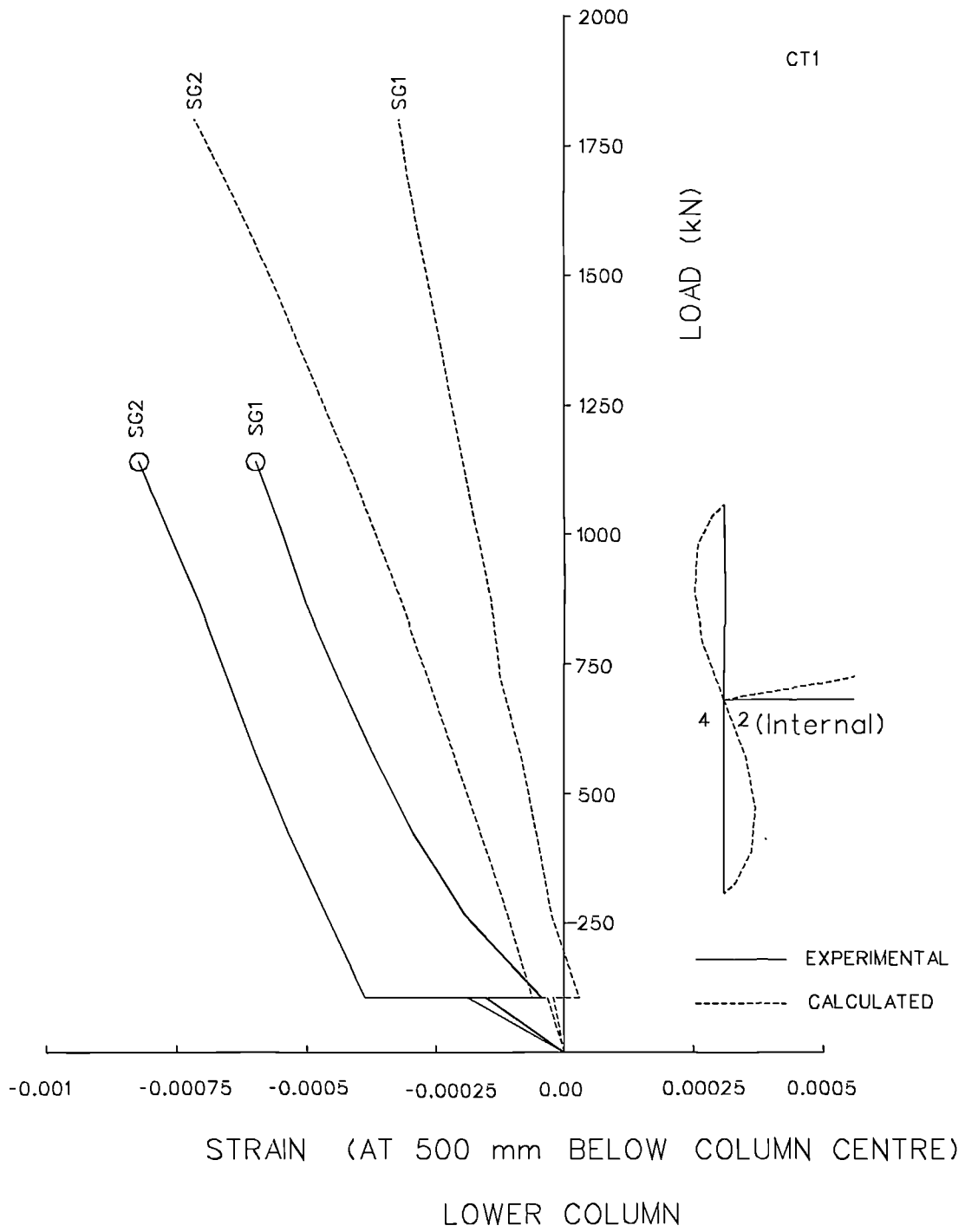


**FIG.5.26 LOAD-STRAIN RESPONSE FOR THE LOWER COLUMN  
(TEST CT1)**

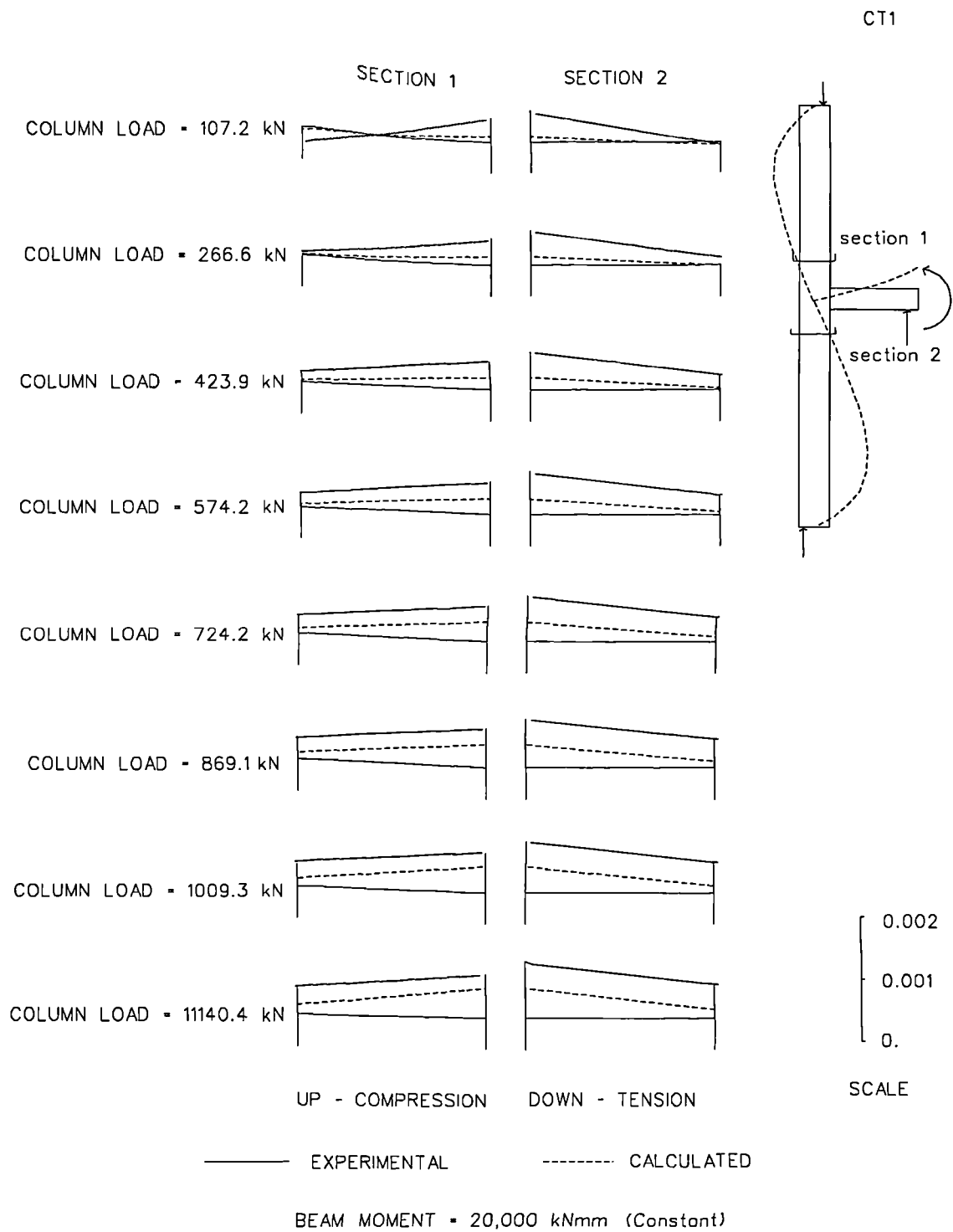


**FIG.5.27 STRAIN PROFILE IN THE COLUMN (TEST CT1)**

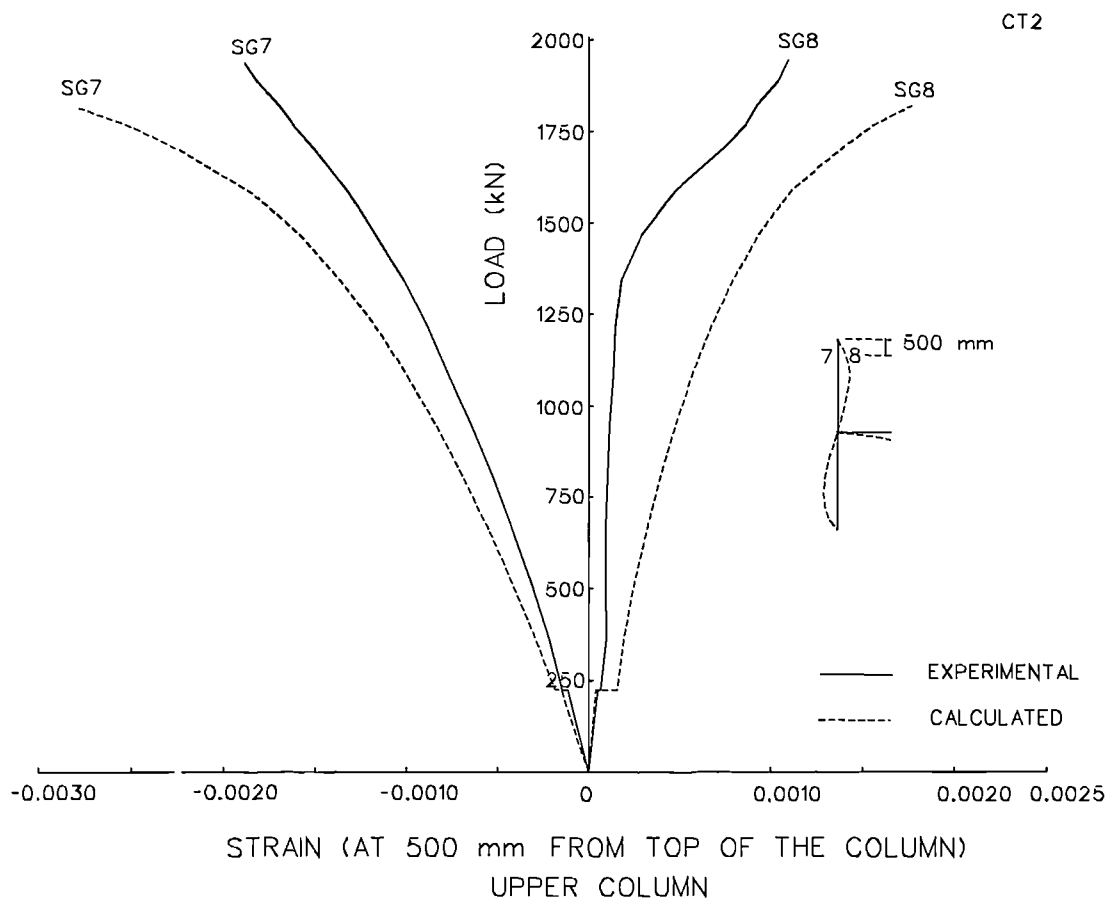


**FIG.5.28 LOAD-STRAIN RESPONSE FOR THE UPPER COLUMN  
(TEST CT2)**

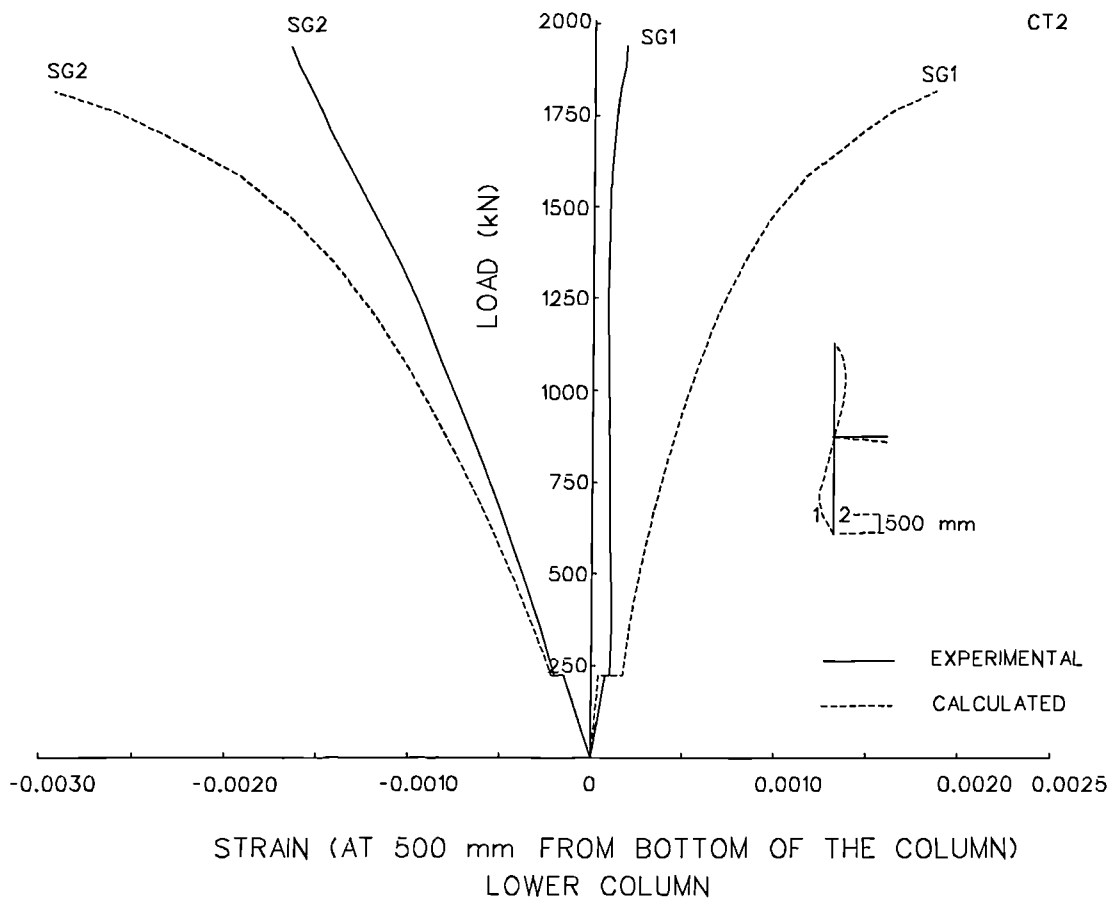


**FIG.5.29 LOAD-STRAIN RESPONSE FOR THE LOWER COLUMN (TEST CT2)**

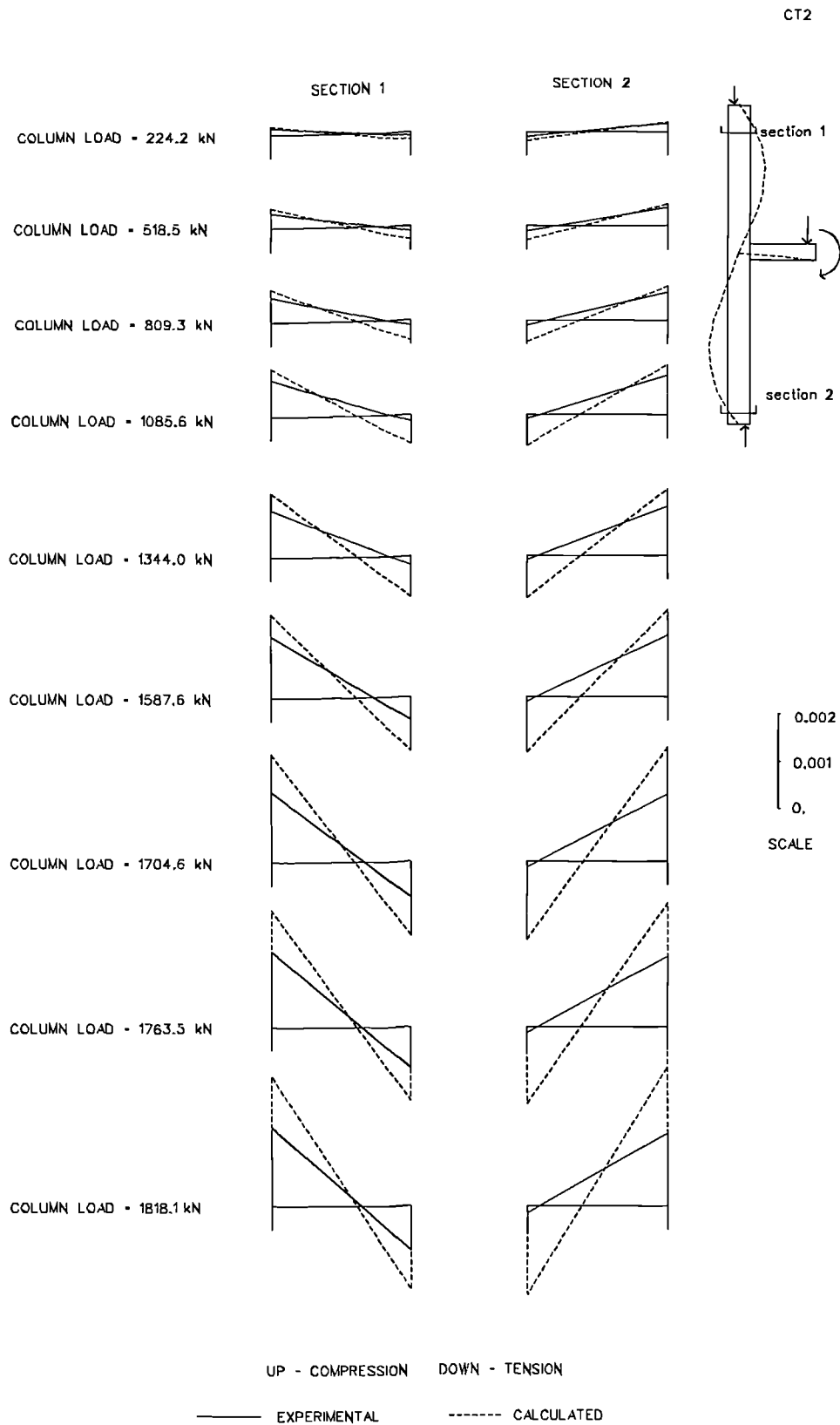


**FIG.5.30 STRAIN PROFILE IN THE COLUMN (TEST CT2)**

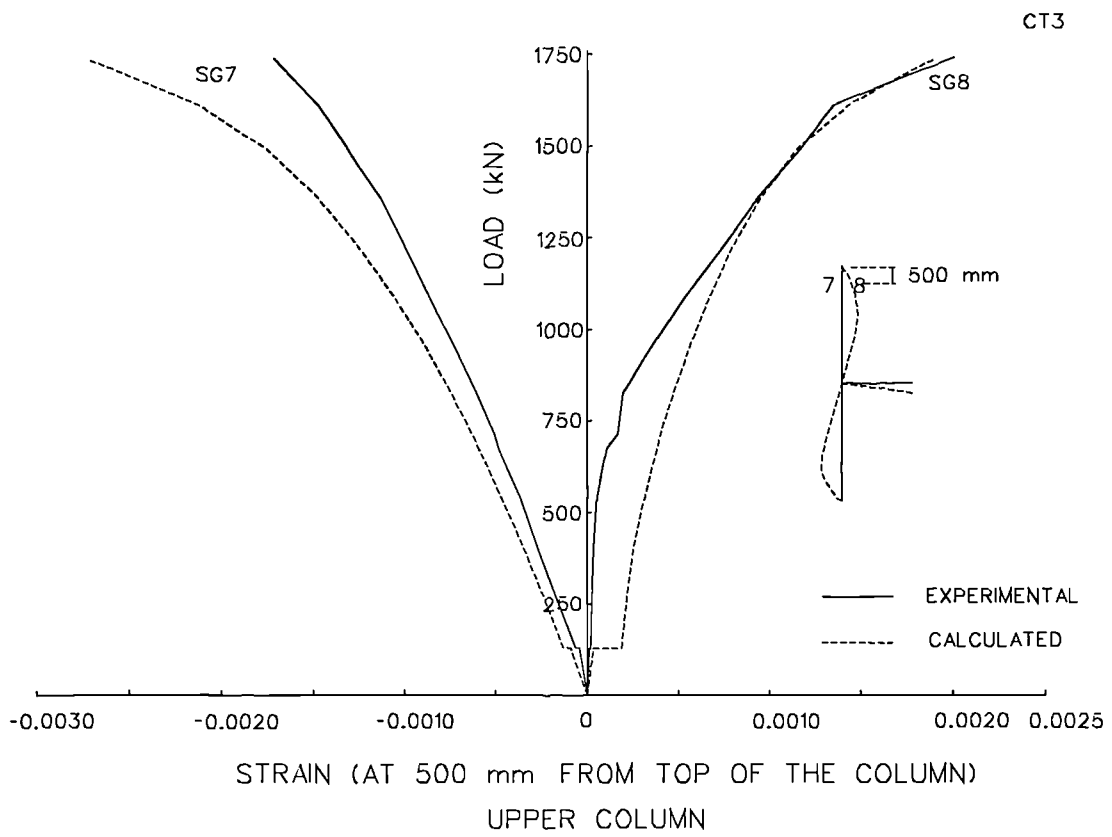


**FIG.5.31 LOAD-STRAIN RESPONSE FOR THE UPPER COLUMN**

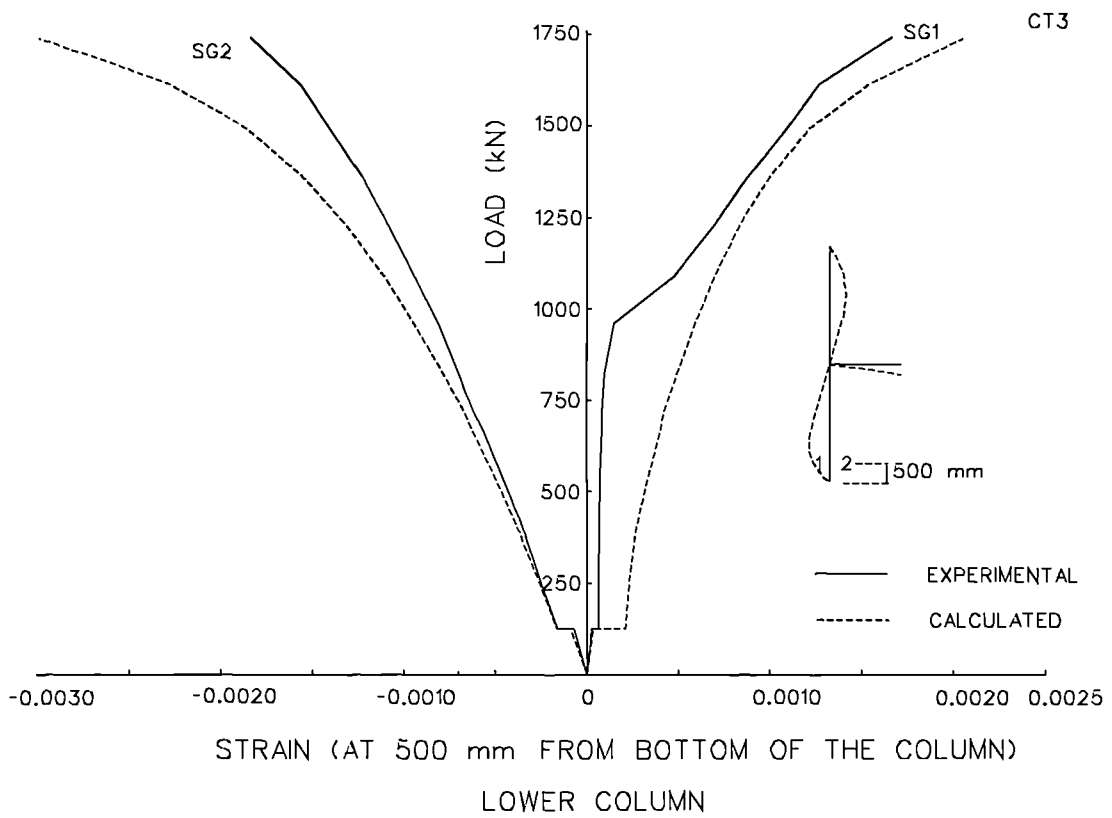


**FIG.5.32 LOAD STRAIN RESPONSE FOR THE LOWER COLUMN**

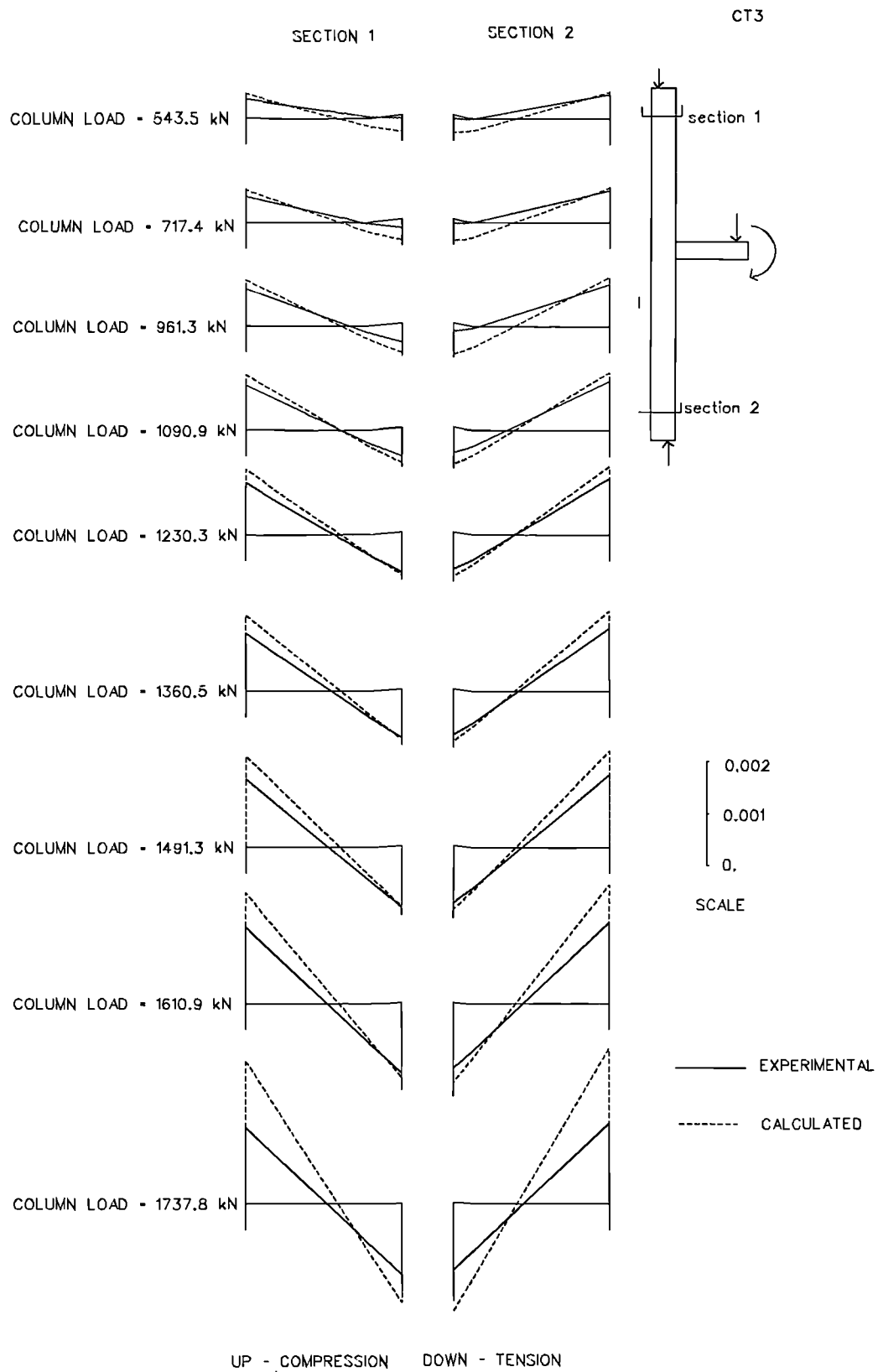


**FIG.5.33 STRAIN PROFILE IN THE COLUMN**

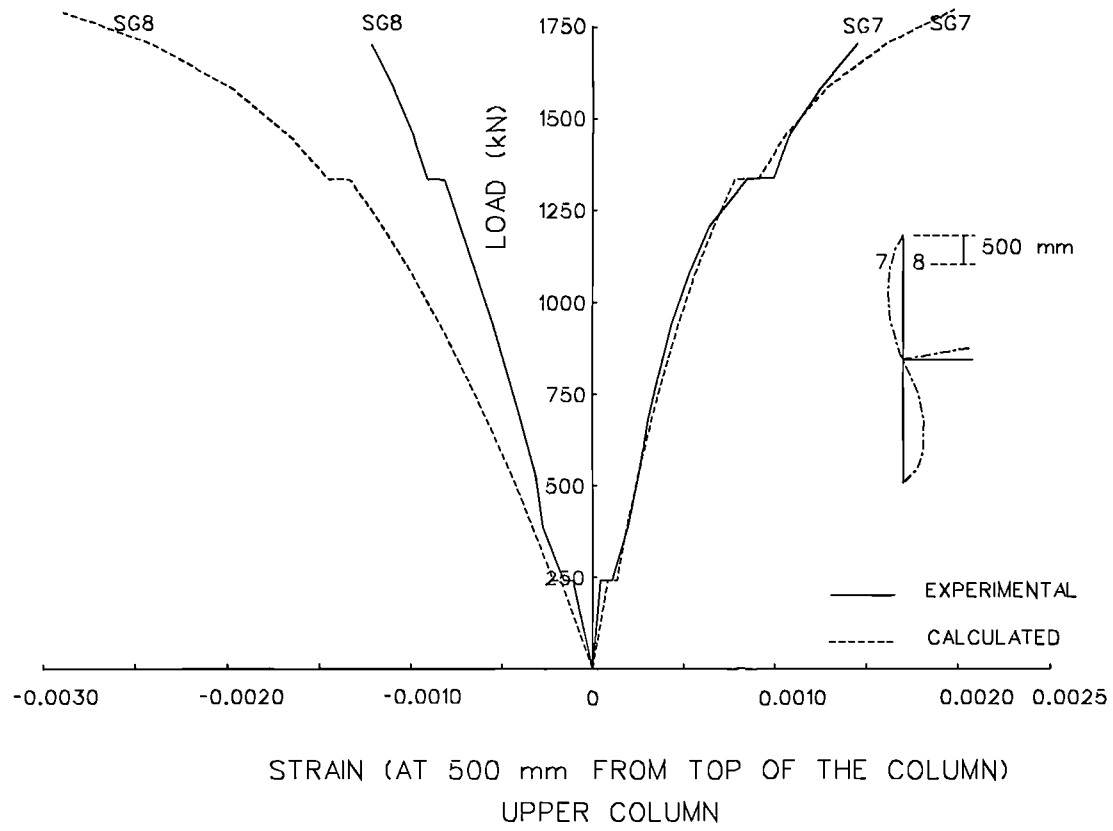


**FIG.5.34 LOAD STRAIN RESPONSE FOR THE UPPER COLUMN**

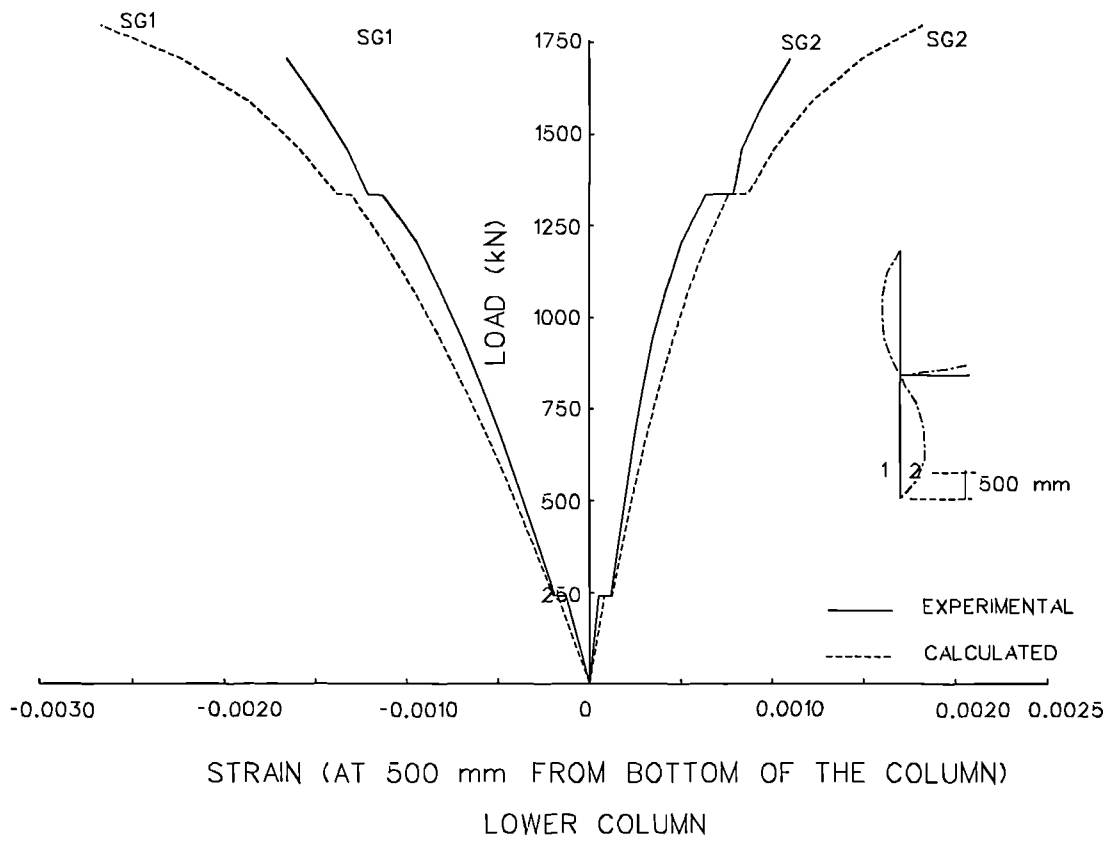


**FIG.5.35 LOAD STRAIN RESPONSE FOR THE LOWER COLUMN**

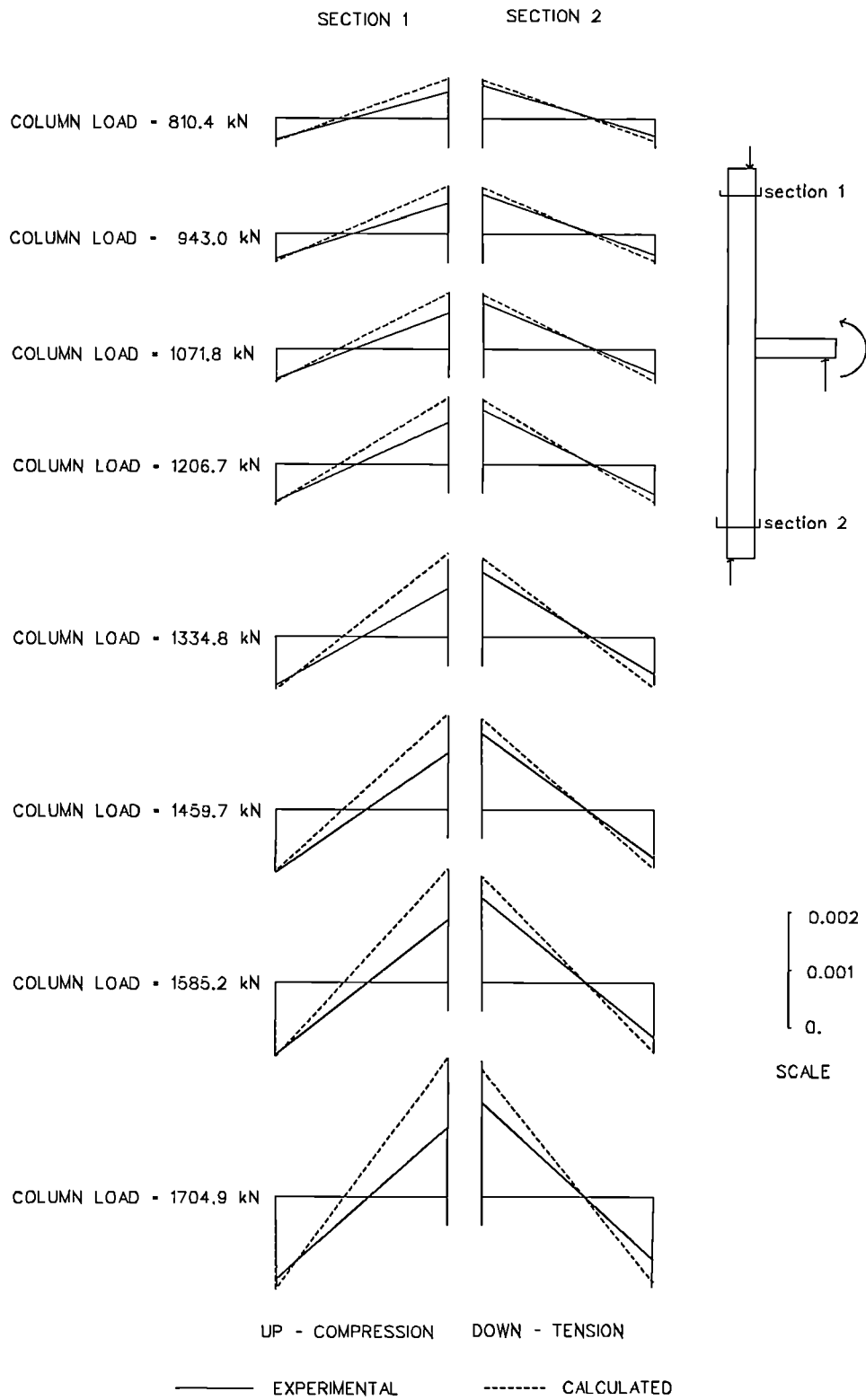


**FIG.5.36 STRAIN PROFILE IN THE COLUMN**

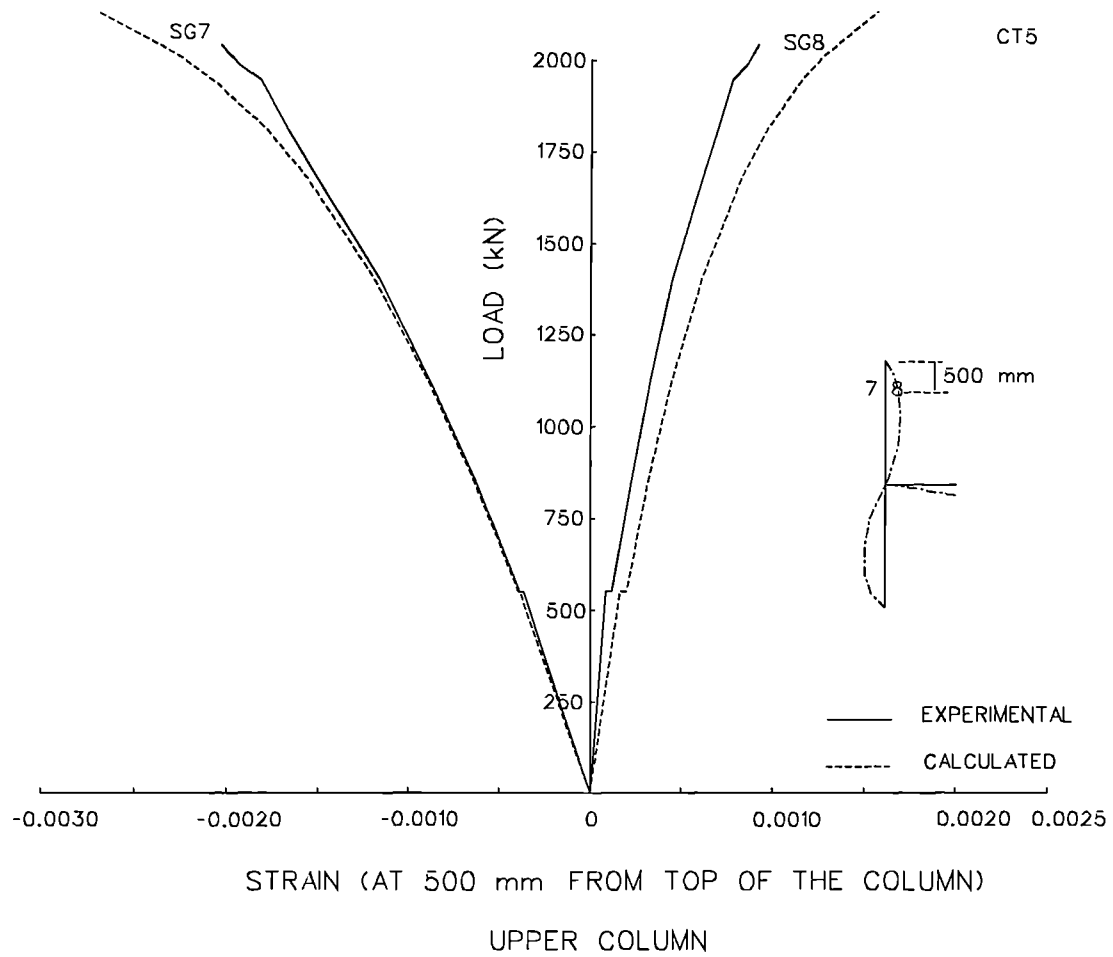


**FIG.5.37 LOAD STRAIN RESPONSE FOR THE UPPER COLUMN**

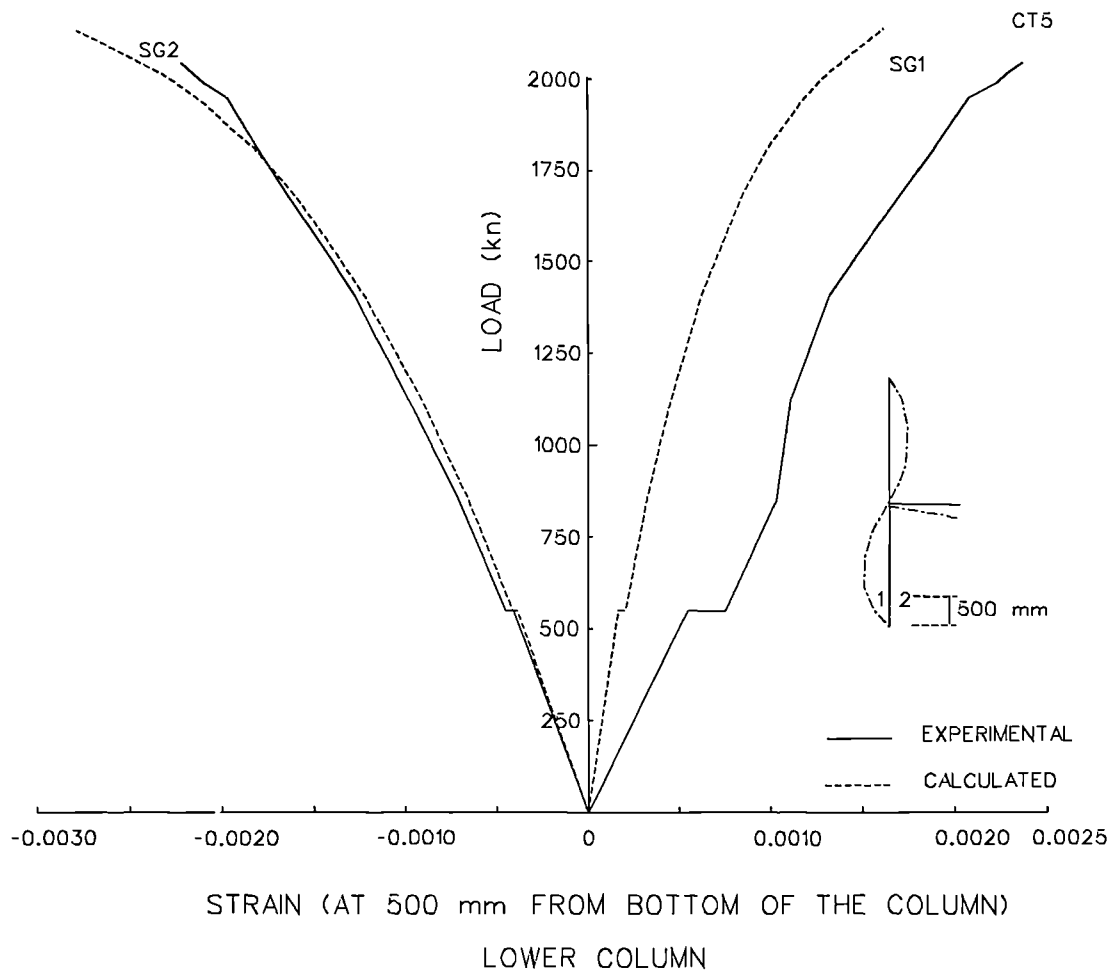


**FIG.5.38 LOAD STRAIN RESPONSE FOR THE LOWER COLUMN**



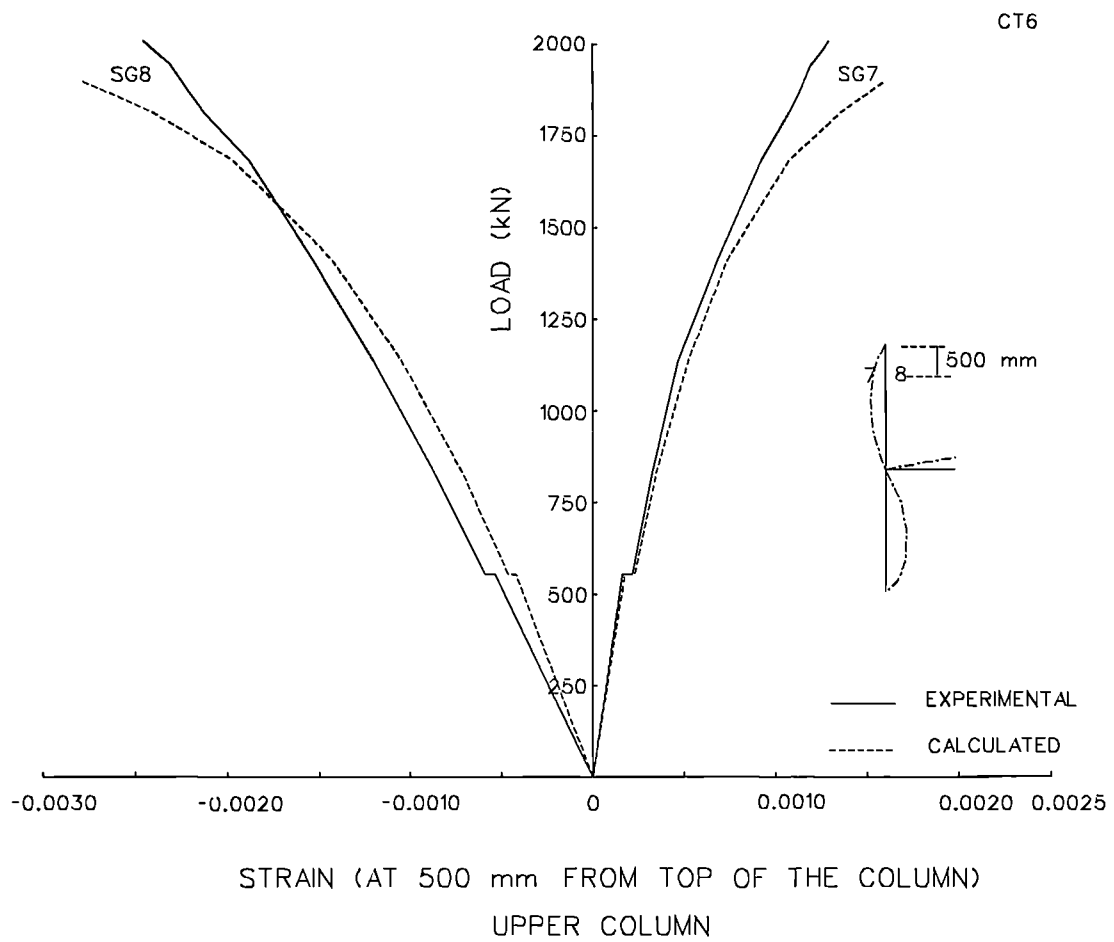


**FIG.5.40 LOAD STRAIN RESPONSE FOR THE UPPER COLUMN**

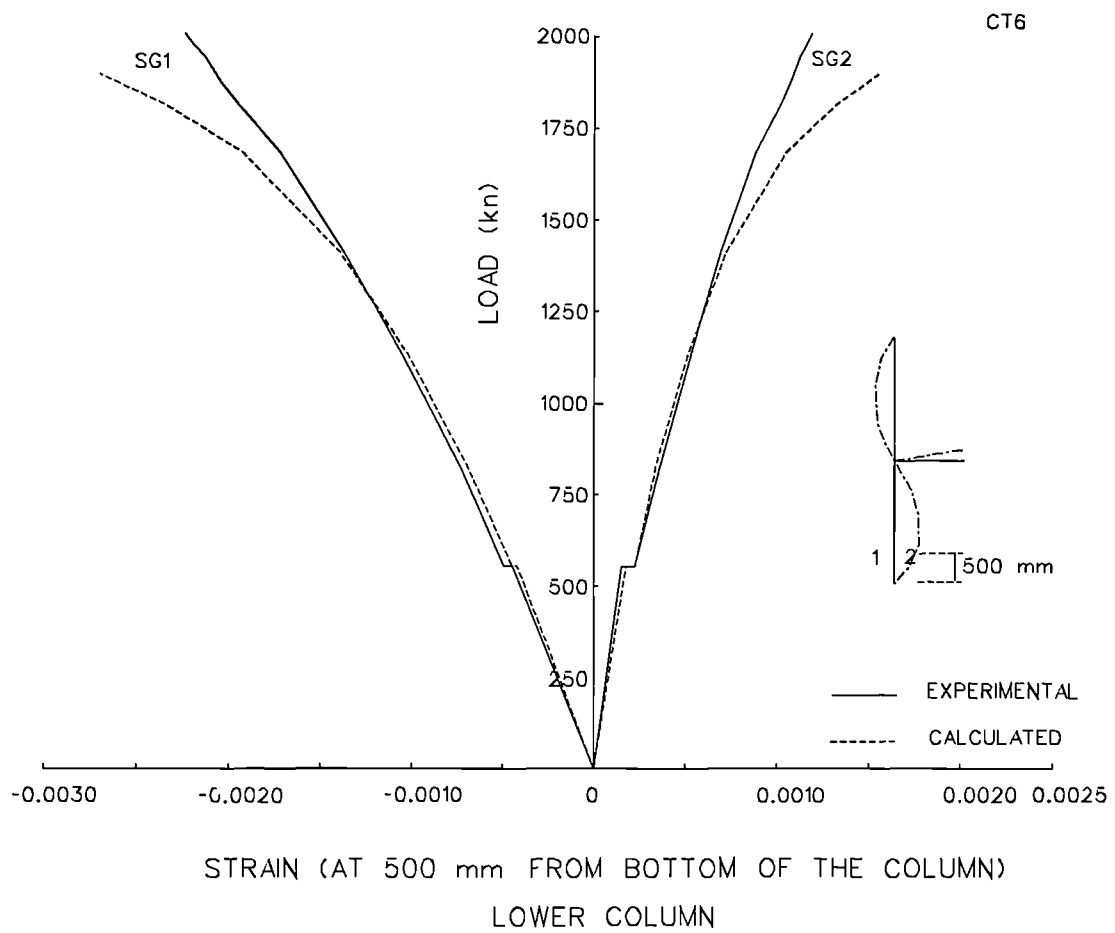


**FIG.5.41 LOAD STRAIN RESPONSE FOR THE LOWER COLUMN**

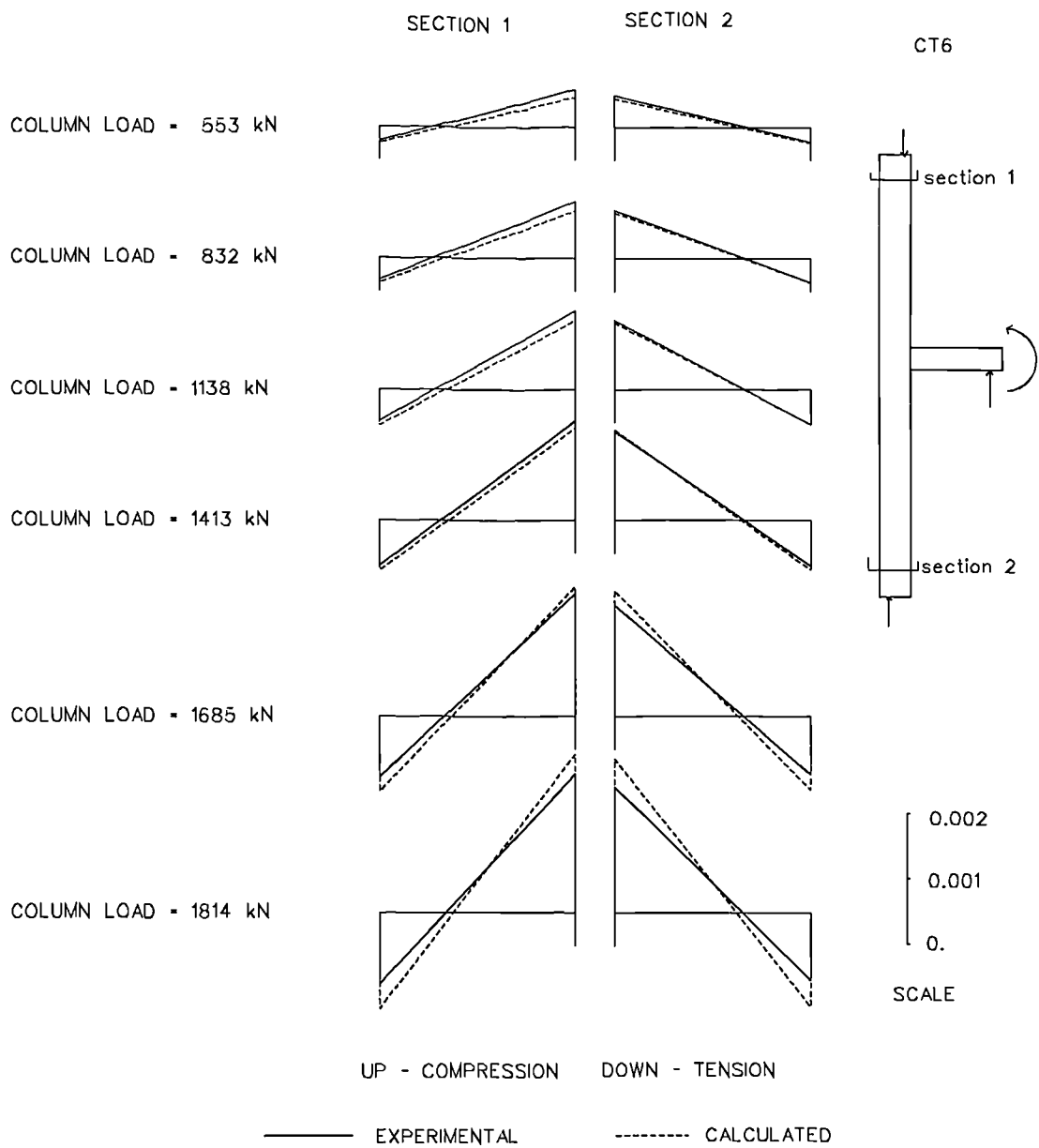


**FIG.5.42 STRAIN PROFILE IN THE COLUMN**

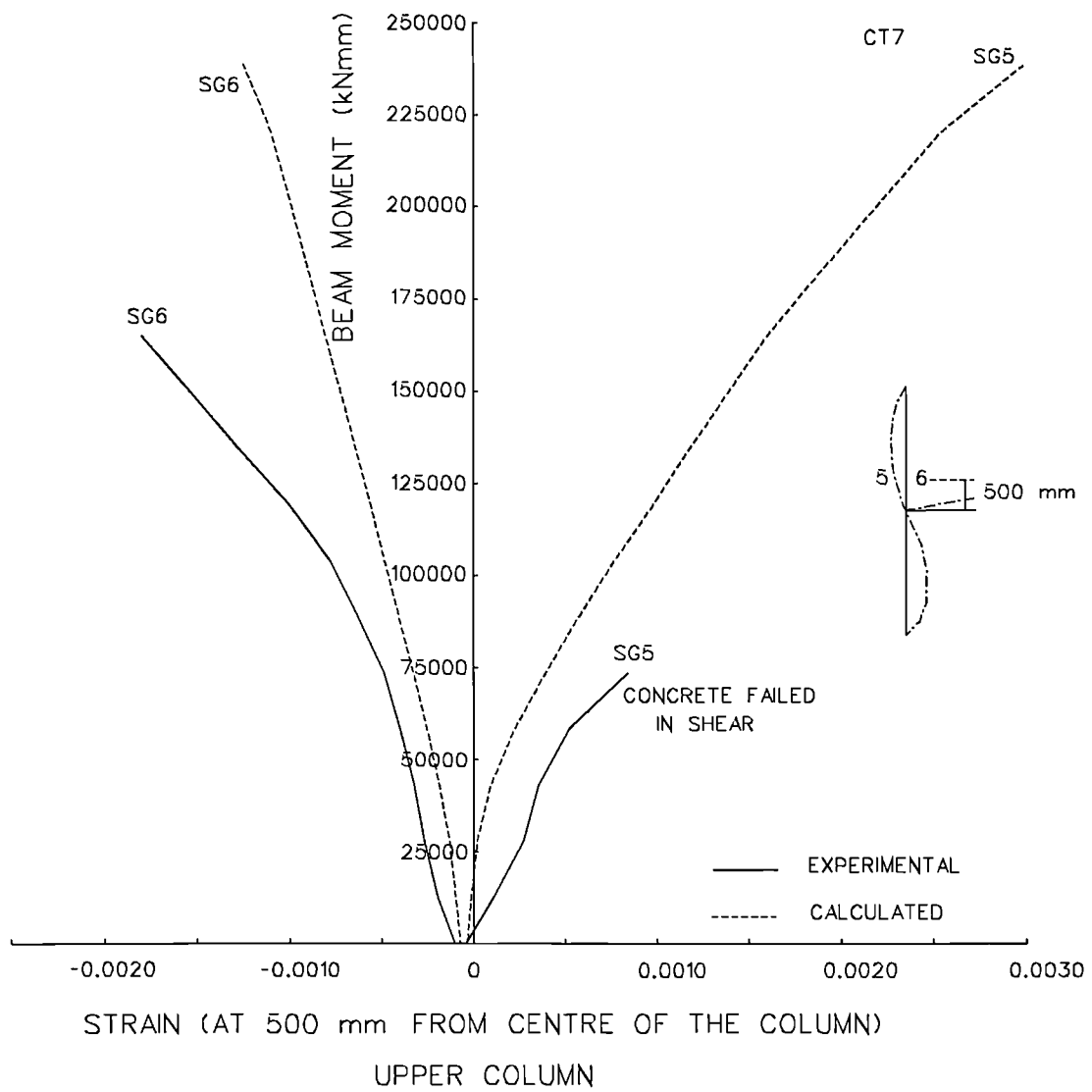


**FIG.5.43 LOAD STRAIN RESPONSE FOR THE UPPER COLUMN**

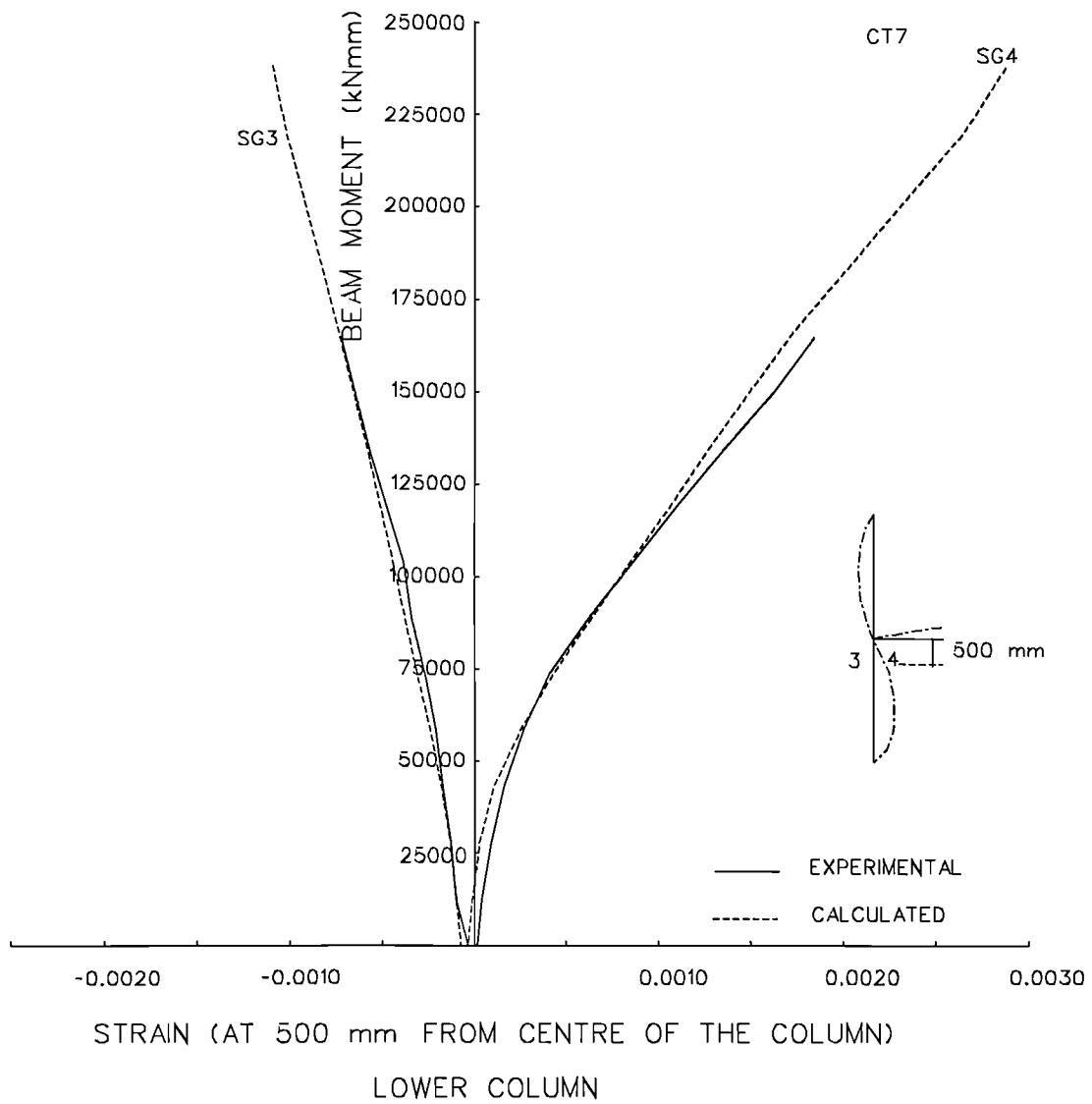


**FIG.5.44 LOAD STRAIN RESPONSE FOR THE LOWER COLUMN**

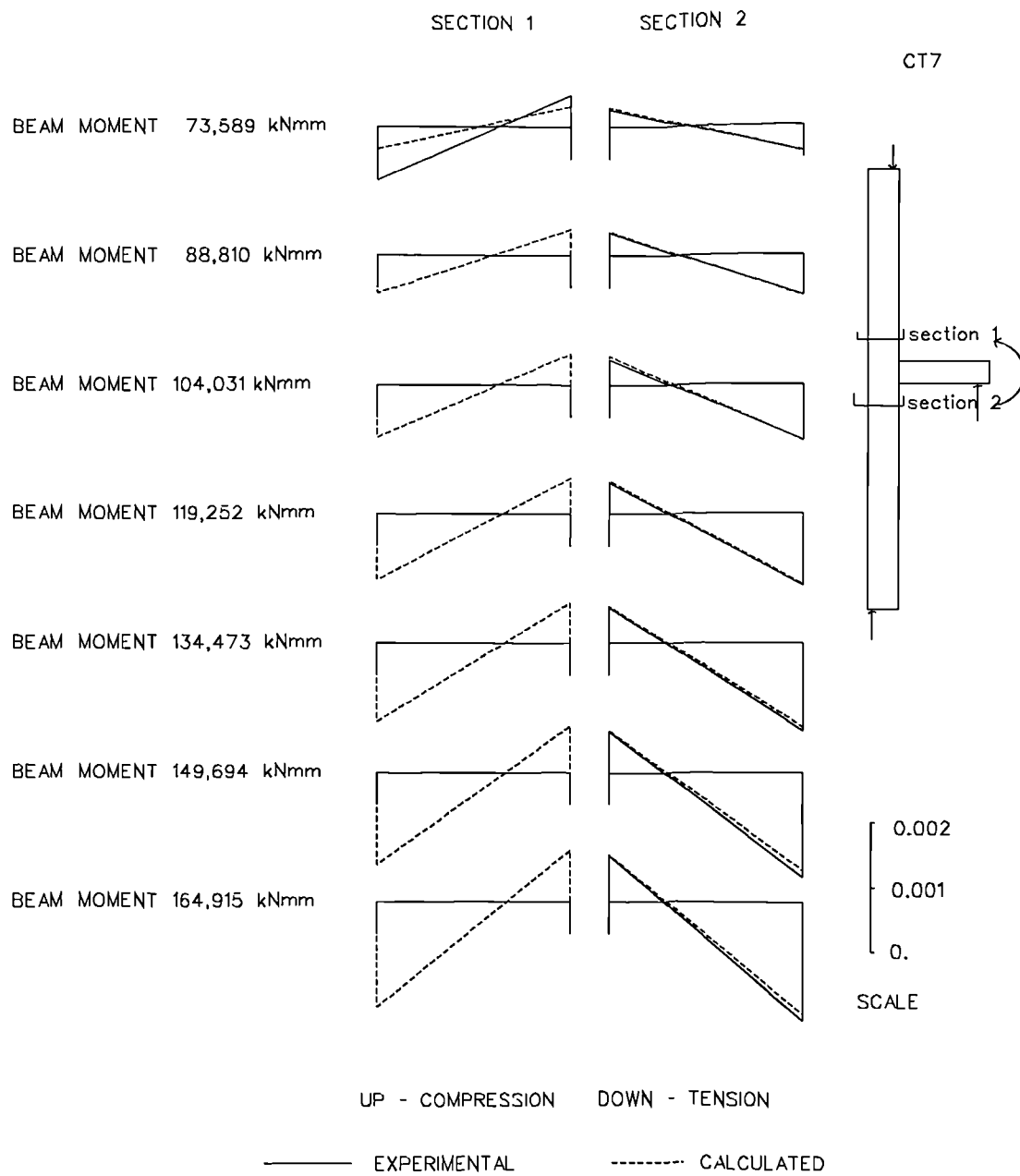


**FIG.5.45 STRAIN PROFILE IN THE COLUMN**

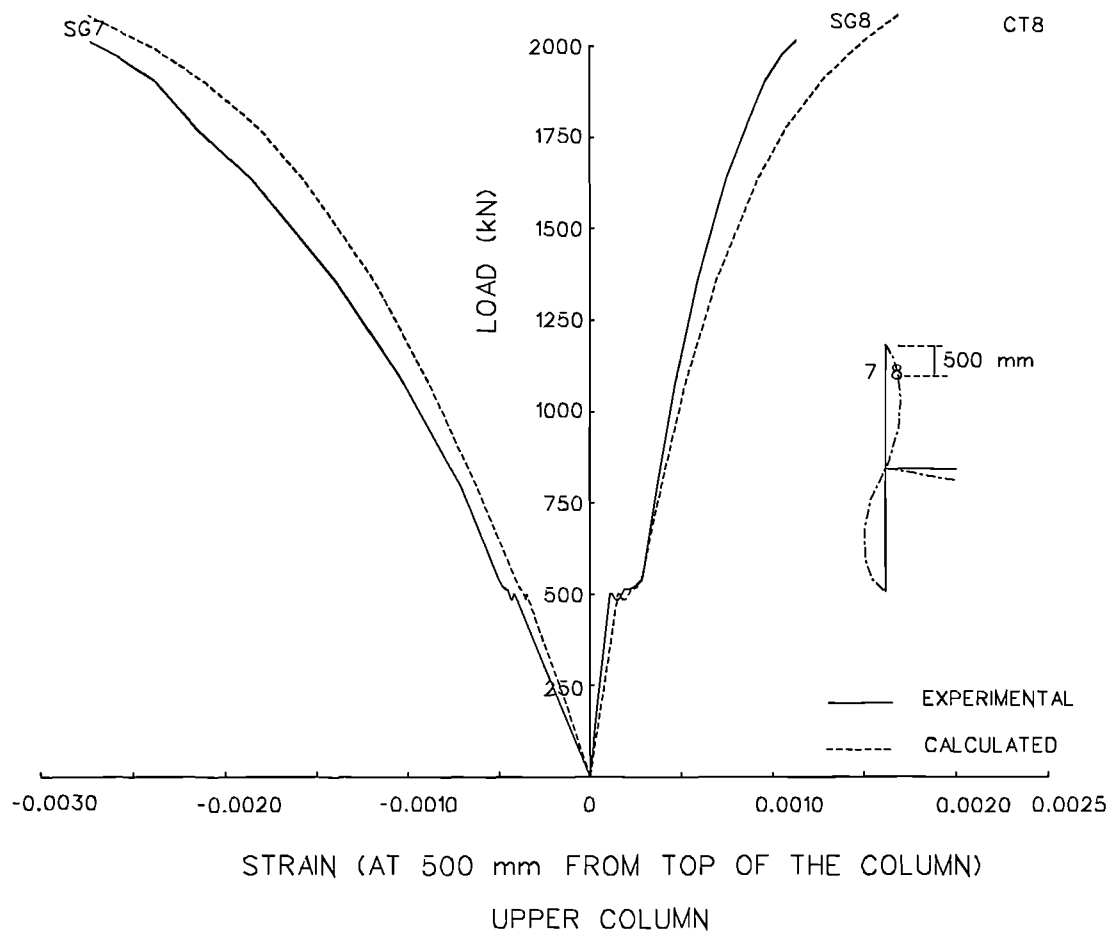


**FIG.5.46 LOAD STRAIN RESPONSE FOR UPPER COLUMN**

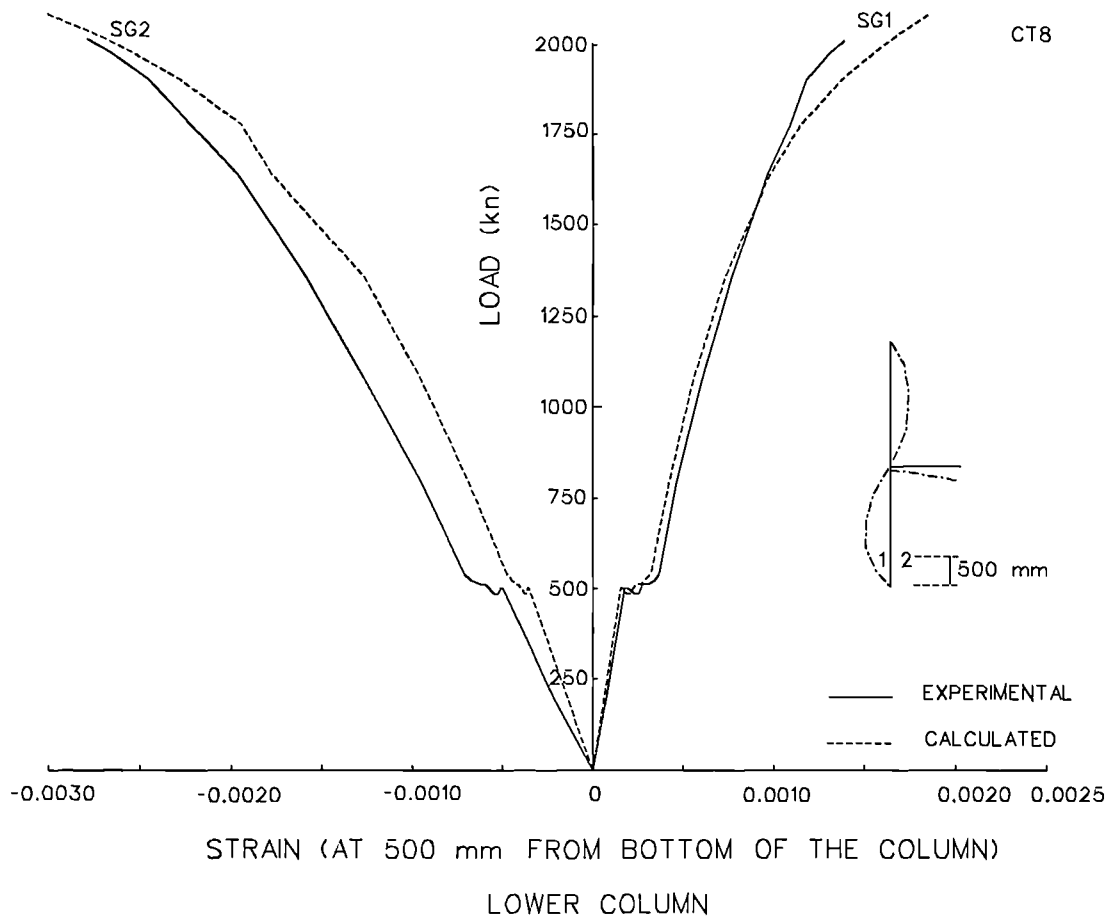


**FIG.5.47 LOAD STRAIN RESPONSE FOR LOWER COLUMN**

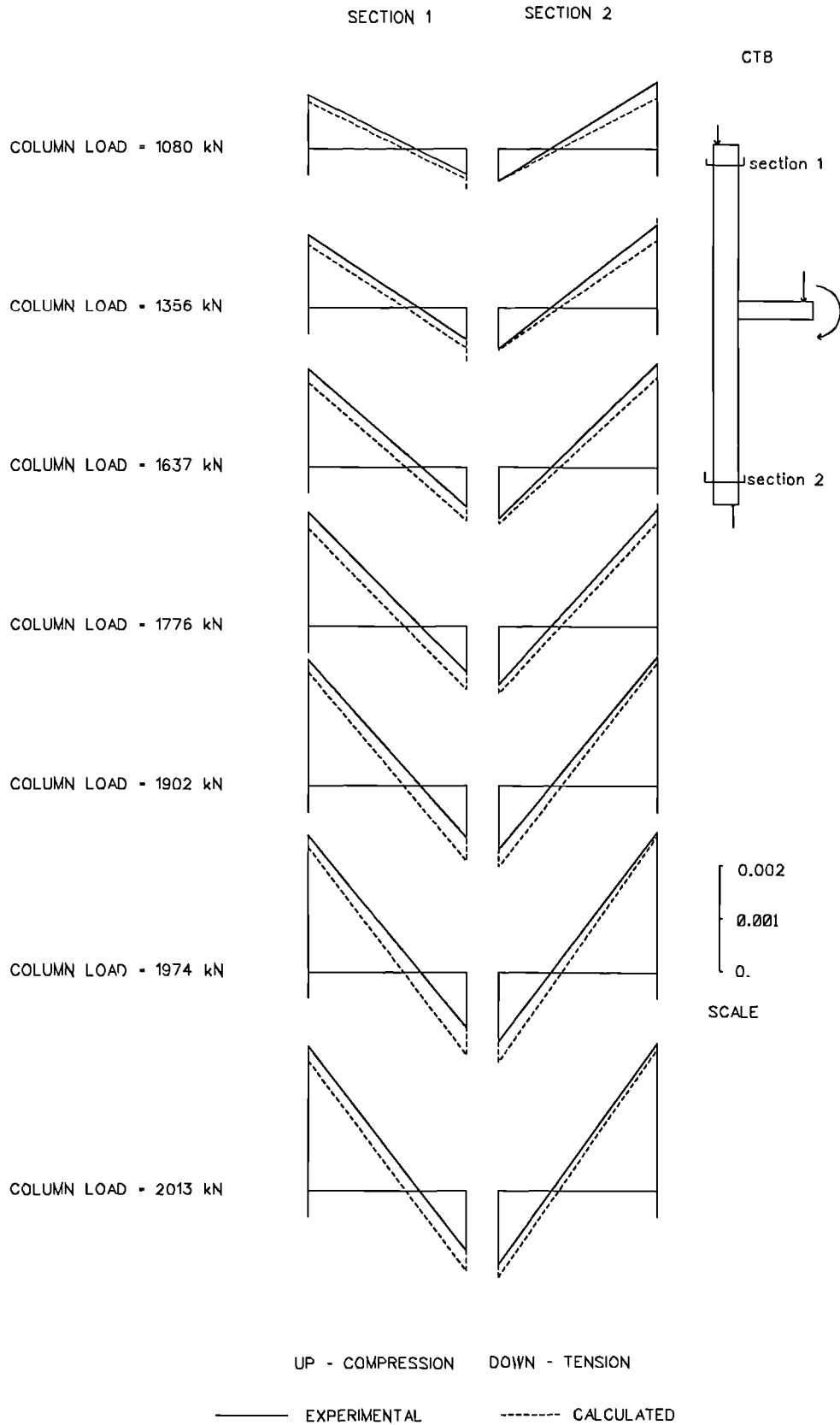


**FIG.5.48 STRAIN PROFILE IN THE COLUMN**

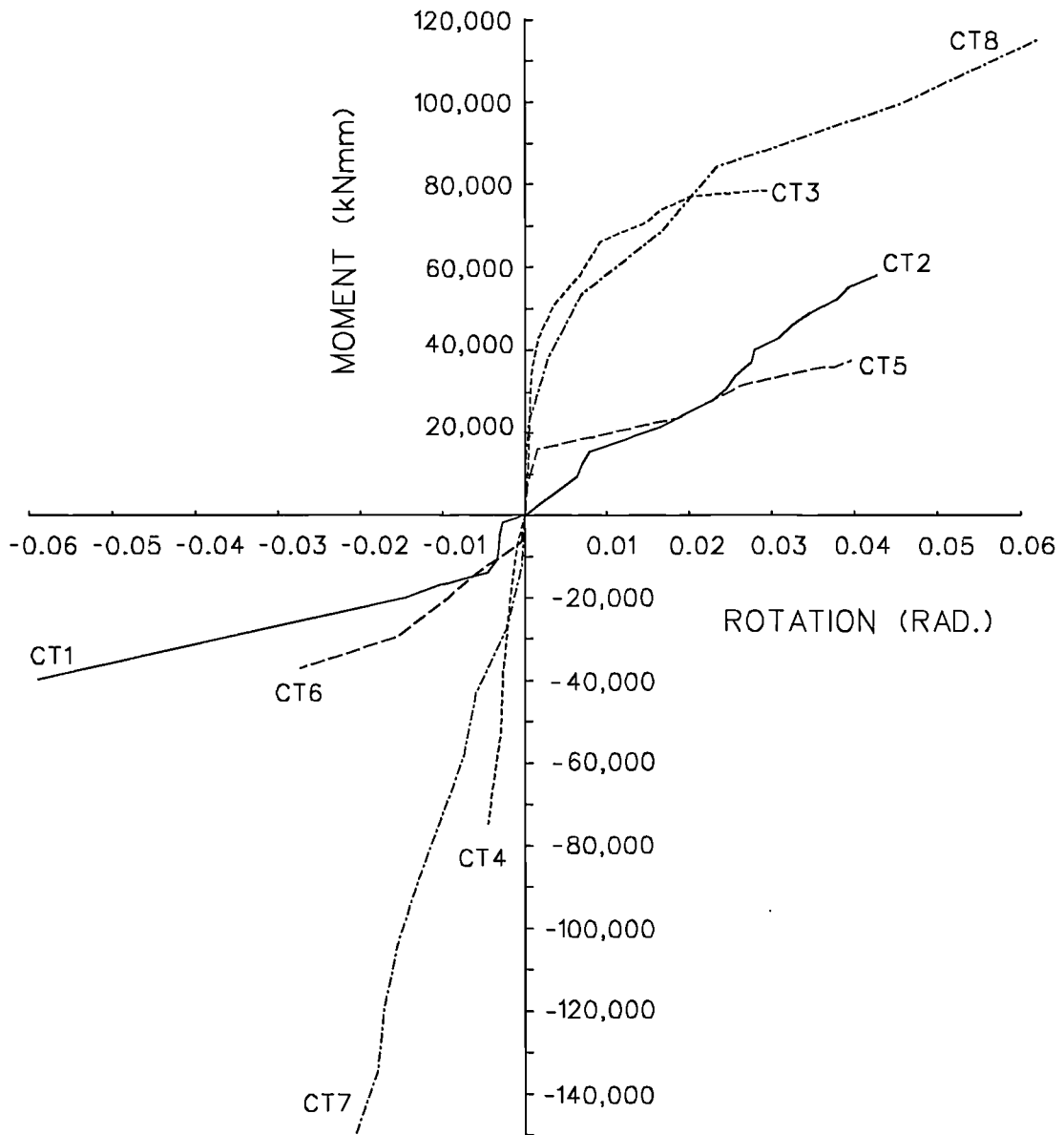


**FIG.5.49 MOMENT ROTATION RELATION FROM TEST CT1-CT8**

## **CHAPTER 6.**

### **VALIDATION OF "SWANSA" WITH EXPERIMENTS FROM OTHER SOURCES**

#### **6.1 INTRODUCTION**

Two types of comparisons are presented in this chapter. Firstly experimental results of reinforced concrete portal frames and secondly analytical results from other sources on single and two-storey reinforced concrete plane frames were considered in the comparison. Experimental results were reported by Ernst et al[65] on six nosway reinforced concrete portal frames. In this test simple portal frames pin-connected at the base were subjected to point-loads along the beam. The point loads were increased uniformly until the frames failed to take further load. Mid span deflections along with the total beam load are compared with the analytical result from the computer program SWANSA. Results of finite element analysis performed on a single and two storey plane frames were reported by Seniwongse[66]. Both the frames were subjected to lateral load while the bottom of the column was rigidly fixed to the base. The above frames were studied by Franklin[67] using another finite element model. The lateral deformation at the loaded floor level is also compared.

#### **6.2 REINFORCED CONCRETE PORTAL FRAMES**

The dimensions of the portal frames, tested by Ernst et al, were selected to demonstrate the ductile behaviour of reinforced concrete portal frames and to cover a practical range of sizes. The frames were of height 6ft (1.8m) and the beams had a nominal span of 12ft (3.6m). The supports at the base were designed as pin joints.

Data for the six frames tested are tabulated below. Frames A40 to C60 were subjected to point loads at the third points of the span and the load was increased up to failure. The frames were tested horizontally.

**TABLE 6.1 GENERAL DATA FOR THE FRAMES CONSIDERED**

Frame	Beam	Column	Concrete	Steel
	type	type	cyl. strength(N/mm <sup>2</sup> )	yield (N/mm <sup>2</sup> )
A40	1	1	29.13	353.5
A60	1	1	39.00	426.0
B40	2	2	29.13	357.7
B60	2	2	39.00	419.4
C40	3	3	29.13	357.7
C60	3	3	39.00	419.4

**TABLE 6.2 DETAILS OF BEAMS AND COLUMNS**

	Width	Height	Cover	Aso	Asi
Beam Type 1	114.3	203.2	38.1	2-#5	2-#5
Beam Type 2	114.3	203.2	38.1	2-#4	2-#6
Beam Type 3	114.3	203.2	38.1	2-#6	2-#4
Column Type 1	114.3	203.2	38.1	2-#5	2-#5
Column Type 2	114.3	203.2	38.1	2-#5	2-#6
Column Type 3	114.3	203.2	38.1	2-#6	2-#5

The above six frames were analysed using the program SWANSA. The stress strain curves adopted for steel and concrete were as defined in BS8110. The material safety factor was taken as 1.0. The compressive stress of concrete in the members was taken as 0.85 of the cylinder strength, as is common practice.

Figures 6.1 to 6.6 show the mid span deflections against the total load on the frame obtained from experiments and from the computer program SWANSA. The ultimate loads are tabulated in Table 6.3 below.

**TABLE 6.3 COMPARISON OF ULTIMATE LOADS**

FRAME	EXPERIMENT	SWANSA	ERROR%
A40	69.4	70.4	1.4
A60	88.9	85.0	-4.4
B40	82.6	73.1	-11.5
B60	93.1	87.3	-6.2
C40	73.0	73.0	-0.0
C60	77.3	87.2	12.8
Average			-1.3
Standard deviation			7.8

In general, the agreement between the computed and experimental ultimate loads is excellent except for B40 and C60, which show errors around 12%, which are acceptable when dealing with concrete structures.

In frame A40 the correlation between the experimental and calculated behaviour of the frame is excellent up to 50 kN. Beyond 50 kN load the experimental curve shows a smooth change in the rate of increase of deflection compared with the theoretical curve which is almost stiff up to near failure.

Frame A60 is similar to A40 except for material strength. The analytical and experimental deflections up to load 60 kN are almost the same. The experimental curve does not show much ductility at failure, and the failure was stated to be due to fracture of a steel bar.

The frame B40 is also similar to frame A40, except for a slight increase in steel strength. In frame B40, the analytical deflection closely follows the experimental pattern except for a slight offset which can be due to initial imperfections. The ultimate load obtained from the program SWANSA is 11.5% less than the experimental values. The failure was in the mid span. In spite of similarity with frame A40, the experimental failure load obtained is much greater. This is reflected in the theoretical curve, which is comparable with that obtained for frame A40. This difference in failure loads could be due to some material or geometrical variations.

Frame B60 is of a higher material strength than frame B40, and is similar to frame A60. This frame also does not show much ductility. The analytical and experimental mid span deflections show excellent agreement. There is a 6.2% variation in the ultimate load.

Experimental observations for frame C40 indicated that the frame had an internal concrete failure due to lack of confining ties[65]. The large

difference in deflections in the later half of the loading history can, therefore, be explained.

Frame C60 also shows a significant difference in deflection behaviour and in the ultimate load. The failure load in this case is not very much different from C40, since the reinforcement and geometrical details are the same for frames C40 and C60. The steel and concrete strengths are higher, and hence the computed failure load is of the order of 90 kN. The failure to reach the above load in the experiment is difficult to explain.

In all cases, the response for what would be serviceability loads are well predicted by the computer program SWANSA in comparison with the experiments

### **6.3 COMPARISON WITH FINITE ELEMENT METHOD**

Seniwongse[66] reported some results on reinforced concrete frames using a finite element program developed by him. The finite element analyses on a single storey and a two storey plane frames are now compared with the results from the computer program SWANSA. Both frames are subjected to sway loading. As reported by Seniwongse these two frames were originally studied by Franklin[67] also using finite element technique. The technique utilises quadrilateral linear strain elements, special frame elements, and bidirectional tie-link elements to analyse the two frames. Seniwongse developed a finite element technique using linear beam elements with bilinear rotational spring elements at each end of the beam element. The literature[66] compares the results from both the analysis. The geometrical data of the frames are given in Fig. 6.7.

The material data used in the analysis are as follows:

Cylinder strength of concrete in compression	= 37.95	N/mm <sup>2</sup>
Yield stress of concrete in compression	= 0.85*37.95	N/mm <sup>2</sup>
Ultimate strain in compression	= 0.003	
Young's modulus of concrete	= 20.01	N/mm <sup>2</sup>
Tensile stress of concrete	= 0.1*0.85*37.95	N/mm <sup>2</sup>

A bilinear curve was used for concrete model, as in the original studies.

Yield stress of steel	= 284.63	N/mm <sup>2</sup>
Ultimate stress of steel	= 351.9	N/mm <sup>2</sup>
Young's modulus	= 200.1	N/mm <sup>2</sup>
Ultimate strain	= 0.15	

The ultimate loads are compared below for both the frames. The load deflection paths are shown in Figs 6.8 and 6.9. It should be noted that the program SWANSA gives excellent agreement with both the finite element results.

**TABLE 6.4 COMPARISON OF ULTIMATE LOAD**

	FRANKLIN	NLACF	SWANSA	ERROR WITH FRANKLIN
One storey frame	5.4	5.4	5.34	-1%
Two storey frame	4.0	3.8	4.28	7%

## 6.4 CONCLUSION

The computer program SWANSA has been shown to give good correlation with results for reinforced concrete frames. It can be safely concluded that the numerical technique which forms the basis of the computer program SWANSA can be used to study and predict the deflected shape and the ultimate capacity of reinforced concrete sway and no-sway plane frames with flexible connections. The numerical technique is indeed capable of analysing space frames, but experimental results for such frames were not found in literature.

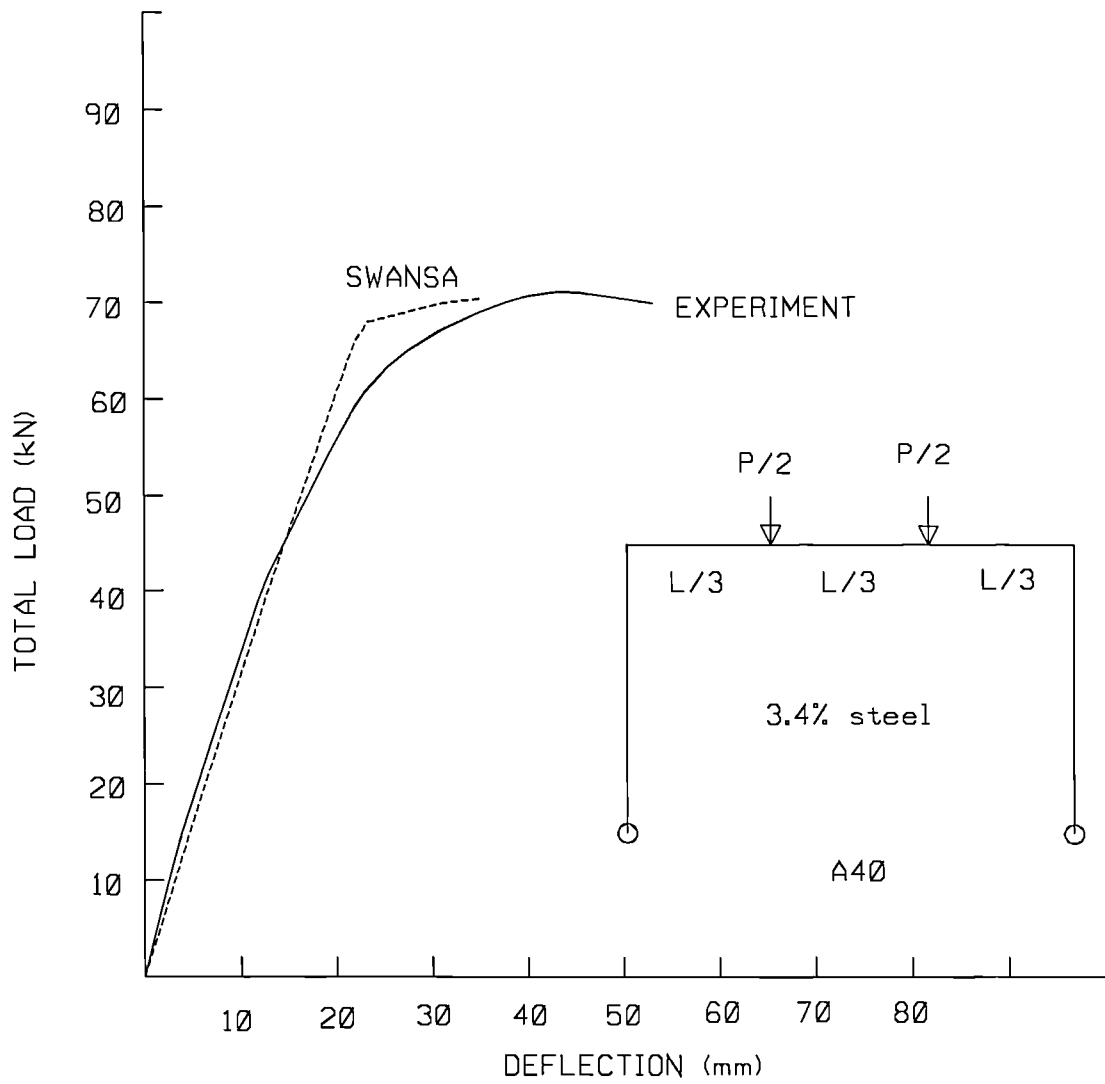


**FIG.6.1 COMPUTED AND EXPERIMENTAL MIDSPAN DEFLECTION FOR FRAME A40**

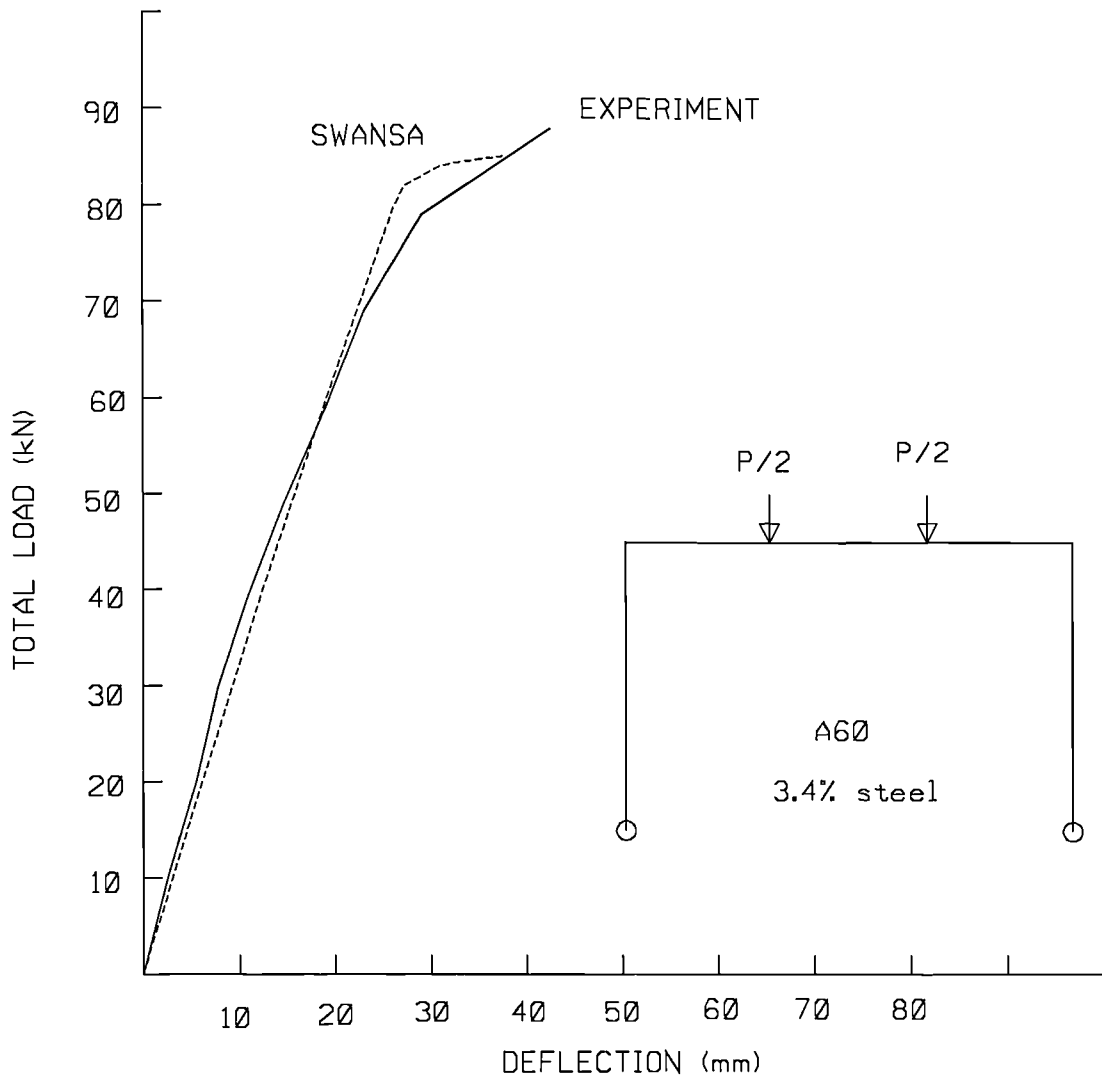


**FIG.6.2 COMPUTED AND EXPERIMENTAL MIDSPAN DEFLECTION FOR FRAME A60**

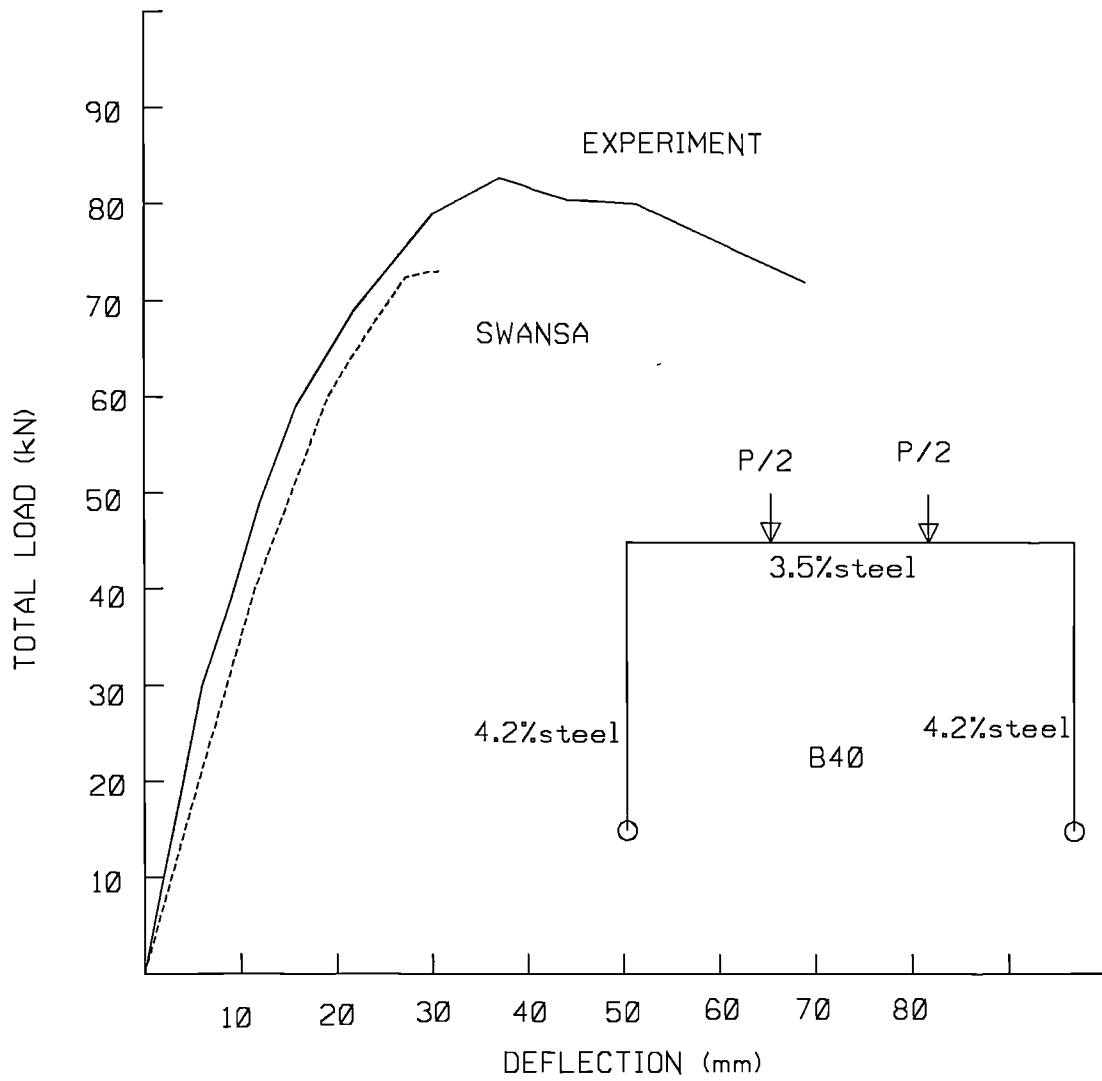


**FIG.6.3 COMPUTED AND EXPERIMENTAL MIDSPAN DEFLECTION FOR FRAME B40**

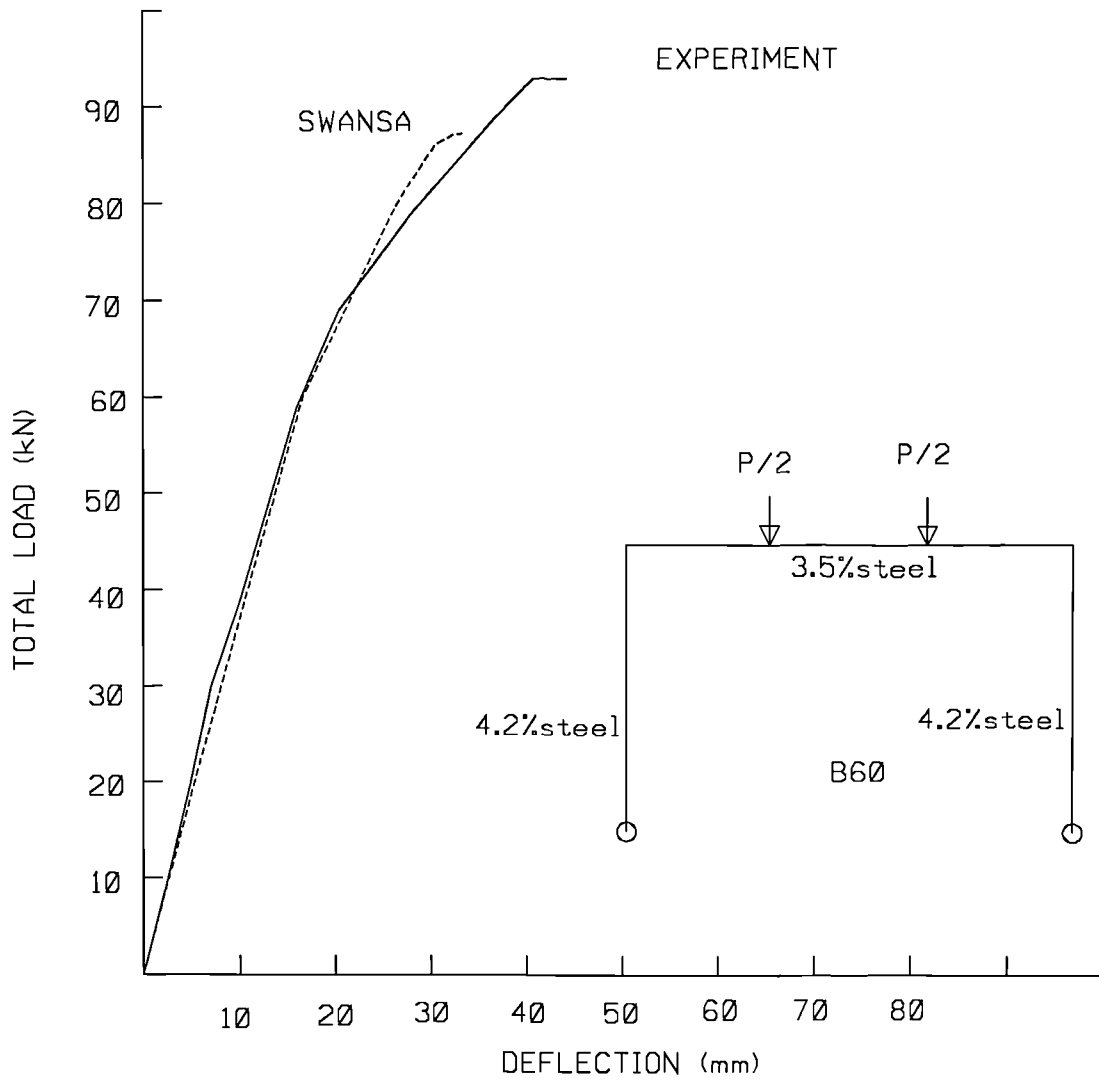


**FIG.6.4 COMPUTED AND EXPERIMENTAL MIDSPAN DEFLECTION FOR FRAME B60**

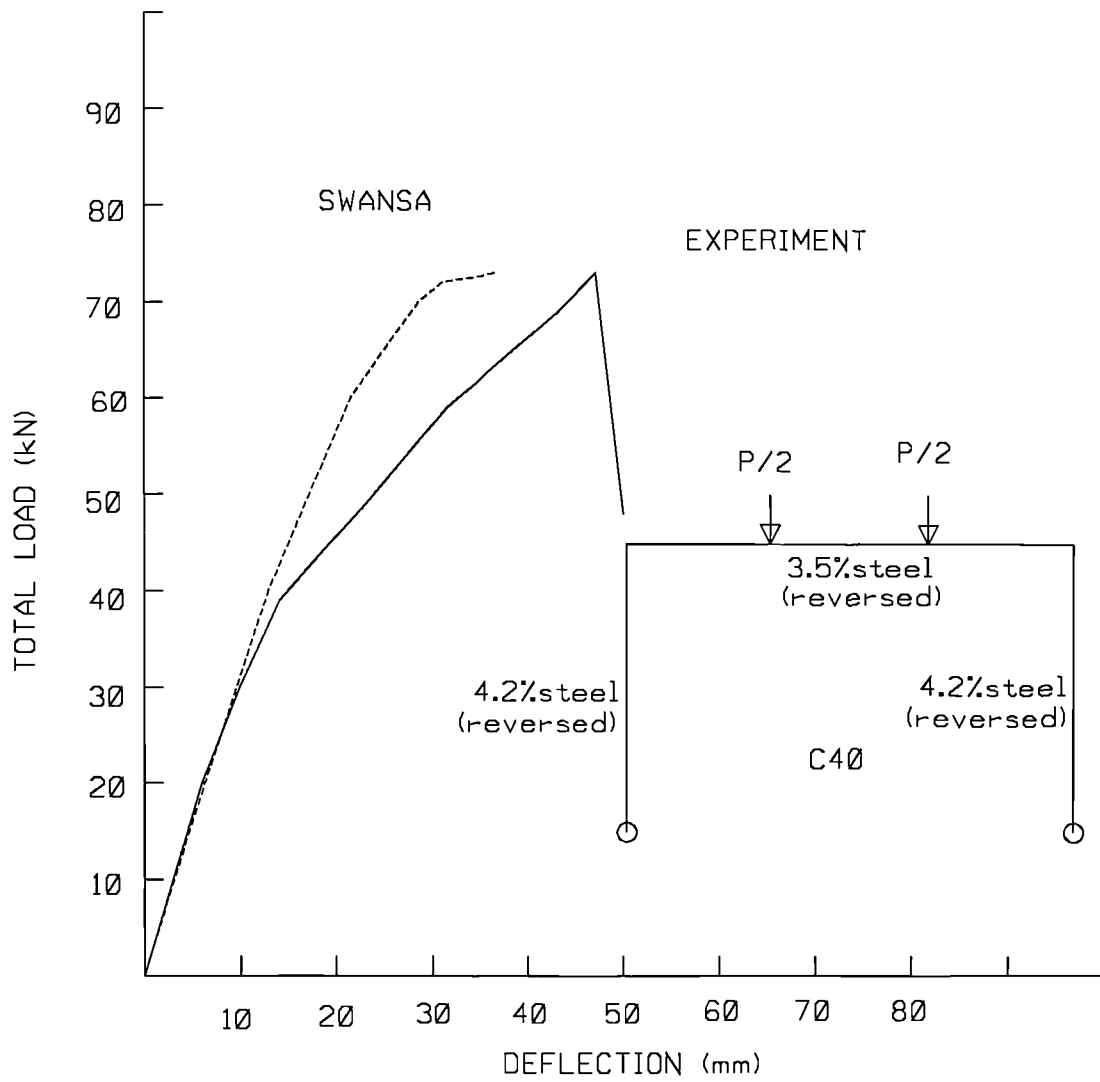


**FIG.6.5 COMPUTED AND EXPERIMENTAL MIDSPAN DEFLECTION FOR FRAME C40**

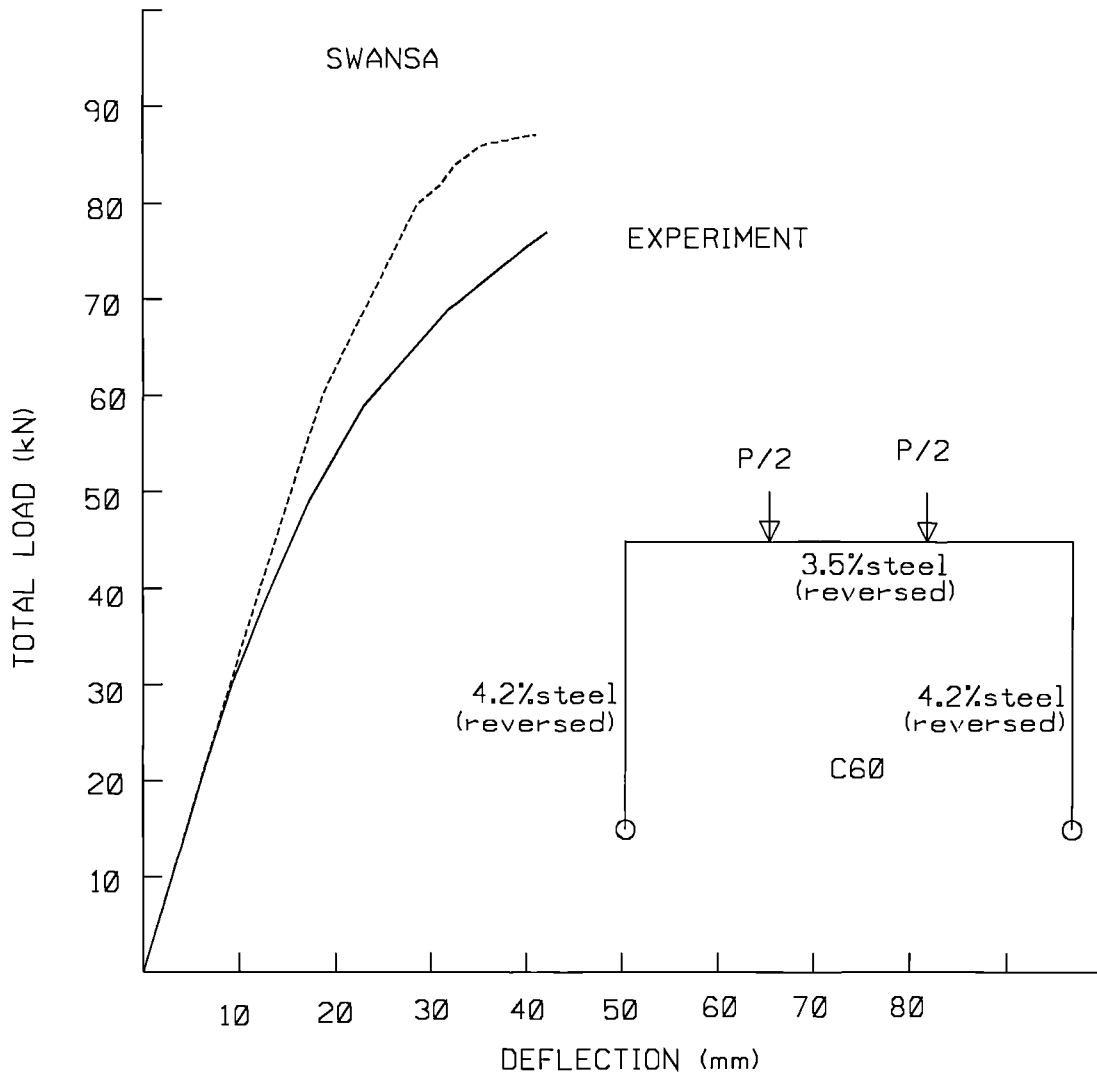
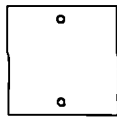
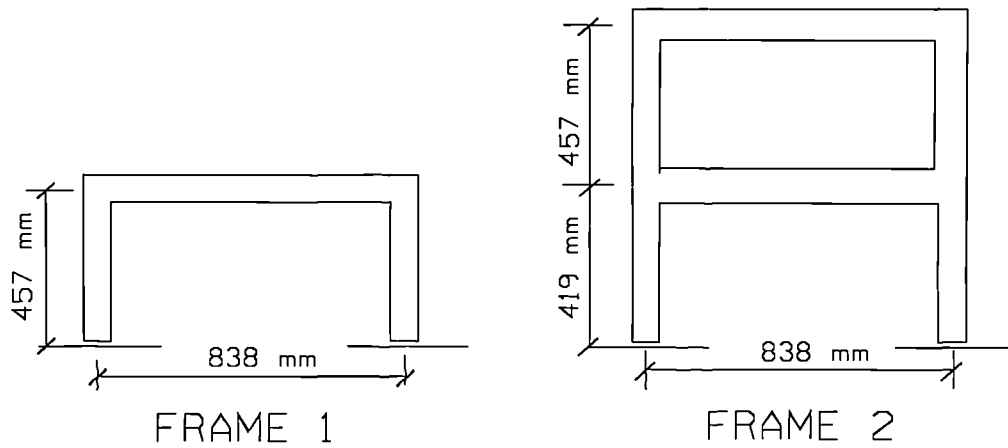


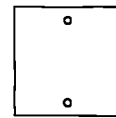
**FIG.6.6 COMPUTED AND EXPERIMENTAL MIDSPAN DEFLECTION FOR FRAME C60**



BEAM SECTION

76x76

Cover 9 mm  
(both)



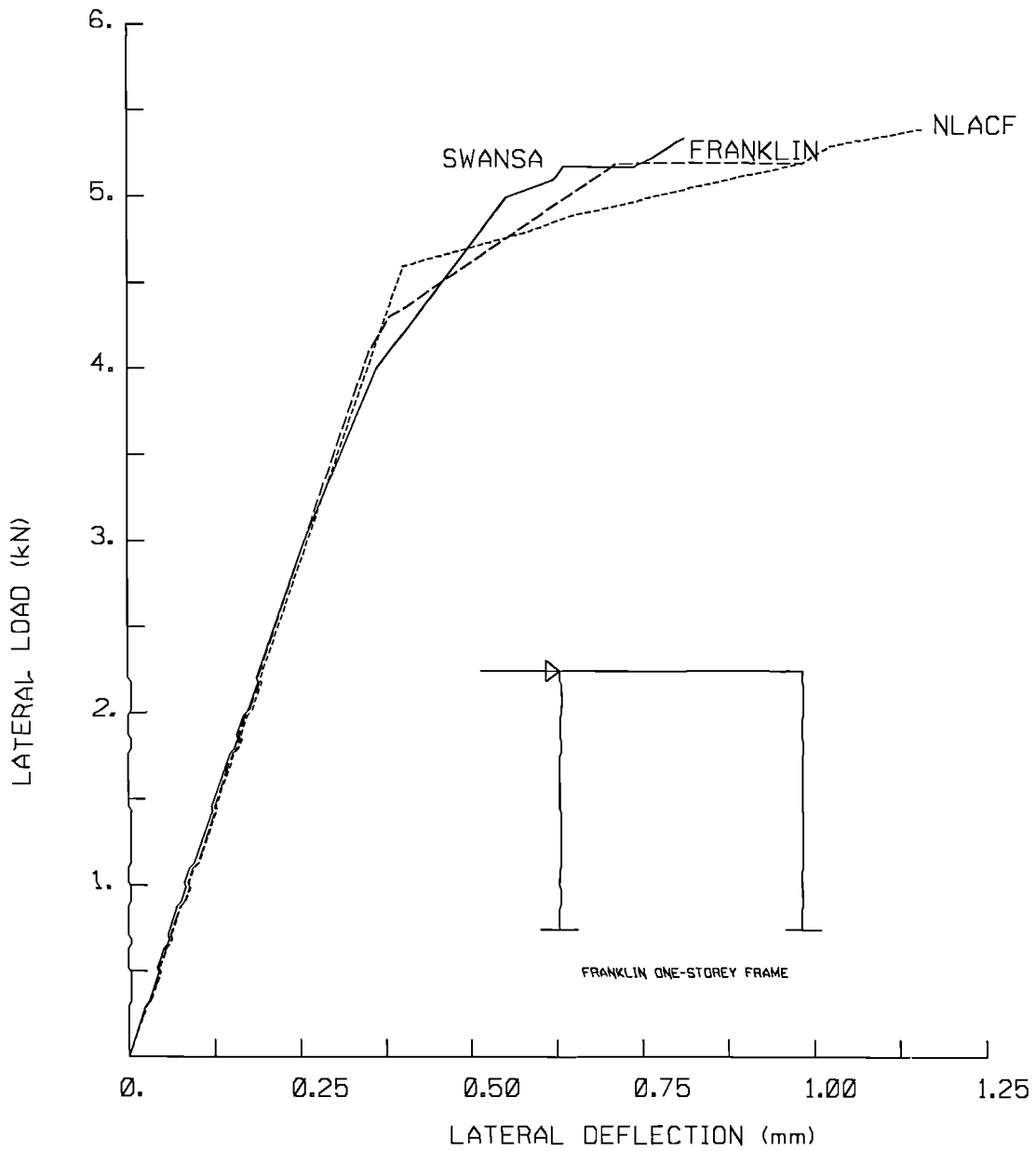
COLUMN SECTION

76x76

Cover 9 mm (inner face)  
Cover 13 mm (outer face)

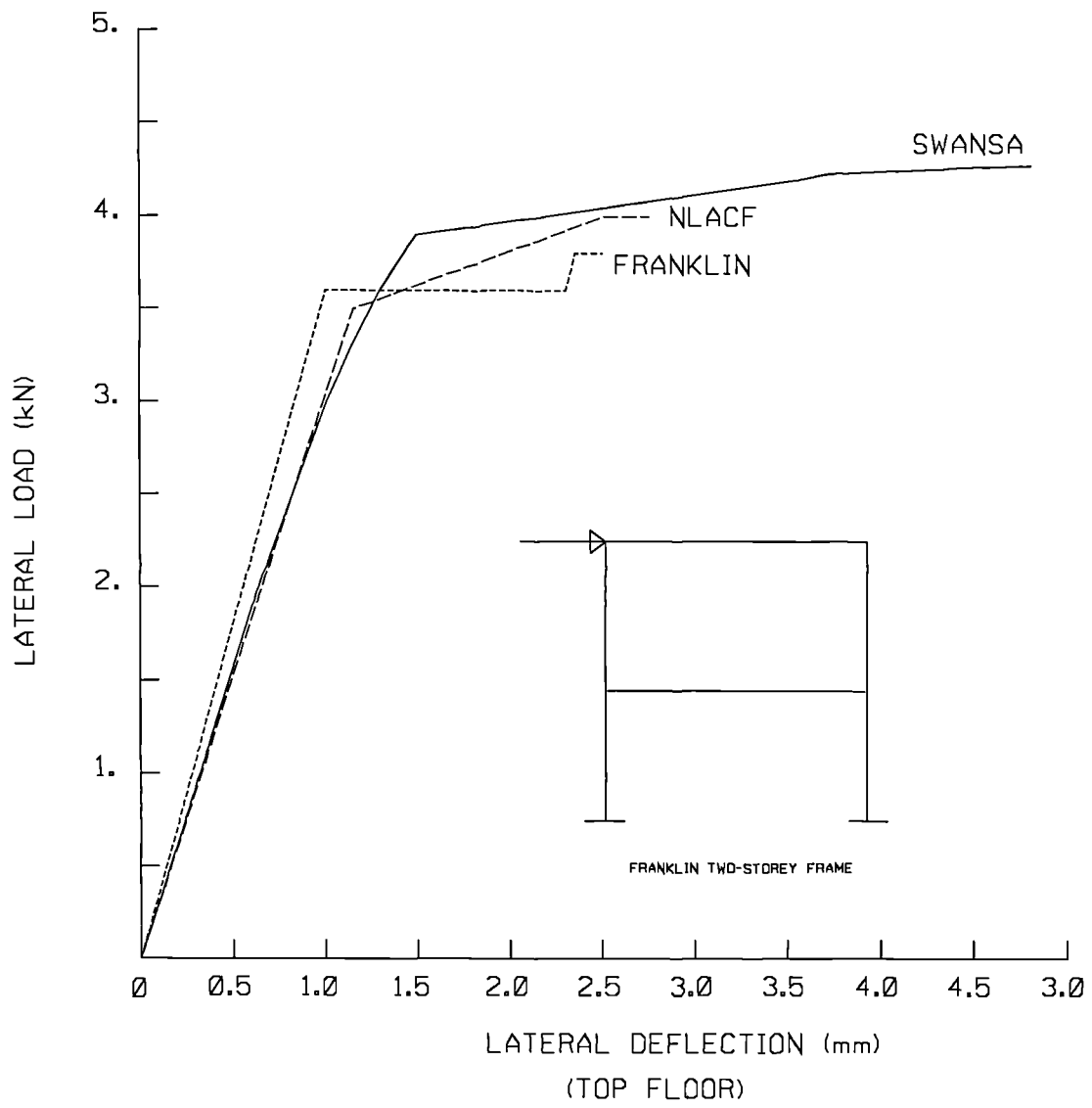
Area of steel = 31.7 sq.mm each

**FIG.6.7 GEOMETRICAL DATA FOR FRANKLIN'S FRAMES**



LATERAL DEFLECTION VERSUS LATERAL LOAD

FIG.6.8 DEFLECTION AT THE FIRST FLOOR LEVEL FOR FRAME 1



LATERAL DEFLECTION VERSUS LATERAL LOAD

**FIG.6.9 DEFLECTION AT THE SECOND FLOOR LEVEL FOR FRAME 2**

# CHAPTER 7

## EXAMPLE ON DESIGN APPLICATION

### 7.1 INTRODUCTION

The current design method as defined in BS8110:1985 suggests that the connections in precast concrete members should be treated as pin-joints. The numerical method described in Chapter 3 demonstrates how a precast concrete frame could be analysed incorporating the semi-rigidity of the connection. It will be shown how the computer program SWANSA based on the above numerical method of non-linear analysis may be used as a design tool. Apart from the normal geometrical and material properties, the additional data required for the analysis is the moment rotation characteristic *of the connection to be used in the frame*. A three-storey two-bay frame is used to demonstrate the procedure that may be adopted.

### 7.2 MODELLING THE STRUCTURE

*Preliminary section properties of the frame were selected from the available precast components based on the requirements of the structure. Assumptions relating to the connection types were also made before starting the computer analysis. It must be understood that the moment rotation data for all the connections used in the frames should be available before the analysis. Most companies dealing with precast structures maintain their own data on connection behaviour. Only the main reinforcement used in flexure was considered in the analysis. All the additional bars such as torsional reinforcement, shear reinforcement and connection reinforcements were not taken into consideration. The analysis does not at present, check the structure*

for shear or torsional strength. Member shear forces and torsional moments obtained from the analysis can be used to check the structure for the above factors. The frame geometry and section data used in the analysis are shown in Fig.7.1. The idealized moment rotation curve of the joint used in the frame is also given that figure.

### 7.3 MATERIAL MODELS

Grade 50 concrete (cube strength) with a partial safety of 1.5 was used in the design. Yield stress of the reinforcement used was  $400 \text{ N/mm}^2$ . A partial safety factor of 1.15 was adopted for the reinforcement. The stress-strain curves and the partial safety factors used in the analysis were in accordance with BS8110:1985.

### 7.4 LOADINGS

The following loads were used in the analysis.

Characteristic dead load on all floors	= 25 kN/m length of beam
Characteristic imposed load on all floors	= 40 kN/m length of beam
Characteristic wind load in middle floor	= 16.667 kN total
Characteristic wind load in top floor	= 8.333 kN total

These loads were combined according to the load factors specified in BS8110:1985. A factor of 1.4 for dead load, a factor of 1.6 for live load and a factor of 1.2 were used for wind load. The exact loads considered in the analysis are given in Table 7.1. Patterned loading was used to obtain the worst instability effects in the columns. The loads  $w_1$  and  $w_2$  given in Table

7.1 are the distributed loads on respective beams as shown in Fig. 7.1. The notation  $F$  represents the lateral load acting at top floor level. The wind load considered at intermediate levels were twice of  $F$ . Three combinations of load cases were considered.

In load case 1 the total of design dead load and design live load on all the beams were factored by 0.1 to initiate the analysis and the factor was increased until the further equilibrium deflected shape could not be found. It must be noted that starting load factor must be small in order to find initial equilibrium deflected shape.

In load case 2, the characteristic dead load was allowed to act on beams marked as  $w_1$  in Fig.7.1. The total of design dead and live load was assigned to beams marked with  $w_2$ . During the analysis the load  $w_1$  was kept constant and load  $w_2$  was varied from an initial load fact of 0.1 until the frame reaches ultimate failure load. The wind load was assumed to be zero in this analysis.

In load case 3 characteristic dead load was assigned to all the beams in the frame and a value of 10 kN was used for the wind load common factor  $F$ . The beam loads were kept constant while the wind load was increased from an initial load factor of 0.1 until structure fails in sway mode.

In all the load case the structure was tested for ultimate load.

## **7.5 JOINT TYPES**

Three types of joints were considered in the analysis as described below.

- Joint type 1    Monolithically cast reinforced concrete connection.
- Joint type 2    Semi-rigid precast concrete connection.
- Joint type 3    Pin jointed as often adopted in current practice.

## 7.6 RESULTS

Fig. 7.2 to 7.10 show bending moment distributions obtained from the computer program SWANSA. This is an option available in the post-processor of the computer program. It may be noted that the maximum column moment for all the three load cases in frame of joint type 1 (Fig 7.4) is 93.1 kNm. This maximum column moment occurs for the load case 3 in which wind is included. The corresponding values are 90.3 kNm for joint type 2 (Fig 7.7) and 83.2 kNm for joint type 3 (Fig 7.10). Corresponding load factors on wind force were 29.8, 23.8 and 4.7 respectively (Table 7.1). The increase in load factor when joint rigidity is considered in the analysis can be observed clearly. Failure of the frames in load case 3, was due to these ultimate moments in the column. The failure moments in column vary slightly due to the different axial loads present for different joint types at failure.

The mechanism by which the structure gains strength, when joint rigidity is included in the analysis, can be noted by studying the bending moment and axial load values given in Fig 7.4, 7.7 and 7.10. Bending moments in the left hand side of the beams in type 1 and type 2 frames change signs. This creates a couple of shear forces in the beams and thereby increases the load in the right column and reduces the load in the left column. This increased column reaction counter balances the wind force. Since these moments are zero in

type 3 frames (with pin joints) the wind force is distributed to all three columns and resisted by cantilever action.

The favourable redistribution of bending by considering joint rigidity is an obvious advantage. The load carrying capacity of a simply supported beam as in the case of type 3 frame (Fig 7.8 and 7.9) is improved considerably when joint rigidity was taken into account (Fig 7.5 and 7.6).

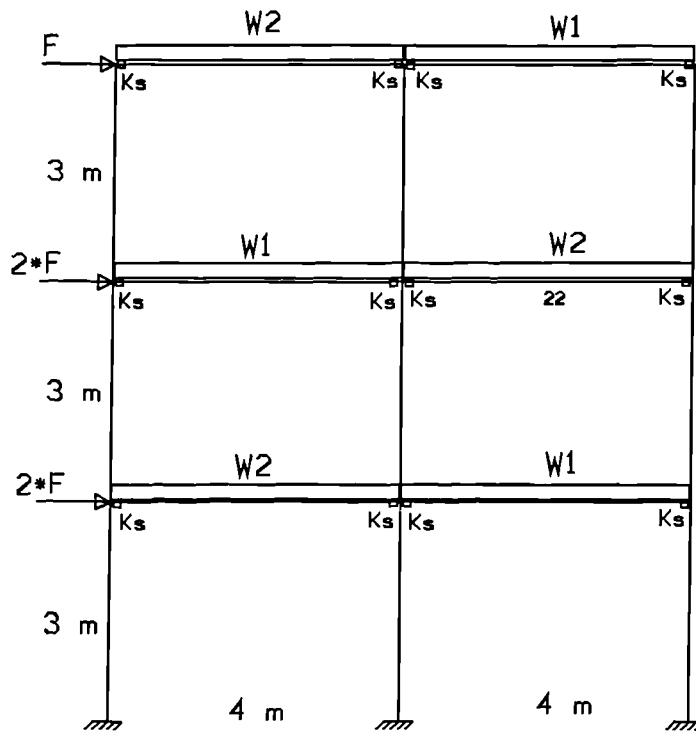
The ultimate load obtained from the analysis are tabulated below. The table shows the design loading and the ultimate load obtained from SWANSA for the three types of joints and for the three loading combinations.

**TABLE 7.1 COMPARISON OF LOAD FACTOR FOR PROPOSED METHOD AND THE OLD METHOD**

LOAD CASE	DESIGN LOAD			ULTIMATE LOAD								
	W1 kN/m	W2 kN/m	F kN	TYPE 1			TYPE 2			TYPE 3		
				W1	W2	F	W1	W2	F	W1	W2	F
1	99.0	99.0	0.0	126.9	126.9	0.0	108.0	108.0	0.0	63.9	63.9	0.0
2	25.0	99.0	0.0	25.0	125.2	0.0	25.0	101.6	0.0	25.0	64.1	0.0
3	25.0	25.0	10.0	25.0	25.0	29.8	25.0	25.0	23.8	25.0	25.0	4.7

It will be observed that, in all cases, the ultimate load obtained under Type 3 is less than the design load. This implies that the structure if designed on the bases of assumed pinned connections will have to be strengthened. The alternative to strengthening of the members would be to use additional structural elements such as shear walls.

The results show that the inclusion of semi-rigid connection behaviour can lead to a tapping of considerable reserves of strength available in the frame. Consideration of the semi-rigid behaviour of connection can thus lead to significant economy in design. This example also shows that the proposed method of analysis can be a valuable design tool.

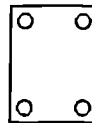


CONCRETE: GRADE 50  
 partial safety factor=1.50

STEEL: YIELD STRESS 460 kN/mm<sup>2</sup>  
 partial safety factor=1.15



SECTION 300x300  
 STEEL 4T20  
 COLUMN



SECTION 300x400  
 STEEL 4T25  
 BEAM

COVER TO CENTRE 50 mm

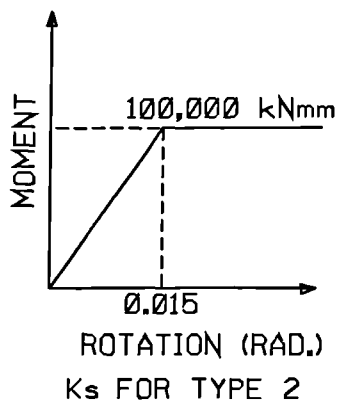
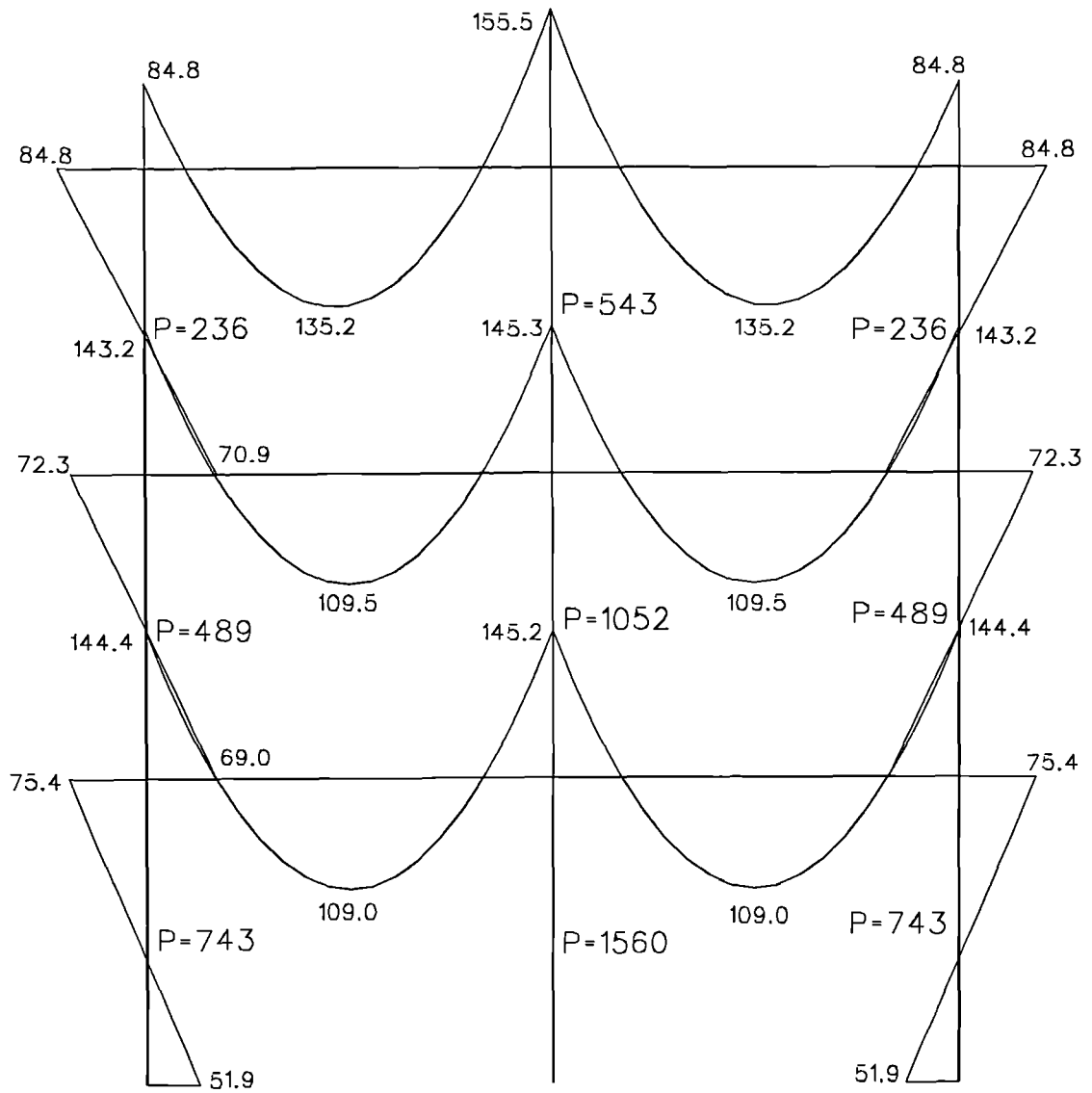
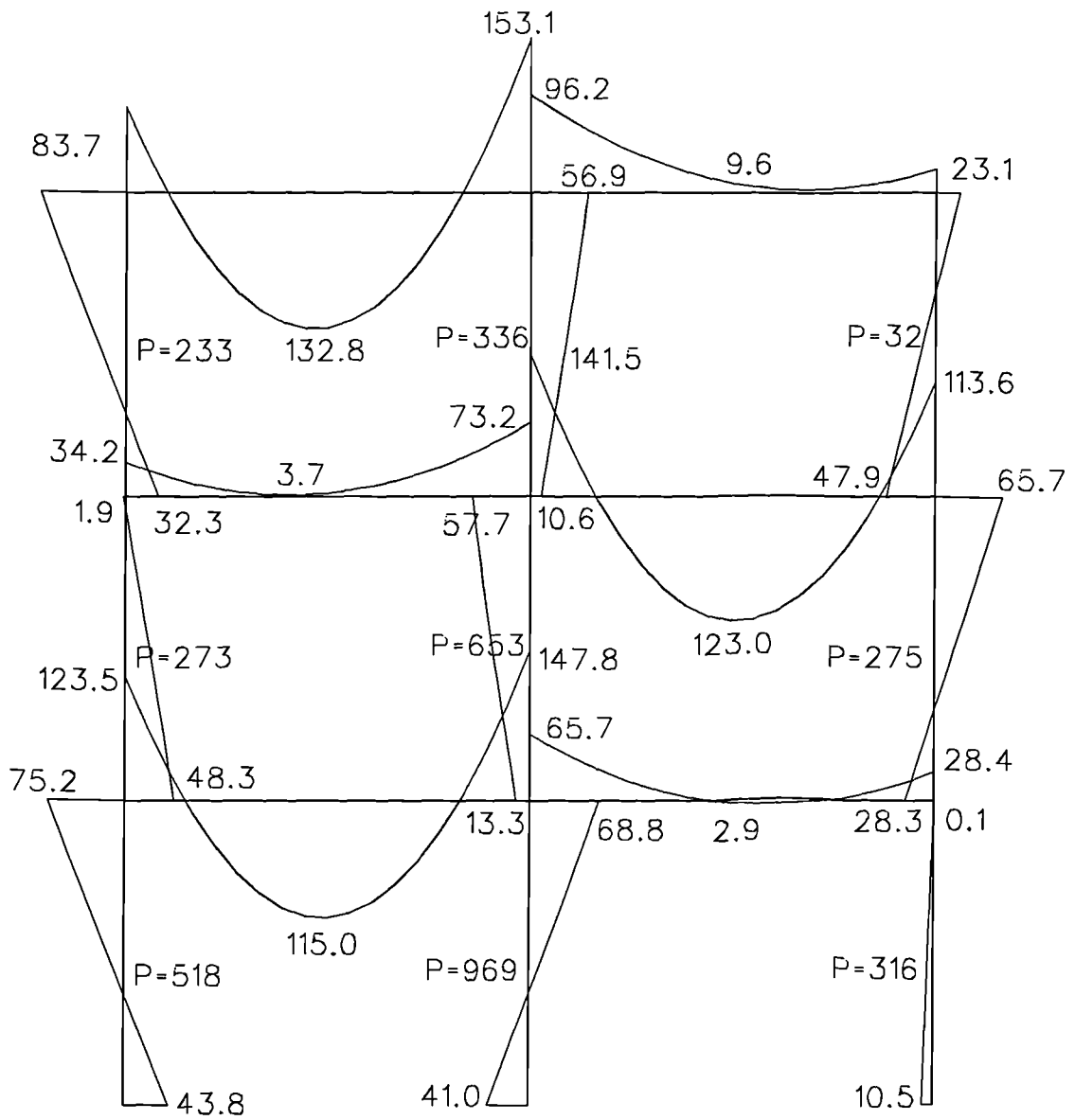


FIG.7.1 GEOMETRICAL DATA OF THE FRAME



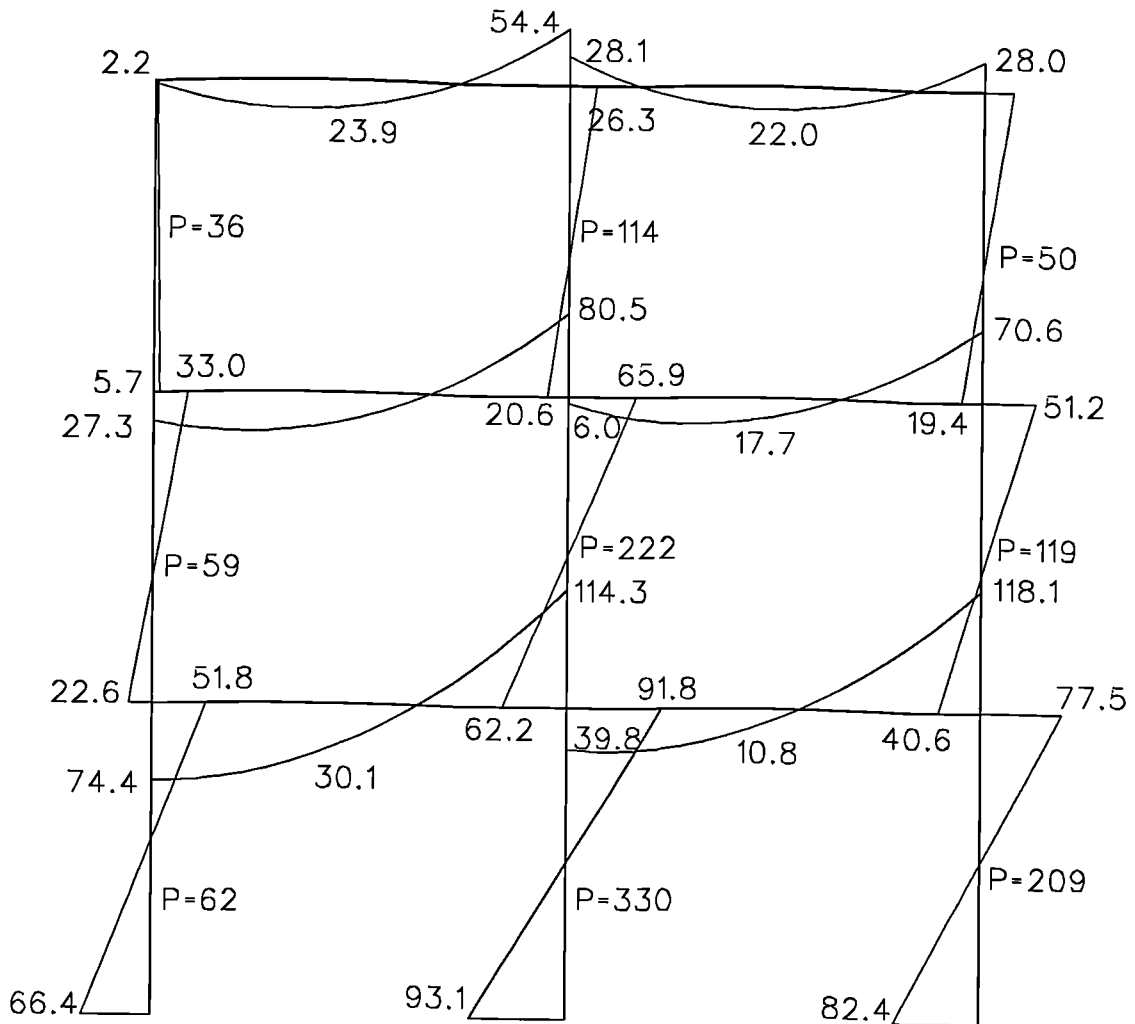
FRAME 1 , LOAD CASE 1

**FIG.7.2 BENDING MOMENT DIAGRAM**



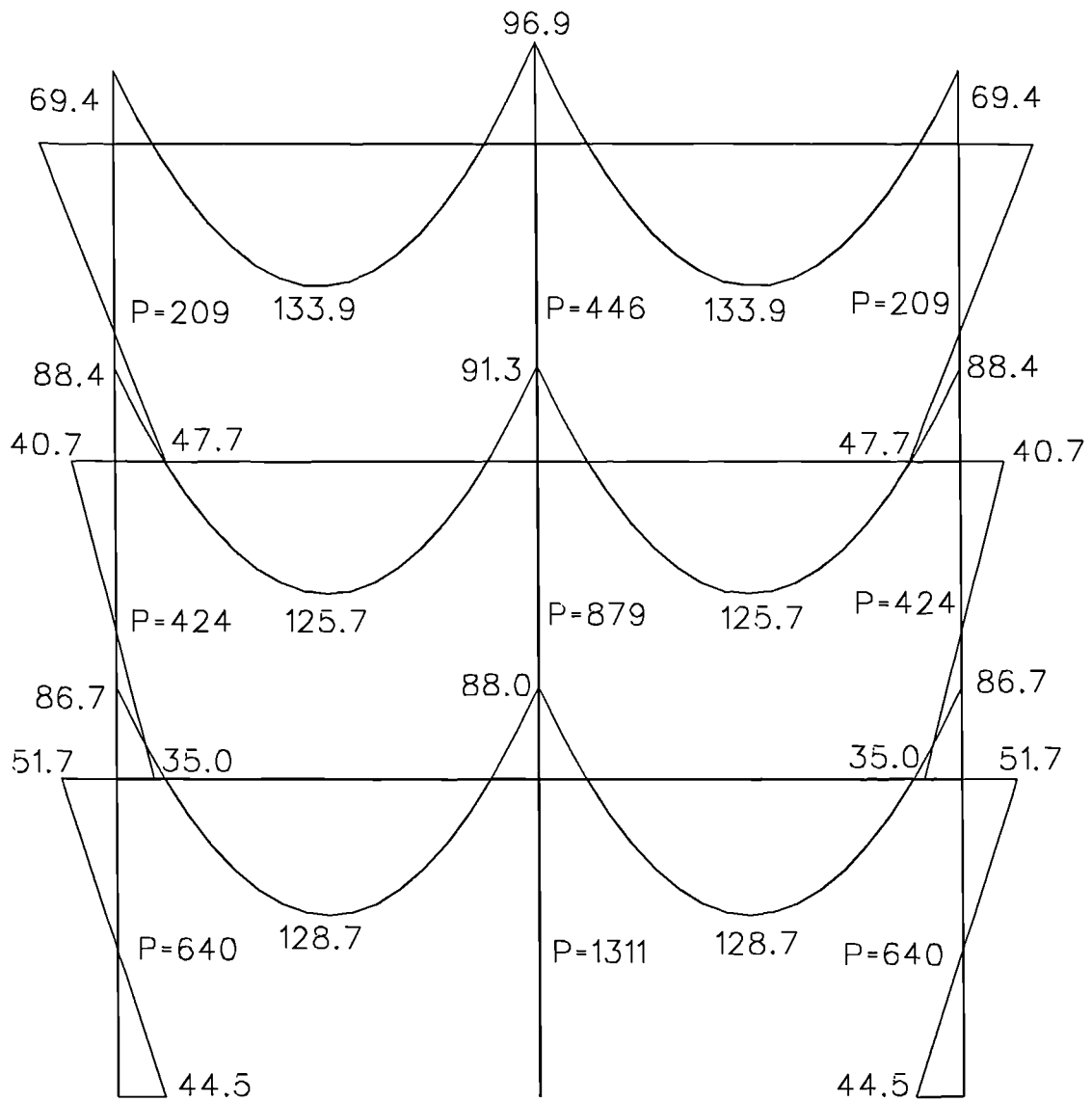
FRAME 1, LOAD CASE 2

**FIG.7.3 BENDING MOMENT DIAGRAM**



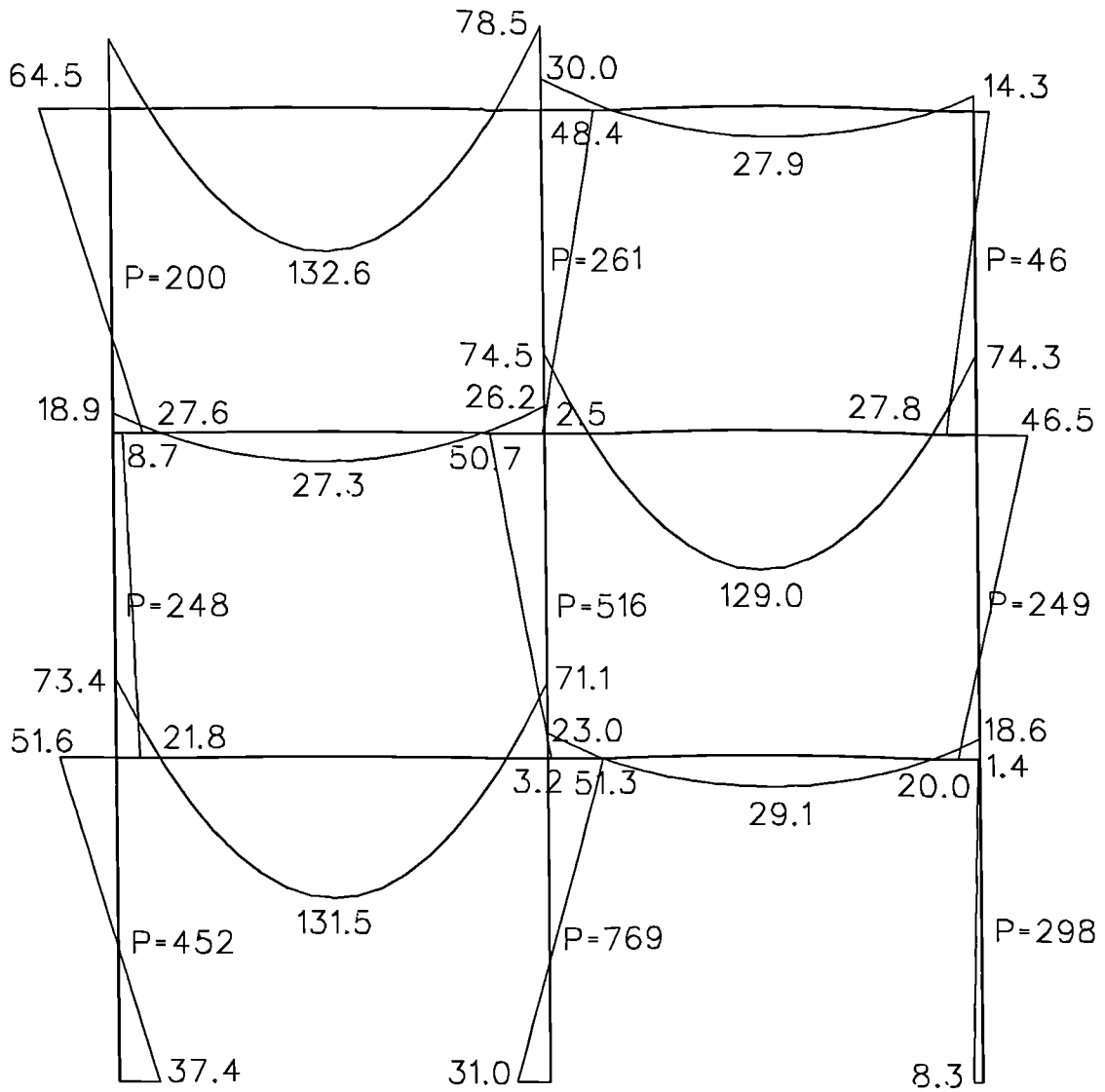
FRAME 1, LOAD CASE 3

**FIG.7.4 BENDING MOMENT DIAGRAM**



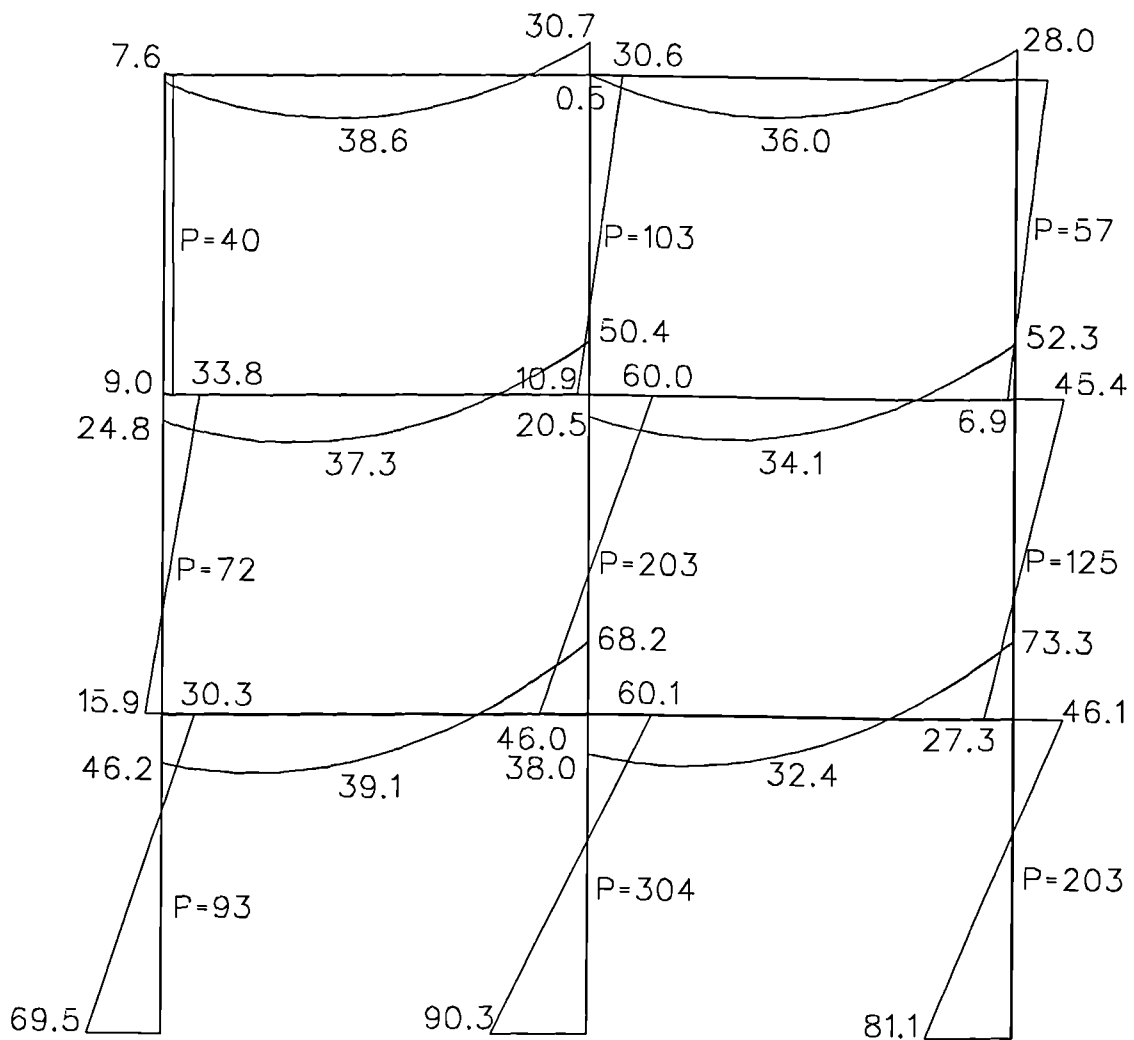
FRAME 2, LOAD CASE 1

**FIG.7.5 BENDING MOMENT DIAGRAM**



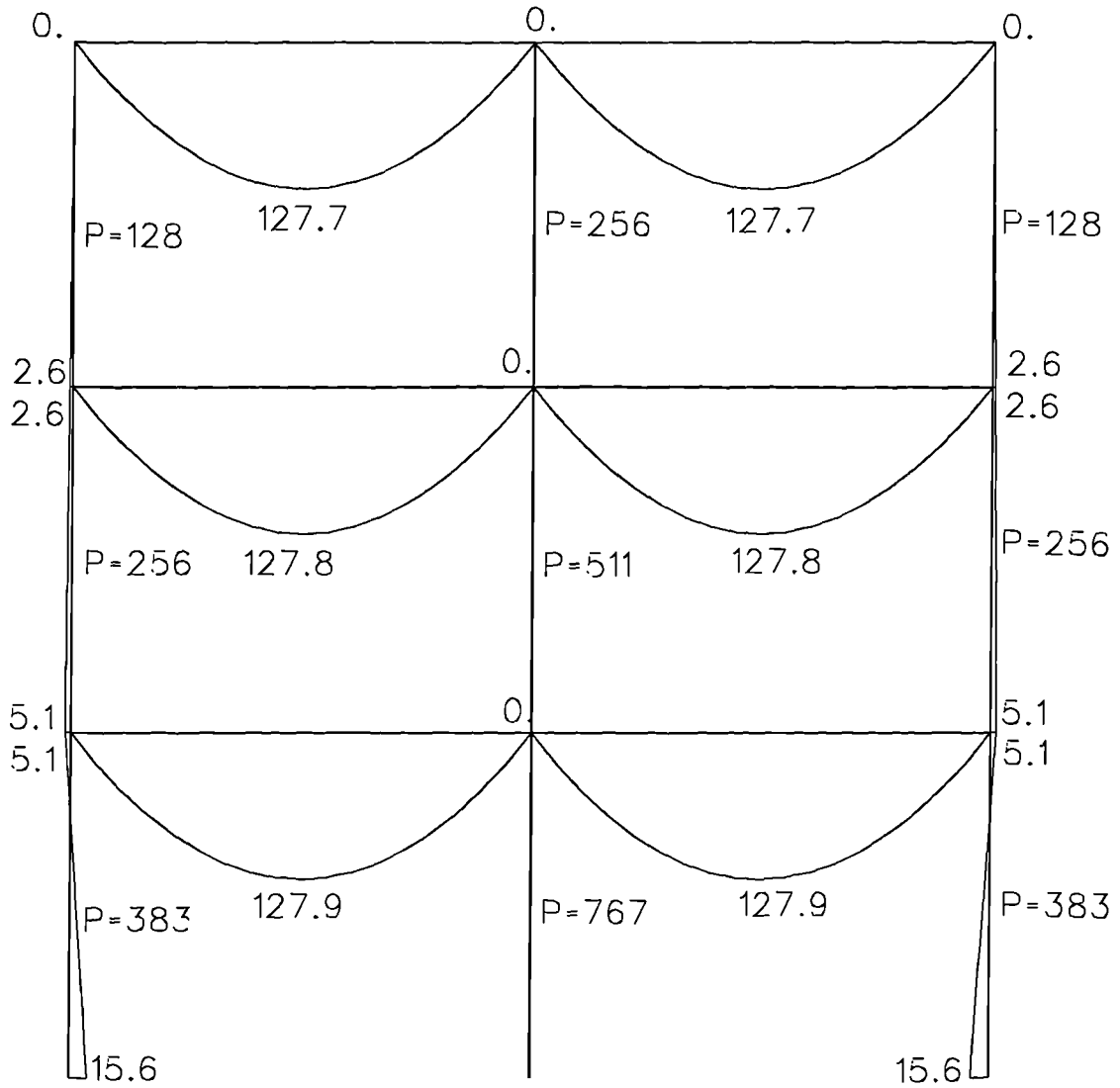
FRAME 2, LOAD CASE 2

**FIG.7.6 BENDING MOMENT DIAGRAM**



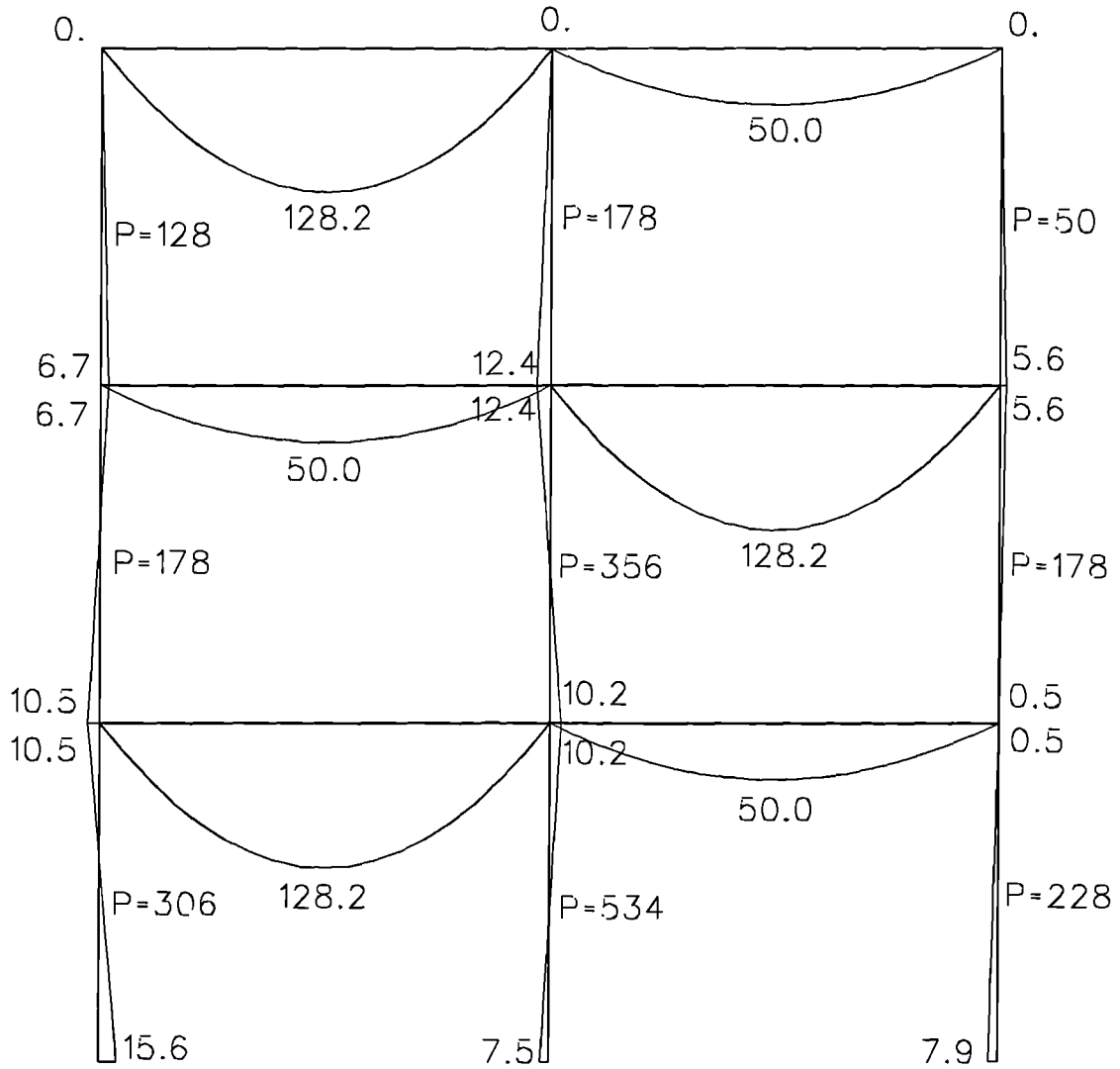
FRAME 2, LOAD CASE 3

FIG.7.7 BENDING MOMENT DIAGRAM



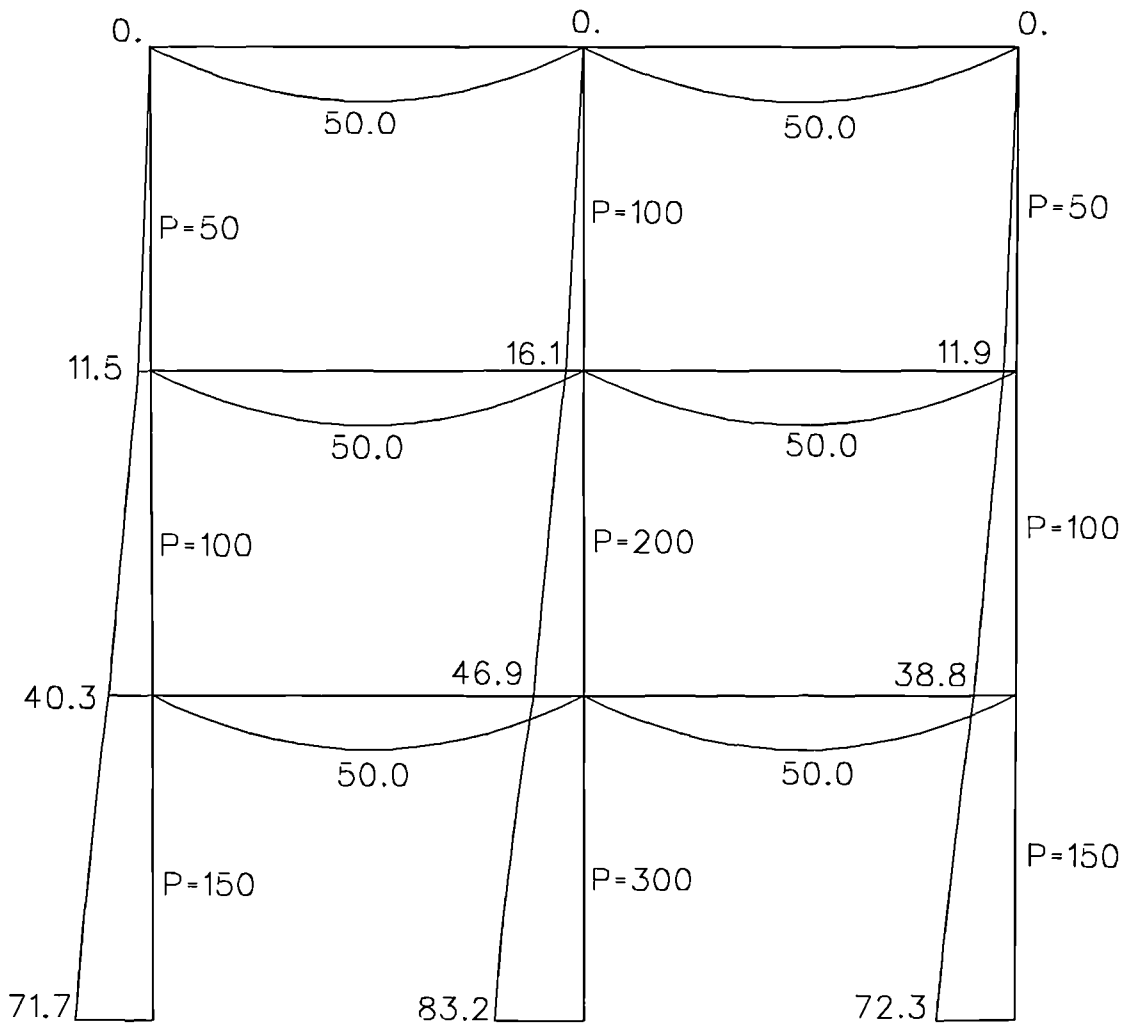
FRAME 3, LOAD CASE 1

**FIG.7.8 BENDING MOMENT DIAGRAM**



FRAME 3, LOAD CASE 2

FIG.7.9 BENDING MOMENT DIAGRAM



FRAME 3, LOAD CASE 3

**FIG.7.10 BENDING MOMENT DIAGRAM**

# CHAPTER 8

## CONCLUSIONS

### 8.1 INTRODUCTION

Traditionally, by making the assumption that the beam to column connection in precast concrete frames is pin-jointed, the design calculations are simplified. The reason for adopting this approach in designing precast concrete frames is that the behaviour of beam column connection and its influence on the stability of the frame has not been well understood. The study carried out in this report has been aimed at achieving a better understanding of behaviour of frames with semi-rigid connections. This has led to the development of an analytical method to study the behaviour of precast concrete frames with flexible connections. Experiments were carried out to validate the new method of analysis.

### 8.2 ANALYTICAL METHOD

The new method of analysis of precast concrete space frames takes into account the semi-rigid nature of connections. The numerical procedure is based on establishing equilibrium deflected shape of the frame for given external forces. By providing suitable moment rotation relations for the joint at ends of beam-columns, the effects of flexible joints are included in the numerical analysis. The method of analysis isolates the torsional effects and direct shear from flexural behaviour of members. Of course, all torsional moments and direct forces are considered in the overall equilibrium requirements.

The member equilibrium at a chosen number of points is satisfied by considering curvatures and material stress-strain characteristics using numerical quadrature procedure. The member deflected shape is then obtained by the generalised Newton-Raphson, following a well established procedure for isolated restrained columns[8]. The advancement is made in considering equilibrium at the nodal points, by establishing a numerically computed stiffness-matrix. The numerical approach allows introduction of semi-rigid joints, with arbitrary moment-rotation characteristics, to be included in the iteration procedure.

Starting with a suitable load factor, the external forces are increased in steps until an equilibrium deflected shape for the frame cannot be found. Such a load is taken as the ultimate load of the frame.

### **8.3 COMPUTER PROGRAM**

The computer program *SWANSA* based on the numerical method developed here, has the following options:

1. Sway and no-sway analysis of 3-dimensional precast concrete frames.
2. Joints can be rigid, pinned or flexible.
3. Any one of the forces or combination of forces can be increased to reach the ultimate load.
4. The output can be presented in a graphical form to view and produce hard copy of deflected shape, bending moment diagrams and shear force diagrams.

The program has been made user friendly, by providing an interactive data entry facility, which allows the user to enter data by answering simple questions or returning default values.

The principal feature of the graphical post-processor is that the results are presented in the form of bending moment, shear force and deflection diagrams, making them more usable by practicing engineers.

#### **8.4 EXPERIMENTAL STUDY**

Experiments were carried out on 8 full scale precast concrete subframes (CT1 to CT8) each consisting of a two-storey continuous column and a short beam, tested primarily to validate the computer program *SWANSA*. Four beam column connections from four participating precast concrete frames manufacturers were used in the experiments. Two frames per each connection details were made. One frame was tested in upward rotation of the beam column connection and the other was tested in downward rotation.

#### **8.5 COMPARISON OF COMPUTED RESULTS WITH EXPERIMENTS**

The above frames were modelled and analysed using the computer program *SWANSA*. Good correlation has been obtained between experimental and computed results. Ultimate loads predicted by the computer program are within 6-7% of the experimental values. Deflection profiles, as well as strain distributions in the frame also show good agreement with the experimental observations. The use of the above computer program as a tool to predict behaviour of precast concrete no-sway frames is well demonstrated in the

comparison of deflections and strains in the members and of the ultimate loads of the frames.

## **8.6 COMPARISON WITH OTHER RESULTS**

The method has been further validated with computational and experimental results available in literature. Experimental results carried out on six portal frames reported by Ernst et al[65] were compared with the analytical results from SWANSA. The comparison of mid span deflections and the ultimate loads was very good. The average error in computing ultimate loads is only 1.3%.

Results on single and two storey plane sway frames based on finite element methods, reported by Seniwongse[66], were also compared with analytical results obtained from the computer program SWANSA. The correlation of lateral deflection at loaded floor level was excellent. The error in ultimate load for the single storey frame is 1% and for the two storey frame is 7%.

## **8.7 DESIGN EXAMPLE**

The computer program *SWANSA* can be used to analyse reinforced concrete frames with or without flexible connections starting from small loads up to failure. The use of the program as a direct computer aided design tool has been demonstrated inside the report. The program can be used as an alternative method of designing a structure. The only other method that could provide a compareably exact solution is the finite element method, but that method is obviously very time consuming in terms of modelling of the structure and evaluation of results. The key features of the numerical method

described in Chapter 3, relating to fewer variables needed for a solution, allow the computations to be carried out faster than the finite element method, yet retain the required accuracy.

## **8.8 FUTURE WORK**

The most critical information required for an analytical study of precast concrete frames is the moment rotation characteristic of the connections. There are two ways of establishing this information. Each contractor can either establish a data set based on experiments or design a connection for a given idealised moment rotation curve. If technology used by the contractor permits, the latter method gives designer the freedom of developing universal design charts for a given set of connections. Unifying connection behaviour and producing design charts would be a worth while operation to undertake.

There are no experimental or analytical data available to study the torsional effects on a space frame. Isolating torsion from the flexure and treating the torsional behaviour linearly, as adopted in this work, may be considered satisfactory at working load level but the torsional effects might dominate near failure where rotations are high. This aspect needs more consideration if the new technique is to be used to study the behaviour of space frames in general.

## REFERENCES

1. BRIGGINSHAW, G F. *A new era for structural frames*. Concrete, Oct 1987.
2. AMEY, D J. *Precast concrete structural frames in the UK.*, Constructional Review, Aug, 1987.
3. Industrial news, *Precast concrete frames-an economic update*. The structural engineer, Vol. 65A, No. 8, Aug. 1987.
4. Industrial news, *The economics of precast frame construction*, The structural engineer, Vol. 63A, No. 7, Jul. 1985.
5. BARFOOT, J. *Precast frames*. Concrete, Apr. 1989.
6. Cavanagh, K. *Future looks bright for prefab industry*. Engineers Australia, May 1988.
7. *Structural joints in precast concrete*. The institution of structural engineers, 1978.
8. VIRDI, K S. and DOWLING, P J. *The ultimate strength of biaxially restrained columns*. Proceeding of the Institution of civil engineers, Mar 1976, Part 2.
9. FRANKLIN, H A. *Nonlinear analysis of reinforced concrete frames and panel*. PhD Thesis: University of California, Berkeley, 1970.
10. VAN DEN BROEK, J A. *Euler's classic Paper 'On the strength of columns'*. American journal of physics, Vol 15, 1947.
11. BLEICH, F. *Buckling strength of metal structures*. McGraw-Hill Book Company, New York, 1952.
12. HORNE, MR. *An historical review on the interaction of plasticity and structural stability in theory and its application to design. Modern developments in frame and slab structures*. Conference by The Institution of Structural Engineers, Nov. 1988.
13. SHANLEY, F R. *Inelastic column theory*. Journal of aeronautical science, 1947.

14. TIMOSHENKO, S P. and GERE, J M. *Theory of elastic stability*. McGraw-Hill international book company, London, 1982.
15. BLEICH, F. *Buckling strength of metal structures*. McGraw-Hill Book Company, New York, 1952.
16. COLLATZ, L. *Functional analysis and numerical mathematics*. Academic Press, New York, 1966.
17. BROWN, P T. and TRAHAIR, N S. *Finite integral solution of differential equations*. Civil Engineering Transactions, Institution of Engineers, Australia, Vol. CE10, No2, Oct. 1968.
18. CHEN, W F. and ATSUTA, T. *Theory of Beam-Columns*, Volume 2 Space behaviour and design, McGraw-Hill, Inc, New York, 1976.
19. WESTERGAARD, H.M. and OSGOOD, W R. Transaction of American Society of civil engineers, Vol 50, 1928.
20. WILSON, E L. *Matrix analysis of non-linear structures*. Proceeding of IInd conference in electronic computing, American society of civil engineers, Sep. 1960.
21. GESUND, H. *Stress and moment distributions in three dimensional frames composed of non-prismatic members made of non-linear material*. Space Structures, Edited by: Davies, R M., Sep. 1966.
22. CRANSTON, W B. *A computer method for the analysis of restrained columns*, Cement and concrete association, Technical report TRA 402, Apr. 1967
23. WARNER, R F. *Biaxial moment thrust curvature relations*, Journal of the Structural division, Proceeding of the ASCE, May 1969.
24. MILNER, H R. *Ultimate load calculations for restrained H-columns under biaxial bending*. The civil engineering transactions of The institution of Engineers, Australia, Apr. 1971.
25. VIRDI, K S. and Dowling, P J. *The ultimate strength of composite columns in biaxial bending*. Proceedings, Institution of civil engineers, Mar. 1973.
26. VIRDI, K S. *Design of circular and rectangular hollow section columns*. Journal of the constructional steel research, Sep. 1981.

27. BRANT, N F A. *Reinforced concrete columns of variable cross section*. PhD Thesis: The City University, London, Sep. 1984
28. BS8110:1985. *Structural use of concrete-Part 1: Code of practice for design and construction*. British standards institution, London, 1985.
29. KONG, F K. and EVANS, R H. *Reinforced and prestressed concrete*. Van Nostrand Reinhold (UK) Co. Ltd. 1987.
30. SIMITSES, G J. and VLAHINOS, A S. *Steel framed structures, Stability and strength*, Edited by: Narayanan, R. 1985.
31. VAART, A. *Elastic stability of space framework*. PhD Thesis: New York University, 1965.
32. CROSS, H. *Analysis of continuous frames by distributing fixed-end moments*. Transaction of ASCE, 96, 1932.
33. LUNDQUIST, E E. *A method of estimating the critical buckling load for structural members*, NACA, Technical Note 717, 1939.
34. NAYLOR, N. *Side sway in symmetrical building frames*. The structural engineer, Apr. 1950.
35. WILLIAM, M. *Matrix structural analysis*, Chichester, New York, 1979.
36. LIVESLEY, R K. and CHANDLER, D B. *Stability functions for structural frameworks*. Manchester University Press, 1962.
37. EKHANDI, S G., SELVAPPALAM, M. and MADUGULA, K S. *Journal of structural Engineers* , 1989.
38. FRAZER, R A., DUNCAN, W J. and COLLAR, A R. *Elementary matrices and some applications to dynamics and differential equations*, Cambridge university press, London, 1938.
39. MacGREGOR, J G., and HUGE, S E. *Stability analysis and design of concrete frames*. Journal of the structural division, Proceedings of the ACSE Vol. 103, No. ST10, Oct. 1977.
40. BAKER, J F., HORNE, M R. and RODERICK, J W. *The behaviour of continuous stanchions*. Proceeding of royal society, vol 198, 1949.
41. STEEL DESIGNERS MANUAL, Crosby Lockwood, London, 1972.

42. MAJID, K I. *Non-linear structures*. Matrix methods of analysis and design by computers, Butterworths, London 1972.
43. GHARPURAY, V. and ARISTIZABAL-OCHOA, D. *Simplified second-order elastic-plastic analysis of frames*. Journal of computing in civil engineering, Vol 3, No. 1 Jan 1989.
44. TURNER, M J., DILL, E H., MARTIN, H C. and MELOSH, R J. *Large deflection of structures subjected to heating and external loads*. Journal of aeronautical science, 27, 1960.
45. ZIENKIEWICZ, O C. and TAYLOR, R L. *The finite element method*, Volume 2, McGraw-Hill book company (UK) Ltd.,
46. HSIAO, K M., HOU, F Y. and SPILIOPOULOS, K V. *Large displacement analysis of elasto-plastic frames*. Computers and structures, Vol.28, No. 5, 1988.
47. NGO, D. and SCORDELIS, A C. *Finite element analysis of reinforced concrete beams*. Journal of the American concrete institute, Vol. 64, No. 3, Mar. 1967,
48. CHANG, W F. *Inelastic buckling and sidesway of concrete frames*. Journal of the structural division, Proceedings of the ASCE, Vol. 93, No. ST2, Apr. 1967.
49. VIRDI, K S. and DAWLING, P J. *A general formulation of the non-linear analysis and stability of space frames*. 2nd International conference on space structures. 1975
50. SEN, T K. *Inelastic H-Column performance at high axial loads*. PhD Thesis, Imperial College, London, 1976.
51. Steel Structures Research Committee, *Report 1*, Department of scientific and industrial research, HMSO, London, 1931.
52. Steel Structures Research Committee, *Report 2*, Department of scientific and industrial research, HMSO, London, 1934.
53. SOMERVILLE, G. and BURHOUSE, P. *Tests on joints between precast concrete members*. Building research station, Engineering paper 45, 1966.
54. ROMSTAD, K M. and SUBRAMANIAM, C V. *Analysis of frame with partial connection rigidity*. Journal of structural division, ASCE 96, 1970.

55. YU, C H. and SHANMUGAM, N E. *Stability of semi-rigid space frames*. Computers and Structures Vol 28, No. 1, 1988.
56. WILSON, W M. and MOORE, H F. *Tests to determine the rigidity of riveted joints in steel structures*. University of Illinois, Engineering Experiment station, Bulletin No. 104, Urbana, USA, 1917.
57. BAKER, J F. *Method of stress analysis*, First Report, Steel structures Research committee, DSIR, UK, 1931.
58. RATHBURN, J C. *Elastic properties of riveted connections*, Transactions of American society of civil engineers, 101, 1936.
59. Monforton, A R. and Wu, T S. *Matrix analysis of semi-rigidly connected frames*. Journal of structural division, American society of civil engineers, 89, ST.6, Dec. 1963.
60. BATHO, C. and ROWAN, H C. *First Report, Second, and final report*, Steel structures Research committee, DSIR, UK, 1931, 1934, 1936.
61. CHEN, W F. and LUI, E M. *Effects of joints flexibility on the behaviour of steel frames*. Computers and Structures Vol. 26, No. 5, 1987.
62. MELCHERS, R E. and KAUR, D. *The behaviour of frames with flexible connections*. 6 th Australian conference on the mechanics of structures and materials. 1982.
63. HSIEH, S H. and DEIERLEIN, G G. *Nonlinear analysis of three dimensional steel frames with semi-rigid connections*. Computers and structures,
64. JONES, S W., KIRBY, P A. and NETHERCOT, D A. *The analysis of frames with semi-rigid connections - A state-of-the-art report*. Journal of constructional steel research, Vol. 3, No. 2, 1983.
65. ERNST, G C, et al. *Basic reinforced concrete frame performance under vertical and lateral loads*, ACI Journal, 1973, April, p261.
66. SENIWONGSE, M. *The deformation of reinforced concrete beams and frames up to failure*, The Structural Engineer, Vol 57B, No 4, 1979, December.
67. FRANKLIN, H A. *Nonlinear analysis of reinforced concrete frames and panels*. PhD Thesis, University of California, Berkeley, 1970.

68. VIRDI, K S. and RAGUPATHY, P. *Stability problems associated with the behaviour of joints in precast sway and nonsway frames, Tests 1-4 on precast concrete subframes*. Report CUSRC/PCF/01, Structures Research Centre, Department of Civil Engineering, City University, London. 1991May.
69. VIRDI, K S. and RAGUPATHY, P. *Stability problems associated with the behaviour of joints in precast sway and nonsway frames, Tests 5-8 on precast concrete subframes*. Report CUSRC/PCF/02, Structures Research Centre, Department of Civil Engineering, City University, London. 1991October.
70. RAGUPATHY, P. *User manual for SWANSA*. Structures Research Centre, Department of Civil Engineering, City University, London. 1991.
71. MAHDI, A A. *Moment-Rotation Behaviour of Connection in Precast Concrete Structures*, PhD Thesis, Department of Civil Engineering, Nottingham University, UK. 1992.
72. CP110:1972. *Code of Practice for the Structural Use of Concrete*. British Standards Institution, London, 1972.

## APPENDIX

The concrete mixes for the columns and beams were designed by the precast frame manufacturers, the specified characteristic strength was Grade 50 concrete.

### GROUT FOR JOINTS

The grout mix used for subframes CT1, CT2, CT5 and CT6 is Conbex 100 grout prepared according to manufactures detail.

The concrete mix used to grout the joint in subframes CT3 and CT4 is given bellow.

Cement	11.88 kg
Sand	11.04 kg
Water	04.56 kg
Aggregate (10 mm)	28.32 kg

Average cube strength = 49.8 N/mm<sup>2</sup>

### FLOOR SLAB

For the floor slab for the specimens CT7 and CT8 which were cast in the Heavy Structures Laboratory has the following mix.

Cement	46.75 kg
Sand	46.20 kg
Water	17.60 kg
Aggregate (20 mm)	107.25 kg

Average cube strength = 55.2 N/mm<sup>2</sup>